SEDIMENT YIELD PREDICTION BASED ON ANALYTICAL METHODS AND MATHEMATICAL MODELLING

by

VP Msadala

Thesis presented in partial fulfilment of the requirements
for the degree of Master of Science in Civil Engineering
at the University of Stellenbosch

Prof. G.R. Basson
Study leader

STELLENBOSCH December 2009

Declaration

By submitting this dissertation electronically, I declare that the entirety of the work contained therein is my own, original work, that I am the owner of the copyright thereof (unless to the extent explicitly otherwise stated) and that I have not previously in its entirety or in part submitted it for obtaining any qualification.

VP Msadala, December 2009

Abstract

A study of the state of reservoir sedimentation in South Africa based on reservoir sediment deposit data, has shown that a considerable number of reservoirs have serious sedimentation problems. The analysis of the reservoir sediment deposit data showed that almost 25% of the total number of reservoirs have lost between 10 to 30% of their original storage capacity. The average storage loss due to sedimentation in South African reservoirs is approximately 0.3% per year while the average annual storage loss for all the reservoirs in the world is 0.8%.

The aim of this research was to develop sediment yield prediction methods based on analytical approaches and mathematical modelling. The sediment yield prediction methods can be used in planning and management of water resources particularly in reservoir sedimentation control. The catchment erosion and sediment yield modelling methods can be applied in temporal and spatial analysis of sediment yields which results are essential for detailed design of water resources, particularly in the identification of critical erosion areas, sediment sources and formulation of catchment management strategies.

Current analytical methods for the prediction of sediment yield have been reviewed.

Nine sediment yield regions have been demarcated based on the observed sediment yields and catchment characteristics. Empirical and probabilistic approaches were investigated. The probabilistic approach is based on analysis of the observed sediment yields that were calculated from reservoir sediment deposit, river suspended sediment sampling data and soil erodibility data. The empirical equations have been derived from regression analysis of the variables that were envisaged to have a significant effect on erosion and sediment yields in South Africa. Empirical equations have been developed and shown to have accurate and reliable predictive capability in six of the nine regions.

The probabilistic approach has been recommended for the prediction of sediment yields in the remaining three regions where reliable regression equations could not be derived.

The predictive accuracy of both the probabilistic and empirical approaches was checked and verified using the discrepancy ratio and graphs of the observed and calculated data.

While the analytical methods are needed to predict the sediment yield for the whole catchment, mathematical modelling to predict sediment yields is applied for more detailed analysis of sediment yield within the catchment. An evaluation of available catchment sediment yield mathematical modelling systems was carried out. The main criteria for the choice of a numerical model to be adopted for detailed evaluation was based on the following considerations: the model's capabilities, user requirements and its application. The SHETRAN model (Ewen et al., 2000) was therefore specifically chosen because of its ability to simulate relatively larger catchment areas (it can handle catchment scales from less than 1km^2 to 2500km^2), its ability to simulate erosion in channels, gullies and landslides, its applicability to a wide range of land-use types and ability to simulate land use changes. Another model, ACRU (Smithers et al., 2002) was also reviewed.

The aim of the model evaluation was to provide a conceptual understanding of catchment sediment yield modelling processes comprising model set up, calibration, validation and simulation. The detailed evaluation of the SHETRAN model was done through a case study of Glenmaggie Dam in Australia. The flow was calibrated and validated using data from 1975 to 1984, and 1996 to 2006 respectively. The results for both the calibration and validation were reasonable and reliable. The sediment load was validated against turbidity derived sediment load data from 1996 to 2006. The model was used to identify sources of sediment and areas of higher sediment yield. The land use of a selected sub-catchment was altered to analyse the impact of land use and vegetative cover on the sediment yield. Based on the results, the SHETRAN model was confirmed to be a reliable model for catchment sediment yield modelling including simulation of different land uses.

Opsomming

'n Studie van die stand van damtoeslikking in Suid-Afrika toon dat daar ernstige toeslikkingsprobleme by baie reservoirs bestaan. 'n Ontleding van die toeslikkingsyfers gegrond op damkomopmetings toon dat omtrent 25% van die totale getal reservoirs tussen 10 en 30% van hulle oorspronklike opgaarvermoë verloor het. Die gemiddelde tempo van damtoeslikking in Suid-Afrika is 0.3%/jaar, wat laer is as die wêreld gemiddeld van 0.8%/jaar.

Die oogmerk met hierdie navorsing was om sedimentlewering voorspellingsmetodes te ontwikkel deur gebruik te maak van analitiese metodes en wiskundige modellering. Die sedimentlewering voorspellingsmetodes kan gebruik word vir die beplanning en bestuur van waterbronne en veral vir damtoeslikking beheer. Die opvangsgebied erosie en die sedimentlewering modelleringsmetodes kan toegepas word in tydveranderlike en ruimtelike ontleding van sedimentlewering. Hierdie inligting word benodig vir die detail ontwerp van waterhulpbronne en veral vir die identifisering van kritiese erosiegebiede, bronne van sediment en die formulering van opvangsgebied-bestuur strategië.

'n Literatuuroorsig oor die huidige metodes vir die voorspelling van erosie en sedimentlewering is gedoen.

Nege sedimentasie streke is afgebaken in Suid-Afrika, gegrond op waargenome damtoeslikkingsdata en opvangsgebied-eienskappe. Proefondervindelike en waarskynlikheidsbenaderinge is ondersoek. Die waarskynlikheidsbenadering is gegrond op die ontleding van waargenome damtoeslikking wat bereken is uit reservoir opmeting data en rivier gesuspendeerde sediment data, asook data oor gronderosie.

Die proefondervindelike metode se vergelykings is afgelei vanuit regressie ontleding van die veranderlikes wat 'n belangrike invloed het op die erosie en sedimentlewering in Suid-Afrika. Daar is bevestig dat die ontwikkelde proefondervindelike (empiriese) vergelykings 'n akkurate en betroubare voorspellingsvermoë in ses van die nege streke het. Die waarskynlikheidsbenadering is aanbeveel vir die voorspelling van

sedimentlewering in die ander drie streke, waar betroubare regressie vergelykings nie afgelei kon word nie. Die voorspellingsakkuraatheid van albei metodes is nagegaan en bevestig deur gebruik te maak van die teenstrydigheidsverhouding en grafieke van die waargenome en berekende data.

Analitiese metodes van sedimentleweringsvoorspelling is nodig vir ‘n volle opvangsgebied, terwyl wiskundige modellering om sedimentlewerings te voorspel gebruik kan word om ‘n meer in diepte ontleding van die sedimentlewering binne ‘n opvanggebied te doen. ‘n Evaluasie van beskikbare wiskundige modelle wat opvangsgebied sedimentlewering kan voorspel, is gedoen. Die hoofkriteria vir die keuse van ‘n model vir gebruik by gedetailleerde ontleding is gegrond op die volgende: die vermoëns van die model, wat verbruikers benodig en die aanwending van die model. Die SHETRAN model (Ewen et al., 2000) is spesifiek gekies weens sy vermoë om relatief groter opvangsgebiede te simuleer (dit kan opvangsgebiede van 1km^2 tot 2500km^2 wees) asook om erosie in kanale, dongas en grondverskuiwing simuleer. Dit kan toegepas word op ‘n wye reeks grondtipes en kan ook die gevolge simuleer as die gebruik van die grond verander. ‘n Ander model, ACRU (Smithers et al., 2002) is ook ondersoek.

Die doel van die modelevaluering was om ‘n konseptuele begrip te kry van sedimentlewering modelleringsprosesse wat die opstelling, kalibrasie, toetsing en simulasies insluit. Die volledige evaluasie van SHETRAN is gedoen deur middel van ‘n gevalle-studie van die Glenmaggiedam in Australia. Die riviervloei is gekalibreer en getoets deur gebruik te maak van data wat strek van 1975 tot 1984, en van 1996 tot 2006 onderskeidelik. Die resultate van beide die kalibrasie en die toetswas redelik en betroubaar. Die sedimentlading is gekalibreer teen velddata van 1996 tot 2006. Die model is gebruik om bronne van sediment te identifiseer, asook gebiede met ‘n hoër sedimentlewering. Die gebruik van die grond op ‘n gekose sub-opvangsgebied is verander om die impak van grondgebruik en plantbedekking op sedimentlewering te ontleed.

Die resultate bewys dat die SHETRAN model ‘n betroubare model is vir groot opvangsgebied sedimentlewering modellering, asook vir die simulasie van verskillende grondgebruike.

Acknowledgements

I wish to acknowledge and express my gratitude to my study leader, **Professor GR Basson** (Director, Institute for Water and Environmental Engineering, Department of Civil Engineering, University of Stellenbosch, South Africa) for his valuable help, assistance and guidance during the execution of this research and preparation of the thesis.

I would like to thank **Water Research Commission** for the funding of this research.

I would like to express my sincere appreciation to **Professor A Rooseboom** for his guidance during the early months of this research.

I am grateful to **Canon Collins Trust** for partial funding of my studies.

I wish to acknowledge **colleagues** in the postgraduate student office (S417) and staff of the **Department of Civil Engineering** for their inspiration.

I am grateful to the **Department of Water Affairs** (DWA) for providing the reservoir survey database and recurrence interval floods.

I would like to acknowledge the assistance given by **Dr. Steve Birkinshaw** of Newcastle University on the application of the SHETRAN model.

Thanks to my wife **Chifundo** and my son **Chipatso** for their love, support and inspiration.

Table of Contents

List of Tables

List of Figures

List of Appendices

Nomenclature

α	Soil porosity
A	Average annual soil loss or flow area
A_e	Effective catchment area
A_H	Size of area consisting of soils with high sediment yield potential
A_L	Size of area consisting of soils with low sediment yield potential
A_M	Size of area consisting of soils with medium sediment yield potential
A_T	Total catchment area or gross annual erosion/soil loss
B	Channel bed width
C	Cover management factor
c	Sediment concentration
C_g	Proportion of ground protected from raindrop/leaf drip erosion by near ground cover such as low vegetation
C_r	Proportion of ground protected against raindrop/leaf drip erosion and overland flow erosion by, for example, rock cover
D_r, D_f	Rates of detachment of material per unit area
F_H	High yield potential factor
F_L	Low yield potential factor
F_M	Medium yield potential factor
h	Water depth
K	Soil erodibility factor
k_f	Overland flow soil erodibility coefficient
K_r	Raindrop impact soil erodibility coefficient
LS	Slope steepness factor
M_d	Momentum squared for leaf drip
M_r	Momentum squared for raindrops falling directly on the ground
Ø	Channel bed porosity
P	Supporting practice factor
Q	Discharge
Q_O	Observed flow discharge
Q_S	Simulated discharge or sediment load
Q	Discharge
$\rho g Q S$	Total input stream power

R	Rainfall erosivity factor
S	Energy slope
S_{DR}	Sediment delivery ratio
S_O	Average river slope
SY, Sy	Sediment yield
SY_{obs}	Observed sediment yield
SY_{sim}	Simulated sediment yield
t	Time
T_C	Critical shear stress for initiation of soil particle motion
T	Overland flow shear stress
V_{50}	Sediment volume after 50 years.
V_S	Sediment velocity
V_t	Sediment volume after t years.
V_W	Storage volume of reservoir
w	Settling velocity of sediment
X_i	Discrepancy ratio
Y_C	Estimated catchment sediment yield value
Y_S	Standardised average yield
z	Depth of loose soil

Acronyms

ANSWERS	Areal Non-point Source Watershed Environmental Response Simulation
CREAMS	Chemicals, Runoff, and Erosion from Agricultural Management Systems
DWA	Department of Water Affairs
EUROSEM	European Soil Erosion Model
GIS	Geographical Information Systems
ICOLD	International Commission on Large Dams
KINEROS	Kinematic runoff and Erosion model
MUSLE	Modified Universal Soil Loss Equation
RUSLE	Revised Universal Soil Loss Equation
USLE	Universal Soil Loss Equation
WEPP	Water Erosion Prediction Project

1.0 INTRODUCTION

1.1 Problem Statement

The problem of elevated sediment concentration in rivers and sediment deposition in reservoirs is currently producing marked effects on land and water resources in southern Africa. The water quality in rivers and reservoirs has been degraded by an increase in suspended sediment. Reservoirs have lost significant proportions of their original storage due to sedimentation. Since reservoirs are beneficial for the provision of storage of water that is required for drinking, irrigation, recreation, hydropower production and flood control, sedimentation has resulted in serious economic losses, and environmental and aesthetic problems. It has therefore become not only important but very necessary to consider erosion and sedimentation issues in the planning and detailed design of proposed dams, reservoirs and water resource projects.

According to Morris and Fan (1998), storage loss is not the only problem resulting from sedimentation in reservoirs; sedimentation also affects the normal operation of reservoirs by obstructing intakes, impacting on low level outlets and accelerating the abrasion of hydraulic machinery.

In order to meaningfully manage sedimentation in rivers and reservoirs, there is a need to understand, define, quantify and/or predict catchment soil erosion and sediment yield. If something cannot be measured, it becomes difficult to manage. While in sedimentation studies, it is not easy to accurately measure the quantities that are involved, reliable predictions of sediment yield can help in the sustainable management of land and water resources.

Most predictions are made pertaining to the amount of sediment that is produced, transported and deposited from a known source to a destination point within a drainage area during a defined period. The major sedimentation quantitative descriptive features are sediment yield and sediment load.

Worldwide, different erosion and sediment yield prediction methods are in use. No single catchment erosion and sediment yield prediction method can be presumed to be applicable to all possible conditions. All methods have limitations and advantages and the choice of the method to apply should consider a number of influencing factors. These factors include: catchment characteristics, site conditions, ecological considerations, dam engineering requirements, availability of time, economics, data requirements and data availability.

Three major approaches for predicting sediment yields have been developed in South Africa namely: direct measurements from reservoir surveys, river suspended sediment sampling and sediment yield maps incorporating the probabilistic approach. The development of these methods was influenced by the availability of sediment yield data, experience and physical analysis of sedimentation and erosion related processes. Notable work in sediment yield prediction methods comprised the development of the new sediment yield map of Southern Africa (Rooseboom et al., 1992). The approach proved a vital tool in sediment yield prediction in South Africa. However, continuous improvement of sediment yield prediction methods is necessary in the wake of changing environments, more data, increased experience and current technological advancements in the sedimentation field. Improved sediment yield prediction methods are essential for sound land and water resources management decision making with respect to dam development and environmental management in the wake of current population increases that are putting a strain on the available land and water resources.

The purpose of this study was to provide a better understanding of erosion and sediment yield and present information for efficient decision making in water resources planning for sedimentation control in rivers, existing and future reservoirs, through the development of sediment yield prediction and analysis methods.

The catchment sediment yield modelling methods will also provide an important decision making tool in the application of relevant catchment soil conservation techniques and formulation of reservoir operation procedures aimed at limiting and controlling sedimentation in reservoirs. Finally, sediment prediction methods would

help in the examination of the extent in which sedimentation could threaten the sustainability of the existing reservoirs.

1.2 Background to erosion and reservoir sedimentation

South Africa is one of the countries in the world that has been actively involved in the research and practical aspects of erosion and sedimentation for a long period of time. Within the last fifty years, a rich knowledge base of erosion and sedimentation has been accumulated through experience and research. It is from this knowledge base that the problem of reservoir sedimentation has been continuously analysed. New prediction methods have been developed as more data has been collected.

1.2.1 Status of reservoir sedimentation in South Africa

The analysis of the reservoir sediment deposit data for South African dams showed that almost 25% of the total number of reservoirs have lost between 10 to 30% of their original storage. Table 1.2.1 shows the results of the assessment of the state of reservoir sedimentation based on reservoir sediment deposit data obtained from the Department of Water Affairs' dam list (DWA, 2006).

Table 1.2.1 State of reservoir sedimentation in South Africa (storage lost as a percentage of the original capacity)

Storage lost (%)	Percentage of dams	Cumulative percentage of dams
0 – 5	28	28
5 – 10	18	46
10 – 20	20	66
20 – 30	6	72
30 – 40	5	77
40 – 50	7	84
50 – 60	8	92
≥60	8	100

Table 1.2.2 shows the annual storage loss in reservoirs in South Africa due to sediment deposition.

Table 1.2.2 Sedimentation in reservoirs (annual storage loss)

Annual storage loss (%)	Percentage of dams	Cumulative percentage of dams
0 – 0.1	28	28
0.1 – 0.2	25	53
0.2 – 0.5	31	84
0.5 – 1	8	92
1 - 1.5	8	100

Analysis of the results showed that the average annual storage loss due to sedimentation in South African reservoirs is approximately 0.3%. This scenario adversely affects the long term sustainability of the reservoirs.

A special case of reservoir sedimentation that confirms the adverse effects of sedimentation is the Welbedacht Dam on the Caledon River in the Free State Province of South Africa (DWA, 2009). Welbedacht Dam was commissioned in 1973. Due to sedimentation, the storage capacity of the Welbedacht Dam reduced rapidly from the original 114 million m^3 to approximately 16 million m^3 during the first twenty years since its commissioning. This reduction in storage created problems in meeting the city of Bloemfontein's demand at an acceptable level of reliability.

A lesson was learnt from the Welbedacht Dam scenario to the extent that further dam developments in the catchment considered the anticipated impacts of sedimentation. Accordingly, Knellpoort Dam that was constructed fifteen years after the commissioning of the Welbedacht Dam was designed and constructed as an off-channel storage dam that is fed by pumping through a 2 km long canal which is equipped with a silt trap to reduce siltation in the main reservoir.

The case of Welbedacht Dam presents one of the challenges in water resource development not only in South Africa but throughout the whole world. Although sediment management strategies encompass many elements, there is need for improved methodologies for sediment yield prediction.

Analytical methods for sediment yield prediction include probabilistic and empirical methods, and are based on observed sediment yield data.

Mathematical models are applied to simulate erosion and sediment yield processes both in time and space. Numerical models are required for spatial and temporal analysis of the sediment yield during the feasibility and detailed design stages of a project. Numerical models can be used to identify the specific sub-catchment that is contributing more sediment into the river or an existing reservoir. Decision makers and planners are then guided on the choice of the optimum sediment management techniques to be adopted for specific catchment sites and conditions. In the end, catchment management techniques aimed at reducing erosion can be directed at the specific problem areas. Climate and human induced changes over a required period of time can also be investigated and analysed using numerical models.

1.3 Objectives

This thesis has focused on the development of analytical methods for sediment yield prediction and the evaluation of mathematical modelling in the detailed analysis of spatial and temporal variability in sediment yield within a catchment. The *key objective* of this thesis is to facilitate a better understanding of the methods for prediction of sediment yield based on analytical methods and mathematical modelling and include:

- To review the current methods for the prediction of sediment yield.
- To develop analytical methods for the prediction of the sediment yield at gauged and ungauged catchments.
- To evaluate mathematical modelling of catchment sediment yield with the main focus of illustrating the aspects of model set up, calibration,

validation and simulation and to improve understanding of spatial and temporal changes.

1.4 Thesis overview

Chapter One of this thesis introduces the topic that was under investigation and the motivation behind the choice of the study topic. An outline of the state of reservoir sedimentation in South Africa has been presented and the potential threat posed by sedimentation in the existing reservoirs has been quantified. The objectives have been laid down.

Chapter Two presents the methodology that was followed in order to achieve the set objectives.

Chapter Three looks at the theory and general concepts of erosion and sedimentation as reported in literature. Erosion and sediment yield relationships have also been reviewed. Background aspects of catchment erosion and sediment yield modelling have been discussed including the various models that are available. More emphasis has been put on the SHETRAN model (Ewen et al., 2000) by reviewing selected case studies that were simulated by SHETRAN in order to give confirmed model capabilities. Finally, a comparative analysis of SHETRAN and ACRU (Smithers et al., 2002) has been done.

Chapter Four addresses current sediment yield prediction approaches and an assessment of the advantages and limitations of current sediment yield prediction methods.

Chapter Five presents the development of new probabilistic and empirical approaches for sediment yield prediction. The acquisition and processing of all relevant data and information that was needed for the development of the methods has been explained. The derivation procedure for the regression equations has been discussed. Worked examples for both the empirical and probabilistic methods have been solved to illustrate the practical implementation of the two methods.

Chapter Six presents an approach to catchment sediment yield mathematical modelling. The reasons behind choosing SHETRAN as the model to be adopted for possible application in catchment sediment yield modelling have been given. The chapter also provides an overview of the study area and how the model was set up. A detailed procedure for flow calibration and validation and sediment load calibration has been provided. The results of the evaluation of numerical modelling have been presented on the ability of the numerical models to simulate the effects of land use changes and identification of areas with high sediment yields.

Chapters Seven and Eight give a summary of the findings and recommendations for further research respectively.

2.0 METHODOLOGY

The development of the analytical methods has been done for catchments within Southern Africa because of the availability of observed data. The detailed evaluation of catchment sediment yield mathematical modelling has been undertaken on a selected catchment in Australia due to data availability. The case study was selected to illustrate the concepts and issues that are mostly encountered in mathematical modelling of sediment yield.

In summary, the methodology that was followed in order to achieve the objectives included the following:

- Literature review of the general concepts and theories in erosion and sedimentation. Various books, scientific journals, reports and guidelines were reviewed.
- Review of current sediment yield estimation methods in Southern Africa.
- Development of new analytical methods for the prediction of sediment yield. Relevant data was collected and analysed in order to derive the empirical and probabilistic relationships.
- Review of mathematical modelling techniques for catchment sediment yield.
- Case study for the application of catchment sediment yield modelling techniques. Aspects of sediment yield modelling that are applicable to different catchments were evaluated. These aspects include: model set up, calibration, validation and analysis of simulations.

3.0 LITERATURE REVIEW

3.1 General concepts and theories in erosion and sedimentation

Erosion is the gradual rubbing, detachment, removal and movement of soil and rock masses by forces of wind and water. Sediment is any particulate matter that can be transported by fluid flow and which eventually is deposited as a layer of solid particles on the bed of a body of water. Sedimentation is the deposition by settling of suspended material (Villiers, 2006).

Erosion and sedimentation embody the processes of erosion, transportation, and deposition of solid particles (Julien, 1998). Erosion within a catchment area produces sediment which later becomes available for transport to water bodies. It has been widely concluded that the whole process of reservoir sedimentation from production, transportation and deposition of sediment is very complex because of the variables that are involved in their occurrence. Additionally, though the processes of production, transportation and deposition seem to be well understood at a small scale, the complexities increase when considering their interaction in large catchments. The concepts and theories governing the processes of sedimentation from erosion, transportation up to deposition were reviewed and discussed. The concepts and theories are significant for a better understanding of the interaction between sediment production and sediment yield at a catchment scale.

Watershed management programmes frequently fail to reduce sediment yield despite large expenditures because the physical nature of the problem is not properly diagnosed (Morris & Fan, 1998). The physical nature of sedimentation is dependent on the processes of erosion and sediment yield.

Erosion and sediment yield are variable both in space and time. Erosion begins with the detachment of a particle from surrounding material (EOEARTH, 2009). Prominent soil detachment mechanisms include raindrop, leaf drip and runoff.

3.1.1 Raindrop and leaf drip erosion.

The impact of falling drops of water has the capacity to detach soil particles from the land surface. The amount and sizes of the soil particles that can be detached with such an impact of falling water depends on the magnitude of the force of the drop or drip upon hitting the land surface. The raindrop and leaf drip may have varying forces of impact. The vegetative cover that determines whether rain falls as raindrop or leaf drip has an effect on the amount of the sediment produced.

According to Smithers and Schulze (2002), the vegetative canopy has an effect of reducing the rainfall energy impact on the soil surface whereby, even if most rainfall intercepted by vegetative canopy, eventually reaches the surface, it does so with much less energy than non-intercepted rainfall. It is reported by Smithers and Schulze (2002) that the raindrops intercepted by the canopy are either fractured into smaller drops with less energy, drip from leaf edges or run down crop stems to the ground. The total rain falling on the canopy cover may come to the ground through either falling or running down the stem in varying proportions. The main controlling parameters for the amount of erosion by raindrop and leaf drip include the fraction of land surface covered by canopy and the height of fall from the vegetative canopy. The fraction of land surface covered by canopy may vary throughout the year. This has a partial effect on the variation of sediment production during the year.

In addition, part of the ground may be covered by non erodible surfaces. All these must be taken into consideration when determining raindrop and leaf drip erosion.

Many studies have been undertaken with the aim of developing methods for estimation of erosion by raindrop and leaf drip. Various empirical erosion models have different parameters that are used to account for vegetative canopy cover. In MUSLE, the cover management factor represented as (C), estimates the effect of ground cover conditions, soil conditions, and general management practices on erosion rates (Sadeghi et al., 2007). ACRU uses a parameter called canopy cover factor. SHETRAN uses an empirical equation to determine the rate of soil erosion by raindrop and leaf drip impact that relates the rate of detachment of soil to raindrop impact soil erodibility coefficient, proportion of ground nearly shielded by ground

cover, proportion of ground shielded by ground level cover and momentum squared of raindrop and leaf drip reaching the ground per unit time per unit area.

In order to illustrate the attempts that have been made to describe the erosion processes resulting from leaf drip and raindrop, the EUROSEM version (Morgan et al., 1998) of leaf drip and raindrop erosion processes will be presented.

According to Morgan et al., (1998), the detachability of the soil by raindrop impact can be expressed as the weight of soil particles detached per unit of rainfall energy. Since there have been various research attempts to correlate the rainfall energy and the weight of the sediment that can be eroded, knowledge of the amount of energy of a falling drop or drip can aid in the prediction of the amount of soil that can be eroded from the ground with respect to various standard soil textures. The EUROSEM User Manual (Morgan et al., 1998) gives the soil detachability in grams per joule for common soil types ranging from clay to sand. Others have managed to define the rate of detachment by raindrop impact as being proportional to the square of rainfall intensity (Beasley et al., 1980).

3.1.2 Erosion and sediment transport by overland flow

Erosion is defined as the wearing away of land surface by detachment and movement of soil and rock fragments through the action of 'moving water' and other geological agents (ICOLD, 1998). The emphasis on the action 'moving water' indicates the intrinsic ability of runoff to detach soil. Soil detachment by runoff contributes significantly to the sediment production process. Overland flow is characterised by sediment entrainment, transport and deposition.

According to Pidwirny (2008), entrainment is the process of particle lifting by the agent of erosion and there is a thin line between entrainment and detachment so much so that it is somehow hard to distinguish between entrainment and detachment. The latter is mostly influenced by fluid drag.

In the EUROSEM User Manual (Morgan et al., 1998), soil detachment by flow and deposition during flow is expressed in terms of settling velocity and transport capacity. The rate of soil detachment due to overland flow on hill slopes of a catchment can also be determined from various empirical relationships that have been developed that aim to relate the rate of soil detachment to other dependent variables such as the shear stress, erodible soil thickness, vegetation cover, rock cover, canopy cover and other factors.

Once the particle is detached, then it is prone to be transported by any transporting medium mostly water and/or wind. Detachment and entrainment can occur in cyclic sequences depending on the prevailing flow conditions. Pidwirny (2008) states that an entrained particle tends to move on as long as the velocity of the medium is high enough to transport the particle horizontally. Pidwirny (2008) further gives four different ways in which transport can occur in the transporting medium:

- Suspension is where the particles are carried by the medium without touching the surface of their origin. This can occur in air, water, and ice.
- Saltation is where the particle moves from the surface to the medium in quick continuous repeated cycles. The action of returning to the surface usually has enough force to cause the entrainment of new particles. This process is only active in air and water.
- Traction is the movement of particles by rolling, sliding, and shuffling along the eroded surface. This occurs in all media of erosion sediment transport.
- Solution is a transport mechanism that occurs only in aqueous environment and it mainly involves the eroded material being dissolved and carried along in water as individual ions.

Particle weight, size, shape, surface configuration, and medium type are the main factors that determine which of these processes operate (Pidwirny, 2008).

3.1.3 Sediment deposition

Once the particles have been detached and/or entrained, they continue to be transported in the given transporting media. Some of the particles become deposited while in transit. Deposition occurs when particle flow velocity is reduced and the forces propelling the particle to move are less than the forces of resistance to transport. The interaction between flow velocity and particle erosion, transport, and deposition is illustrated by Pidwirny (2008) using Figure 3.1-1. Pidwirny (2008) states that the curved line marked "erosion velocity" describes the velocity required to entrain particles from the surface and further explains that the entrainment of silt and clay needs greater velocities than larger sand particles owing to the fact that silt and clay have the ability to form cohesive bounds between particles. Therefore, greater flow velocities are required to break the bonds and move these particles.

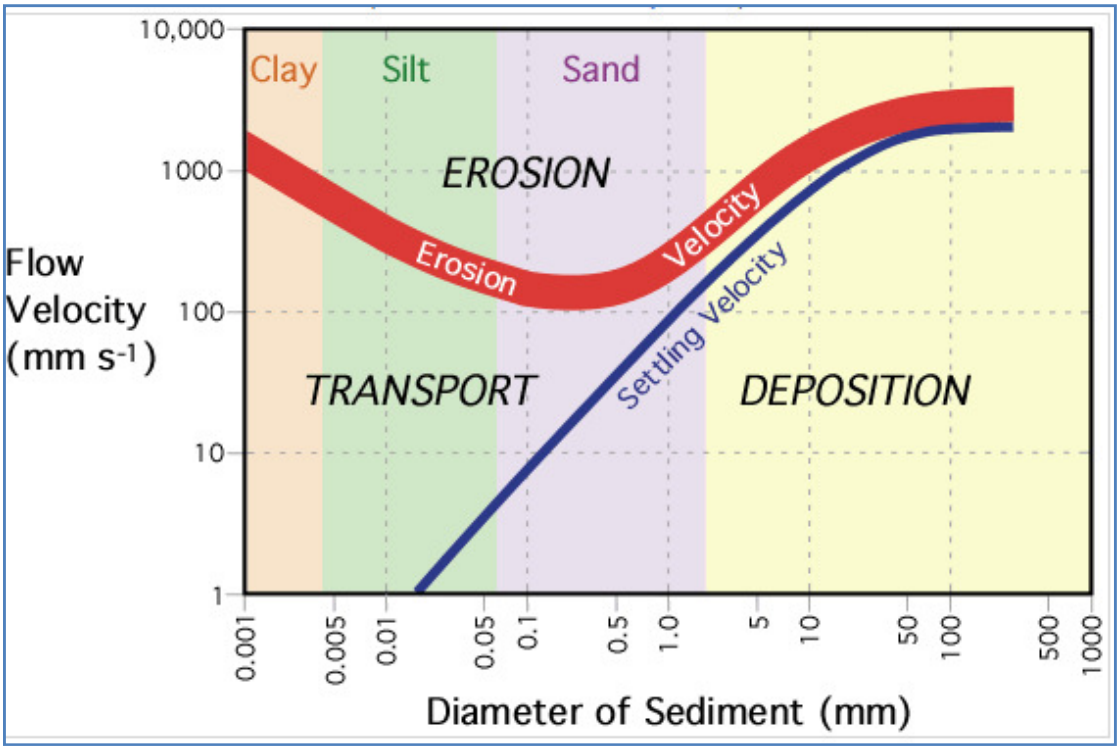

Figure 3.1-1 The relationship between flow velocity and particle erosion, transport and deposition. (Source: PhysicalGeography.net) (Pidwirny, 2008)

From Figure 3.1-1 above, the line labelled "settling velocity" shows at what velocity certain sized particles fall out of transport and are deposited (Pidwirny, 2008). The illustration shows the interaction between flow velocity, erosion, transport, settling velocity and deposition of particles of varying sizes in the form of clay, silt or sand.

The yellow band describes the relationship between “erosion velocity” and “settling velocity” for larger sized particles. The curves indicate that greater flow velocities are required to entrain larger sized particles from the stream’s bed and banks and also to make them fall out of transport and be deposited. The “erosion velocity” is slightly lower than the “settling velocity” for similar larger sized particles.

The complexity of the interaction is one of the reasons why a quantitative analysis of the sediment supplied to a stream from a watershed is usually difficult to perform as pointed out by Julien (1998). In other words, while it is possible to quantify sediment transport capacity (as will be illustrated in paragraph 3.1.4), sediment supply to streams or dams is affected by parameters such as deposition and entrainment, which cannot be accurately deciphered within the typically vast watershed areas encountered in practice.

Julien (1998) stated that physical processes involved in the spatial and temporal variations of all the parameters describing upland erosion from local rainstorms and bank erosion processes exacerbate the complexity of quantifying sediment supply.

3.1.4 Sediment transport capacity and sediment load

The transporting capacity is determined by the characteristics of the river channel and other factors. Every sediment particle that passes a given stream cross-section must satisfy the two conditions below (Julien, 1998):

- It must be eroded somewhere in the catchment above the cross section
- It must be transported by the flow from the place of erosion to the cross section.

It was concluded from the above conditions that the rate of sediment transport depends on the transport capacity of the stream and availability of sediment. Julien (1998) went further to say that the amount of transported material in the stream therefore would depend on two groups of variables:

(a) Characteristics and quantity of material made available for transport (characteristic variables): catchment topography, geology, rainfall intensity, magnitude and duration, weathering, vegetation, surface erosion, sediment supply from tributaries, mineralogy, soil type and land use.

(b) Sediment transport capacity (defining variables): channel geometry, width, depth, shape, wetted perimeter, slope, vegetation, roughness, velocity distribution, turbulence and uniformity of discharge.

The sediment that is transported by the river has varying sizes in terms of diameter. In regions where the sediment transported in the river is relatively coarse consisting of sand, gravel or coarser particles it is possible to hydraulically determine the sediment yield (Basson, 2008). Sediment yield is the quantity of sediment that has been mobilised from a known catchment area size which is passing through a river channel's reference point in a given time interval. Sediment quantitative analysis is sometimes expressed as total sediment load in a stream. The sediment transport capacity is determined as function of hydraulic conditions and the shape of the stream cross section.

Many attempts have been made to try to relate the quantity of material made available for transport, transport capacity and sediment sizes. Figure 3.1-2 below gives the general sediment transport capacity and supply relationship.

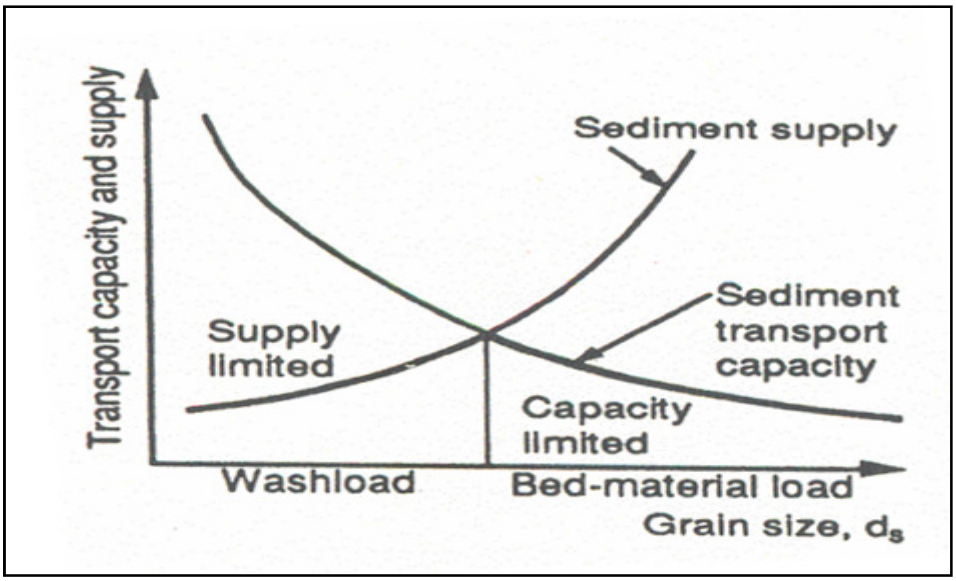

Figure 3.1-2 Sediment transport capacity and supply relationship (Julien, 1998)

From Figure 3.1-2 it can be seen that for finer sized sediment, the transport capacity of the stream is much higher than the sediment supplied (up to some limiting grain size). The wash load is availability limited and it is therefore not possible to do a direct quantitative analysis of the sediment yield for a flow discharge on a particular river.

The criteria for the determination of the sediment yield for finer sediment, typically less than 0.06mm which generally use regression analysis, will be presented in paragraph 3.1.5. Methods of direct measurement of sediment load will be explained in Chapter 4.

3.1.5 Empirical methods for erosion and sediment yield estimation

Empirical methods of erosion and sediment yield estimation are based on regression and probabilistic analysis of observed erosion or sediment yield against erosion and sediment controlling processes. Empirical methods use equations or relationships derived through analysis of observed data pertaining to erosion and sedimentation. Regression is the development of equations to predict a dependent variable based on two or more independent variables. Based on this concept, empirical equations can be developed for the prediction of sediment load or sediment load from data pertaining to factors that control the sediment yield.

One of the empirical equations that were developed to compute soil losses (mainly resulting from rill and sheet erosion at a given site) is the Universal Soil Loss Equation (USLE) (Wischmeier and Smith, 1978). Further improvements have been undertaken on the USLE method resulting in the Modified Universal Soil Loss Equation, MUSLE (Williams, 1975) and Revised Universal Soil Loss Equation, RUSLE (Renard et al., 1991).

The USLE equation:

$$A = RKLSCP \qquad 3.1$$

Where

A = long term average soil loss per unit area (tonne.ha^{-1}.annum^{-1})
R = an index of annual rainfall erosivity, (MJ.mm.ha^{-1}.h^{-1}.annum^{-1})
K = soil erodibility factor (tonne.h.MJ^{-1}.mm-^{1})
LS = slope length and gradient factor (dimensionless)
C = cover and management factor (dimensionless) and
P = support practice factor (dimensionless).

The above parameters (R, K, L, S, C, and P) are calculated independently and are then multiplied to determine the soil loss. The structure of the MUSLE equation is similar to the USLE, with the exception that the annual rainfall erosivity factor is replaced with the runoff factor comprising the product of the surface runoff and the peak runoff rate for the sub-basin (Williams, 1975). The modification of USLE by Williams (1975) was done because there was need to allow for direct prediction of sediment yield based on runoff characteristics. In the RUSLE empirical model, the basic equation is the same as in the USLE but the parameters (R, K, L, S, C, and P) were significantly improved using greatly improved data. Similarly, in both RUSLE and MUSLE, the factors are computed independently and the annual soil loss is obtained from the multiplication of the average values.

3.2 Erosion and sediment yield relationship

Not all sediment particles that are eroded from the catchment area upstream of a specified point along a river or at the reservoir manage to reach that specific point or the reservoir. The process of deposition described in paragraph 3.1.3 is responsible for deposition of sediment before they get to the reservoir. While in most cases, the deposition would be as a result of limited transporting capacity of flow discharge, in some cases, it could be as a result of natural storages and ponds that trap the sediment within the catchment. While some deposited sediment become entrained back again into the transporting medium, there is still more chance that some sediment would still be deposited between the sediment source point and the hypothetical destination due to inadequate transport capacity.

One of the relationships that have been derived between erosion and sediment yield include the sediment delivery ration, S_{DR}. Sediment delivery ratio denotes the ratio of the sediment yield (SY) at a given stream cross section to the gross erosion (A_T) from the watershed upstream from the measuring point (Julien, 1998). Whereby, the following mathematical relationship is applied:

$$SY = A_T S_{DR} \quad 3.2$$

Equation 3.1 calculates the gross erosion therefore the sediment delivery ratio was being applied to compute the sediment yield. According to Julien (1998), the sediment delivery ratio is generally dependent on the size of the catchment area. Development of these sediment yield and drainage area relationships requires data on observed sediment yields to validate the relationship between the sediment yield and erosion.

The sediment delivery ratio can only be applied to catchments that are homogeneous with respect to hydrology, erosion and sediment characteristics on which the model results were verified on. According to Birkinshaw (2006) the sediment yield/catchment area relationships can be direct or inverse depending of catchment characteristics. Therefore the concept of sediment delivery ratio is applicable in catchments where reliable calibration was done and the catchment areas are homogeneous.

3.3 Temporal and spatial variability in sediment yields

Sediment yield varies both in time and space. Knowledge of the extent of the temporal and spatial variability in sediment yields is significant in the context of resource allocation for sediment control measures. According to a study by Guyot et al., (1994) on sediment transport in the Rio Grande, the Andean river of the Bolivian Amazon drainage basin, it was found that most transport occurs during the three months of the year in which the river has high water flows. The period contributed up to 90% of the annual load.

The determining factors for an increase or decrease in sediment yield with time depend on the site specific conditions. In some circumstances, annual variability in sediment yield can just be a reflection of the variability in precipitation and runoff.

Batalla et al. (1994) reported about an investigation of the temporal variability of the suspended sediment load in a Mediterranean sandy gravel-bed river where marked temporal variability was caused by seasonal effects, progressive exhaustion of sediment available to be transported during sequences of storm events and extremely high sediment concentration during individual floods.

A cumulative plot of the observed sediment load has the ability to indicate the temporal variability in sediment yield by inspecting the slope changes in the graph of the cumulative water discharge against cumulative sediment discharge.

The same factors that have been reported to be responsible for the temporal variability of sediment yield have the ability to influence the spatial variability in sediment yield as long as there is possibility of spatial variability in the controlling variables within a catchment area. The temporal variation can be seasonally, annually and even inter-annually. It therefore emphasises the need for longer term sampling records for a detailed understanding of the temporal variation in sediment yield and in order to draw realistic conclusions from observations.

(Guyot et al., 1994) reported that the spatial variability was very strong in the Rio Grande to the extent that one sub-catchment would have almost fifty times the sediment yield observed in the other region.

Theoretically, it is therefore possible to discover that in a catchment, only 20% of the total catchment is contributing to over 80% of all sediment. Olive et al. (1994) reported that most sediment in the Murrumbidge River, New South Wales in Australia was generated from a localised area from one of the tributaries and was only transported for a short distance through the main Murrumbidge River before being deposited in the reservoir. This means that the longest water course is not necessarily the major sediment source.

3.4 Catchment erosion and sediment yield modelling

3.4.1 Models for erosion and sediment yield modelling

(a) Background

Numerical models are very useful tools in the estimation of erosion and sediment yield from a watershed and analysis of land-use impacts on sediment generation (Schmidt et al., 2008). Modelling of erosion and sediment yield plays a significant role during the design stages of a project particularly in the development of effective catchment management and sediment control strategies. This is in most cases achieved by spatially distributed models that have the ability to provide spatially distributed information on erosion and sediment yield within the catchment which can be used for planning catchment management and sediment control strategies. The spatial information is either presented in the form of data for individual grid squares making up the catchment or sub-catchment that can be calculated as single computational units.

Models can be fully physically-based, empirically-based or mixed empirical and physically-based (Randle et al., 2006). This classification is applied with reference to the description of the hydrological processes that are involved. Parameters used in the physically-based models are measured and/or are assessed from field data and conditions that describe the physical characteristics and properties of the catchment. Physically-based models can represent the catchment as either lumped or distributed. Physically-based, spatially-distributed modelling systems have particular advantages for the study of basin change impacts and applications to basins with limited records (Basson & Di Silvio, 2008). The capability to simulate land use changes by a model is significant where there is need to examine the effectiveness of applying site/sub-catchment specific soil conservation techniques within the watershed.

A considerable number of models have been developed over the years to simulate and predict flow processes and sedimentation loads in order to predict sediment yields from catchments. These numerical models have the ability to simulate spatial and temporal variation of sediment yields. The basic application of numerical models

requires information such as meteorological and topographical data as well soil properties and vegetation characteristics.

(b) Empirically based models

Empirically based models are derived from what is experienced or seen rather than on theoretical grounding of erosion and sediment processes. Empirical equations are developed using data collected from specific geographical areas; application of these equations should be limited to areas represented in the base data (Randle et al., 2006). Development of the equations mostly makes use of regression and statistical analysis Erosion and sediment yield in a catchment is determined by the following factors according to Strand and Pemberton (1982):

- Rainfall amount and intensity
- Soil type and geologic formation
- Ground cover and land use
- Topography
- Upland erosion rate, drainage network density, slope, shape, size, and alignment of channels
- Runoff
- Sediment characteristics-grain size, mineralogy, etc.
- Channel hydraulic characteristics

Few empirical methods have been developed to compute sediment yield as a function of the catchment area as explained in 3.3. The drainage characteristics are used in empirical relationships. However, it is mostly the Universal Soil Loss Equation (USLE) or its modified versions such as MUSLE that has been widely applied in most empirically based models.

The mathematical models have their algorithm for the computation of erosion and sediment yield based on the USLE parameters or its modified versions as explained in 3.1.5. The ACRU model (Agro hydrological modelling system of the Agricultural

Research Unit, South Africa) uses the Modified Universal Soil Loss Equation (MUSLE) for the estimation of sediment yield (Smithers et al., 2002).

(c) Physically based models

Physically-based models are based on physical and theoretical interrelationships between erosion and sediment yield controlling processes. They have the ability to simulate erosion and sediment yield both in time and space. The models give a detailed description in time and space of the flow and transport processes that are involved in erosion and sediment yield. Some of the available physically based models include: SHETRAN (Ewen et al., 2000) and Water Erosion Prediction Project (WEPP) (Nearing et al., 1989),

Other models include: Areal Non-point Source Watershed Environmental Response Simulation (ANSWERS) (Beasley et al., 1980), Hydrological Simulation Programme – Fortran (HSPF) (Bicknell et al., 1997), Chemicals, Runoff, and Erosion from Agricultural Management Systems (CREAMS) (Kinsel, 1980), Kinematic runoff and Erosion model (KINEROS) (Woolhiser et al., 1990) and European Soil Erosion Model (EUROSEM) (Morgan et al., 1998).

(d) Mixed empirical and physically based models

Mixed empirical and physically based models are based on both empirical and theoretical erosion and sediment yield processes.

3.4.2 ACRU and SHETRAN

The models that have been outlined in paragraph 3.4.1 were reviewed with respect to three major considerations: being applicable to relatively larger catchment sizes, ability to simulate erosion and sediment yield on a continuous basis and the ability to simulate wide range of land-use types and land cover.

Two models were selected for further evaluation namely ACRU and SHETRAN. A detailed evaluation of the relevant literature on SHETRAN will be presented in the following paragraphs.

SHETRAN, is a physically based, spatially distributed, hydrological and sediment yield modelling system applicable at the river basin scale (Ewen et al., 2000). It uses the application of physical and mathematical relationships by utilising internally coded equations and functions to simulate erosion, transport and sediment deposition processes in the catchment for both overland and channel flow.

The ACRU model gives event by event catchment sediment yield estimation by the application of Modified Universal Soil Loss Equation, MUSLE (Smithers, 2002; Williams, 1975). No detailed evaluation will be presented on ACRU but the main distinguishing factors and similarities of these two models will be presented in section 3.5.

3.4.3 The SHETRAN model

SHETRAN is characterised by its comprehensive nature and capabilities for modelling subsurface flow and transport (Ewen et al., 2000). The SHETRAN model uses a grid network to describe the catchment areas and links as river networks.

It is a three dimensional model that has a column of horizontal layers underlying each grid square in the vertical direction within each soil layer. The layers represent the soil thickness and the top layer surface represents the overland surface. Flow is routed from surface, subsurface and up to the channel or gullies (Ewen et al., 2000). According to Ewen et al. (2000), the three major components of the SHETRAN model responsible for physical process modelling are water flow, sediment transport and solute transport. Figure 3.4-1 illustrates the information exchange among the three components.

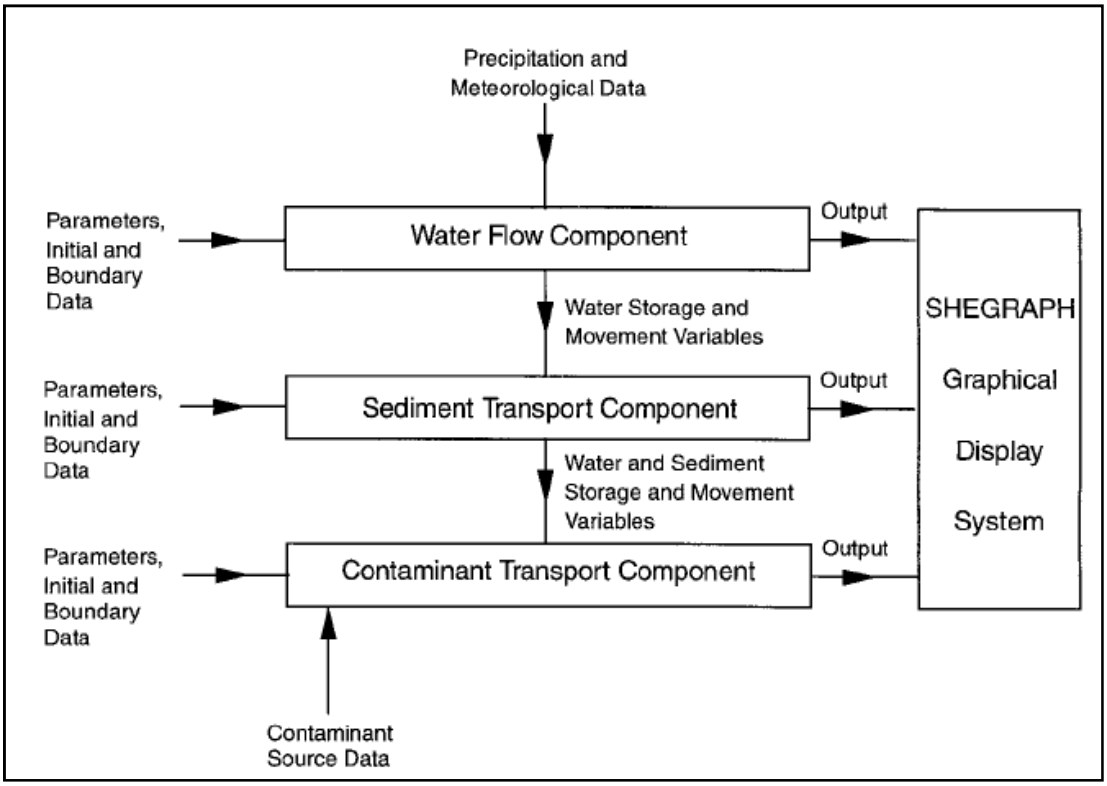

Figure 3.4-1 Information exchanges in SHETRAN (Ewen et al., 2000)

SHETRAN uses the following compulsory modules to run a basic simulation:

- Frame module - This module is the main body of the model and it contains input parameters that are generally shared among various and to allow all modules to perform coordinated activities.

- Evapo-transpiration module – This module calculates potential evapo-transpiration from vegetation, soil, and water surfaces; evaporation from wetted canopies, bare soil, dry channels, free water surfaces and also computes plant transpiration.

- Overland/channel module – This module computes the depth of surface water on the ground surface and in stream channels and calculates the flow of surface water across the ground surface and in channels.

- Variably saturated subsurface module – This modules simulates three dimensional flow of water in the subsurface soil scheme including seepage

The rest of the modules that are related to the sediment transport and contaminant transport component of the model are optional. These optional modules are: bank module, snowmelt module, sediment yield and contaminant transport module. For purposes of sediment erosion and transport modelling, the inclusion of the sediment yield module becomes a necessity. The erosion processes that can be modelled include the raindrop impact, leaf drip impact and runoff (both channel and overland flow).

The hydrological processes that are represented by SHETRAN are shown in Figure 3.4-2.

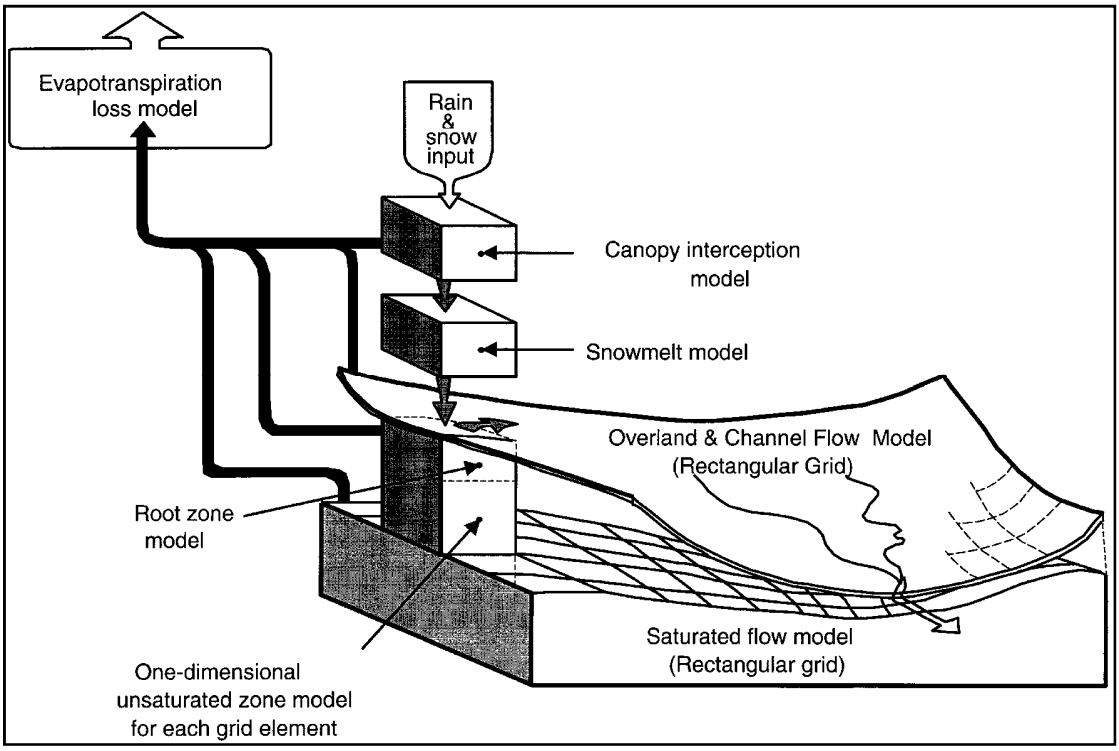

Figure 3.4-2 Schematic diagram of the SHETRAN hydrological component (Bathurst, 2002)

The model applies different equations to compute the above hydrological processes of evapo-transpiration, interception, infiltration, runoff and erosion (De Figueiredo, 2008). The Penman-Monteith equation is applied to compute evapo-transpiration. Interception of rainfall on vegetation canopy is based on Rutter storage model (1971/1972). The Boussinesq equation is applied for the two dimensional flow in the

saturated zone. One-dimensional flow in the unsaturated zone is based on the Richards (1931) equation.

Saint Venant equations (1871) are used for two-dimensional overland flow and one dimensional channel flow with respect to water depth and velocity. Only processes that are directly related to the erosion and sediment yield components of the model have been explained in detail in the following paragraphs below.

The sediment transport component of the model simulates soil erosion and transport on ground surface and in stream channels. The model computes the rate of detachment of soil by raindrop and leaf drip impact, rate of sediment detachment by channel and overland flow, sediment transport capacity for overland and channel flow, deposition, re-suspension/entrainment and infiltration of sediment.

The overland and channel flows are expressed by the following equations:

$$\frac{\partial(ch)}{\partial t} + (1-\alpha)\frac{\partial z}{\partial t} + \frac{\partial g_x}{\partial x} + \frac{\partial gy}{\partial y} = 0 \qquad \text{Overland flow} \qquad 3.3$$

$$\frac{\partial(Ac)}{\partial t} + (1-Ø)B\frac{\partial z}{\partial t} + \frac{\partial(AcV_s)}{\partial x} = q_s \qquad \text{Channel flow} \qquad 3.4$$

Where h is water depth (m), c is sediment concentration (m^3m^{-3}), α is the soil porosity (decimal fraction), g_x and g_y are volumetric sediment transport rates per unit width in the x,y directions respectively ($m^3s^{-1}m^{-1}$), t is the time (s), z is the depth of loose soil (m), A is the flow area (m^2), Ø is the channel bed porosity (decimal fraction), B is the channel bed width (m), V_s is the sediment velocity (ms^{-1}) and q_s is the sediment input from bank erosion and overland flow supply per unit channel length ($m^3s^{-1}m^{-1}$). Equations 3.3.and 3.4 have been adapted from De Figueiredo (2008).

Figure 3.4-3 shows the representation of the processes of soil detachment by raindrop and leaf drip impact, modified by ground cover, canopy cover and surface water layer in the SHETRAN erosion and sediment yield component.

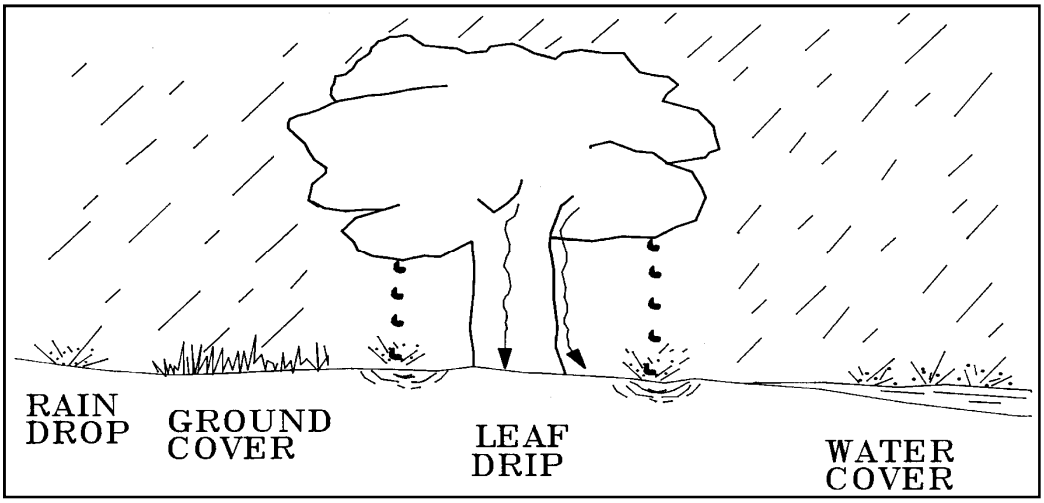

Figure 3.4-3 Soil detachment by raindrop and leaf drip impact (Bathurst, 2005)

The following equations are applied to compute soil erosion from raindrop and leaf drip impact and overland flow respectively (Bathurst, 2005):

For raindrop and leaf drip impact (Equation 3.5)

$$D_r=K_r F_w\left(1-C_g-C_r\right)(M_r+M_d) \qquad 3.5$$

For overland flow (Equation 3.6)

$$D_f = K_f(1-C_r)\left(\frac{T}{T_c}-1\right) \qquad T > T_c \qquad 3.6$$

Where

D_r and D_f = the respective rates of detachment of material per unit area ($\frac{kg}{m^2 s}$)

K_r = raindrop impact soil erodibility coefficient (J^{-1})

k_f = overland flow soil erodibility coefficient ($\frac{kg}{m^2 s}$);

C_g = proportion of ground protected from drop/drip erosion by near ground cover such as low vegetation

C_r = proportion of ground protected against drop/drip erosion and overland flow erosion by, for example, rock cover

M_r = momentum squared for raindrops falling directly on the ground ((kg m s^{-1}) m^{-2} s^{-1})

M_d = momentum squared for leaf drip ((kg m s^{-1}) m^{-2} s^{-1})

T = overland flow shear stress (N m^{-2}); and

T_C = critical shear stress for initiation of soil particle motion (N m^{-2})

The factor F_w accounts for the effect of a surface water layer in protecting the soil from raindrop impact (dimensionless).

Overland sediment transport uses the advection-dispersion equation (2D) with terms for deposition and erosion by raindrop and leaf drip impact and overland flow. Channel sediment transport applies the advection-dispersion equation (transport in network of 1D channels) with terms for deposition and erosion and for infiltration into bed (Wicks and Bathurst,1996). The Engelund and Hansen (1967) equation for total load or the Yalin (1963) bed-load formulae are used to compute transport capacity.

3.4.4 Selected SHETRAN modelling case studies

The following SHETRAN modelling case studies provide some of the specific model capabilities that have been confirmed by other users as reported in literature.

SHETRAN was applied and tested for the Waitetuna catchment (170km^2) in New Zealand (Schmidt, 2008). The model was set up and was altered to simulate different land-use scenarios in order to explore land-use impacts on sediment generation and to suggest catchment management alternatives. The land scenario was changed in two scenarios namely: completely under pasture and secondly completely converted back to native forest. The model managed to predict the adverse impacts that could have happened in the event of land use change to pasture in some of the sub-catchment.

It was then recommended, based on the model predicted results, that the critical sub-catchment should not be changed into pasture land but rather should remain under native forest. SHETRAN's ability to predict the impacts of possible future climate change on runoff and sediment yield was demonstrated in an application to the 701km^2 Cobres basin in Portugal (Bathurst et al., 1996). This demonstrates the

advantage of using SHETRAN an erosion and sediment yield model in the wake of current climate change issues.

SHETRAN basin-scale, landslide erosion and sediment yield model was applied to simulate a major landsliding event in the upper 505 km^2 of the Llobregat basin, in the eastern Spain, in November 1982.
The model simulated sediment yield that was estimated at 2670–14630 t/km^2 demonstrated the ability of SHETRAN to simulate the basin-scale landslide response to a rainfall event (Bathurst, 2006).

According to Birkinshaw (2006), the SHETRAN model was also used to study the relationship between sediment yield and basin area. Such results are important in the determination of the increase or decrease in the sediment yield when the catchment area increases in size.

3.5 General comparative analysis of SHETRAN and ACRU models

The SHETRAN model capabilities were compared with ACRU after a review and investigation of the SHETRAN model as explained in this thesis and the experience gained from using the ACRU model.

Table 3.5.1 ACRU and SHETRAN comparative analysis

Parameter	**ACRU**	**SHETRAN**
Rainfall Daily Input	Uses daily data	Uses hourly data
Spatial distribution of data	GIS raster	Grid squares and links
River/channel sediment routing	No channel or river sediment is routed	Channel sediment can be routed including estimation of the proportion of sediment coming from channel erosion
Discharge data output	Daily	Both hourly and daily

Sediment particle distribution	All sediment are routed as a single load	Has the ability to give results indicating the proportion of the amount sediment of a specific sediment size group
Output of water depths and water tables	Only soil water content results can be generated	Can provide data on sub-surface and surface levels for water in the soil
Sediment process routing method	Uses MUSLE	Uses empirical mathematical equations from literature that describe physical characteristics of flow and land interaction that result in erosion, transport and sediment deposition
Temporal variation in sediment yields	Capable of generating time series of flow	Capable of generating time series of flow
Typical Maximum catchment size (km^2)	10000	2500
Land use change simulation	Y	Y
Overland flow: Rainfall Excess	Y	Y
Overland flow: Upward Saturation	Y	Y
Erosion process: Raindrop impact/Overland flow	Y	Y
Erosion Map	Y	Y
Erosion process: Rilling	Y	N
Erosion process: Crusting	Y	N
Erosion process: Gullying	N	Y
Erosion process: Channel banks	N	Y
Erosion process: Land sliding	N	Y
Land Use	Mainly agricultural	Most vegetation types

4.0 CURRENT SEDIMENT YIELD PREDICTION APPROACHES IN SOUTH AFRICA

4.1 Background

Several methods are applied to predict the sediment yield of a watershed. The common method (in addition to direct measurements) that has mostly been applied in South Africa for estimation of sediment yield has been the application of the sediment yield maps (Rooseboom et al., 1992).

The sediment yield map and the accompanying probabilistic approach was developed using data from observed sediment yields and catchment erodibility.

Three main techniques have been widely applied in the prediction and estimation of sediment yield in South Africa. The methods include use of sediment yield maps, reservoir deposit data and sediment load-discharge rating curves.

4.2 Sediment yield maps

This methodology was developed by Rooseboom et al. (1992). It was developed based on data from erodibility maps, statistical analysis of observed sediment yield values obtained from reservoir survey data and river sampling, location and size of catchments and other information on relevant geographical and environmental factors that were deemed to have significant influence on erosion and sediment yield in a catchment.

The whole of Southern Africa was divided into regions of relatively uniform yield potential to minimise the effect of high sediment yield variability at national scale. To determine the regions, the following important factors were considered: soil erodibility with respect to soil type, catchment slopes and land use, availability of sufficient recorded sediment yield data to make meaningful statistical analysis per region, boundaries of river catchments and rainfall characteristics.

A total of nine main regions were delineated across Southern Africa. The nine regions were further divided into areas with higher, medium and lower sediment yield potential shown on an erodibility index map. The methodology is based on the assumption that the ratio between the observed sediment yields is constant for higher, medium and lower sediment yield potential areas.

The detailed approach that is followed when predicting sediment yield using the sediment yield maps include:

(a) The region in which the required catchment falls is determined. A map indicating the three sediment yield potential classes is used to determine the areas covered by the three sediment yield potential classes in the required catchment. Figure 4.2-1 shows the erodibility index map and regions.

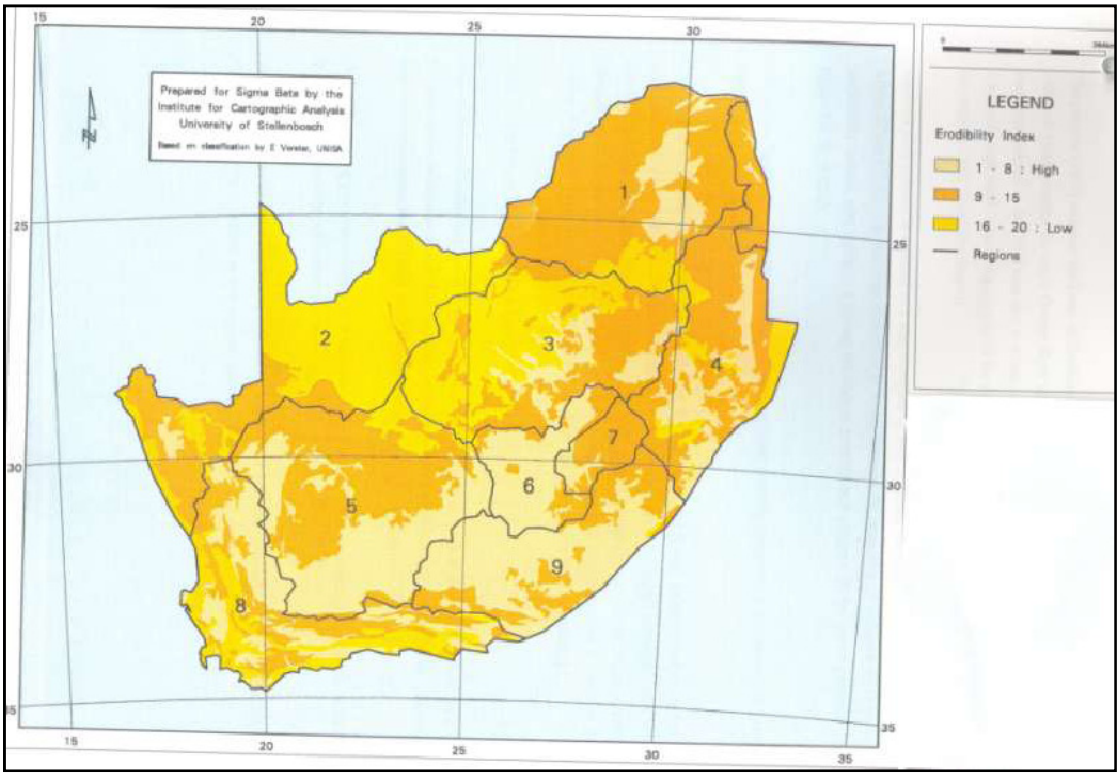

Figure 4.2-1 Erodibility indices and sediment yield regions

(Rooseboom et al., 1992)

(b) Table 4.2-1 is used to obtain mean standardised sediment yield values for any of the regions under consideration. It also gives the sediment yield factors for each region.

Table 4.2.1 Factors for converting standardised yield values to site-specific values (Rooseboom et al., 1992)

Region	Standardised average yield ($t/km^2.a$)	Sediment yield factors		
		F_H	F_M	F_L
1	49	2.23	1	0.92
2	N/A	N/A	N/A	N/A
3	82	1.87	1	0.35
4	155	1.44	1	0.18
5	30	2.69	1	N/A
6	335	1	1	N/A
7	203	N/A	N/A	1
8	35	1	1	0.23
9	185	1	1	N/A

(c) Confidence bands curves as shown in Figure 4.2-2, give a multiplication factor for the required confidence band in relation to the catchment area. The multiplication factors are multiplied with the regional average standardised sediment yield.

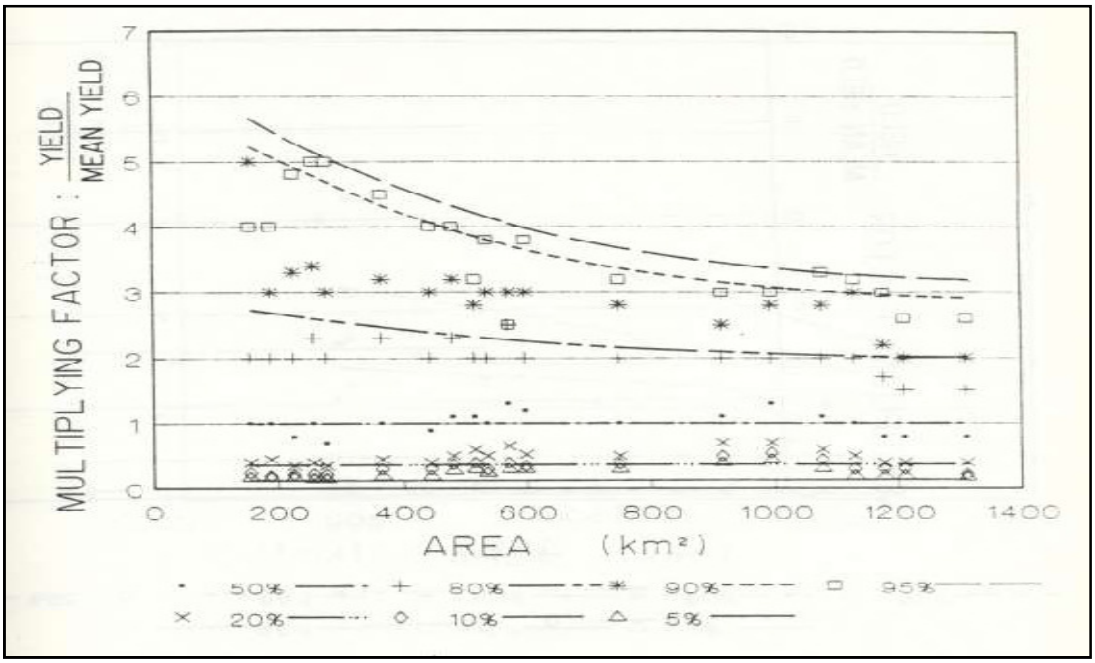

Figure 4.2-2 Confidence Bands (Rooseboom et al., 1992)

(d) Equation 4.3-1 is used to estimate the sediment yield of an ungauged catchment.

$$Y_C = Y_S \left[F_H \frac{A_H}{A_T} + F_M \frac{A_M}{A_T} + F_L \frac{A_L}{A_T} \right] \quad 4.3.1$$

Where:

Y_C = Estimated catchment sediment yield value (t/km^2.a)
Y_S = Standardised average yield (t/km^2.a)
F_H = High yield potential factor (from Table 4.2.1 above)
F_M = Medium yield potential factor (from Table 4.2.1 above)
F_L = Low yield potential factor (from Table 4.2.1 above)
A_H = Size of area consisting of soils with high sediment yield potential
A_M = Size of area consisting of soils with medium sediment yield potential
A_L = Size of area consisting of soils with low sediment yield potential
A_T = Total catchment area (km^2)

4.3 Reservoir sediment deposit data

It is possible to calculate the sediment yield from reservoir deposit data. In semi-arid regions that have high rainfall intensity, the storage capacity of a reservoir is usually in the order of the mean annual runoff and the reservoirs therefore trap approximately 97% of the sediment yield (Basson, 2008). Therefore the loss in storage is taken as a true reflection of sediment accumulation.

Any reservoirs whose trap efficiencies fall below the required percentage of 97% cannot be used in the determination of the sediment yield because of the unreliable sediment deposit data.

The data on sediment deposit in reservoirs is obtained from the Department of Water Affairs or a re-survey can be done. Sediment volumes are calculated from the analysis of the observed decrease in the reservoir storage volume during re-surveys with respect to previous surveys or initial volume at commissioning.

An equation proposed by Rooseboom (1992) below is used to compute the equivalent fifty (50) year sediment volume, based on the sediment volume after a known period, preferably after 10 or more years.

$$\frac{V_t}{V_{50}} = 0.376 ln \frac{t}{3.5} \qquad 4.3\text{-}2$$

Where

V_t = sediment volume after t years.
V_{50} = sediment volume after 50 years.
t = time (years).

The sediment yield S_y is then computed using the equation 4.3.3.

$$Sy = \frac{1.35 \times V_{50}}{50 \times A_e} \qquad 4.3.3$$

Where

Sy = Sediment yield in tonnes per annum per square kilometre
A_e = Effective Catchment Area

After 50 years of deposition, the sediment density is used as 1.35t/m^3.

4.4 River sediment sampling

Sediment yield can be determined from the cumulative plots of observed sediment load versus cumulative water discharge. The plot shows that the graphical relationship between cumulative sediment load and cumulative water discharge at a location along a river reach with the sediment yield being given by the slope of the curve. A sample plot of a cumulative sediment load versus discharge on the Orange River in South Africa is given in Figure 4.4-1 (Rooseboom et al., 1992).

Another direct measurement method of determining sediment yield is river water sampling. In this method, the rate of sediment transport expressed as either a sediment discharge (total load) or sediment concentration is presented as a function of water flow discharge and plotted on a graph which is termed “sediment rating curve”. The total load constitutes both bed load and suspended sediment.

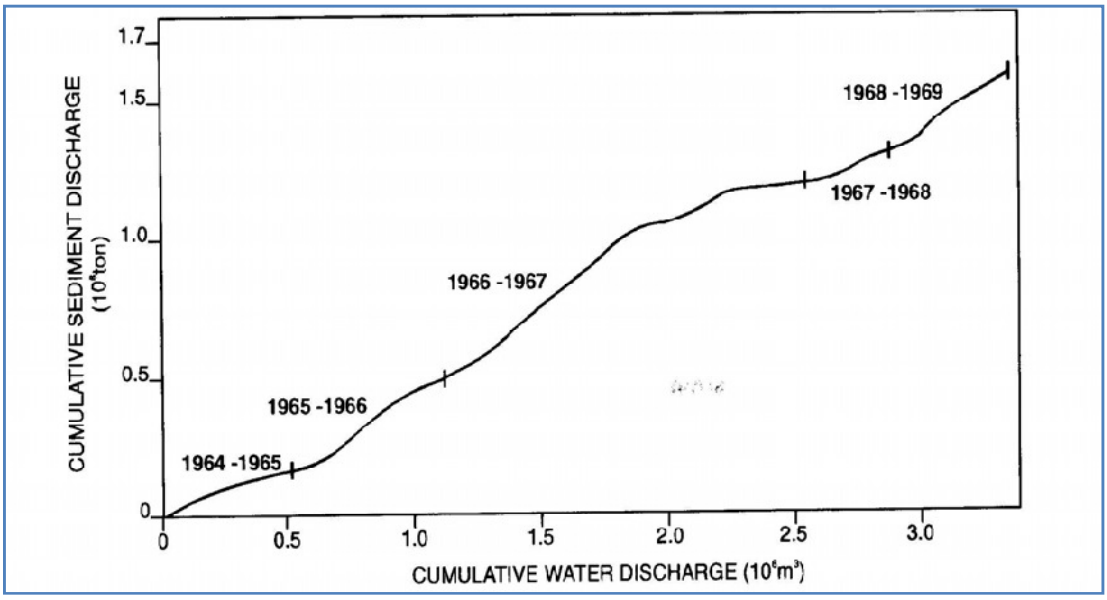

Figure 4.4-1 Cumulative sediment load versus discharge on the Orange River in South Africa (Rooseboom et al., 1992)

However, according to Basson (2008) bed sediment loads are difficult to obtain mostly due to too high flow velocities and large bed dunes that are encountered during sampling. In this case, a factor of 1.25 has often been applied to suspended sediment grab sample data to take into account the bed load and non-uniformity in suspended load across the river where the calculation of the bed load component is not possible (Rooseboom et al., 1992). The concentrations are related to the discharge in order to get the sediment load. The sediment rating curve method is very reliable for the determination of the sediment yield when there is good correlation between the observed discharge and sediment loads/concentration, a sufficiently long period of sampling is available and large infrequent floods are considered.

5.0 NEW PROBABILISTIC AND EMPIRICAL APPROACHES FOR SEDIMENT YIELD PREDICTION

5.1 Introduction

The current sediment yield prediction methods have been applied with success. However, there is a need to improve the previous sediment yield maps methodology. This is justified by the fact that there has been an increased availability of additional sediment yield data since the previous report (Rooseboom et al., 1992) was prepared and the need to incorporate current technological advancements in sediment yield methods.

An empirical method was also investigated to predict the sediment yield based on the unit stream power theory. The probabilistic approach was based on the analysis of newly calculated sediment yield data and revised erosion hazard maps. The empirical approach was based on the relationships established from the observed sediment yield and the selected variables that have a marked effect on the expected sediment yield in a given homogeneous region.

5.2 Sources of Information

The observed sediment yields were obtained from two types of data sources. These sources are reservoir survey data and river suspended sediment sampling data. Reservoir survey data provided information on reservoir deposit sediment volumes.

The sediment yield calculation method that makes use of reservoir deposit data is based on the general concept that any reduction in storage volume of a reservoir that is observed through reservoir surveys is directly related to the amount of sediment being accumulated in the reservoir. The sediment yields had to be recalculated in order to incorporate added data since the preparation of the 1992 sediment yield maps (Rooseboom et al., 1992).

The reservoir survey data was obtained from the Department of Water Affairs (DWA) dam list of 2006 and individual reservoir survey reports. The DWA dam list provided most of the historical information on surveyed and re-surveyed reservoirs

and dams such as: the name of the dam, height at full supply level, survey dates and the period (in years) between the surveys and re-surveys with their corresponding storage volumes at the time of surveying.

The erodibility indices were obtained using the Revised Universal Soil Loss Equation (RUSLE) erosion factors processed in a Geographical Information Systems (GIS) framework. The main input parameters in the GIS framework comprised maps showing the following erosion factors: rainfall erosivity, soil erodibility, topography factor and cover factor (Basson et al., 2009).

5.3 Quality of data, analysis and validation

The criteria for the analysis of the validity of the data in order to ensure its integrity were based on the following considerations:

- Records or period between surveys to be longer than ten (10) years
- Reliable high reservoir sediment trap efficiency (at least 97% and above)
- Raised or lowered dams

In order to determine reliable sediment yields, the raw data for individual dams was analysed based on these considerations. This resulted in the reduction in the number of dams.

Raised and lowered dams whose sediment volumes could not be reliably determined from the net cumulative sediment curves were also discarded. The reservoir storage volume during the original and/or preceding surveys was supposed to be reliable and not be significantly affected by possible raising and lowering of the dam.

5.3.1 Mean Annual Runoff and Trap Efficiency

The Mean Annual Runoff (MAR) was applied in the determination of the trap efficiency. The trap efficiency of a reservoir is defined as the ratio of the quantity of sediment deposited with respect to the total sediment inflow (ICOLD, 1989). Not all sediment passing through a reservoir is trapped. The quantification of the amount of

sediment trapped with respect to what passes into the reservoir is termed 'the trap efficiency'. In order to ascertain the 'trap efficiency' for each of the dams under consideration, the MAR had to be determined. The trap efficiency is indicated by the ratio of the storage volume (V_W) against the MAR of the reservoir. The MAR was acquired from maps and appendices obtained from the Surface Water Resources of South Africa 1990 (WR90) (Midgley et al., 1994).

The MAR of any catchment area was calculated from the summation of individual MARs of each of the quaternary sub-catchments forming the whole catchment area under consideration based on the MAR value given for uniquely coded quaternary sub-catchment as illustrated in Figure 5.3-1 extracted from WR90 (Midgley et al., 1994).

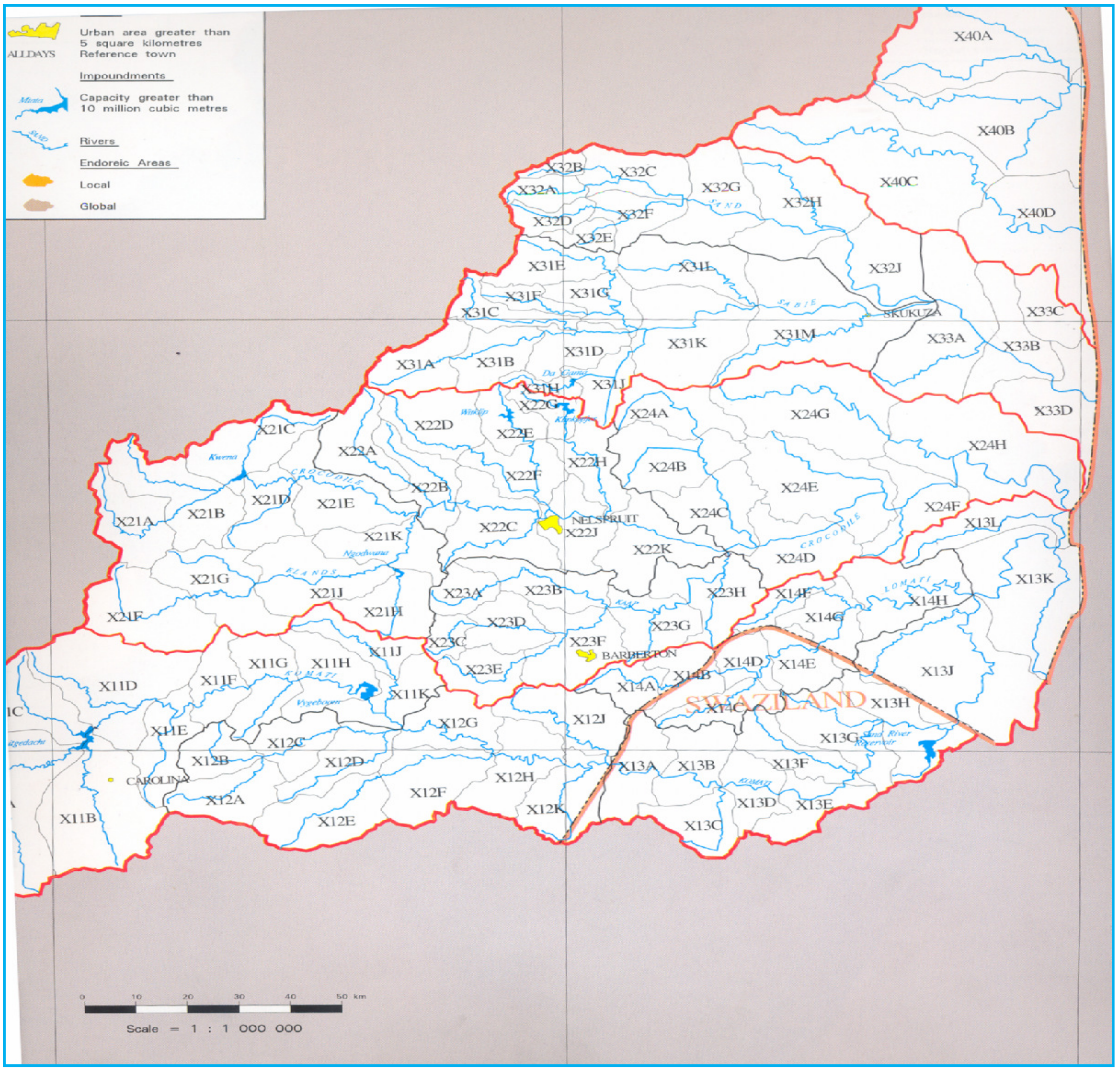

Figure 5.3-1 Sub-quarternary and quarternary sub-catchments for MAR computation (Midgley et al., 1994))

5.3.2 Effective Catchment Area

The effective catchment areas were generated by GIS. The effective catchment area (A_e) refers to the significant area for a reservoir or a dam as regards to the computation of the sediment yield particularly where there is another dam falling within its gross catchment area. The effective catchment area is therefore that part of the total drainage area upstream of a dam that contributes to the sediment being deposited in a reservoir.

The MAR is directly related to the total catchment area above a point of reference for a dam. While the sediment yield is computed using the effective catchment area. The general approach is based on the assumption that the sediment that accumulate in a reservoir are produced from the effective catchment in particular cases where there is another dam upstream which is relatively large and has a reliable high reservoir sediment trap efficiency since all sediment resulting from the upstream drainage area are trapped by the upstream dam, while the water inflow into a reservoir comes from the total drainage area upstream.

In the sediment yield computation, the area to be used depended also on the period during which the dams upstream (if any) became operational. In other words; where there was a dam upstream which became into operation at a later stage outside the survey data period, the total area during the period of no dam upstream was used instead of the effective catchment area.

5.4 Determination of sediment yields from reservoir sediment deposit data

The detailed information that was needed in the estimation of the sediment yield from reservoir sediment deposit data included the following:

- Name and reference code of the dam
- The heights at full supply level during recorded surveys.
- The storage volumes.
- The year in which the dam became operational

- The mean annual runoff
- The catchment area and sediment density

The reservoir survey data was used to determine the quantity of sediment deposited in the reservoir by way of comparing the water storage volume changes between two or more successive surveys. A similar procedure as explained in section 4.3 was used to compute the sediment yield by employing equations 4.3-2 and 4.3-3.

Graphical analysis was applied when the available data was enough to predict the volume of sediment in the dam after or at fifty (50) years from a graph as illustrated in Figure 5.4-1. A logarithmic trend line was fitted through the data points because of the assumption that a logarithmic relationship exists between sediment deposit volume and time (Rooseboom et al., 1992) and the use of an average density of sediment after fifty years. This is due to the consolidation characteristics of fine sediment (clay and silt). In the case of Olifantsnek Dam the volume at fifty years could be read from the graph as shown by arrows in Figure 5.4-1 or by calculating it using the trend line equation.

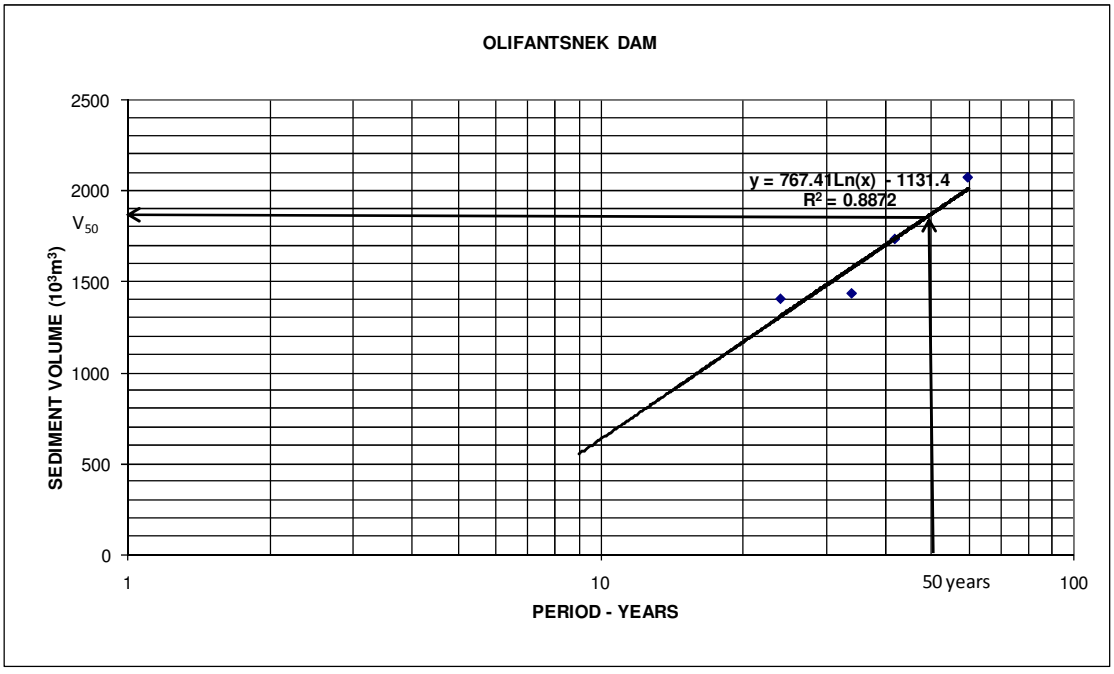

Figure 5.4-1 Graphical analysis of the sediment volume after fifty years

A number of dams that were once raised or lowered have had their sediment yield converted from sediment deposit data. The detailed calculations of the sediment volume at fifty (50) years for raised and lowered dams did not follow the normal summation method of sediment volume in a dam, but rather a cumulative sediment volume was plotted from the dam's data where possible.

This is illustrated by an example of Grassridge Dam (a case of a raised dam) whose tabular presentation of sediment deposit data is shown in Table 5.4.1.

Table 5.4.1 Grassridge Reservoir deposit data

Grassridge Reservoir Deposit Data			
Year	Vol ($10^6 m^3$)	Height at FSL (m)	Gauge Plate (m)
1924	77.55	1056.93	14.05
1931	70.20	1056.93	14.05
1935	59.80	1056.93	14.05
1946	51.90	1056.93	14.05
1948	60.86	1057.84	14.96
1952	59.00	1057.84	14.96
1966	58.40	1057.84	14.96
1975	53.78	1057.84	14.96
1984	49.58	1057.84	14.96
2000	46.20	1057.84	14.96

This resultant graphical plot of the cumulative sediment yield in the reservoir is shown in Figure 5.4-2. This graph was used to calculate the sediment volume at fifty years.

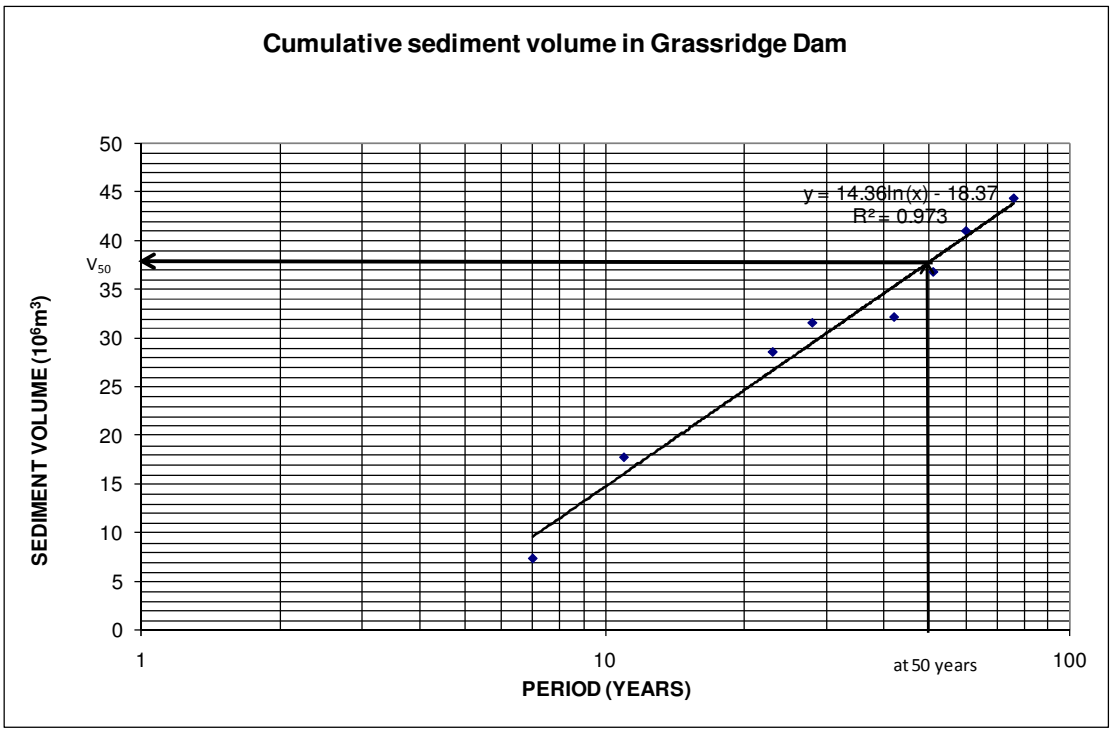

Figure 5.4-2 Cumulative sediment volume in Grassridge Reservoir

In the event that this approach could not be carried out with greater reliability, a raised or lowered dam was discarded. A reliable cumulative sediment volume graph was taken as the one that gave the required sediment volume at fifty years depending on its observed regular pattern and number of data points.

There were notable differences in the newly calculated sediment yields for similar dams in comparison with those of the 1992 sediment yield map (Rooseboom et al., 1992). This was expected and could be accounted to the following factors:

- Normal changes in sediment transport trends and behaviour with time that might happen in a drainage area that were not captured by previous surveys.
- Increased dam survey data for the dams from additional bathymetric re-surveys

Some of the newly calculated sediment yields were higher for similar dams when compared with those of the 1992 sediment yield map (Rooseboom et al., 1992) and vice versa. Analysis of the overall trend in the sediment yields showed that the newly calculated sediment yields are comparatively higher. It was concluded that sediment production is not reducing in South Africa.

5.5 Calculation of sediment yields from river suspended solids data

Where possible, the sediment load at a gauging station could be determined from river suspended solids data. The Department of Water Affairs historical flow records for approximately two hundred (200) gauging stations were obtained. The major problem was that the sediment data sets were for short periods and not representative enough to be considered as reliable. The sediment load was computed from the relationship between the suspended solid concentration and the discharge.

The sediment load was determined from the trend line of the relationship between the suspended sediment concentration and discharge. The mean annual sediment load was found by applying a factor of 1.25 to cater for bed load (Rooseboom et al., 1992). Out of 200 gauging stations, only eight stations could have their sediment load reliably determined because of inadequate suspended solid concentration data (short record).

5.6 Probabilistic sediment yield prediction methodology

The probabilistic approach was based on the previous report's fundamental assumptions of Rooseboom et al. (1992).

The main underlying assumption is that sediment transport is influenced by sediment availability and in turn sediment availability is influenced by soil erodibility or soil erosion hazard. This was rather a crude assumption considering the dominant role of other significant sediment controlling factors that could also affect the sediment yield. The probabilistic analysis approach used the following data: dam and river catchment areas, erosion hazard classes and observed sediment yields per region (from reservoir sediment deposit data and river suspended sediment data) whose acquisition and processing has been explained in detail in the preceding paragraphs.

5.6.1 Demarcation of new regions

The current identification and demarcation of the new regional boundaries was based on the latest calculated sediment yields and soil erosion data, including the latest

water erosion prediction map of South Africa (Le Roux et al., 2008), hydrological parameters such as watershed quaternary boundaries and flood regions. The regional demarcation was necessitated by the need to have relatively homogeneous regions. According to Rooseboom et al. (1992), the geographical considerations and the availability of data played a role in determining the boundaries of the homogeneous regions.

Selection of the new boundaries for sediment yield regions was based on similar considerations. The availability of adequate sediment yield data for analysis was based on the number of observed sediment yields within a proposed sediment yield region. A map showing observed sediment yield by catchment for the whole of Southern Africa was created in GIS. The soil erosion data was prepared in GIS on a map of Southern Africa showing ten erosion hazard classes. The erosion hazard classes were based on the improved water erosion, cover-factor and topography-factor maps of Southern Africa. The new water erosion prediction map is based on a simplification of the Revised Universal Soil Loss Equation (RUSLE) (Renard et al., 1994). The flood regions were based on the homogeneous flood regions shown in the Drainage Manual (SANRAL, 2006).

A total of nine new homogeneous sediment yield regions were identified. Figure 5.6-1 shows the previous sediment yield regions (Rooseboom et al., 1992) and the new sediment yield regions. Appendix A shows the erosion hazard classes for each of the new sediment yield regions.

The new boundaries for sediment yield regions were traced manually on a map showing observed sediment yields for river gauge and dam catchments, rivers and drainage regions. Manual overlay of the erosion hazard map (Le Roux, 2008) and the homogeneous flood regions map (SANRAL, 2006) was done using transparent paper to capture homogeneous flood regions and erosion hazard areas. The availability of adequate data for analysis was done by manual computation of the number of observed sediment yields falling in a proposed sediment yield region. The manually demarcated sediment yield regions were electronically delineated using GIS.

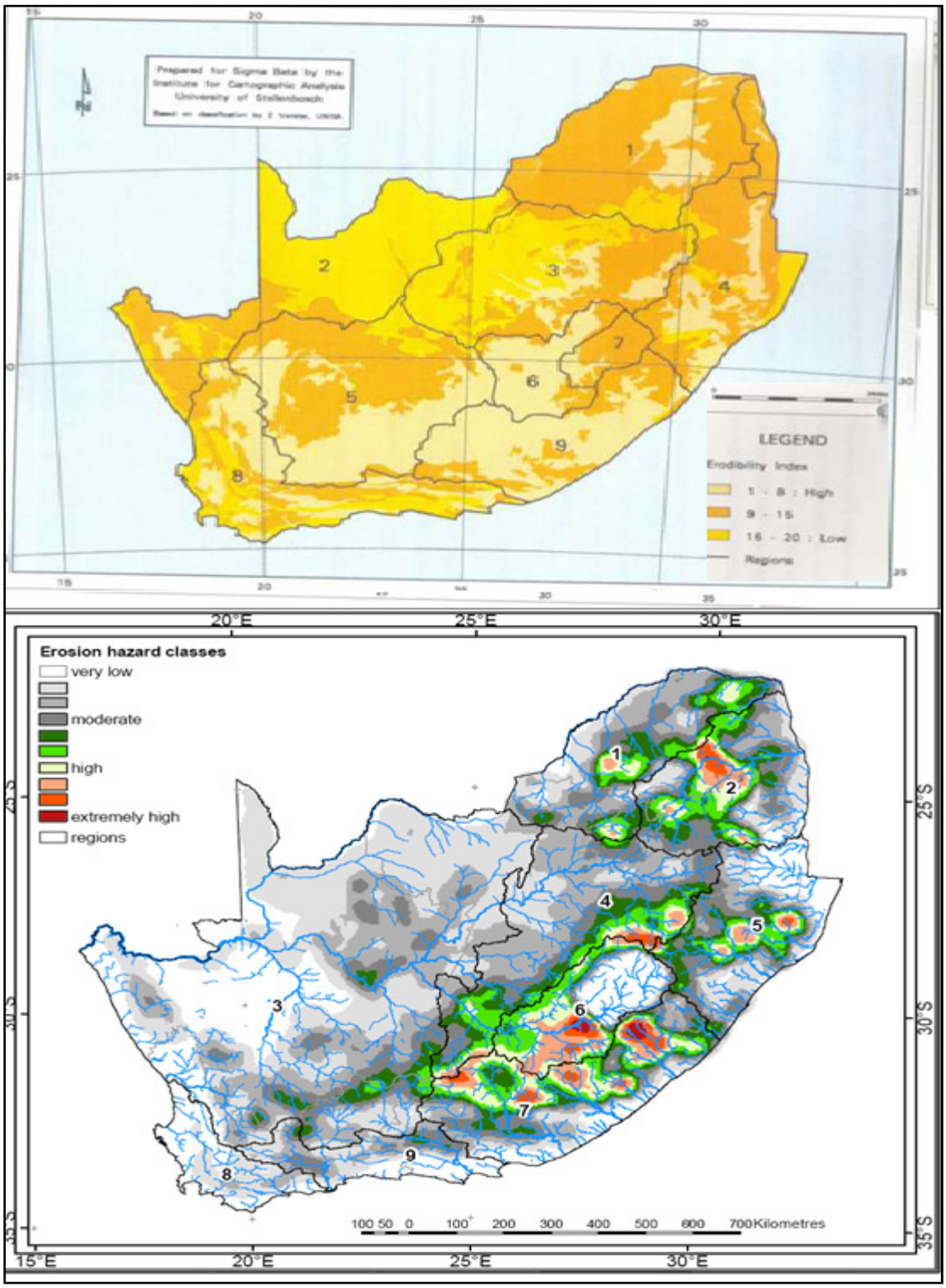

Figure 5.6-1 Previous (top) (Rooseboom et al., 1992) and current sediment yield regions (bottom) showing erodibility indices and erosion hazard classes respectively

Upon demarcating the regions, attention was focused on the determination of the correlation between the RUSLE generated average erosion rates (from the improved erosion map) against the observed sediment yield. This was done to determine the relationship between RUSLE based average erosion rates and the observed sediment yields. This relationship was expected to be used for further prediction of sediment yield in ungauged catchments based on average erosion rates.

Analysis of data (see Figure 5.6-2) was carried out by means of statistic functions in a GIS (ArcMap) and correlation graphs (Le Roux, 2009). For each catchment with an observed sediment yield, the soil erosion based on RUSLE in tonnes/ha/annum was computed using a GIS spatial data statistical analysis tools. The erosion rates in tonnes/ha/annum were converted into sediment yields in t/km^2.a. The observed sediment yields were plotted against the RUSLE simulated sediment yields for each region.

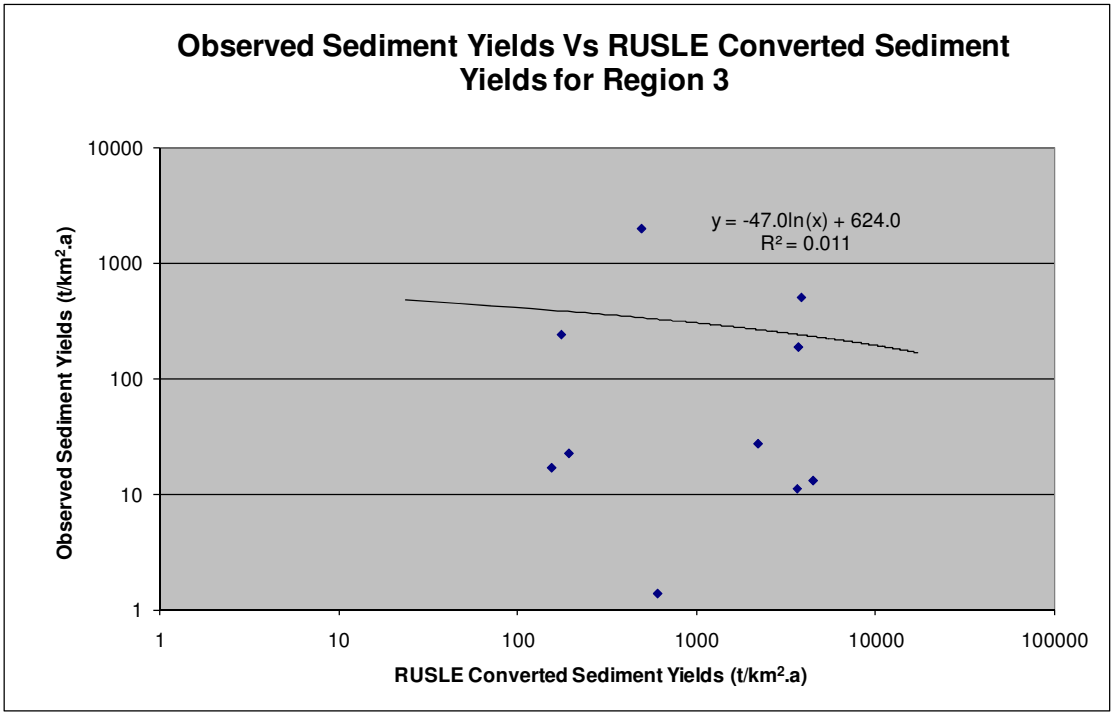

Figure 5.6-2 Observed sediment yields vs. RUSLE simulated sediment yields for Region 3

Analysis of the results as illustrated in Figure 5.6-2 (for Region 3) indicated very poor correlation between the mean erosion rates and observed sediment yields. The other sediment yield regions had poor results, which were also characterised by very low r-square values. According to Le Roux (2008), the main reason for the failure of

the correlation of erosion loss rates and observed sediment yield could be that the mean net soil loss (i.e. the sediment yield at the outlet) in a catchment is bound to differ from the mean total soil erosion (i.e. the total sediment produced in the catchment) due to varying delivery and deposition trends in the catchment that depend on specific catchment characteristics which are highly variable.

Consequently, an attempt to correlate the average erosion loss rates and sediment yield was discontinued. The development of an erosion risk database at national scale for South Africa in the form of erosion hazard classes was pursued. This was used in the development of the probabilistic method.

5.6.2 Erodibility indices and sediment yield regions

The erodibility index represents the relative ability of earth material to resist erosion (Annandale, 1995). Ten erosion hazard classes were identified using GIS spatial data analysis based on the RUSLE. The water erosion prediction map of South Africa was generated from a combination of the effect of cover and crop management factor "C' and physical soil erosion contributing factors of rainfall erosivity, soil erodibility, topography and vegetation cover. According to Le Roux et al. (2006), RUSLE groups the many influences on the erosion process into five categories comprising climate, soil profile, relief, vegetation and land use and land management practices. The categories are known as erosion factors indicated by R, K, LS, C and P respectively. The RUSLE model is expressed by equation 5.1 (Renard et al., 1994):

$$A = R.K.L.S.C.P \qquad 5.1$$

Where

A = Expected annual soil loss (tonnes ha^{-1} yr^{-1})

R = Rainfall erosivity in (MJ mm ha^{-1} h^{-1} yr^{-1})

L and S = Topographic factors that describe hill slope length and hill slope steepness (dimensionless) respectively

K = Soil erodibility in (Mg ha h ha^{-1} MJ^{-1} mm^{-1})

C and P = cover-management practices and support practices' factors that describe land use respectively

The four major factors of rainfall erosivity, topography, soil erodibility and land cover were calculated from new maps generated in GIS framework using improved input data.

These erosion hazard classes were classified in terms of an index scale of one to ten for the whole of southern Africa whereby Class 1 is very low erosion hazard and Class 10 is extremely high erosion hazard. The proportion of area covered by specified hazard classes per catchment was calculated for all the dam and river catchments using GIS-based spatial analysis tools.

For example, the total effective catchment area of Albasini Dam in Region 1 was computed as 501km^2. Out of this total area; 145 km^2 falls under erosion index 4, 352 km^2 falls under erosion index 5 and 4 km^2 is covered by erosion hazard class of index 5. A weighted average was calculated to provide a single dominant erosion hazard class per catchment based on the proportionate areas. The computation of a single dominant erosion hazard class was done for all river and dam catchments which had an observed sediment yield. For the purpose of the probabilistic analysis, each observed sediment yield was associated with its corresponding dominant erosion hazard class. The weighted average erosion hazard class was converted to the nearest integer in the range of 1 to 10 to provide a single hazard class per catchment.

5.6.3 Probabilistic analysis of observed sediment yield data

The probabilistic analysis was done using the following types of data:

(i) Dam and river catchment area sizes and proportionate areas covered by each soil erosion hazard potential index
(ii) Observed sediment yields per region

The final data set for the observed sediment yields per region is attached in **Appendix B.**

Each observed sediment yield value had a corresponding dominant erosion hazard class. The dominant erosion class was then linked to its sediment yield value for further probabilistic analysis. The previous probabilistic approach (Rooseboom et al., 1992) had three erodibility indices. The probabilistic approach in this thesis has applied ten indices (referred to as erosion hazard classes) in order to improve the classification. For each dam and river catchment, the dominant erosion hazard class was recorded. Appendix C gives the data for the computation of the dominant erosion hazard class per catchment and the determination of potential factors for Region 7. A summary of the results in Appendix C is given in Table 5.6.1. The sediment yield values for dam and river catchments with similar erosion hazard class were grouped together.

Table 5.6.1 Computation of sediment potential factors

	Erosion Hazard Class									
	1	2	3	4	5	6	7	8	9	10
Group of Observed Sediment Yields ($t/km^2.a$)	1509	840	158	210	262	219	558	617		
	193	306	4	37	12	378	279	888		
	106	95	156		589	19	209	207		
		49	136				152			
							236			
Median	193	200	146	123	262	219	236	617		
Standardised Average Yield ($t/km^2.a$)	209	209	209	209	209	209	209	209		
Sediment Potential Factor	0.923	0.958	0.698	0.589	1.255	1.049	1.129	2.952		

The median values for the sediment yield values with similar dominant erosion hazard class were computed as shown in Table 5.6.1. The similar procedure as shown in Table 5.6.1 for region 7 was done for all the sediment yield regions to determine the sediment potential factors given in Table 5.6.2

The main assumption in the analysis was that the standardised average yield (taken as the sediment yield at 50% exceedance probability) for each region is related to the median of each group of observed sediment yield with similar dominant erosion hazard class in a region. The relationship is indicated by the ratio of the median values and the standardised average yield which is termed “sediment potential factor”

(see Table 5.6.1). The sediment potential factors for each of the sediment yield regions are shown in Table 5.6.2.

The observed sediment yield values for each of the nine regions were then plotted on a probability graph to determine their distribution.

The following logarithmic distributions were investigated to select the distribution that would best fit the data.

(i) Log Normal Distribution
(ii) Log Pearson Type III Distribution
(iii) General Extreme Value Distribution (Using Mean Moments)
(iv) General Extreme Value (using Probable Mean Moments)

The logarithmic distributions were chosen because they were found to give good results when fitted to sediment yield data (Rooseboom et al., 1992). The final adopted graphical distribution depended on the distribution that fitted the data well. The observed data was plotted on the electronic probability paper in Microsoft Excel whereby the observed sediment yield values were on the vertical axis and probability values on the horizontal axis. The Cunnane plotting position was used. The Log Pearson Type III Distribution was found to give better results for the data in regions 1 and 8. The Log Normal distribution was found to be best suited to data for regions 2, 3 and 6. In regions 4, 5, 7 and 9, the data was fitted with a distribution line between the Log Normal and Log GEV_{mm} distributions in order to achieve a better fit.

Appendix D shows the various distributions that were plotted using the observed sediment yields for all nine sediment yield homogeneous regions. The sediment yield value at 50% probability of exceedance as read from the regional distribution plot was taken as the standardised average yield given in Table 5.6.2 for that region.

Table 5.6.2 Sediment potential factors

REGION	Standardised Average Yield ($t/km^2.a$)	SEDIMENT POTENTIAL FACTORS									
		F_1	F_2	F_3	F_4	F_5	F_6	F_7	F_8	F_9	F_{10}
1	73	0.000	0.000	0.638	1.511	0.997	1.504	1.755	0.000	0.000	0.000
2	73	0.000	4.984	2.977	1.043	0.513	1.000	0.438	1.236	0.000	0.000
3	33	0.033	0.501	1.445	1.334	0.778	0.000	0.000	0.000	0.000	0.000
4	102	0.000	2.202	0.781	1.104	2.974	0.827	0.941	0.623	1.081	0.000
5	241	0.000	0.415	1.580	0.503	2.374	1.322	0.844	3.139	0.000	0.000
6	621	0.000	0.000	0.000	0.000	0.000	0.859	1.044	1.171	0.000	0.000
7	209	0.923	0.958	0.698	0.589	1.255	1.049	1.129	2.952	0.000	0.000
8	103	0.672	1.334	0.423	0.000	0.000	0.000	0.000	0.000	0.000	0.000
9	53	0.184	1.719	2.076	0.000	0.000	0.000	0.000	0.000	0.000	0.000

F_n Sediment potential factor for erosion hazard class n (n = 1 to 10) obtained using the procedure outlined in Table 5.6.1

5.6.4 Multiplication factors, confidence intervals and limits

The distribution that fitted the regional observed data well as described in section 5.6.3 was used for the determination of the confidence limits. The confidence limits are required to act as envelope values on the regional standardised average sediment yield. The standardised average yields were obtained from the probability distribution graph at 50% exceedance probability. A 50% exceedance probability indicates that 50% of the predicted values could be lower or 50% of the predicted values could be higher. By default a multiplication factor of 1 is applied at 50% probability of exceedance when equation 5.2 is used without considering confidence limits

The confidence limit graphs were plotted with the multiplication factors as the parameters on the vertical axis and the catchment areas on the horizontal axis. The multiplication factor was obtained from the ratio of the observed sediment yield against the standardised average yield. The multiplication factors describe the relationship between the observed sediment yields and the standardised average yield. Observed sediment yields that were greater than the standardised average yield in a particular region gave factors that were greater than one (1) and vice versa. The multiplication factors indicate the variability in the observed sediment yields with respect to the standardised average yield. The confidence bands' lines were manually fitted along the data points on the graph of the relationship between the multiplication factor and catchment area. The graphs for the sediment yield confidence bands for each region have been shown in **Appendix E.** These confidence bands have been plotted with respect to catchment areas. Just like in the previous methodology (Rooseboom et al., 1992), there were some regions where the effect of the size of catchment area on the confidence limit could not be reliably ascertained. In such cases, a constant factor was adopted for the whole range of catchment sizes.

5.6.5 Steps for the prediction of sediment yields – probabilistic approach

The proposed procedure for the prediction of the sediment yields for an ungauged catchment based on the above statistical analysis of the regional data is as follows:

(a) Establishment of the region in which the specific dam under investigation falls.

(b) Determination of the boundary of the catchment and tracing of this boundary on an electronic copy or hard copy of the map showing the ten erosion hazard indices.

(c) Computation of the area covered by each of the erosion indices that are found in the catchment.

(d) Calculation of the proportion of the area out of the total catchment area (i.e. 100% = 1) that is covered by each of the specific erosion hazard indices.

(e) The sediment yield for an ungauged catchment is predicted using the equation 5.2 below whereby the proportion of the area out of the total catchment area that is covered by each of the specific erosion hazard indices is multiplied by the corresponding sediment potential factor for that particular class and the summation of the values across all classes are then multiplied by the standardised average sediment yield value (t/km^2.a) for the specific region:

$$\mathbf{SY_{est}} = \mathbf{SY_{sty}}\left\{\mathbf{F_1}\frac{\mathbf{A_1}}{\mathbf{A_T}} + \mathbf{F_2}\frac{\mathbf{A_2}}{\mathbf{A_T}} + \mathbf{F_3}\frac{\mathbf{A_3}}{\mathbf{A_T}} + \mathbf{F_4}\frac{\mathbf{A_4}}{\mathbf{A_T}} + \mathbf{F_5}\frac{\mathbf{A_5}}{\mathbf{A_T}} + \mathbf{F_6}\frac{\mathbf{A_6}}{\mathbf{A_T}} + \mathbf{F_7}\frac{\mathbf{A_7}}{\mathbf{A_T}} + \mathbf{F_8}\frac{\mathbf{A_8}}{\mathbf{A_T}} + \mathbf{F_9}\frac{\mathbf{A_9}}{\mathbf{A_T}} + \mathbf{F_{10}}\frac{\mathbf{A_{10}}}{\mathbf{A_T}}\right\} \quad 5.2$$

Where

SY_{est} = Estimated median sediment yield value (t/km^2.a)

SY_{sty} = Standardised average sediment yield value (t/km^2.a) for the specific region.

The standardised average sediment yield is obtained from Table 5.6.2 with respect to the region. F_1, F_2, F_3, F_4, F_5, F_6, F_7, F_8, F_9 and F_{10} are sediment potential factors to be obtained from Table 5.6.2.

The probabilistic approach for the computation of a sediment yield using equation 5.2 requires that the estimated median sediment yield (SY_{est}) value be multiplied by a factor to get the estimated sediment yield value with respect to the required exceedance probability. The multiplication factor, which is dependent on the preferred confidence band, catchment area size and sediment yield region is obtained from sediment yield confidence bands' graphs for each region that have been attached in

Appendix E. The determination of the sediment yield confidence bands is described in section 5.6.4.

The relationship is shown below:

$$SY_{\text{fest}} = Multiplication\ Factor \times SY_{est} \quad 5.3$$

Where

SY_{fest} = Factored estimated median sediment yield value (t/km^2.a)

5.6.6 Verification of results

In order to check the extent of the predictive accuracy of this probabilistic method, the sediment yields that were computed using equation 5.2 were checked using the discrepancy ratio test at 50% exceedance probability. The technique compares all the predicted sediment yields against all the observed sediment yields using the discrepancy ratio, x_i, whereby each predicted value is divided by the corresponding actual observed value. The discrepancy ratio x_i, should be a good indicator of the predictive accuracy of the probabilistic approach in predicting the sediment yield.

In mathematical terms the discrepancy ratio would be given by the following relationship:

$$\frac{SY_{sim}}{SY_{obs}} = x_i \quad 5.4$$

Where

SY_{sim} = Simulated sediment yield

SY_{obs} = Observed sediment yield

The simulated sediment yields refer to the sediment yields calculated using equation 5.2. The simulated sediment yields using equation 5.2 were divided by their corresponding observed sediment yields in Appendix B for all the regions. The following relationship was obtained relating to the calculated value of x_i.

$0.33 \leq x_i \leq 3$; 81% of the data was in this range

$0.5 \leq x_i \leq 2$; 68% of the data was in this range

$0.67 \leq x_i \leq 1.5$; 43% of the data was in this range

The ranges of the discrepancy ratios obtained in the current statistical approach were compared with those obtained in the previous statistical approach (Rooseboom et al., 1992) and the results were:

$0.33 \leq x_i \leq 3$; 70% of the data was in this range (Rooseboom et al., 1992)

$0.5 \leq x_i \leq 2$; 47% of the data was in this range (Rooseboom et al., 1992)

$0.67 \leq x_i \leq 1.5$; 32% of the data was in this range (Rooseboom et al., 1992)

The results for individual regions are shown in Table 5.6.3 for the probabilistic approach in this thesis.

Table 5.6.3 Discrepancy ratio results for the probabilistic method

Region	Obs.	Percentage of the data in this range		
	n	$0.67<x_i<1.5$	$0.5<x_i<2.0$	$0.33<x_i<3.0$
1	18	41	64	77
2	25	36	68	84
3	7	71	71	86
4	30	44	66	72
5	12	33	61	83
6	8	56	67	89
7	19	46	65	77
8	14	26	60	80
9	9	44	78	89

These ranges are within the limits of acceptable predictive accuracy considering the complex nature of the spatial variability in sediment yield. However, these values have been computed at 50% probability of exceedance implying that a factor of one (1) has been adopted for all calculated sediment yield values. For higher or lower confidence bands, the multiplication factors from Appendix E are applied. Caution must be taken when applying these factors to avoid over prediction. The probabilistic methodology/approach appears to over predict very small observed sediment yields

and under predict high sediment yields at 50% probability of exceedance. This is evidenced by the relationship between the observed data and simulated data on the graphs in **Appendix F**. For example, the graph for region 1 in Appendix F shows higher calculated sediment yields in the vertical axis for corresponding low observed sediment yields in the horizontal axis. This is because the method is based on the general concept of regional sample median assumed at 50% probability of exceedance.

In essence, the estimation of the sediment yield is developed from the average of the observed data series which is taken as the 50^{th} percentile. Since theoretically a percentile is the value of a variable below which a certain percent of observations fall (Wikipedia, 2009), the estimated median sediment yield value calculated by equation 5.2 gives a sediment yield value below which 50% percent of observed sediment yields fall. The probabilistic method developed around the 50^{th} percentile value should typically over predict probably at least half of the sediment yields. The estimated median sediment yield calculated using equation 5.2 acts as a reference point whose main application is to provide a sediment yield value that has a 50% exceedance probability. This results in problems in regions where there is high variability in the sediment yield values from the lowest to the highest.

The standardised average yield itself may be already over predicting some small sediment yield in the region. This is the reason why data points on the graphs in Appendix F are characterised by poor scatter along the line of perfect fit. The probabilistic approach does not derive direct relationships between the observed and calculated sediment yields. The method calculates a value that statistically masks all values below it depending on the specified probability of exceedance. For example at 50% exceedance probability, the method calculates a value whereby almost 50% of the data in the original sample size would have been below it.

The results given in Appendix F show that for some low observed sediment yields, say less than $100t/km^2.a$, the method gives relatively higher simulated yields. Similarly, the higher observed sediment yields above the standardised average yield appear to be under predicted. In practice to avoid over predicting or under predicting,

two possible measures could be undertaken. The first measure would be to check the predicted sediment value at 50% confidence band against the nearest observed yield value within the region and compare the results. Secondly, the graphs for the statistical distribution (probability of exceedance) of the observed sediment yields for each region, shown in **Appendix D**, can be used to compare the predicted value against the expected sediment yield value from the graph at any specific probability of exceedance. In other words, the probabilistic distribution of the observed sediment yields for each region gives an estimate of the general variation of the expected sediment yields within a given region.

Depending on the comparative results, an appropriate confidence band can be adopted. If the estimated median sediment yield is found to be lower than the comparative sediment yield, then the factors provided in the confidence bands' graphs in Appendix E can be used depending on the preferred confidence band and applicable catchment area. The discrepancy ratio test outlined in Table 5.6.3 is considered a significant measure of the predictive accuracy of sediment yield prediction approaches in sedimentation engineering particularly where multiplication factors are applied to achieve higher confidence levels.

5.6.7 Illustration of the application of the probabilistic method

An example of a dam requiring the prediction of a sediment yield will be solved to illustrate the application of the method outlined above.

A dam has been proposed at a location just upstream of Darlington Dam. The total catchment area of the dam is 10396km^2.

This dam falls in sediment yield Region 7 according to the sediment yield map in Figure 5.6-1 (bottom). The erosion hazard class statistics for the area under consideration are given in Table 5.6.4.

Table 5.6.4 Case study area statistics – probabilistic method

Erosion Index	Area (km^2)	Proportion to the total
1	0	0
2	102	0.009
3	4038	0.388
4	3991	0.383
5	1795	0.172
6	445	0.043
7	25	0.002
8	0	0
9	0	0
10	0	0
TOTAL	**10396**	**1**

From Table 5.6.2, the standardised average yield for Region 7 is 209t/km^2.a. In order to be conservative, the preferred confidence band for this estimate needs to be 80%.

Using Table 5.6.2 above the sediment potential factors for this region are as reproduced in Table 5.6.5:

Table 5.6.5 Region 7 erosion potential factors

REGION	Standardised Average Yield (t/km^2.a)	F_1	F_2	F_3	F_4	F_5	F_6	F_7	F_8	F_9	F_{10}
7	209	0.923	0.958	0.698	0.589	1.255	1.049	1.129	2.952	0.000	0.000

Equation 5.2 is used to convert the *Standardised average yield* value to the *Estimated median sediment yield value*, SY_{est}.

$$SY_{med} = 209[(0.923 \times 0) + (0.958 \times 0.009) + (0.698 \times 0.388) + (0.589 \times 0.383) + (1.255 \times 0.172) + (1.049 \times 0.043) + (1.129 \times 0.002) + (2.952 \times 0) + (0 \times 0) + (0 \times 0)]$$

$$= 160 t/km^2.a$$

A comparative check on this calculated value to the actual measured yields for comparable catchments has been done on Darlington Dam downstream of the proposed site and it has a value of 210t/km^2.a which is higher than the estimated median sediment yield of 160t/km^{2}a.

Since the calculated sediment yield value at 50% confidence is slightly lower than the nearest regional observed sediment yield, a higher confidence band can be applied to compute a sediment yield that is closer to the actual measured yields for comparable catchments. A confidence band of 80% can be adopted and the multiplication factor is read on the graph for Region 7 in Appendix D as 1.34 for a catchment area of 10396km^2.

The estimated sediment yield value at the required confidence band of 80% is:

= Estimated median sediment yield × Multiplication factor

= 160t/km^2.a × 1.34 = 214t/km^2.

The results show that at 80% exceedance probability, the calculated sediment yield value for this catchment is slightly higher than the standardised average yield and that of the catchment of the nearest observed sediment yield.

5.7 Empirical sediment yield prediction methodology

The objective was to find out if empirical relationships could be established that could provide a means of predicting the sediment yield from data of the significant variables that are involved in sediment yield processes. An investigation was done on the significant variables that would form part of the empirical equations to be derived through regression analysis. The unit stream power formed the theoretical basis for the development of the empirical method.

5.7.1 Concept of total input stream power

The rate of energy dissipation that would be required to transport material is related to the rate of material to be transported according to the general concept of physics. According to Yang (1996), the sediment transport rate is directly related to unit stream power. Therefore, sediment transport can be described by the following total input stream power relationship:

$$\mathbf{Q_s} \propto \frac{\mathbf{\rho gQS}}{\mathbf{w}} \qquad 5.5\text{-}1$$

Where

$Q_s =$ Sediment load

$Q =$ Discharge

$S =$ Energy slope

$w =$ Settling velocity of sediment

$\rho g Q S$ = Total Input Stream Power (ρg is assumed constant)

Equation 5.5-1 assumes that there is a sediment transport capacity based on local hydraulic conditions and sediment characteristics. This is generally true for coarse sediment (sand and gravel), but in the South African condition where about 75% of the sediment transported consists of clay and silt fractions, the sediment transport capacity is high, but the sediment availability from the catchment could be limited. Therefore, additional variables had to be considered in equation 5.5-1 to account for the sediment availability. In other words, there is joint effect of both sediment production and transport capacity controlling factors related to hydraulic conditions and sediment characteristics.

The settling velocity was therefore replaced by a weighted Erodibility Index (EI_w) to account for sediment production. The catchment area (A) was also added to describe the sediment source spatial extent and characteristics. There was also consideration of the region to account for different climatic conditions in the country and also the need to work out the analysis on a relatively homogeneous region. The discharge (Q) was based on a recurrence interval flood proposed to be the 1:10 year flood (established from regression analysis checks of all available recurrence interval floods in Table 5.7.1). The energy slope (S) for a catchment was taken as the average river slope.

5.7.2 Dependent and independent variables

(a) Sediment load

The sediment load was taken as the dependent variable. The average sediment loads were derived from resurveys of sediment deposits in reservoirs and river sediment load sampling data. A critical component of the conversion of sediment deposit volume into mass is the variable density of the sediment deposits (Rooseboom et al., 1992). Equation 5.5-2 proposed by Rooseboom et al. (1992) was used to compute the equivalent fifty (50) year sediment volume.

$$\frac{V_t}{V_{50}} = 0.376 ln \frac{t}{3.5} \qquad 5.5\text{-}2$$

Where

V_t = sediment volume after t years.
V_{50} = sediment volume after 50 years.
t = time (years).

The average density after 50 years is taken as 1.35t/m^3 in South Africa (Rooseboom et al., 1992). The sediment volume after t years was calculated from reservoir re-survey data in the dam list (DWAF, 2006). Equation 5.5-2 was used to convert the sediment volume after t years to a 50 year sediment volume. Alternatively, the 50 year sediment volume was obtained from graphs of sediment volume with time as explained in section 5.4. Using the average density after 50 years, the 50 year sediment volume was converted to a 50 year sediment load in tonnes. The sediment load in the regression model in tonnes per annum was obtained from the 50 year sediment load by assuming equal annual sediment deposit. The sediment loads from river suspended sediment sampling were obtained directly from river suspended sediment concentration data.

(b) Weighted erodibility index

The development of the erodibility indices has been explained in paragraph 5.6.2. The weighted erodibility index basically provides a quantitative measure of the following parameters: climate, soil profile, relief, vegetation, land use and land management practices based on the Revised Universal Soil Loss Equation (RUSLE) model. The inclusion of the weighted erodibility index per catchment in the regression analysis as one of the variable parameters proved to be a significant parameter for further derivation of the equations.

(c) River network density

River network drainage density can be classified as one of the factors that determine the catchment's sediment yield according to Strand and Pemberton (1982). It can be assumed that with all factors equal, for the same catchment area, longer length of river channel per unit area must be able to transport more sediment than shorter river channels within the catchment. This suggests that the river network density should be a significant variable in sediment load computations.

Drainage density is a measure of the length of stream channel per unit area of basin (Goudie, 1984). This measurement can vary according to the map scale used, as smaller scale maps will contain less drainage detail than larger scale maps resulting in lower drainage densities where small scale maps are used when compared to large scale maps. This is illustrated in Figure 5.7-1 where the difference in level of detail between rivers mapped at 1: 50 000 scale is shown compared to rivers mapped at 1: 500 000 scale. Theoretically using Figure 5.7-1, the drainage density calculated from the 1: 50 000 data is 1.02km/km^2 while drainage density from the 1: 500 000 data is calculated to be 0.12 km/km^2. At a scale of 1:500 000; only 0.12km length of rivers per km^2 of catchment can be shown due to reduced details. In order to calculate the drainage density, the rivers that were mapped at 1: 500 000 scale obtained from the Department of Water Affairs (DWA) were used. Future application of the developed equations should therefore adopt the 1:500 000 scale for computation of the river network density data across the study area to ensure consistency in the approach.

Spatial data analysis of river channel length per dam or river catchment of known area size was done in ArcGIS. The length of river channels was calculated in meters (m). The drainage density for each catchment was finally obtained by the division of the total stream length (km) by the catchment area (km^2) for each of the selected catchments to arrive at a drainage density in m/km^2 for each of the selected catchments.

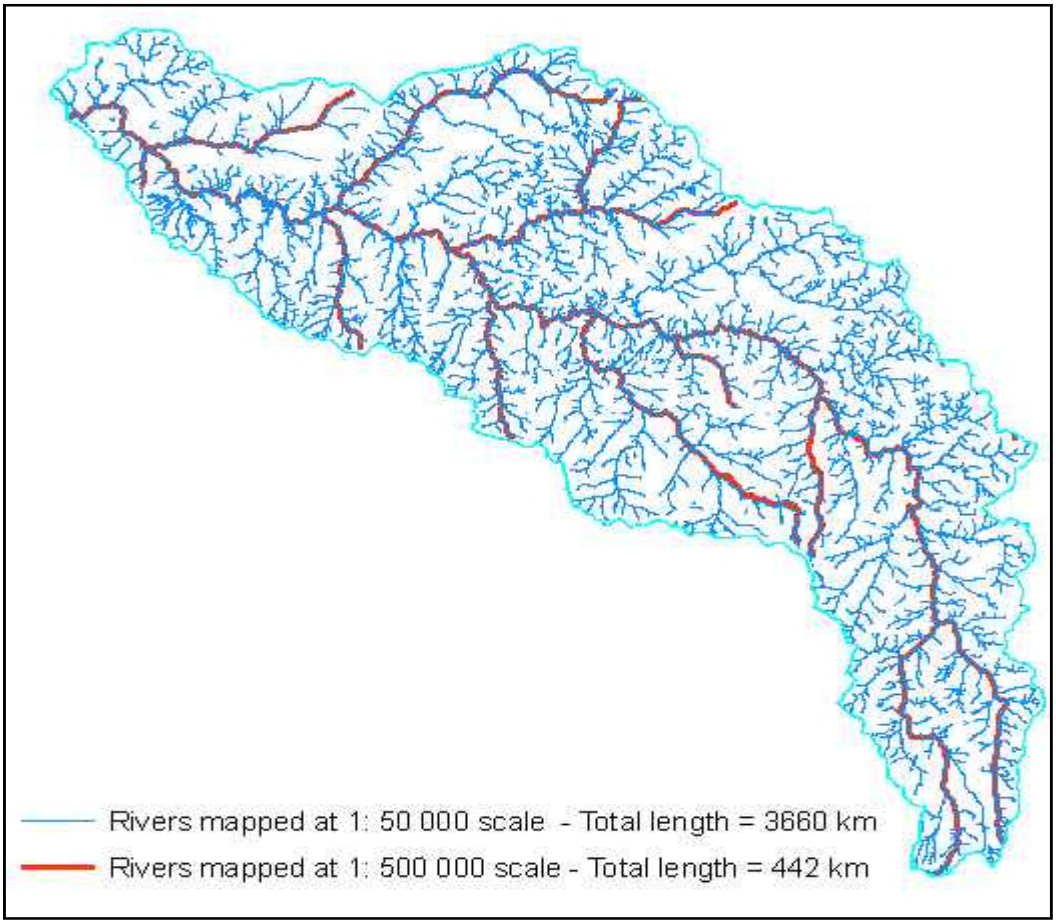

Figure 5.7-1 Illustration of scale effect on total stream length per catchment

(d) Recurrence interval flood

In the original application of the unit stream power, the instantaneous discharge was used in the relationship to describe the sediment transport. However, when considering sediment load over a long period of time then an effective discharge passing through a point along a river or a reservoir would best be represented by a recurrence interval flood, since more sediment is transported during floods than the average runoff from the catchment. All available recurrence interval floods were checked as shown in Table 5.7.1.

Table 5.7.1 Analysis of an optimum recurrence interval flood

			$0.67<x_i<1.5$						$0.5<x_i<2.0$						$0.33<x_i<3.0$			
Region	Obs. *n*		Q_2	Q_5	Q_{10}	Q_{20}	Q_{50}	Q_{100}	Q_2	Q_5	Q_{10}	Q_{20}	Q_{50}	Q_{100}	Q_2	Q_5	Q_{10}	Q_{20}
1	18	%	50	22	50	50	50	50	72	28	78	83	77	72	94	50	94	94
		r^2	0.59	0.59	0.67	0.68	0.68	0.64	0.59	0.59	0.67	0.68	0.68	0.64	0.59	0.92	0.68	0.68
2	25	%	32	40	40	40	40	40	68	76	72	76	68	68	88	88	88	88
		r^2	0.88	0.89	0.89	0.89	0.89	0.89	0.88	0.89	0.89	0.89	0.89	0.89	0.88	0.89	0.89	0.89
3	7	%	60	71	100	57	42.8	43	14	86	100	71	43	42	57	100	100	100
		r^2	0.8	0.97	0.99	0.94	0.93	0.94	0.8	0.97	0.96	0.94	0.93	0.94	0.8	0.97	0.96	0.94
4	30	%	13	43	40	40	40	40	16	50	50	53	57	53	33	77	76	76
		r^2	0.98	0.81	0.82	0.82	0.82	0.78	0.98	0.81	0.81	0.82	0.82	0.78	0.98	0.81	0.81	0.82
5	12	%	50	50	42	41	61	42	75	75	75	75	68	66	100	91	91	75
		r^2	0.92	0.9	0.88	0.87	0.86	0.85	0.92	0.9	0.88	0.87	0.86	0.85	0.92	0.9	0.88	0.87
6	8	%	-	-	-	-	-	-	-	-	-	-	-	-	-	-	-	-
		r^2	-	-	-	-	-	-	-	-	-	-	-	-	-	-	-	-
7	19	%	42	42	42	38	38	38	74	68	84	73	73	73	89	94	95	94
		r^2	0.85	0.87	0.88	0.87	0.86	0.87	0.85	0.87	0.87	0.87	0.86	0.87	0.85	0.87	0.87	0.87
8	14	%	50	50	57	50	50	50	60	60	64	64	71	71	86	86	93	93
		r^2	0.67	0.68	0.73	0.68	0.67	0.67	0.67	0.68	0.68	0.68	0.67	0.67	0.67	0.68	0.68	0.68
9	9	%	33	33	44	44	33	33	56	56	56	56	56	56	74	74	78	78
		r^2	0.86	0.87	0.89	0.88	0.88	0.88	0.86	0.87	0.87	0.88	0.88	0.88	0.86	0.87	0.87	0.88

The values in Table 5.7.1 were obtained from different combinations of the regression analysis by varying the recurrence flood interval and leaving the rest of the independent variables intact. The data column (in Microsoft Excel) for recurrence interval floods was substituted with different recurrence interval flood datasets and the predictive accuracy of the subsequent regression equations was recorded. Analysis of the results in Table 5.7.1 showed that the best results were obtained from the application of the 1:10 year recurrence interval flood. The 1:10 year recurrence interval flood gave consistent results based on the value of the r-square and the discrepancy ratio results for each of the recurrence interval floods in all the regions.

(e) Average river slope

This was taken as the average slope of the longest watercourse in the catchment.

(f) Homogeneous regions and catchment areas

The sediment yield or sediment load must be related to the catchment area within a homogeneous region. It was therefore decided that the regression analysis should include the parameter of the catchment size as one of the variables based on the concept of sediment delivery ratio explained in 3.2. It has also been observed in the confidence bands' graphs in Appendix E that the sediment yield is related to the catchment area size.

(g) Other variables

Other additional variables could also have an effect on the sediment load. However, it was recognised that not all these parameters could be incorporated in the regression analysis. The adopted variables for regression analysis were only those that were seen to have a dominant effect in the correlative analysis within the prescribed theoretical basis.

5.7.3 The concept of multiple regression analysis

Regression represents a mathematical equation expressing one random variable as being correlatively related to another random variable or to several random variables (Yevjevich, 1972). Linear regression analysis is the investigation of an optimum mathematical model that can best predict one variable in terms of another variable. Multiple regression analysis is done when more than two variables are involved.

5.7.4 Results and derived equations

In order to carry out the multiple regression analysis, both the dependent variable of sediment load and the other variables were logarithmically transformed. According to Rooseboom et al. (1992), sediment transport is a hydrological process and therefore is a function of the same parameters that influence all hydrological processes. It has been observed that while hydrological data are usually strongly skewed, the logarithms of the data have a near symmetrical distribution (Hazen, 1914). The variables were logarithmically transformed to achieve a better regression fit. A column of the sediment load as a dependent variable and five columns comprising the recurrence interval flood, average river slope, river network density, catchment area and weighted erodibility index were created in Excel. The regression analysis was performed in Microsoft Excel (2007) using Data Analysis tools. The proposed equations showing the results of the derived coefficients after regression analysis and correlation against observed data are shown in Table 5.7.2:

Table 5.7.2 Empirical equations based on regression analysis

Region	Proposed Equation
1	$Q_S = 22Q_{10}^{0.98}S_0^{-0.19}R_{nd}^{0.10}A_e^{0.10}EI_w^{0.95}$
2	$Q_S = 10Q_{10}^{0.44}S_0^{0.27}R_{nd}^{0.46}A_e^{0.88}EI_w^{-1.42}$
3	$Q_S = 354163Q_{10}^{1.62}S_0^{1.50}R_{nd}^{-3.73}A_e^{0.24}EI_w^{3.36}$
4	$Q_S = 0.61Q_{10}^{0.58}S_0^{0.28}R_{nd}^{0.88}A_e^{0.80}EI_w^{-0.92}$
5	$Q_S = 1432Q_{10}^{1.31}S_0^{0.74}R_{nd}^{-1.32}A_e^{0.41}EI_w^{-0.30}$
6	-
7	$Q_S = 30Q_{10}^{0.36}S_0^{0.33}R_{nd}^{0.29}A_e^{0.61}EI_w^{0.58}$

8	$Q_S = 0.003Q_{10}^{-0.25}S_0^{1.27}R_{nd}^{1.62}A_e^{1.26}EI_w^{-0.57}$
9	$Q_S = 0.0013Q_{10}^{-0.87}S_0^{-0.05}R_{nd}^{3.14}A_e^{1.15}EI_w^{2.26}$

Where:

Q_s = Sediment load (t/a)

Q_{10} = A flood of a recurrence interval of 1 in 10 years (m^3/s)

R_{nd} = River network density (m/km^2)

A_e = Effective Catchment Area (km^2)

E_{IW} = Weighted Erodibility Index according to sub-catchment areas

S_o = Average river slope (%)

The above 1:10 year flood, river network density, effective catchment area and average river slope can be calculated using standard hydrological/GIS methods. The weighted Erodibility Index can be found using data from Erodibility Index maps as illustrated in Paragraph 5.7.7 with respect to the area and its corresponding erodibility index.

5.7.5 Parameters for measurement of the degree of correlation

An acceptable degree of correlation depends on the objective of the model. A model can be developed to either predict or to quantify. The objective determines an acceptable level of correlation or accuracy. The correlative association of the known random variables can not entirely explain the total variation of the dependent variable, in this case the sediment load. This simplistic representation of the variables means that the neglected variables would result in an unexplained part of the variation that is mostly quantified by the degree of correlation and/or confirmation of the predictive accuracy. The main parameter that was applied to measure the degree of correlation was the coefficient of multiple determination referred to as the r-square.

Consideration of a good r-square depends on several factors such the nature of the variable being predicted, the size of the sample and results of other test statistics on regression and correlation.

5.7.6 Verification and analysis of results

It should be pointed out that the number of observations in all the nine regions was very small to allow the splitting of the sample and use portions of the data for independent verification of the results of the empirical model. Nevertheless, test application of the approach of the split sample in two regions (Regions 1 and 2) that had relatively larger sample sizes showed that the predictive accuracy of the empirical method is relatively good based on the model objectives. Table 5.7.3 shows data that was used for split sample analysis in Region 1. Ten observations were applied to derive regression equations.

The results were used to predict the sediment loads in eight independent observations within the same region. The similar procedure was done for Region 2 and the summary of results for both regions is shown in Table 5.7.4.

Table 5.7.3 Split sample analysis for Region 1

ID	Station Name	Log Sediment Load (Q_S)	Log 1:10 Year Recurrence Interval Flood ($Q_{1:0}$)	Log Average Slope, S_o (river)	Log River Network Density (R_{nd})	Log(A_e)	Log Erodibility Index (EI_w)	Calculated Sediment Load (t/a)	Observed Sediment Load
1	Albasini Dam	4.62	2.290	0.367	1.651	2.700	0.674		
2	Bospoort Dam	4.94	2.322	0.250	2.077	2.764	0.570		
3	Buffelspoort Dam	4.17	1.903	0.517	2.340	2.065	0.695		
4	Cross Dam	4.59	2.190	0.602	2.121	2.480	0.838		
5	Doorndraai Dam	4.81	2.176	0.312	2.108	2.587	0.736		
6	Hans Strijdom Dam	4.61	2.681	0.420	2.178	3.636	0.789		
7	Hartebeespoort Dam	5.58	2.789	0.441	2.120	3.541	0.793		
8	Klein-Maricopoort Dam	4.30	2.301	0.225	2.184	2.918	0.605		
9	Klipvoor Dam	4.78	2.342	0.124	2.056	3.673	0.545		
10	Koster Dam	3.90	2.041	0.236	1.955	2.461	0.498		
11	Kromellenboog Dam	4.86	2.371	0.320	2.069	2.783	0.567	38435.104	73011.64
12	Lehujwane Dam	4.32	2.061	0.086	2.177	2.302	0.509	31288.52	21102.37
13	Madikwe Dam	4.30	2.176	0.253	2.186	2.496	0.547	27307.205	19745.89
14	Marico-Bosveld Dam	4.77	2.230	0.500	1.972	2.977	0.674	18359.148	59333.65
15	Mzhelele Dam	5.36	2.724	0.699	3.048	2.920	0.845	115410.28	230846.72
16	Olifantsnek Dam	4.70	2.708	0.373	2.011	2.698	0.595	128226.75	50513.35
17	Roodeplaat Dam	4.82	2.360	0.312	2.185	2.838	0.693	66781.883	65417.98
18	Vaalkop Dam	5.32	2.886	0.143	2.095	3.593	0.523	193772.94	207876.60

Table 5.7.4 Results of split sample predictive accuracy analysis

Region	Obs.	Percentage of the data in this range		
	n	$0.67<x_i<1.5$	$0.5<x_i<2.0$	$0.33<x_i<3.0$
1	18	50	63	88
2	25	42	58	77

Graphs were plotted for all regions to analyse the relationship between the observed sediment loads against calculated sediment loads using the derived regional empirical equations given in Table 5.7.2.

Predictive accuracy checks were done by way of inspection of the graphs, determination of the r-square and calculation of the extent of deviation (using the discrepancy ratio concept). APPENDIX G shows the plot of the results of the observed sediment loads against calculated sediment loads using the empirical method. Table 5.7.5 shows results of the discrepancy ratio test for each region.

Table 5.7.5 Discrepancy ratio results for the empirical method

Region	Obs.	Percentage of the data in this range		
	n	$0.67<x_i<1.5$	$0.5<x_i<2.0$	$0.33<x_i<3.0$
1	18	50	78	94
2	25	40	72	88
3	7	100	100	100
4	30	40	50	76
5	12	42	75	91
6	8	-	-	-
7	19	42	84	95
8	14	57	64	93
9	9	44	56	78

The r-squares in Table 5.7.1 for the 1:10 year recurrence interval flood were analysed. Analysis of the graphs in Appendices F and G and the discrepancy ratio results in Tables 5.6.3 and 5.7.5 for the probabilistic and empirical approaches respectively gave the following observations.

a. Region 1 has the lowest r-square (based on the results in Table 5.7.1) but the predictive accuracy of the regression equation, based on the discrepancy ratio, is still satisfactory when one considers the general behaviour of sediment and the ranges of acceptable predictive accuracy.

b. Region 3 results appear theoretically good. But the few observations might be contributing undue leverage on the regression equation which is typical of regression analysis results when insufficient data is used i.e. few observations (Wasson, 1994). Additionally, Region 3 falls in part of the region that was also difficult to derive satisfactory results in the previous report (Rooseboom et al., 1992) due to insufficient data and high variability in observed sediment yields.

c. No reliable equation was developed for region 6 due to poor data.

d. Regions 7 and 8 have one outlier each that appear to be over predicting the low sediment yields. However, the outliers have been checked to have no significant effect on the overall predictive accuracy of the regression equation.

e. Regions 3 and 9 have fewer observations. The number of observations has significant influence on the predictive accuracy and statistical significance of the regression equations.

Based on the issues raised in paragraph 5.7.6 (a - e), the regression equations with most reliable predictive accuracy are for those of regions 1, 2, 4, 5, 7 and 8. With the exception of Region 6, which regression equation has been completely discarded due to poor data, recommendations on region 3 and 9 regression equations will be made after the comparative analysis of the probabilistic and empirical method in paragraph 5.8.

5.7.7 Illustration of the application of the empirical method

The methodology presented in the preceding section will be illustrated with a hypothetical dam that needs to be constructed on the Crocodile River. For planning purposes, the sediment yield from its total catchment area of 2600km^2, needs to be predicted.

It has been determined that the dam has Rietvlei dam upstream which has reliable high trap efficiency. Rietvlei dam has a catchment area of 490km^2. The effective catchment area, A_e of this hypothetical dam is therefore 2110km^2. The dam is located in Region 1 of the new sediment yield regions in Figure 5.6.1 (bottom) or in Appendix A.

From Table 5.7.2 an applicable regression equation for the determination of the sediment load (Q_s) for Region 1 is shown below.

$$Q_S = 22Q_{10}^{0.98}S_0^{-0.19}R_{nd}^{0.10}A_e^{0.10}EI_w^{0.95} \qquad 5.6$$

The rest of the parameters were calculated as detailed below.

(a) Flood peak discharge for a recurrence interval of 10 years, Q_{10}

The results of the flood frequency analysis at the dam site are summarised in Table 5.7.6:

Table 5.7.6 Flood frequency analysis

Probability of Exceedance (%)	50	20	10	5	2	1	0.5
Flood Peak (m^3/s)	229	499	727	975	1346	1670	2019

Therefore, a flood with a recurrence interval of 1 in 10 years (Q_{10}) is 727m^3/s

(b) River network density, R_{nd}

The river network density at a scale of 1:500 000 was computed as 160m/km^2.

(c) Average river slope, S_o

The average slope of the longest river was computed to be 0.8%

(d) Weighted Erodibility Index, E_{IW}

Table 5.7.7 shows the sub-catchment areas and their corresponding erodibility indices.

Table 5.7.7 Case study area statistics – empirical method

Erodibility Index	Area (km^2)	Proportion to the total
1	0	0
2	0	0
3	0	0
4	0	0
5	420	0.2
6	630	0.3
7	1060	0.5
8	0	0
9	0	0
10	0	0
TOTAL	**2110**	**1**

From Table 5.7.7, the weighted erodibility index, E_{IW} is 6.3.

The predicted sediment load using equation 5.6 above and substituting the computed parameters is as follows:

$$Q_s = 22 \times 727^{0.98} 0.8^{-0.19} 160^{0.10} 2110^{0.10} 6.3^{0.95}$$

Q_S = 300160t/a

The predicted sediment yield = $\frac{300160}{2110}$ = 142t/km^2.a. As recommended it is helpful to compare the results with neighbourhood dams' sediment yields. Neighbouring dams to the hypothetical dam that have an observed value are Rietvlei Dam upstream and Hartebeespoort Dam downstream with sediment yields of 35.95t/km^2 and 110.23t/km^2 respectively. The computed sediment yield is slightly higher.

5.8 Comparison of the empirical and probabilistic approaches

Table 5.8.1 shows the comparative analysis of the empirical and probabilistic methods.

Table 5.8.1 Comparative analysis of empirical and probabilistic methods using the discrepancy ratio

Region	Obs. *n*	Percentage of the data in this range					
		$0.67<x_i<1.5$		$0.5<x_i<2.0$		$0.33<x_i<3.0$	
		Empirical	Probabilistic	Empirical	Probabilistic	Empirical	Probabilistic
1	18	50	41	78	64	94	77
2	25	40	36	72	68	88	84
3	7	100	71	100	71	100	86
4	30	40	44	50	66	76	72
5	12	42	33	75	61	91	83
6	8	-	56	-	67	-	89
7	19	42	46	84	65	95	77
8	14	57	26	64	60	93	80
9	9	44	44	56	78	78	89

Based on the discussions in paragraph 5.7.6, the empirical method is comparatively the most reliable prediction method for sediment yield. It can be concluded from the discussions in paragraph 5.7.6 and paragraph 5.6.6 that the most reliable method to adopt for region 1, 2, 4, 5, 7 and 8 should be the empirical method. The empirical method is not being recommended in regions 3 and 9 because of the relatively small sample sizes. Region 6 had poor data. Therefore, the empirical method should be applied in regions 1, 2, 4, 5 7 and 8. By implication, sediment yield predictions for sediment yield regions 3, 6 and 9 should make use of the probabilistic method. Since regression equations for regions 3 and 9 have been provided in Table 5.7.2, it is possible to apply them but caution should be exercised since the equations were derived from smaller sized samples. Comparative checks against neighbouring observed sediment yields are highly recommended.

6.0 SEDIMENT YIELD MATHEMATICAL MODELLING

6.1 Justification for the choice of the SHETRAN model

The identification and choice of the best possible model to utilize in sediment yield modelling depends on a number of factors. Due to the multitude of models that have been developed to simulate erosion and sediment yield from a watershed, the choice of a suitable model to utilize is a challenging task. Some models are easy to apply, others are complex and often require extensive hydrological modelling skills.

The important aspects that need to be taken into consideration when choosing a numerical model to utilize include the following: catchment area size, data requirements (for setting up, calibration and validation), specific output parameters sought, stream/channel sediment simulation capability, flexibility for use in the anticipated actual catchment conditions, specific land use type that can be handled, simulation type (continuous or single event), erosion processes that can be simulated, adequate knowledge of specific intrinsic physical processes that the model can simulate, user requirements etc.

Table 6.1.1 shows the typical scale ranges of the size of the catchment areas that can be handled by the various models.

Table 6.1.1 Typical model area size range capabilities

Model	ACRU	SHETRAN	ANSWERS	WEPP	EUROSEM
Typical maximum model scale ranges	<10000 km^2	<2500 km^2	<50 km^2	<2.6 km^2	Small basin

Adapted from Basson and Di Silvio (2008)

The following are ranges of the effective catchment areas whose sediment yield was calculated for South Africa based on reservoir sediment deposit data and river sediment sampling data. Table 6.1.2 below gives an indication of the typical catchment area size ranges in South Africa based on the dam and river catchment areas in Appendix B

Table 6.1.2 Catchment area ranges for the observed sediment yields

Area range	Number of dams/rivers with an observed sediment yield	Percentage
0 - 50 km^2	9	6
50 - 100 km^2	13	9
100 - 1000 km^2	66	47
1000 - 2500 km^2	17	12
>2500 km^2	36	26

The SHETRAN and ACRU models have the capability to handle at least seventy percent (70%) of the typical area ranges.

The analytical sediment yield prediction methods have been developed based on data from southern Africa and are applicable to catchments in southern Africa. The domain of applicability of the SHETRAN model (as a conceptual model and model code (Refsgaard, 2007)) based on literature review showed that it is suitable for use in detailed analysis of sediment yield in a catchment. A conceptual model is a description of reality in terms of verbal descriptions, equations and governing relationships that purport to describe reality (Refsgaard, 2007).

The SHETRAN model can use input variables and parameter values for different land use types. The domain of applicability of the SHETRAN model is dependent on the ability to carry out model calibration and validation for specific catchment conditions. The case study was chosen for a catchment in which the aspects of model set up, calibration and validation could be evaluated in detail. Based on such validation results, the SHETRAN model can be used for sediment yield prediction in catchments with similar model conditions whether in southern Africa or anywhere in the world since it was not developed for specific catchments.

6.2 Description of the study area

The application of SHETRAN was reviewed through a case study of the catchment of Glenmaggie Dam in Australia. This catchment was chosen because of the availability of reliable meteorological and flow data.

This data is important in order to be able to reliably set up and run the model, and to successfully calibrate and validate the model results.

The total catchment area is 1901km^2, which was represented by 475 grid squares of 2km by 2km each. The grid size was limited by the number of columns and rows that the model can handle since it has a maximum allowable number of basic grid elements in the x and y direction. However, similar larger grid sizes have been successfully simulated by the model users elsewhere (SHETRAN Version 4, 2008b). The elevations ranged from around 1700 masl (highest point) to 70 masl at the lowest point located at the outlet of the Glenmaggie Dam.

Two dominant soil types within the catchment are loamy-sandy and sandy-loamy. The three main types of vegetation are temporary grassland, permanent grassland and forest. Major land uses are pasture and forest. Average annual precipitation is 800mm/year with low lying areas receiving around 450mm of precipitation per year and higher lying areas getting an average annual precipitation of 1250mm.

6.3 Model set up

The catchment description parameters outlined in paragraph 6.2 were applied in the model. The period of the sediment yield study was from 1975 to 2006. The meteorological and flow data was available for the whole of this period. The basic time step was taken as one hour.

Figure 6.3-1 shows the catchment boundary of Glenmaggie Dam (situated on the bottom right hand corner of the catchment) and rain gauge and flow gauging stations' location. Five meteorological stations were used for input of meteorological data within the catchment and these are: 225221, 225230, 225209, 225217 and 225219. These are the significant stations that have been used for both model calibration and verification. One external rain gauge station that was used for rainfall data input only is 83024 which is located at the northern tip of the catchment.

The catchment boundary was delineated from maps by hand through visual analysis of the contours. The ground surface elevations for each grid square and river network elevations for each link were obtained from Digital Elevation Maps through processing using AUTOCAD. The river network was established from maps by hand.

The rainfall distribution with respect to position of rainfall/meteorological stations was determined using the Thiessen polygon method. Average hourly rainfall data and daily evapo-transpiration data was used for the stations indicated in Figure 6.3-1.

Figure 6.3-2 shows the catchment palette as generated by SHETRAN with variations in the elevation indicated by grid square colour contrast. The rivers are shown as links between the grid squares.

The land cover distribution was analysed and assessed from photos, maps and satellite images. The soil distribution, depths and catchment geology were obtained from relevant technical reports, soil maps and visual inspection of the soils at road cuttings. The vegetation cover for the catchment comprised mainly of temporary grassland, permanent grassland and forest.

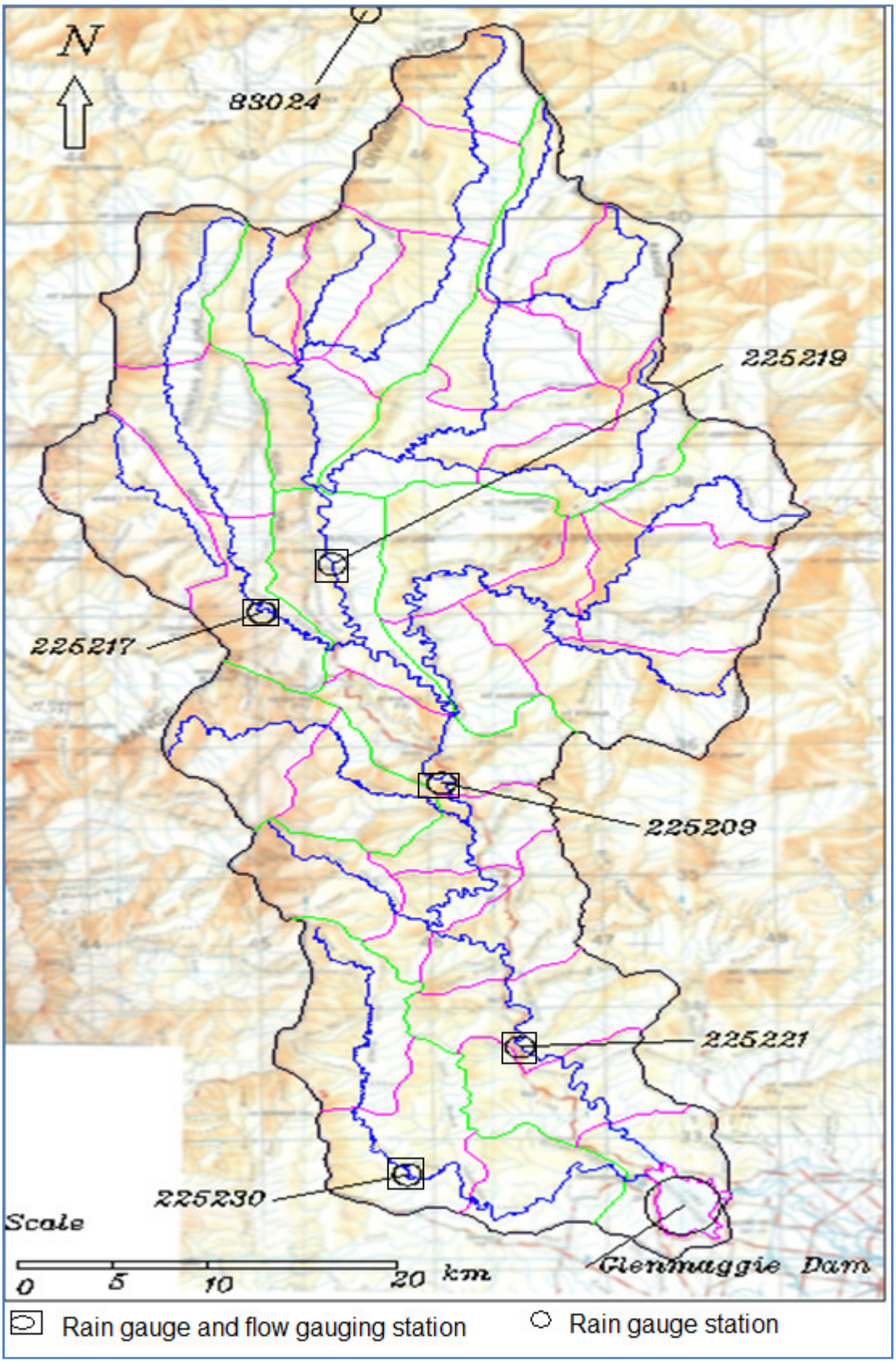

Figure 6.3-1 Study area showing Glenmaggie Dam with rain gauge and flow gauging stations

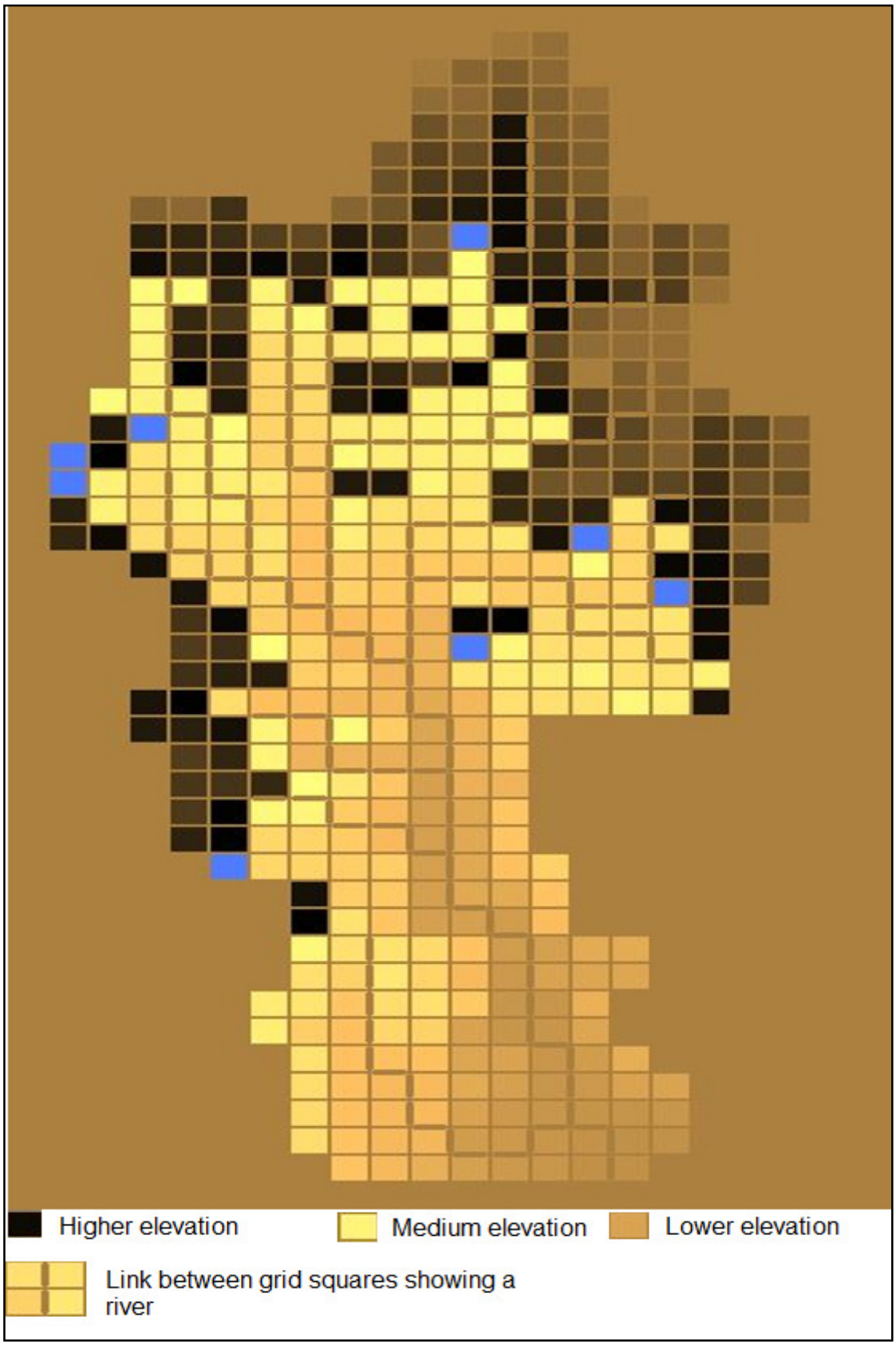

Figure 6.3-2 SHETRAN generated catchment palette showing elevation and rivers as links

The canopy and leaf parameters such as canopy drainage, canopy storage and vegetation cover indices were based on standard parameters specified in SHETRAN Version 4 User Guide (2008) for various standard vegetation types. Although more detailed vegetation types could be distinguished, the number of vegetation types was limited to the allowable cumulative maximum of individual parameters for vegetation, soils, rainfall stations and meteorological stations that the model can ably handle per simulation.

The Manning's roughness coefficient for channels was set between 0.033 and 0.04 (Strickler resistance coefficients between 30 and 25 respectively). The Manning's roughness coefficient for overland flow was set at an average of 0.03. There were four soil types set up in the whole catchment in three different layers. The saturated hydraulic conductivity in the x, y and z direction was set up at an average of 4m per day. The simulated soil porosity ranged from 0.16 around the bedrock to 0.412 in the upper layers. Data for the rest of the relevant parameters was entered for each of the grid squares and links.

The sediment yield component was set up with input data pertaining to some of the following significant parameters:

(i) Mobile sediment concentration
(ii) Raindrop and leaf drip soil erodibility coefficient (J^{-1})
(iii) Overland flow soil erodibility ($kgm^{-2}s^{-1}$)
(iv) Channel bank erodibility coefficient ($kgm^{-2}s^{-1}$)
(v) Average height that drips fall from canopy to ground (m)
(vi) Bulk dry soil density (kg m-^{3})
(vii) Fractional clay content of soil
(viii) Threshold depth of loose soil above which erosion is zero

6.4 Flow calibration

Upon setting up the appropriate hydrological, meteorological, spatial and initial data, the model was calibrated against observed flow for the period from 1975 to 1984. The most significant hydrological and flow calibration parameters that were slightly

adjusted included the following: roughness/resistance (Manning) for overland and channel flow, saturated conductivity and unsaturated conductivity and soil depths. The discharge data from 1975 to 1984 was used for calibration of the flow. The graphs showing the results of the calibration at flow gauging stations 225221, 225230, 225209, 225217 and 225219 are attached in **Appendix H**.

The model uses hourly rainfall for its simulation but the actual observed hourly rainfall data was not available. Therefore, daily rainfall was used in the simulation by disaggregating it into average hourly rainfall. The hourly output flow data was generated after each time step which depends on the available rainfall volume per hour. The model has the ability to reduce the basic time step depending on the rainfall volume.

The accuracy of the calibration was checked through visual inspection of the hydrographs based on experience as well as determination of the degree of correlation. The other criteria for checking the degree of calibration was inspection of the scatter along the line of perfect fit. During flow calibration from 1975 to 1984, the calculated r-squares ranged from 0.5 to 0.72 for the four given stations. All stations except flow gauging station 225230 have better scatter around the line of perfect fit. Nevertheless, the peak discharge rates for significant storms appear to be simulated better at flow gauging station 225230.

However, peak flows appeared to be overestimated by the model, possibly because of the modelling of the soil properties and river networks. The flow could also be overestimated because of some of these reasons: poor representation of the land cover and vegetation properties which in turn may not properly describe the natural soil infiltration rates, the effect of ponding/sinks within the catchment, small natural depressions within the catchment could not be clearly modelled by lack of capacity to simulate water falling into natural sinks and river sinuosity not being accurately represented because of the scaling resulting in theoretically straight rivers contrary to the actual river network configuration in the field.

However, the overestimation of the flow was found to have minimal repercussions on the accuracy of the final calibrated sediment yield and sediment load.

In conclusion, the extent of the correlation is deemed reasonable considering the time period that the flow was being simulated and size of the mesh that was applied which could not adequately represent some natural catchment conditions such as infiltration and storage due to scaling problems. According to Bathurst (2002), use of large grid squares (up to 2 km x 2 km) may introduce scaling problems. The other reason could be the length of the calibration period which could likely be affected by some temporal changes not just resulting from meteorological factors but other human induced factors. In most SHETRAN calibrations, shorter periods are used hence it is easier to achieve better correlation since the chance of encountering significant temporal changes that may be contributed by other factors could be minimal.

Nevertheless, the calibrated flow is sufficient for sediment yield prediction purposes.

6.5 Flow validation

Due to availability of sufficient data, it was possible to split the sample and use one continuous period for calibration (1975 to 1984) and the other period for validation. Therefore, flow validation for the SHETRAN model was done using independent data from the period 1996 to 2006. It was done by comparing the simulated flow against the flow that was measured at four flow gauging stations: 225221, 225230, 225209 and 225219. There was no observed flow data for validation at flow gauging station 225217. The validation hydrographs are shown in Appendix I for flow gauging stations 225221, 225230 and 225209. Analysis of the correlation or lack of correlation between observed and simulated flow was done based on the value of the r-square and the scatter of the data around the line of perfect fit. These quantitative measures of accuracy were applied in general without fixing any specific level of accuracy to confirm the model validation. Highly correlated data is characterised by an r-square of around 0.8 in most SHETRAN simulations reported in literature.

Table 6.5.1 shows values of the r-square for flow calibration and validation results at the five gauging stations.

Table 6.5.1 Comparison of the calibration and validation results

Flow gauging station	Calibration r-square	Validation r-square
225221	0.531	0.610
225230	0.610	0.249
225209	0.578	0.583
225217	0.723	-
225219	0.631	0.486

The validation results were compared against the calibrated hydrographs' accuracy for three of the flow gauging stations. Flow validation for the period from 1996 to 2006 gives relatively the same and a higher r-square value compared to those obtained during the calibration for flow gauging stations 225209 and 225221 respectively. The r-squares of the stations 225221 and 225209 appear to be statistically low but these values are significantly better and reasonable considering the size of the sample that was used in the analysis which had over 90,000 observations.

Flow validation results at flow gauging station 225230 did not show very good correlation. There was poor scatter along the line of perfect fit and an r-square of 0.249 was obtained which was significantly low. The poor correlation could be as a result of the failure by the model to accurately simulate sub-catchment characteristics and conditions such as soils and topography.

It can be seen that the correlation is better for flow gauging stations in the upper catchments than at the flow gauging station just upstream of Glenmaggie Dam. The simulated flood flows for the flow gauging station closer to the dam are higher than observed flows.

This can be explained by the fact that actual amount and extent of infiltration of water as it is flowing from upstream water courses to the dam may not be sufficiently and accurately defined by the model's algorithm of infiltration and capillary rise during flow routing whereby the model assumes that much of the flow reaches the dam without considering sinks and river meandering among other things.

The validation at the three stations 225221, 225230 and 225209 closer to the outlet of the catchment (at the dam) was assumed to be a true representation of the internal catchment's behaviour since the initial calibration was done from the upstream to the outlet of the catchment.

6.6 Sediment load calibration and validation

There was not enough data for sediment load calibration using total suspended solid concentration observations at the flow gauging stations. However, there was data on turbidity measurements at flow gauging stations 225221 and 225209. A relationship that shows the correlation between suspended solid concentration and turbidity derived by Randerson et al. (2005) was used. The equation that was chosen out of the four derived equations was the one that gave the maximum possible concentration at any specific turbidity. The relationship according to Randerson et al. (2005) is given by equation 6.6.

$$y = 2.06x \qquad 6.6$$

Where
y = turbidity (NTU)
x = concentration (mg/L)

Using the discharge data, turbidity and the relationship in equation 6.6, the sediment load-discharge curves for flow gauging stations 225221 and 225209 were plotted as shown in Figures 6.6-1 and 6.6-2.

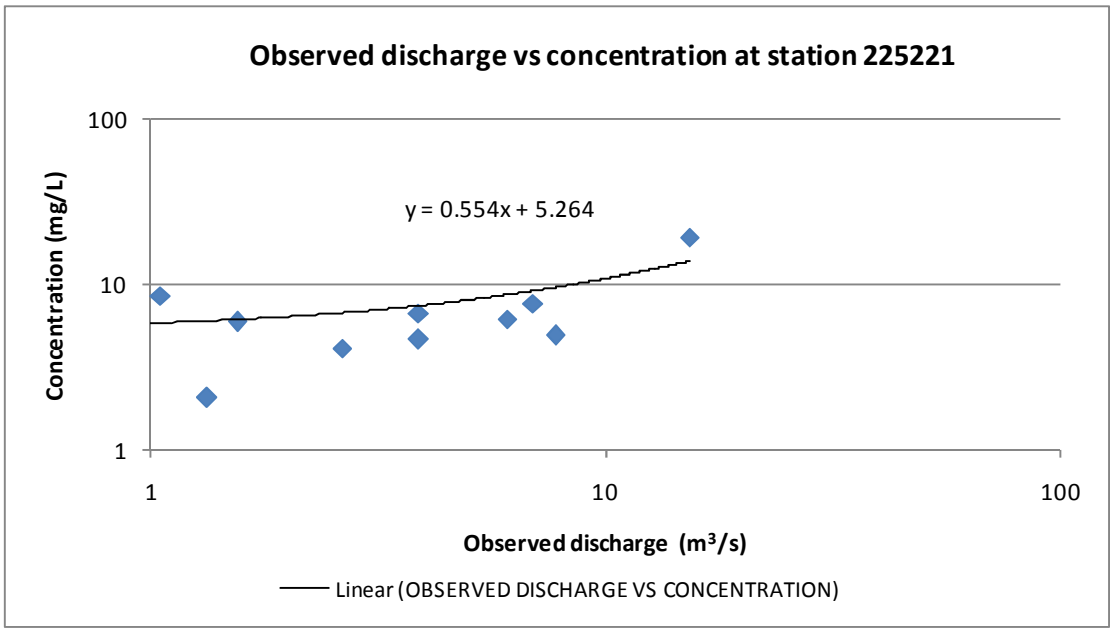

Figure 6.6-1 Sediment load – discharge rating curve for the flow gauging station 225221

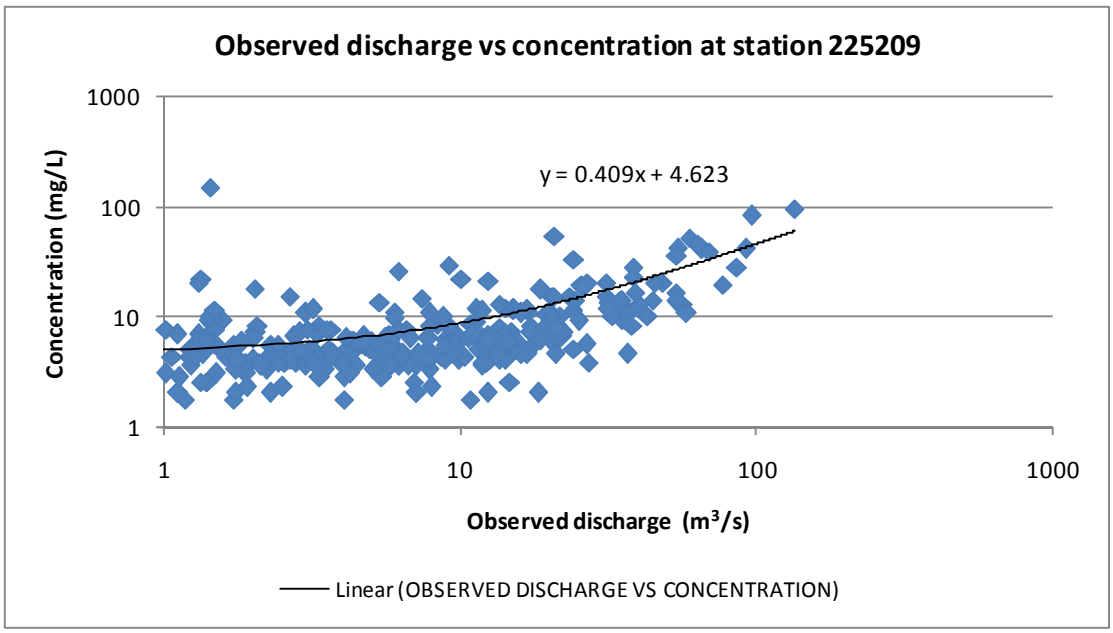

Figure 6.6-2 Sediment load – discharge rating curve for the flow gauging station 225209

The model was calibrated against the sediment load in the dam calculated from the relationship between turbidity and sediment concentrations with respect to the sediment load-discharge rating curves in Figures 6.6-1 and 6.6-2. Sediment yield calibration sensitive parameters included some of the following: mobile sediment concentration, raindrop and leaf drip soil erodibility coefficient (J^{-1}), overland flow soil erodibility ($kgm^{-2}s^{-1}$), channel bank erodibility coefficient ($kgm^{-2}s^{-1}$). The results of the calibration are attached in **Figures 6.6-3 and 6.6-4**. The sediment load calibration was done on the main river only. The small river that joins the case study dam on the right bank was not included in the sediment yield predictions. Therefore, its poorly calibrated and validated flow results did not affect the sediment yield predictions.

It can be seen that the model simulates relatively higher cumulative sediment load at flow gauging station 225209. The over prediction of the cumulative sediment load at this flow gauging station did not significantly affect the results. The results could still be applied in detailed design of water resources development with the increased sediment load presumably being considered as a necessary conservative value.

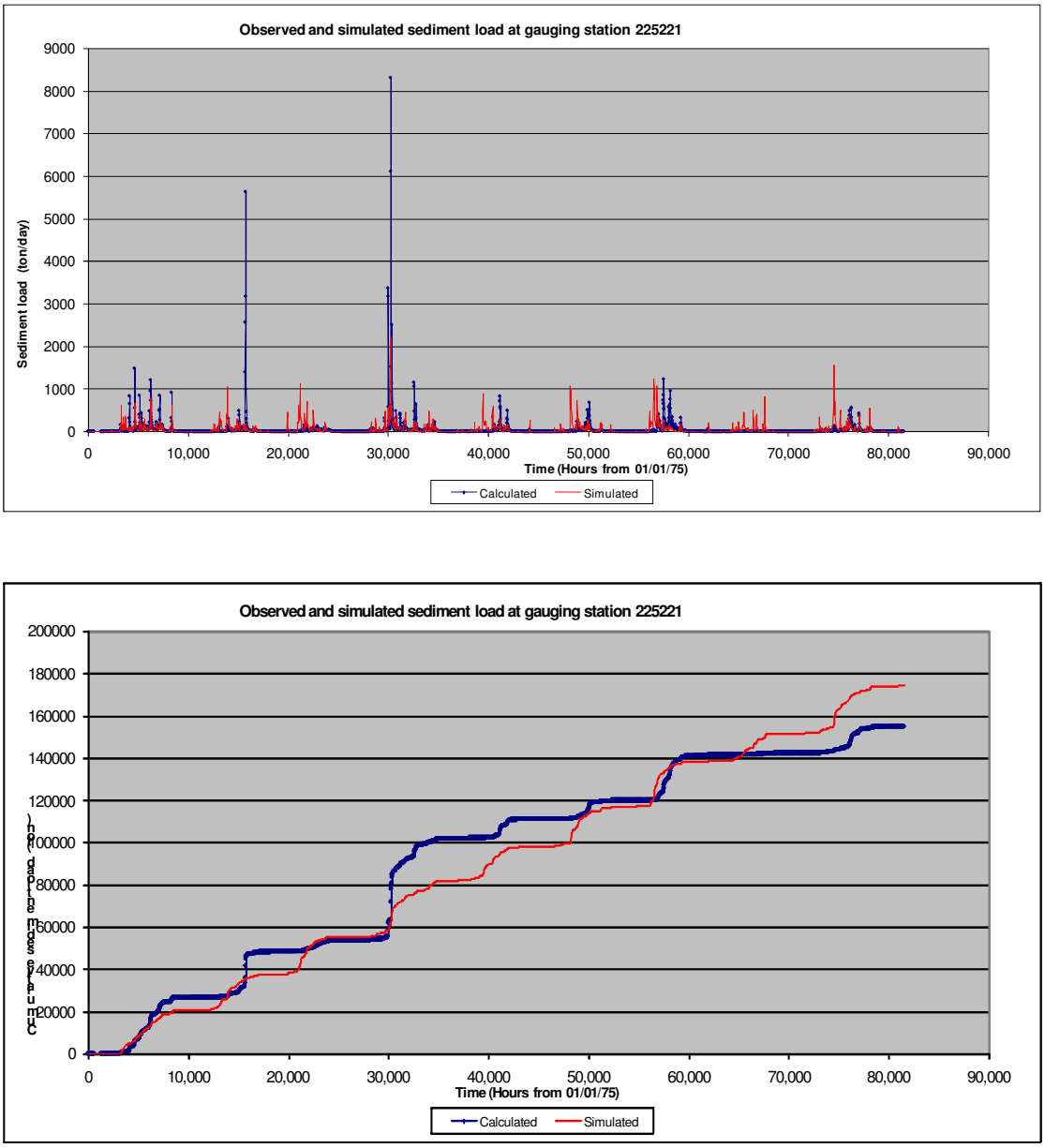

Figure 6.6-3 Sediment load calibration for station 225221

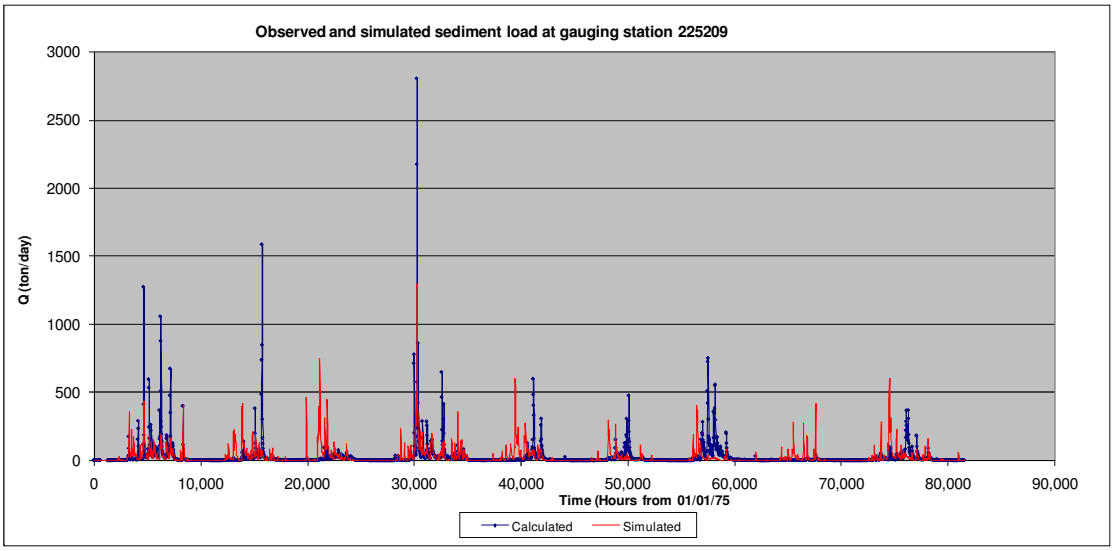

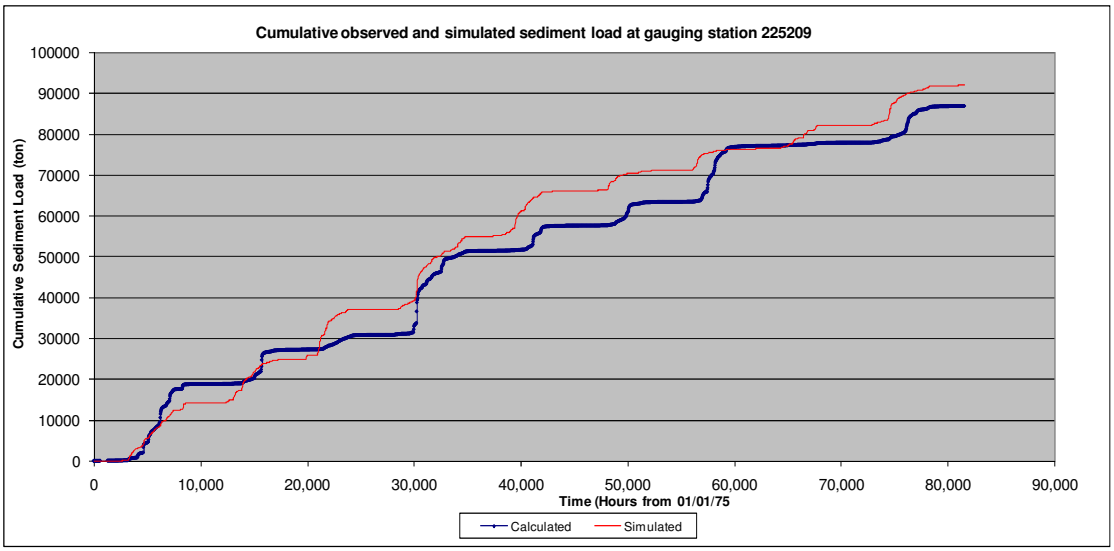

Figure 6.6-4 Sediment load calibration for station 225209

Table 6.6.1 shows some of the sediment load calibration parameter values.

Table 6.6.1 Significant sediment load calibration parameter values

Parameter	**Average/Range**
Raindrop and drip soil erodibility	$0.1J^{-1}$
Overland flow soil erodibility	$1.3x10^{-12}$ to $7.0x10^{-11}$ $kgm^{-2}s^{-1}$
Channel bank erodibility coefficient	$1.0x10^{-11}$ $kgm^{-2}s^{-1}$
Threshold depth of loose soil above which erosion is zero	0.05m

Table 6.6.2 gives the calculated and simulated (calibrated) sediment yield.

Table 6.6.2 Sediment yield calibration for the period from 1975 to 1985

Flow gauging Station	Calculated sediment yield (turbidity derived) ($t/km^2.a$)	SHETRAN simulated sediment yield ($t/km^2.a$)
225221	10.02	10.61
225209	6.40	6.65

The sediment yield was calculated using the average annual sediment load and dividing it by the specific area under investigation. The assumptions that were made in the derivation of the sediment yields could be unreliable. For example the adopted relationship between turbidity and concentration might not be reliable for the site specific conditions at the two gauging stations. The limited turbidity data at the flow gauging stations could have also affected the results with respect to the sediment load-discharge rating curve.

The results were verified by running the simulation using the calibrated sediment load parameters during the period from 1996 to 2006. The results of the sediment load validation for flow gauging stations 225221 and 225209 are shown in Appendix J. The relatively higher simulated cumulative sediment load could be as a result of high simulated flows observed during flow validation during the same period and temporal variability in the watershed hydrologic response, soils, bank sediment characteristics and land use/cover (Randerson et al., 2005) since the model was not changed to account for such changes. For example, the proportion of the ground covered by vegetation could have changed over time. The model could only capture a representative vegetative cover which could not be very accurate and hence might have affected the sediment load. It is therefore not very impossible to have a slightly higher validated sediment load as seen in Appendix J.

Based on the results, temporal variation of the sediment load could also be assessed by inspecting the slope of the cumulative sediment load graph over the simulation period. There were observable variations in the sediment load between years of high rainfall volumes than low rainfall volume years confirming the capability of the model to compute temporal variations in sediment yield.

6.7 Identification of high sediment yield areas

SHETRAN has the capability to show the sediment yield from each sub-catchment area within the watershed. The SHETRAN model can be instructed to calculate the sediment load at any grid square or link within the catchment. In order to investigate potential sources of sediment, four sub-catchment areas were assessed. The sub-catchments are labelled 1 to 4 and they have been delineated by a red boundary as shown in Figure 6.7-1.

Each of the four sub-catchments had a pour point on a river for sediment load simulation from upstream. The simulation to identify the sub-catchment that has the highest sediment yield was done for the period starting from 1996 up to 2006. The results are summarised in Table 6.7.1.

Table 6.7.1 Results showing sediment yields from each sub-catchment area

Sub-catchment number	Area (km^2)	Cumulative sediment load (ton)	Calculated sediment yield ($t/km^2.a$)
1	52	400	0.7
2	240	16000	6.20
3	36	200	0.5
4	248	18000	6.72

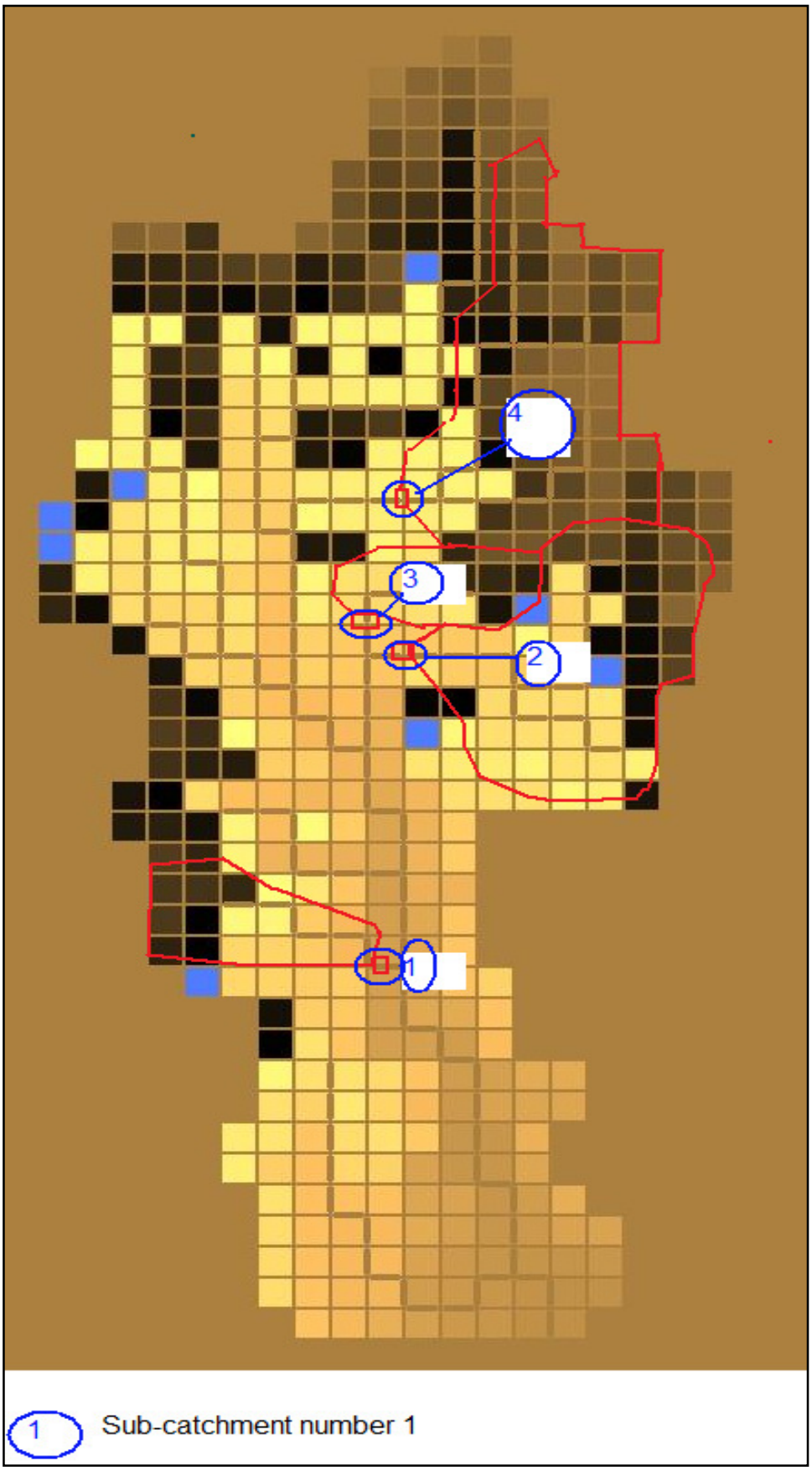

Figure 6.7-1 Sediment yields from sub-catchment areas

The cumulative plot of the sediment load for each of the sub-catchments in Table 6.7.1 are attached in **Appendix K**. Sub-catchment 4 has the highest sediment yield while sub-catchment 3 has the lowest sediment yield. Sub-catchment 4 is in an upland area with steeper slopes and permanent grassland. Erosion could be comparatively higher in this area. Sub-catchment 2 comprises of a native forest. This could be the reason why the sediment yield is not as high as that of sub-catchment 4. The low sediment yield in sub-catchments 1 and 3 could be because of the size of the streams in the catchment which are not bigger enough and hence the transport capacity of the sediment is low. In addition it could also suggest the possible scenario of the dominant erosion process in the catchment being bank and channel erosion.

6.8 Investigation of land use change effects on sediment yield

Table 6.8.1 gives the simulated sediment yield at flow gauging stations 225219 and 225217.

Table 6.8.1 Simulated sediment yield at flow gauging stations 225217 and 225219

Gauging Station	Simulated sediment yield (t/km^2.a)
225217	8.20
225219	8.20

In Table 6.8.1 above the simulated sediment yield was the same at the two flow gauging stations. The two flow gauging stations have different catchment areas and observed temporal discharge but the model simulated the same sediment yield due to similar land uses. The flow gauging stations 225217 and 225219 are shown in Figure 6.8-1. When the land use was changed from temporary grassland to permanent grassland for the catchment of the flow gauging station 225217, the simulated sediment yield reduced from 8.20t/km^2.a to 7.70t/km^2.a.

Although the reduction was just 7% of the original sediment yield, it can be concluded that the model responds reasonably to catchment land use changes.

Based on the results, further investigations can be done to find the best alternative solution for erosion control within the relevant sub-catchment.

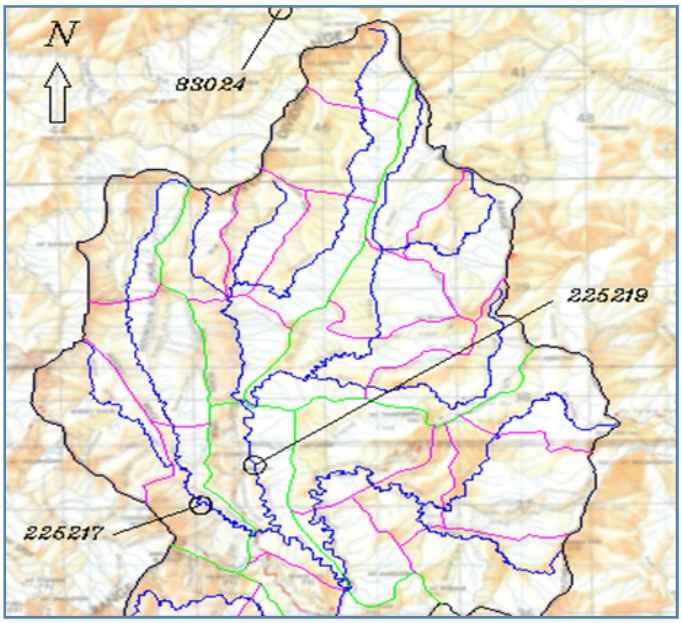

Figure 6.8-1 Investigation of the effect of vegetative cover changes on sediment yield

6.9 Conclusions on the application of the SHETRAN modelling system

SHETRAN is written in FORTRAN 77. The SHETRAN modelling system has two versions. These are SHETRAN Windows and SHETRAN Standard. The SHETRAN Windows version cannot run sediment and solute transport. Sediment and solute transport can only be run in the SHETRAN standard version (SHETRAN Version 4, 2008). The SHETRAN Standard version does not have a graphical user interface (GUI). The SHETRAN Standard version uses text files to run the model. The model takes more time to set up since data is entered and edited in text files. The user must be able to prepare and generate a certain amount of data independently before applying it in the modelling system. It took approximately five months to know how to use the modelling system and how to set up and run the model. However, with prior experience in using the model, the time taken to come up with the results can be significantly reduced. Additionally, the time and ease in the use of the model depends on the data requirements and availability, size of the catchment and the nature of the simulations to be done.

7.0 CONCLUSIONS

If the current state of reservoir sedimentation in South Africa is to continue at the rate it is happening, it is likely that serious problems on water yield will be encountered in the near future. This scenario provides a grim picture on the long term sustainability of the existing reservoirs unless appropriate sediment control measures are put in place. One of these measures includes accurate prediction of sediment yields in existing and future reservoirs. This information is essential in the feasibility studies, planning and management of water resources with respect to sedimentation control and management.

The current sediment yield prediction methods have been reviewed. The need for revision has been explained. Nine relatively homogeneous sediment yield regions were demarcated across South Africa. Two sediment yield prediction methods have been developed. These methods include probabilistic and empirical methods. The probabilistic method has been developed using statistical analysis of regional data on observed sediment yields and erodibility indices based on Rooseboom et al., (1992). The observed sediment yields were calculated from reservoir sediment deposition data and river sediment sampling. The empirical method has been developed from regression analysis of variables that control sediment yield with respect to the South African conditions namely floods, soil erodibility, river network density, catchment area and river slopes.

The empirical and probabilistic methods of sediment yield prediction are important for decision making in the feasibility studies and planning of water resources. In the detailed design of water resources, the use of numerical models particularly physically based distributed models is proving to be very significant particularly in the prediction of spatial and temporal variability of erosion and sediment yield within the catchment. In this regard, two physically based numerical models have been reviewed and evaluated. These models are SHETRAN (Ewen et al., 2000) and ACRU (Smithers et al., 2002). The former has been reviewed in detail including the identification of a case study for the evaluation of the aspects of model set up, calibration, validation and simulation.

These models cannot be used without calibration and validation against flow and observed sediment loads. The validity of the modelling systems for site specific conditions can be judged by the results of the validation.

7.1 Criteria for the choice of a sediment yield prediction method

The empirical method is relatively more reliable based on the predictive accuracy check tests that have been done. The probabilistic method appears to be overestimating low value sediment yields as observed from the graphical plots of observed sediment yields against calculated sediment yield values especially for sediment yields below 100t/km^2.a. It has therefore been proposed that sediment yield prediction for regions 1, 2, 4, 5, 7 and 8 should be done using the derived empirical equations in Table 5.7.2. Regions 3, 6 and 9 should make use of the probabilistic method. The derived empirical equations and probabilistic approach can be applied in predicting sediment yields in rivers, lakes, reservoirs and estuaries. Detailed analysis of the temporal and spatial variability in sediment yield within the catchment can be done using physically based distributed models such as SHETRAN and ACRU.

7.2 Numerical model constraints and strengths

A review of the application of SHETRAN as an erosion and sediment yield model has showed that the model can be successfully used to simulate sediment yield in a catchment. Calibration of the sediment load was done at two flow gauging stations on the rivers close to the case study dam where calibration data was available. Upon calibrating and validating, the model was successfully used to predict sources of sediment. This helped in the identification of catchment areas with high or low sediment yields. The model was applied in the prediction of the effect of land use change on the sediment yield. The response of the model to land use change was also reasonable and credible.

One of the constraints in the application of numerical models is the availability of sediment load and flow data to be used for sediment and flow calibration and/or validation respectively. It is therefore imperative that systematic measurements of sediment loads and flows should continue to be undertaken in important and strategic rivers for future use. SHETRAN uses hourly rainfall data and hourly time steps which could be a problem in South Africa especially in large catchments. The model can however run with average daily rainfall that has been disaggregated into hourly rainfall. Data on sediment loads and flows would provide a wealth of information for flow and sediment yield calibration and validation and in turn boost the successful application of sediment yield prediction models.

8.0 RECOMMENDATIONS

There is need for more future research in the prediction of sediment yields in ungauged catchments. It has been observed that the role of sediment storage could have a significant impact on the sediment yields observed in some South African catchments. Though quantification of sediment storage is generally problematic especially for large catchments according to Slaymaker and Spencer (1998), future research on the role of storage on the observed sediment yields in South Africa should provide an insight into the problem of lack of better correlation between the gross erosion as computed using the Revised Soil Loss Equation and the observed sediment yields. Such research would also determine whether possible depleting sediment storage capacity in some catchments would trigger future increases in sediment yields than currently predicted.

Future research on predicting sediment yields should also be directed towards investigating the climate change impacts on sediment loads and sediment yields. From the findings it has been observed that the sediment yields are correlated to the 1:10 year flood. In the event of increases in floods due to climate change in future, there is need for research to determine the corresponding increase in sediment budgets and the cost of water resources management for sediment control due to climate induced changes. Potential regions that would have their sediment loads increased by floods could be identified and the relevant mitigating measures could be undertaken.

9.0 REFERENCES

Basson, G.R., and Di Silvio, G. (2008). Erosion and sediment dynamics from catchment to coast. UNESCO. International Hydrological Programme, Technical Documents in Hydrology, No 82.

Basson, G.R., Rooseboom, A., Le Roux, J., Gibson, L. and Msadala, V.P. (2009). Sedimentation and sediment yield maps for South Africa. Water Research Commission Project K5/1765. Progress Report.

Bathurst, J.C., Moretti, G., El-Hames, A., Moaven-Hashemi, A., and Burton A. (2005). Scenario modelling of basin-scale, shallow landslide sediment yield. Valsassina, Italian Southern Alps, Natural Hazards and Earth System Sciences 5: pp. 189–202.

Bathurst, J.C., Burton, A., Clarke, B.G., and Gallart, F. (2006). Application of the SHETRAN basin-scale, landslide sediment yield model to the Llobregat basin, Spanish Pyrenees. HYDROLOGICAL PROCESSES 20, pp. 3119–3138. Wiley InterScience (www.interscience.wiley.com).

Batalla, R.J., and Sala, M. (1994). Temporal variability of suspended sediment transport in Mediterranean sandy gravel bed river. IAHS Publication 224.

Beasley, D.B., Higgins, L.F., and Monk, E.J. (1980). ANSWERS. A model for watershed planning, Trans., Am. Soc. Agric. Eng., 23: pp. 938-944.

Bicknell, B.R., Imhoff, J.C., Kittle, J.L., Donigian, A.S. and Johanson, R.C. (1997). Hydrological Simulation Program--Fortran: User's manual for version 11: U.S. Environmental Protection Agency, National Exposure Research Laboratory, Athens, Ga., EPA/600/R-97/080.

Birkinshaw, S.J., and Bathurst, J.C. (2006). Model study of the relationship between sediment yield and river basin area. Earth Surface Processes and Landforms 2006, 31(6): pp. 750-761.

Conroy, W.J., Hotchkiss, R. H., and Elliot W. J. (2006). A coupled upland-erosion and instream hydrodynamic-sediment transport model for evaluating sediment transport in forested watersheds. American Society of Agricultural and Biological Engineers, Vol. 49(6): pp. 1713−1722.

De Figueiredo, E.E. (2008). Sediment yield modelling at micro-basin and basin scales in semi-arid regions of Brazil. Sediment dynamics in changing environments. IAHS Publication 325: pp. 157 -166.

Department of Water Affairs. (2006). Dam list. Ministry of Water and Environmental Affairs, Republic of South Africa.

Encyclopaedia of Earth (2009).
http://www.eoearth.org/article/Soil_erosion_and_deposition surfed on 31 July 2009.

Ewen, J., Parkin, G., and O'Connell, P.E. (2000). SHETRAN: Distributed river basin flow and transport modelling system. Proceedings of the American Society of Civil Engineers, Journal of Hydrologic Engineering 5, pp. 250-258.

Guyot, J.L., Bourges, J., and Cortex, J. (1994). Sediment transport in Rio Grande, an Andean river of the Bolivian Amazon drainage basin. Variability in stream erosion and sediment transport, IAHS Publication 224, pp. 223-231.

International Commission On Large Dams. (1989). Sedimentation control of reservoirs, Guidelines, Bulletin 67.

Julien, P.Y. (1998). Erosion and sedimentation. Cambridge University Press.

Kinsel, W.G. (1980). CREAMS: A field scale model for Chemicals, Runoff, and Erosion, in Agricultural Management Systems. U.S. Department of Agriculture, Conservation Report no. 26, pp. 640.

Le Roux, J.J., Morgenthal, T.l., Malherbe, J., Smith, H.J., Weepener, H.L., and Newby, T.S. (2008). Water erosion prediction at a national scale for South Africa. Water SA 34 (3), pp. 1-10.

Ma, N. (2006). Mathematical modelling of water soil erosion and sediment yield in large catchments. MSc thesis, Stellenbosch University.

Midgley, D.C., Pitman W.V., and Middleton, B.J. (1994). Surface Water Resources Of South Africa (WR90). Water Research Commission, Volume I – VI (Appendices) and Volume I – VI (Maps), WRC Report Nos (298/1.1/94, 298/1.2/94, 298/2.1/94, 298/2.2/94, 298/3.1/94, 298/3.2/94, 298/4.1/94, 298/4.22/94, 298/5.1/94, 298/5.2/94, 298/6.1/94, 298/6.2/94.

Morgan, R.P.C., Quinton, J.N., Smith, R.E., Covers, G., Poesen, J.W.A., Auerswald, K., Chisci, G., Torri, D., and Styczen, M.E. (1998). The European Soil Erosion Model (EUROSEM): A dynamic approach for predicting sediment transport from fields and small catchments. Earth surface process and landforms, Vol. 23, pp. 527-544.

Morgan, R.P.C., Quinton, J.N., Smith, R.E., Govers, G., Poesen, J.W.A., Auerswald, K., Chisci, G., Torri, D., Styczen, M.E., and Folly, A.J.V. (1998). The European Soil Erosion Model (EUROSEM): Documentation and user guide.

Morris, G.L., and Fan, J. (1998). Reservoir sedimentation handbook: design and management of dams, reservoirs and watersheds for sustainable use. McGraw Hill.

Nearing, M.A., Foster, G.R., Lane, L.J., and Finker, S.C. (1989). A process-based soil erosion model for USDA-Water Erosion Prediction Project technology. Transactions of the American Society of Agricultural Engineers, vol. 32, no. 5, pp. 1587-1 593.

Phillips, J.D., (1991). Fluvial sediment budgets in the North Carolina Piedmont, Geomorphology, 4, pp. 231-241.

Pidwirny, M., Sidney D. (2008). Soil erosion and deposition. Encyclopaedia of Earth (Washington, D.C.: Environmental Information Coalition, National Council for

Science and the Environment <http://www.eoearth.org/article/Soil_erosion_and_deposition>http://www.eoearth.org/article/Soil_erosion_and_deposition.

Randerson, T.J., Fink, J.C., Fermanich, K.J., Baumgart, and Ehlinger, T. (2005). Suspended solids – turbidity correlation in Northeastern Wisconsin streams. AWRA.

Randle, T.J., Yang, C.T., and Daraio, J. (2006). Erosion and sedimentation manual. U.S. Department of the Interior, Bureau of Reclamation, Technical Service Centre. Sedimentation and River Hydraulics Group Denver, Colorado.

Refsgaard, J.C. (2007) Hydrological modelling of river basin management, Doctoral Thesis, Geological Survey of Denmark and Greenland, Danish Ministry of the Environment.

Renard, K.G., Foster G.R., Weesies, G.A., McCool D.K., and Yoder D.C. (1994). RUSLE Users Guide. Predicting soil erosion by water: A guide to conservation planning with the Revised Universal Soil Loss Equation. USDA, Agriculture Handbook No. 703, Washington DC, USA.

Renard, K.G., Foster, G.R., Weesies, G.A., and McCool, D.K. (1991). Predicting soil erosion by water. A guide to conservation planning with the Revised Universal Soil Loss Equation (RUSLE). USDA Agricultural Research Service, Tucson, AZ, USA, Report.

Renard, K.G., FOSTER, G.R., WEESIES, G.A., and PORTER, J.P. (1991). RUSLE: Revised Universal Soil Loss Equation. J. Soil and Water Cons., 46(1), pp. 30-33.

Rooseboom, A., Verster, E., Zietsman, H.L., and Lotriet, H.H. (1992). The development of the new sediment yield map of South Africa. WRC Report No. 297/2/92, Water Research Commission. Pretoria, South Africa.

Sadeghi, S.H., Mizuyama, T., and Vangah, B.G. (2007). Conformity of MUSLE estimates and erosion plot data for storm-wise sediment yield estimation. Terr. Atmos. Ocean. Sci., Vol. 18, No. 1, pp. 117-128.

South African National Roads Agency Limited. (2006). Drainage Manual, 5th Edition

Schmidt, J., Elliot, S., and McKergow, l. (2008). Land use impacts on catchment erosion for the Waitetuna catchment. New Zealand. Sediment dynamics in changing environments. IAHS Publication 325, pp. 453 -457.

SHETRAN Version 4. (2008). User Manual. Viewed on 14th February 2009, http://www.ceg.ncl.ac.uk/shetran

SHETRAN Version 4. (2008b). Example Data sets. Viewed on 14th February 2009 http://www.ceg.ncl.ac.uk/shetran

Slaymaker, 0., and Spencer, T. (1998). Physical Geography and Global Environmental Change. Addison Wesley Longman Ltd, Essesx, UK.

Smithers, J., Schulze, R. (2002). ACRU Agrohydrological Modelling System User Manual Version 3.0.0.

Strand, R.I., and Pemberton E.L. (1982). Reservoir sedimentation technical guidelines for Bureau of Reclamation. U.S. Bureau of Reclamation, Denver, Colorado, pp. 48.

Villiers J.W.L. (2006). 2D modelling of turbulent transport of cohesive sediment in shallow reservoirs. MSc thesis, Stellenbosch University.

Waterinformation. (2009). http://www.waterinformation.co.za, surfed on 20th July 2009 .

Wicks, J. M., and Bathurst, J. C. (1996). SHESED: A physically based, distributed erosion and sediment yield component for the SHE hydrological modelling system. Journal of Hydrology, 175 (1996), pp. 213-238.

Wicks, J.M., Bathurst, J.C., and Johnson, C.W. (1992). Calibrating SHE soil-erosion model for different land covers. ASCE Journal of Irrigation and Drainage Engineering, 118, pp. 708-723.

Williams, J. R., and Berndt, H.D. (1977). Sediment yield prediction based on watershed hydrology. Trans. Am. Soc. Agric. Eng., 20, pp. 1100-1104.

Williams, J.R. (1975). Sediment yield prediction with universal equation using runoff energy factor, In: Present and Prospective Technology for Predicting Sediment Yields and Sources. USDAARS, 40, pp. 244-252.

Wischmeier, W. H., and Smith, D. D. (1965). Predicting rainfall-erosion losses from cropland east of the Rocky Mountains. Agriculture Handbook No. 282, Washington DC.

Wischmeier, W.H., and Smith, D.D. (1978). Predicting rainfall erosion losses - a guide to conservation planning. USDA, Washington DC, Agricultural Handbook, pp. 537.

Woolhiser, D.A., Smith, R.E., and Goodrich, D.C. (1990). KINEROS, A Kinematic Runoff and Erosion Model: User Manual. U.S. Department of Agriculture, Agricultural Research Service, ARS-77, pp. 130.

Yalin, M.S. (1963). An expression for bed-load transportation. J. Hydraulics Division ASCE, 98(HY3), pp. 221-250.

APPENDIX A ERODIBILITY INDICES FOR EACH SEDIMENT YIELD REGION

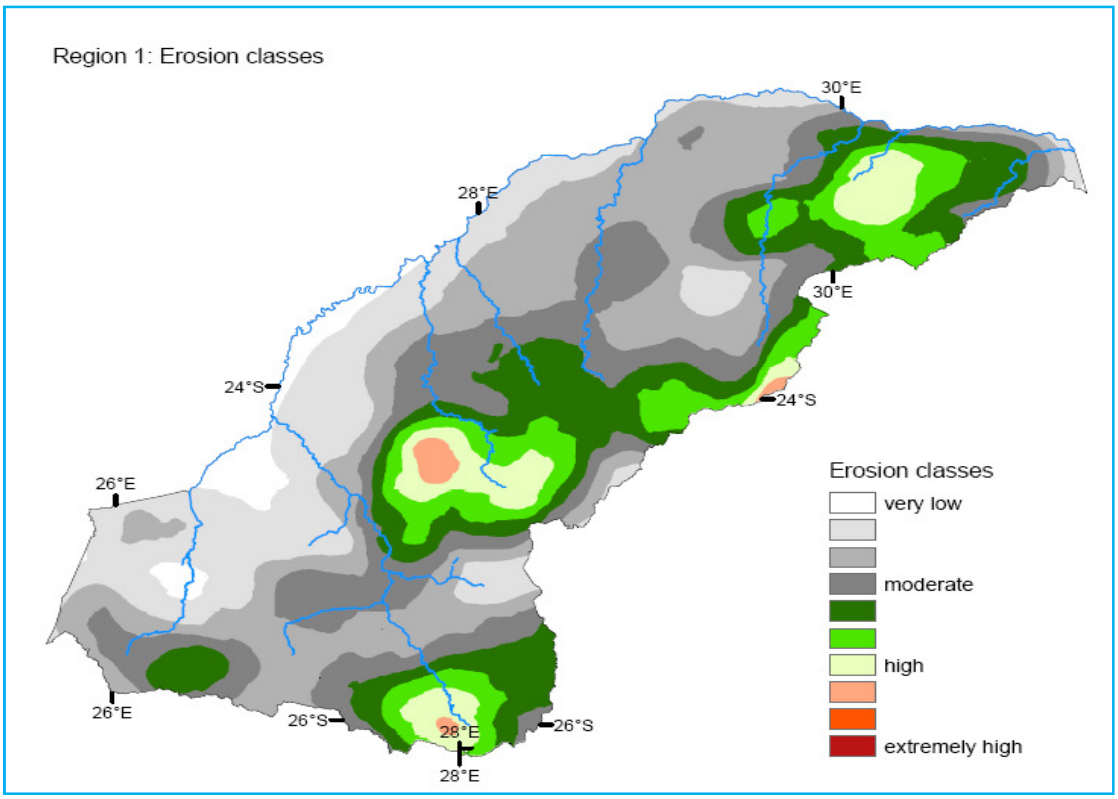
Region 1: Erosion classes
30°E
28°E
30°E
24°S
24°S
26°E
26°E
26°S
28°E
26°S
28°E
Erosion classes
very low
moderate
high
extremely high

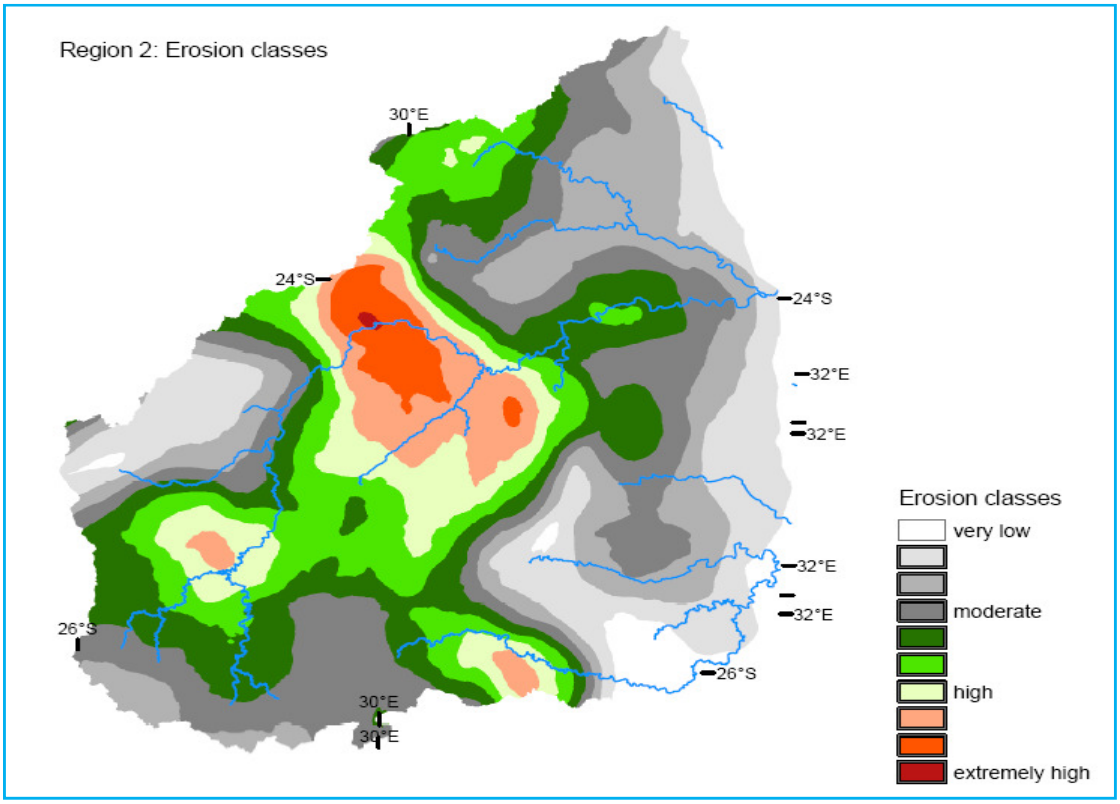
Region 2: Erosion classes
30°E
24°S
24°S
32°E
32°E
32°E
32°E
26°S
26°S
30°E
30°E
Erosion classes
very low
moderate
high
extremely high

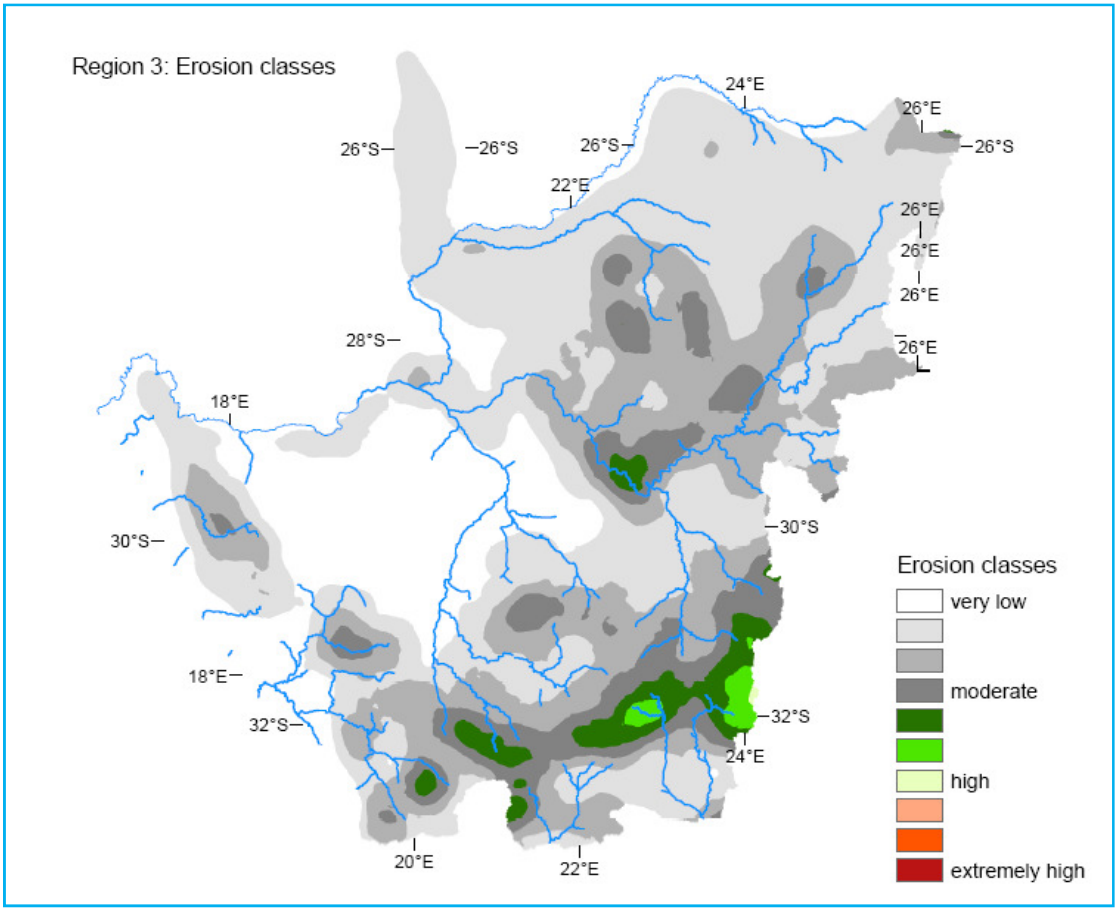
Region 3: Erosion classes
24°E
26°E
26°S
22°E
28°S
18°E
30°S
32°S
20°E
Erosion classes
very low
moderate
high
extremely high

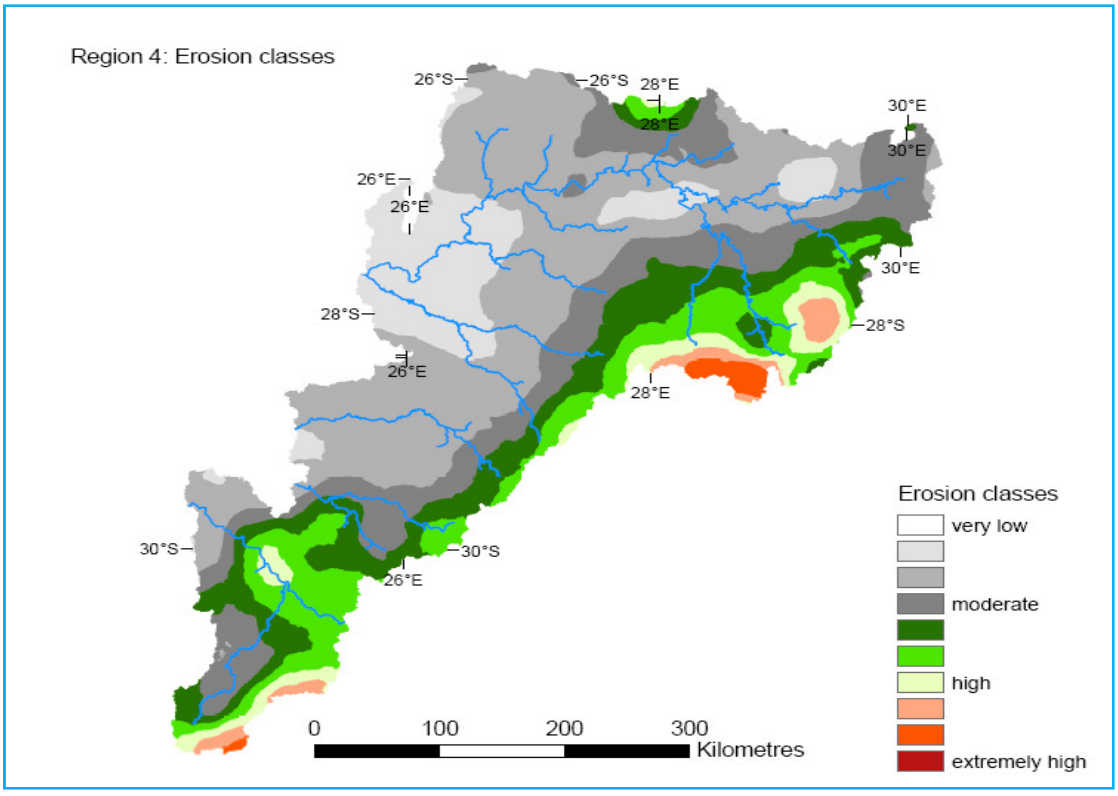
Region 4: Erosion classes
26°S
28°E
30°E
26°E
28°S
30°S
0
100
200
300
Kilometres
Erosion classes
very low
moderate
high
extremely high

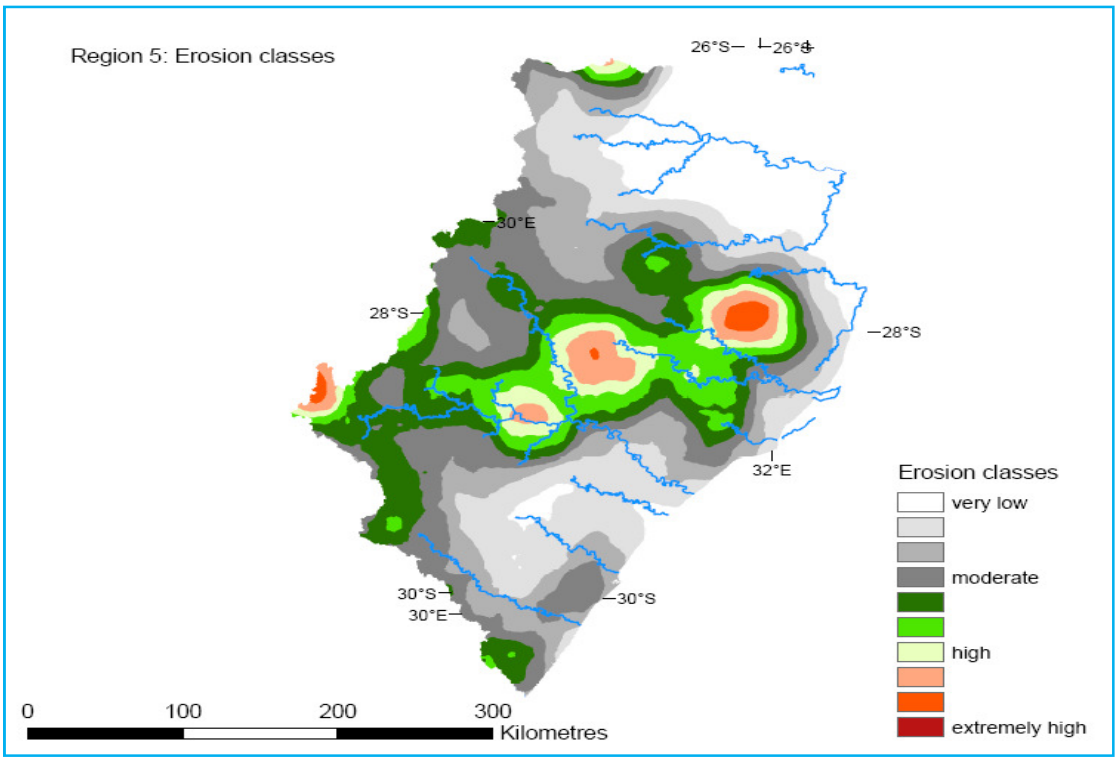
Region 5: Erosion classes
26°S
26°E
30°E
28°S
28°S
32°E
30°S
30°S
30°E
Erosion classes
very low
moderate
high
extremely high
0
100
200
300
Kilometres

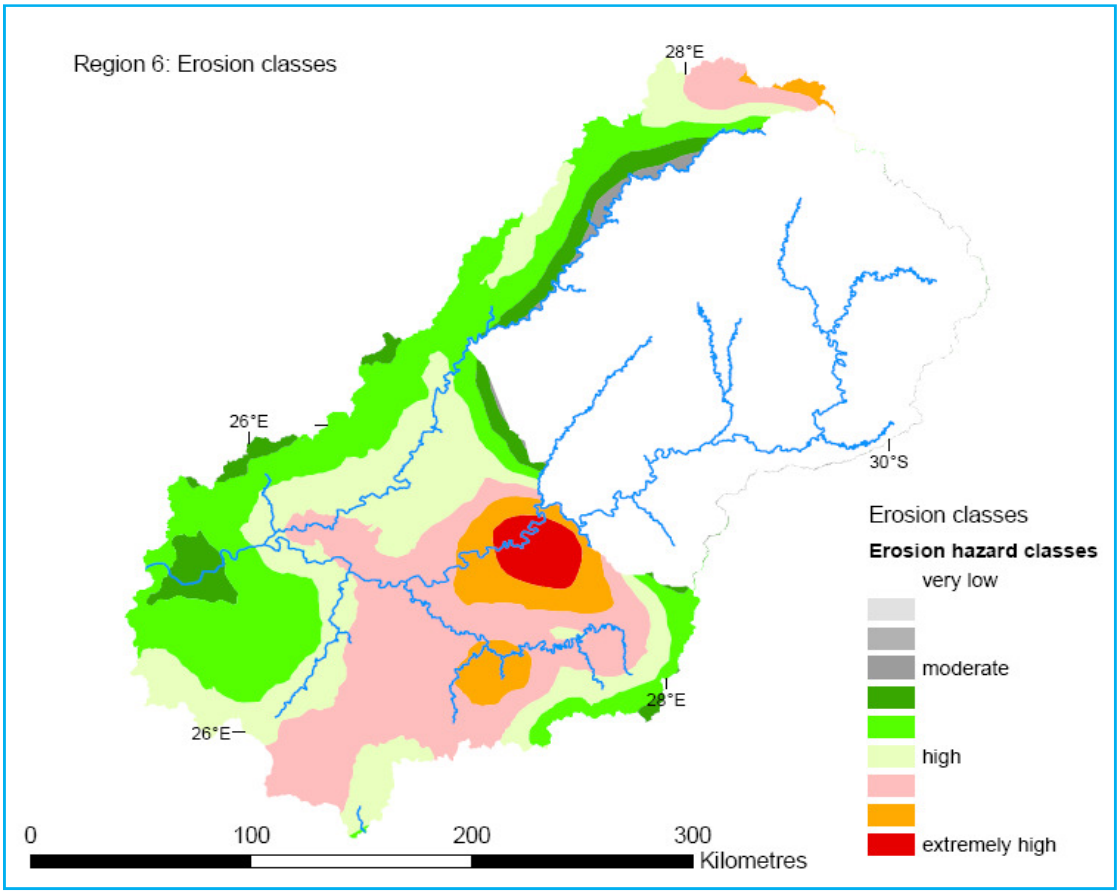
Region 6: Erosion classes
28°E
26°E
30°S
28°E
26°E
Erosion classes
Erosion hazard classes
very low
moderate
high
extremely high
0
100
200
300
Kilometres

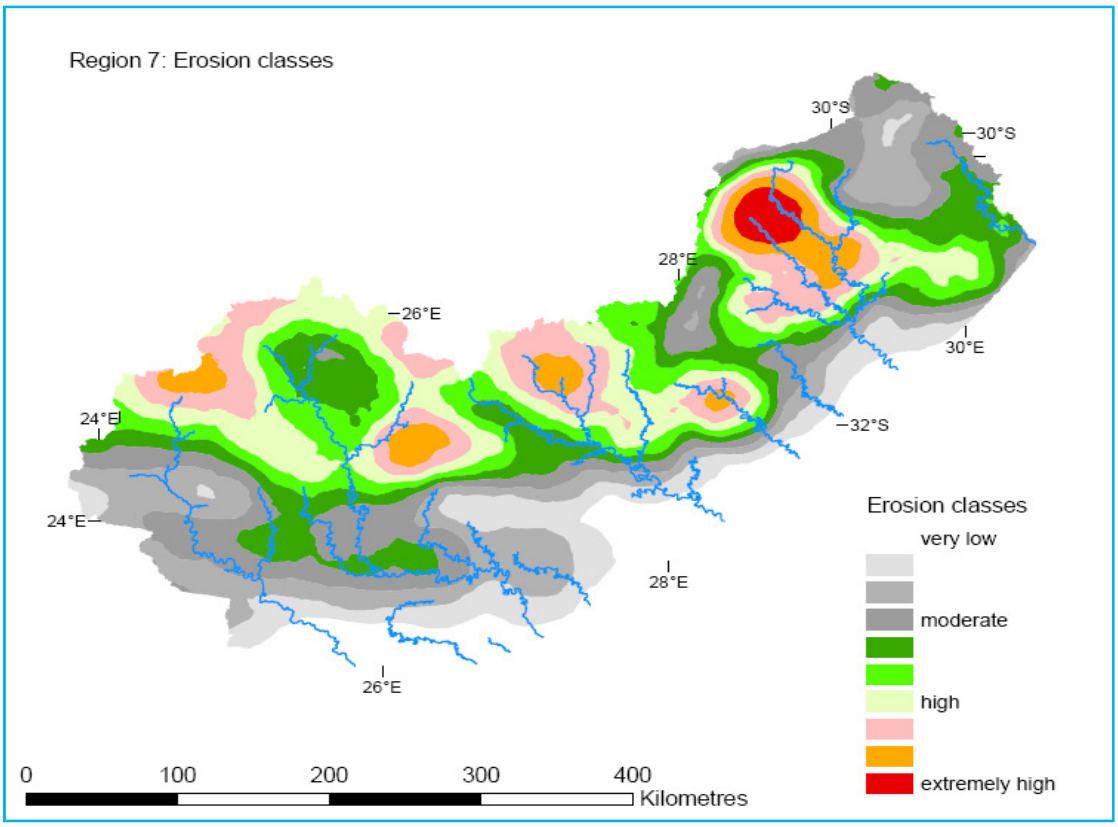
Region 7: Erosion classes
30°S
30°S
28°E
26°E
30°E
32°S
24°E
24°E
28°E
26°E
Erosion classes
very low
moderate
high
extremely high
0
100
200
300
400
Kilometres

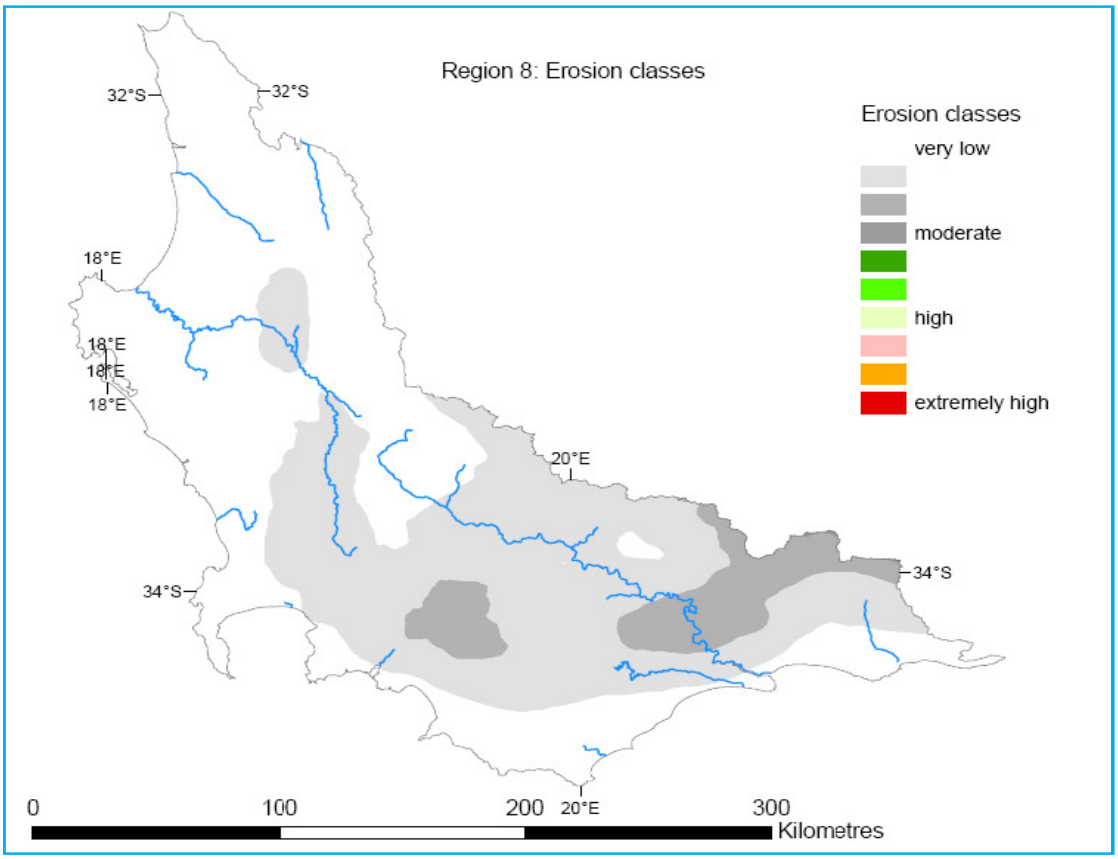
Region 8: Erosion classes
32°S
32°S
18°E
18°E
18°E
18°E
20°E
34°S
34°S
Erosion classes
very low
moderate
high
extremely high
0
100
200
20°E
300
Kilometres

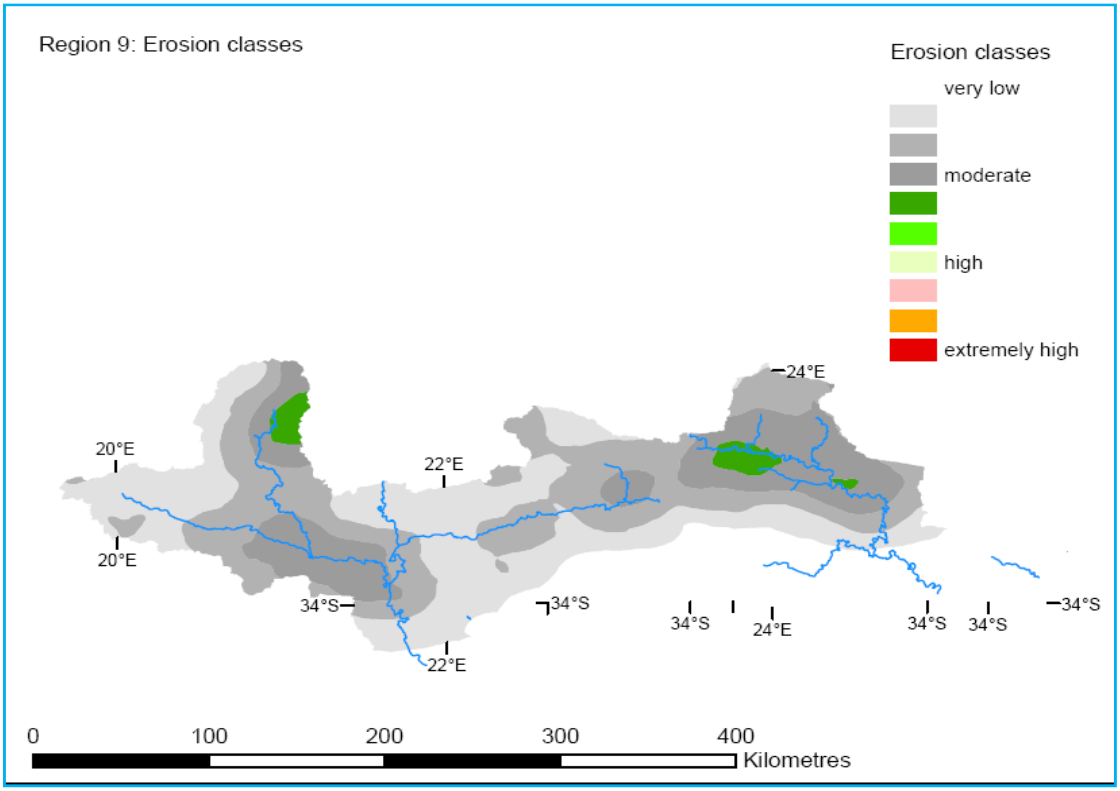
Region 9: Erosion classes
Erosion classes
very low
moderate
high
extremely high
20°E
20°E
22°E
22°E
24°E
24°E
34°S
34°S
34°S
34°S
34°S
34°S
0
100
200
300
400
Kilometres

APPENDIX B FINAL ADOPTED SEDIMENT YIELD VALUES

Name	Station No	Sediment Yield (t/km^2.a)	Effective Catchment Area (km^2)	Region
Albasini Dam	A9R001	84	501	1
Bospoort Dam	A2R006	152	580	1
Buffelspoort Dam	A2R005	126	116	1
Cross Dam		129	302	1
Doorndraai Dam	A6R001	167	387	1
Gert Combrink Dam	A6R004	15	176	1
Hans Strijdom Dam		9	4329	1
Hartebeespoort Dam	A2R001	110	3474	1
Klein-Maricopoort Dam	A3R002	24	828	1
Klipvoor Dam	A2R012	13	4708	1
Koster Dam	A2R011	27	289	1
Kromellenboog Dam	A3R003	120	607	1
Kudube Dam (Leeukraal)	A2R016	15	389	1
Lehujwane Dam	A3R005	105	201	1
Madikwe Dam		63	313	1
Marico-Bosveld Dam	A3R001	63	948	1
Ngotwana Dam	A1R001	41	504	1
Olifantsnek Dam	A2R003	101	499	1
Rietvlei Dam	A2R004	35	490	1
Roodeplaat Dam	A2R009	95	689	1
Vaalkop Dam	A2R014	53	3918	1
Blyderivierspoort Dam	B6R003	25	1235	2
Bronkhorstspruit Dam	B2R001	77	1244	2
Buffelkloof Dam	B4R004	25	279	2
Da Gama Dam	X3R001	339	44	2
Ebenezer Dam	B8R001	156	126	2
Hans Merensky Dam	B8R002	27	89	2
Klaserie Dam	B7R001	122	168	2
Klipkoppie Dam	X2R002	219	77	2
Kwena Dam	X2R005	36	950	2
Longmere Dam	X2R001	226	32	2
Loskop Dam	B3R002	48	3973	2

Name	Station No	Sediment Yield (t/km^2.a)	Effective Catchment Area (km^2)	Region
Magoebaskloof Dam	B8R003	73	81	2
Middel Letaba	B8R007	520	1051	2
Nooitgedag Dam	X1R001	31	1583	2
Ohrigstad Dam	B6R001	40	85	2
Rietfontein Dam		53	86	2
Rietspruit Dam	C2R007	62	392	2
Rust de Winter Dam	B3R001	25	1127	2
Trichardsfontein Dam	B1H022	72	11	2
Tzaneen Dam	B8R005	248	284	2
Vlugkraal Dam	B4R002	46	14	2
Vygeboom Dam	X1R003	93	1541	2
Witklip Dam	X2R003	402	60	2
Corumana		330	6271	2
Massingir		245	63350	2
Disaneng Dam	D4R003	22	3817	3
Gamkapoort Dam	J2R006	41	14535	3
Leeu-Gamka Dam	J2R002	26	2030	3
Oukloof Dam	J2R003	48	155	3
Spitskop Dam	C3002	11	14845	3
Victoria West Dam	D6R001	44	311	3
Upington		205	117932	3
Allemanskraal Dam	C4R001	411	2405	4
Armenia Dam	D2R002	96	260	4
Bloemhof Dam	C9R002	75	30601	4
Boskop Dam	C2R001	11	2172	4
Erfenis Dam	C4R002	163	4188	4
Grootdraai Dam	C1R002	63	7057	4
Jericho Dam	W5R001	245	211	4
Kalkfontein Dam	C5R002	100	8664	4
Klerkskraal Dam	C2R003	18	1272	4
Klipdrif Dam	C2R005	15	875	4

Name	Station No	Sediment Yield (t/km^2.a)	Effective Catchment Area (km^2)	Region
Koppies Dam	C7R001	126	2145	4
Kriegerspoort Dam		32	638	4
Krugersdrif Dam	C5R004	104	4453	4
Loch Athlone Dam	C8R005	95	122	4
Lucretia Dam		25	374	4
P.K. Le Roux Dam/ Vanderkloof	D3R003	137	17858	4
Rusfontein Dam	C5R003	184	868	4
Saulspoort Dam	C8R004	111	731	4
Tierpoort Dam	C5R001	128	918	4
Vaal Dam	C1R001	163	25678	4
Barrage - Vaal		85	31145	4
Leewkraal		100	9936	4
Oranjerivierbrug		630	22834	4
Paardeberg		312	14175	4
Sannaspos		304	931	4
Standerton		193	7958	4
Upington		205	16911	4
Wilge		32	1455	4
Albert Falls Dam	U2R003	31	731	5
Chelmsford Dam	V3R001	236	838	5
Craigie Burn Dam	V2R001	656	156	5
Goedertrouw Dam	W1R001	524	1275	5
Hammarsdale Dam		100	48	5
Hazelmere Dam	U3R001	714	382	5
Henley Dam	U2R005	74	219	5
Hluhluwe Dam	W3R001	203	725	5
Jericho Dam	W5R001	245	211	5
Kilburn Dam	V1R004	756	30	5
Klipfontein Dam	W2R001	121	281	5
Midmar Dam	U2R001	93	931	5
Pongolapoort Dam	W4R001	1038	10927	5
Spioenkop Dam	V1R001	581	803	5

Name	Station No	Sediment Yield (t/km^2.a)	Effective Catchment Area (km^2)	Region
Wagendrift Dam	V7R001	167	755	5
Woodstock Dam	V1R003	318	875	5
Colenso		571	4198	5
Intulembi		133	8806	5
Bethulie Dam	D3R001	519	232	6
Gariep Dam	D3R002	392	28091	6
J.L. De Bruin Dam		13	976	6
Aliwal-North		623	13465	6
Bethulie	D3H002	778	14105	6
Caledon River @ Lesotho		1141	934	6
Caledon River @ Slabbertswag	D2H016	832	659	6
Jammersdrift		621	4448	6
Bridle Drift Dam	R2R003	1509	252	7
Darlington Dam	N2R001	210	10397	7
Doringrivier Dam	S2R002	617	310	7
Elandskuil Dam	C2R006	158	22	7
Grassridge Dam	Q1R001	236	3507	7
Gubu Dam	S6R001	840	16	7
Katrivier Dam	Q9R001	306	262	7
Kommandodrift Dam	Q4R002	152	2627	7
Laing Dam	R2R001	95	834	7
Loerie Dam	L9R001	193	149	7
Maden Dam		49	31	7
Mtata Dam	T2R001	262	882	7
Nahoon Dam	R3R001	106	478	7
Ncora Dam	S5R001	219	1775	7
Nuwejaars Dam		4	519	7
Poortjie Dam		156	26	7
Van Ryneveldspas Dam	N1R001	207	3666	7
Waterdown Dam	S3R001	12	583	7
Xilinxa Dam	S7R002	378	209	7

Name	Station No	Sediment Yield (t/km^2.a)	Effective Catchment Area (km^2)	Region
Xonxa Dam	S1R001	888	1476	7
Buffelsfontein	Q8H001	589	173	7
Doornhoek	S3H002	558	811	7
Grootvlakte		279	803	7
Hougham Abramson		209	13305	7
Jansenville		136	1921	7
Roberts Kraal		19	974	7
Bellair Dam	J1R002	57	509	8
Clanwilliam Dam	E1R002	206	1954	8
Duiwenhoks Dam	H8R001	43	147	8
Elandskloof Dam	H6R002	236	51	8
Keerom Dam	H4R002	87	389	8
Korentepoort Dam	H9R001	123	35	8
Lakenvallei Dam	H2R002	118	86	8
Miertjieskraal Dam	J1R004	16	254	8
Pietersfontein Dam	H3R002	260	114	8
Poortjieskloof Dam	H3R001	156	86	8
Roode Elsberg Dam	H2R001	344	53	8
Stettynskloof Dam		49	60	8
Wemmershoek Dam	G1R002	450	86	8
Goudmyn/Rooiburg		10	1	8
Nieuwkloof		69	397	8
Calitzdorp Dam	J2R001	149	165	9
Churchill Dam	K9R001	10	354	9
Floriskraal Dam	J1R003	145	4029	9
Impofu Dam	K9R002	7	486	9
Kammanassie Dam	J3R001	53	1527	9
Kouga Dam	L8R001	18	3856	9
Prinsrivier Dam	J1R001	129	753	9
Raubenheimer Dam	J3R003	6	52	9
Stompdrift Dam	J3R002	75	5249	9

APPENDIX C DETERMINATION OF SEDIMENT POTENTIAL FACTORS

		Erosion Hazard Class												
Station Name	**Total Area (km^2)**	**1**	**2**	**3**	**4**	**5**	**6**	**7**	**8**	**9**	**10**	**Observed Sediment Yield**	**Weighted Erosion Hazard Class**	**Dominant Erosion Hazard Class**
Bridle Drift Dam	252	132	120	0	0	0	0	0	0	0	0	1,509	1.48	1
Darlington Dam	10,397	0	102	4038	3991	1795	445	25	0	0	0	210	3.86	4
De Mistkraal	1,871	0	0	0	1871	0	0	0	0	0	0	37	4.00	4
Doringrivier Dam	310	0	0	0	0	0	0	119	191	0	0	617	7.62	8
Elandskuil Dam	22	0	0	14	8	0	0	0	0	0	0	158	3.35	3
Grassridge Dam	3,507	0	0	0	118	316	634	2395	44	0	0	236	6.55	7
Gubu Dam	16	0	16	0	0	0	0	0	0	0	0	840	2.00	2
Katrivier Dam	262	0	156	83	23	0	0	0	0	0	0	306	2.49	2
Kommandodrift Dam	2,627	0	0	0	0	93	510	813	511	701	0	152	7.46	7
Laing Dam	834	99	601	134	0	0	0	0	0	0	0	95	2.04	2
Loerie Dam	149	149	0	0	0	0	0	0	0	0	0	193	1.00	1
Maden Dam	31	0	31	0	0	0	0	0	0	0	0	49	2.00	2
Mtata Dam	882	0	0	0	139	393	282	67	0	0	0	262	5.31	5
Nahoon Dam	478	415	63	0	0	0	0	0	0	0	0	106	1.13	1
Ncora Dam	1,775	0	0	0	0	40	958	705	72	0	0	219	6.46	6
Nuwejaars Dam	519	0	108	378	32	0	0	0	0	0	0	4	2.85	3
Poortjie Dam	26	0	0	26	0	0	0	0	0	0	0	156	3.00	3
Van Ryneveldspas Dam	3,666	0	0	0	12	69	684	150	1936	814	0	207	7.74	8
Waterdown Dam	583	0	31	19	104	357	73	0	0	0	0	12	4.72	5
Xilinxa Dam	209	0	0	0	0	83	113	13	0	0	0	378	5.66	6
Xonxa Dam	1,476	0	0	0	0	0	0	341	904	231	0	888	7.93	8
Buffelsfontein	173	0	0	0	0	164	9	0	0	0	0	589	5.05	5
Doornhoek	811	0	0	0	0	0	16	591	204	0	0	558	7.23	7
Grootvlakte	803	0	0	0	0	27	345	431	0	0	0	279	6.50	7
Hougham Abramson	13,305	0	0	0	402	1767	3016	3887	2980	1253	0	209	6.83	7
Jansenville	1,921	0	423	928	403	168	0	0	0	0	0	136	3.16	3
Roberts Kraal	974	0	0	0	0	235	574	159	7	0	0	19	5.94	6

APPENDIX D REGIONAL GRAPHS FOR STATISTICAL ANALYSIS

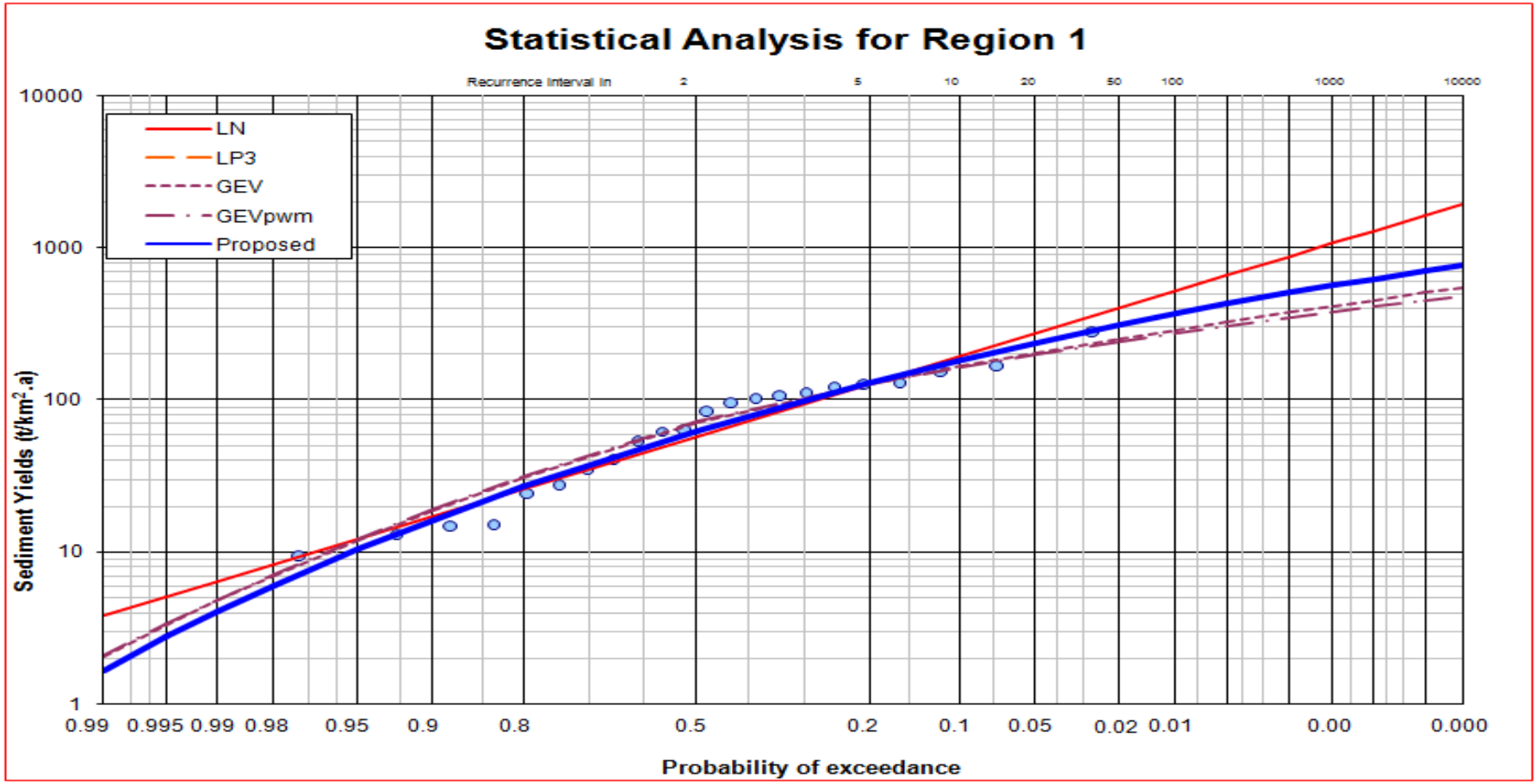

Statistical Analysis for Region 1

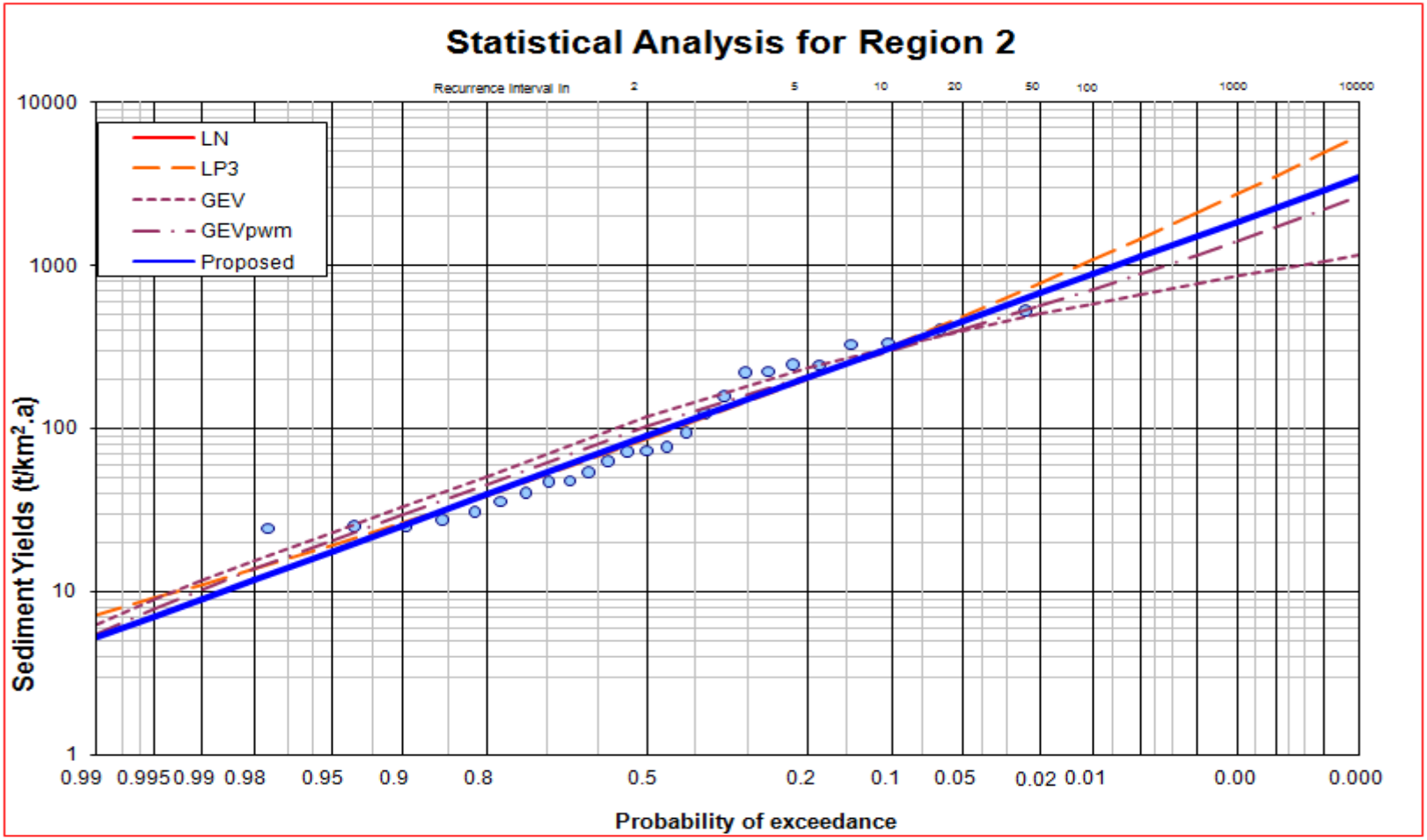

Statistical Analysis for Region 2

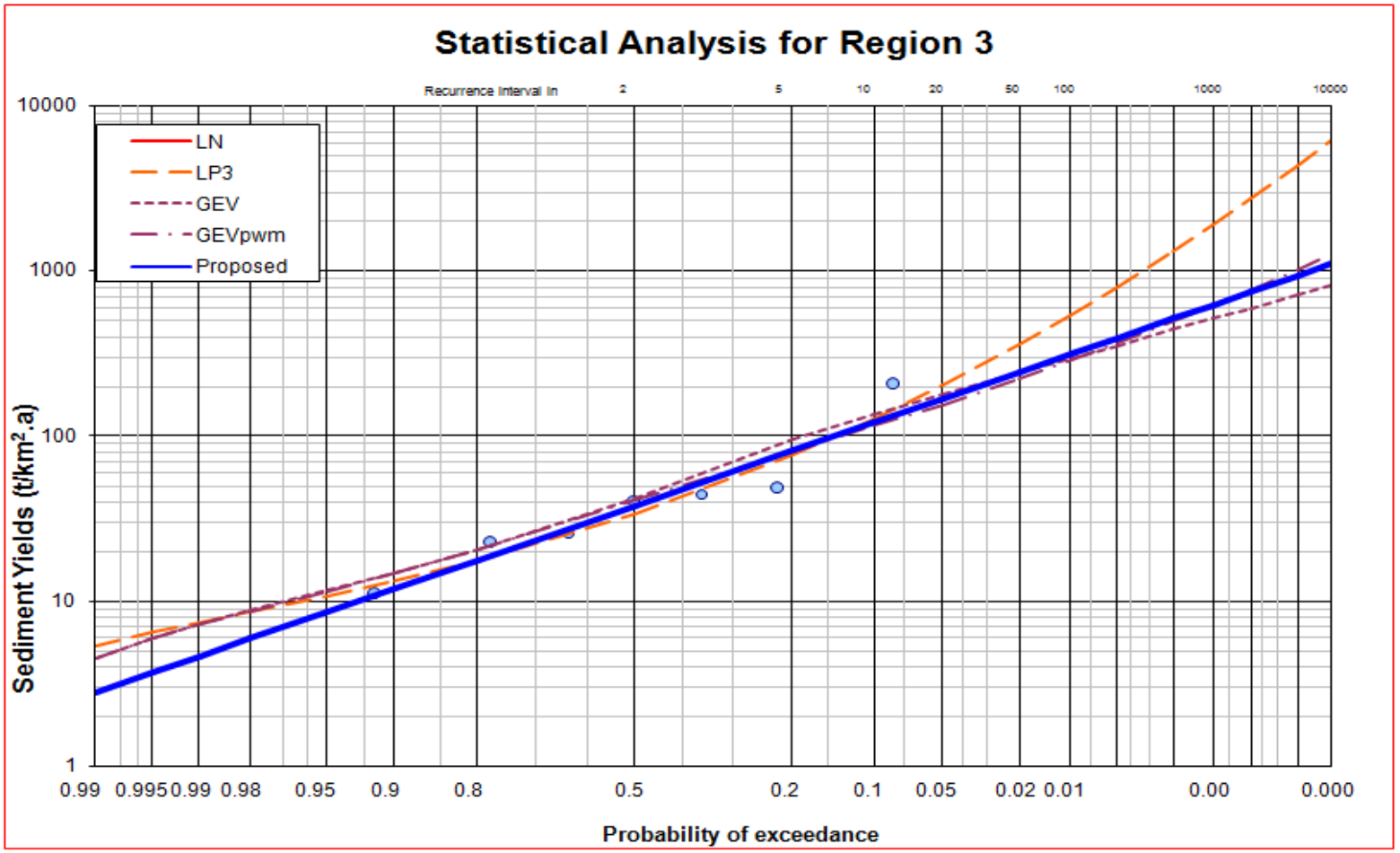

Statistical Analysis for Region 3

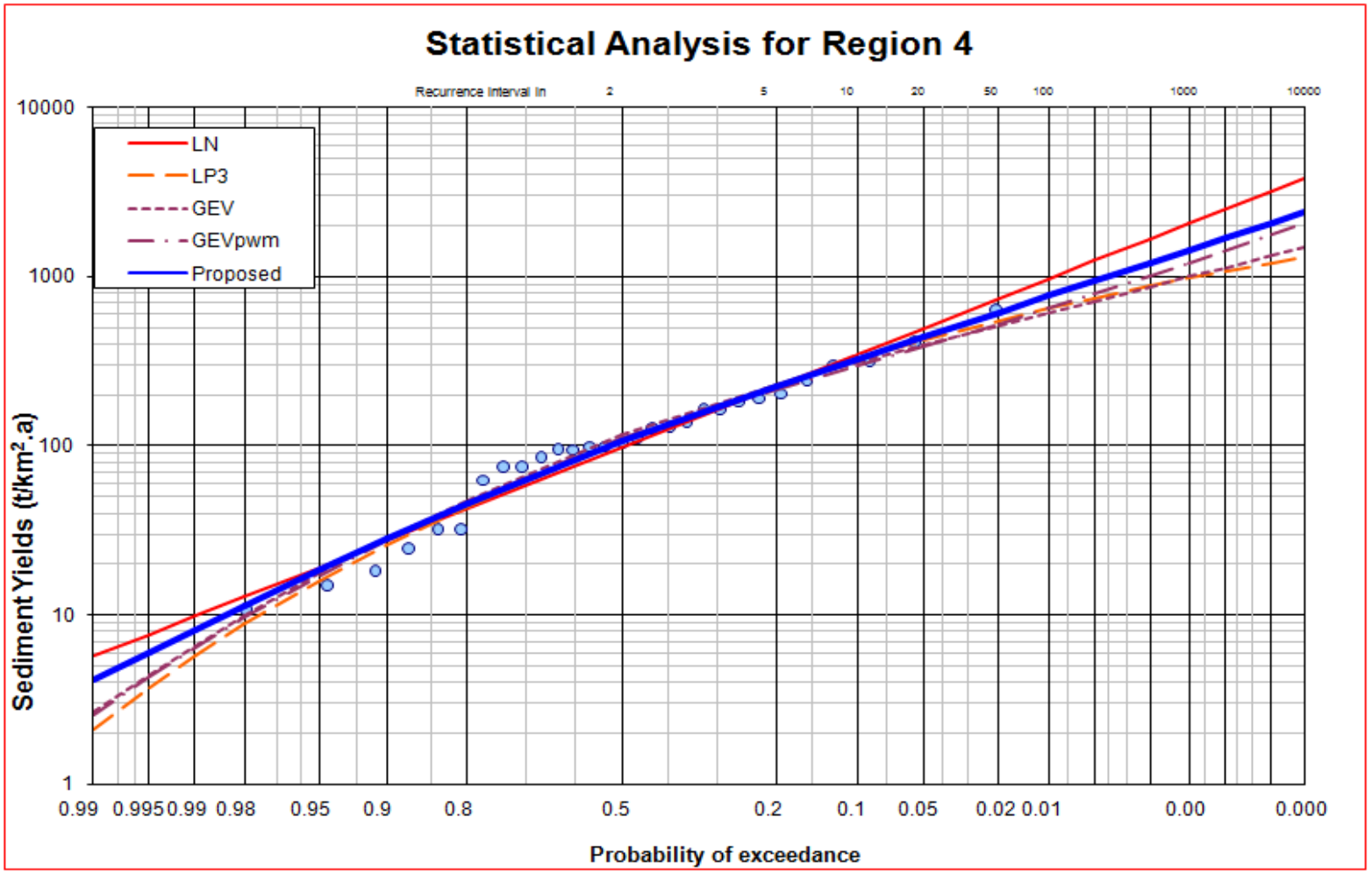

Statistical Analysis for Region 4

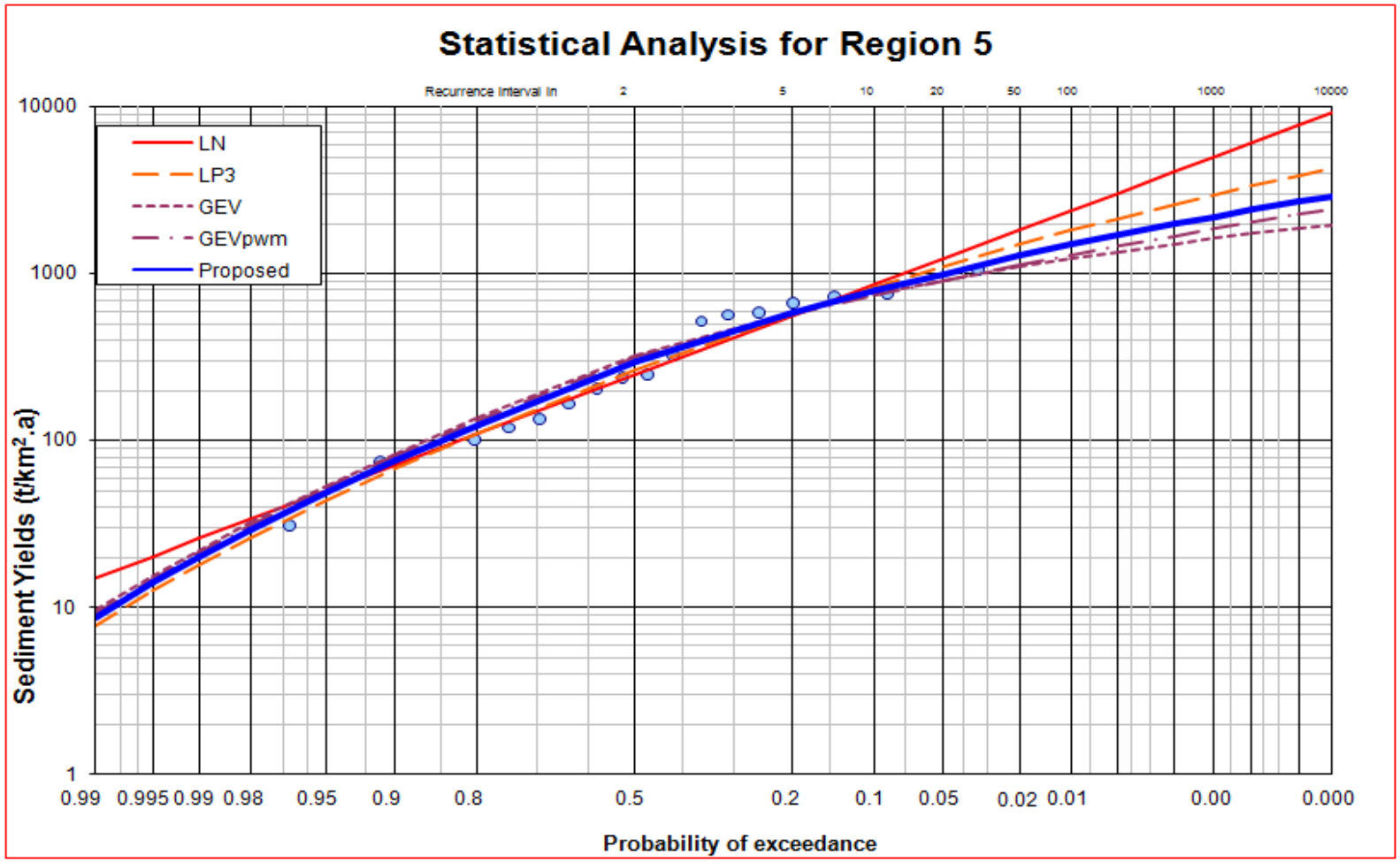

Statistical Analysis for Region 5

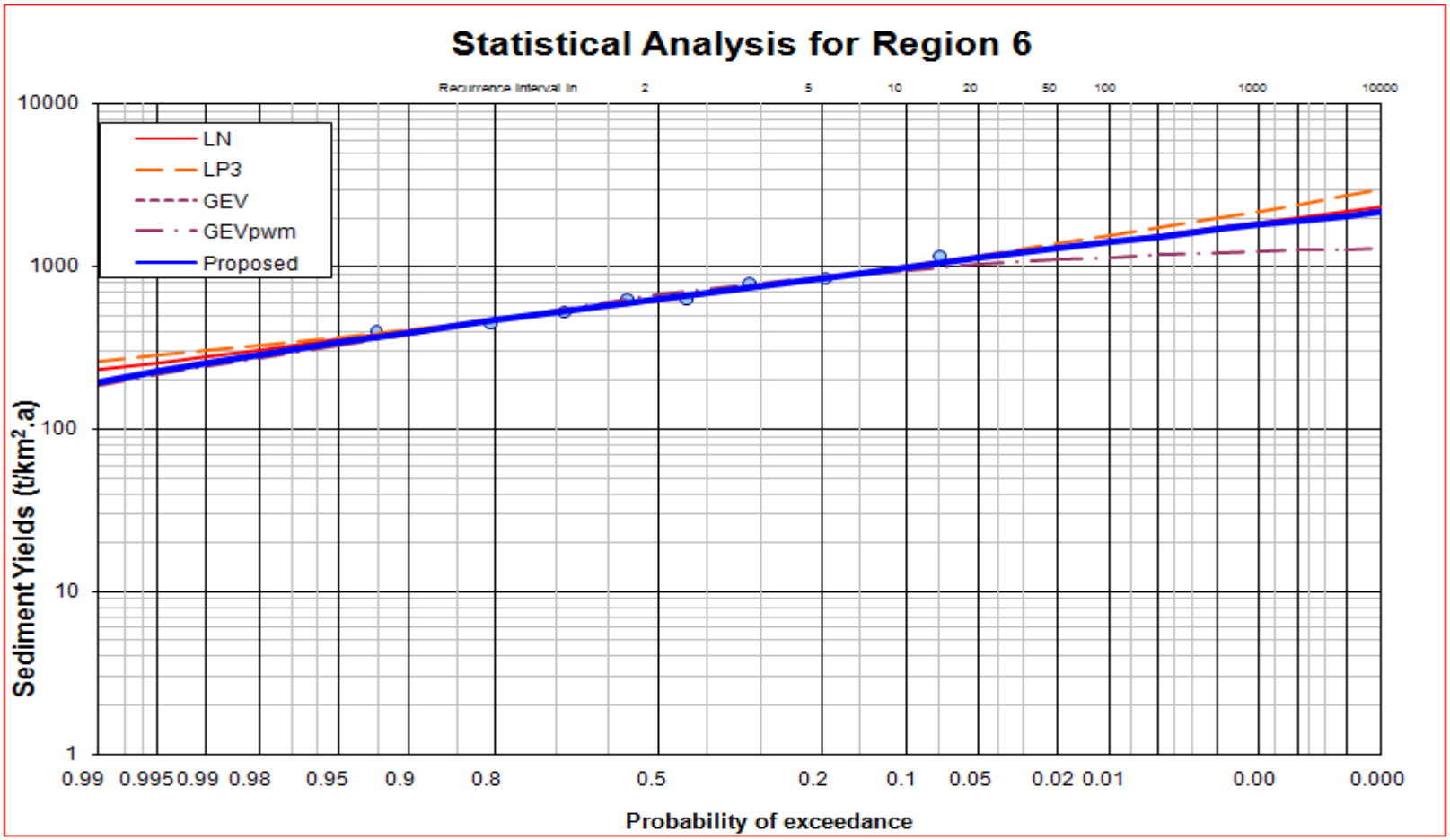

Statistical Analysis for Region 6

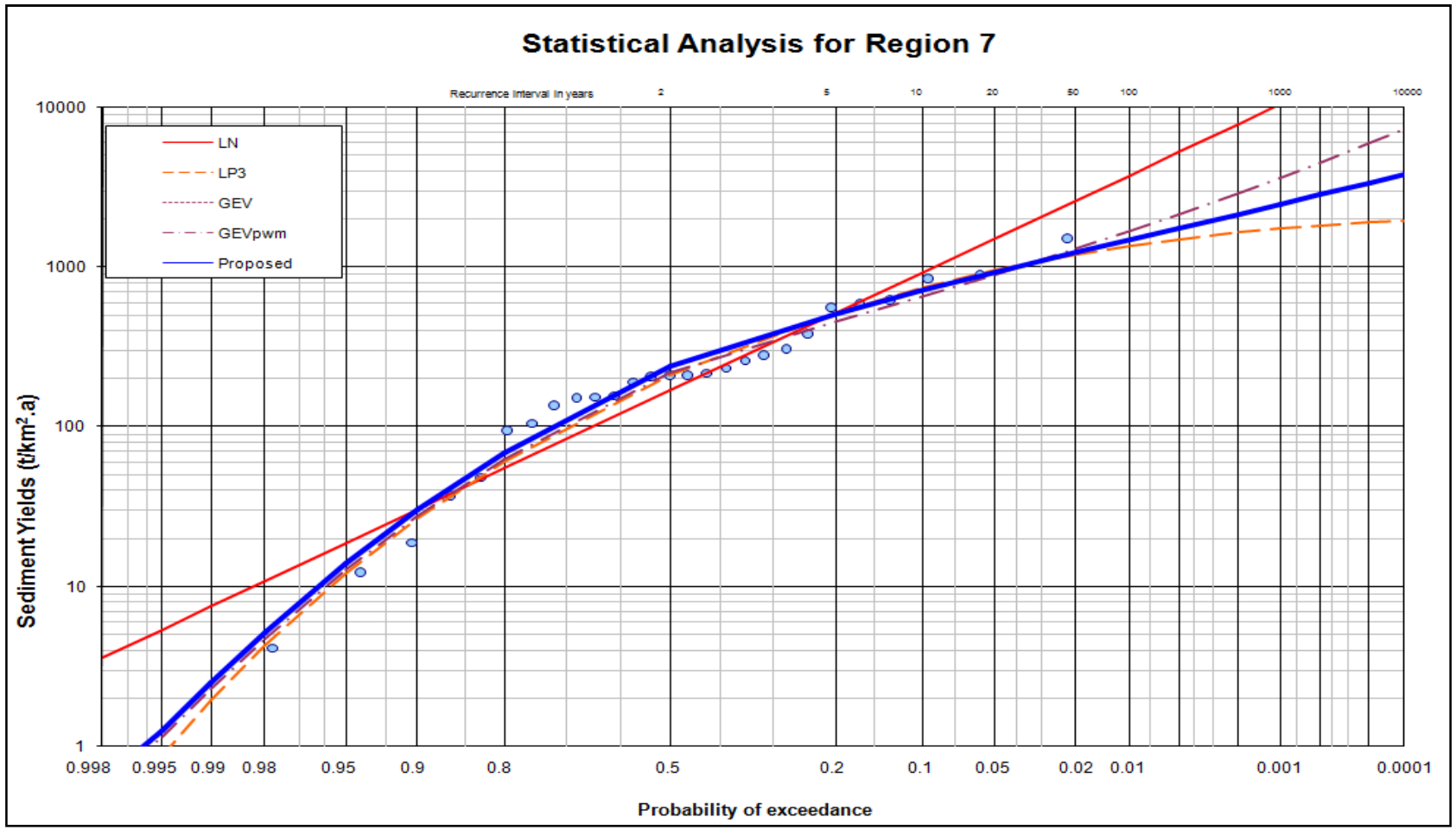

Statistical Analysis for Region 7

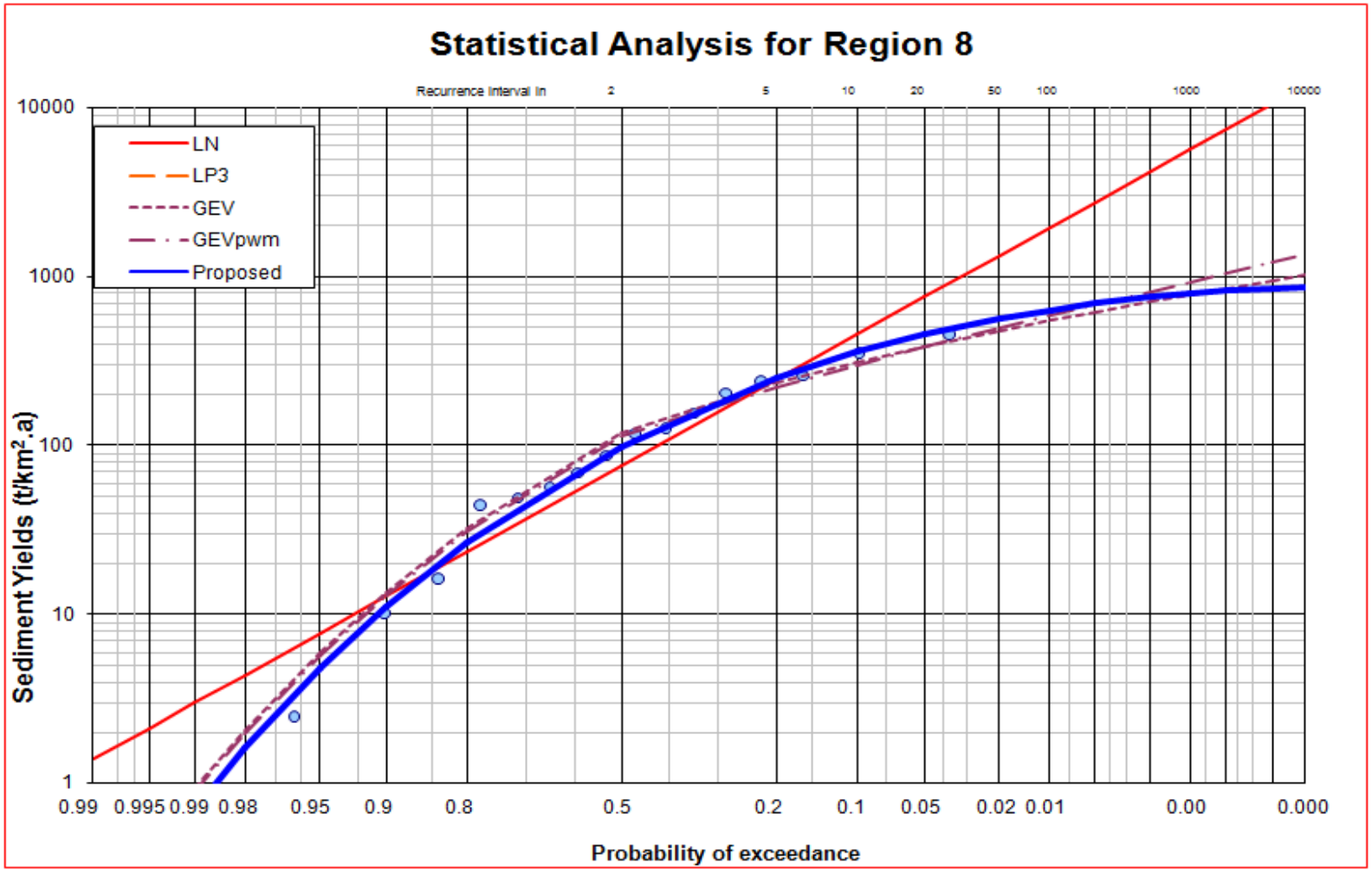

Statistical Analysis for Region 8

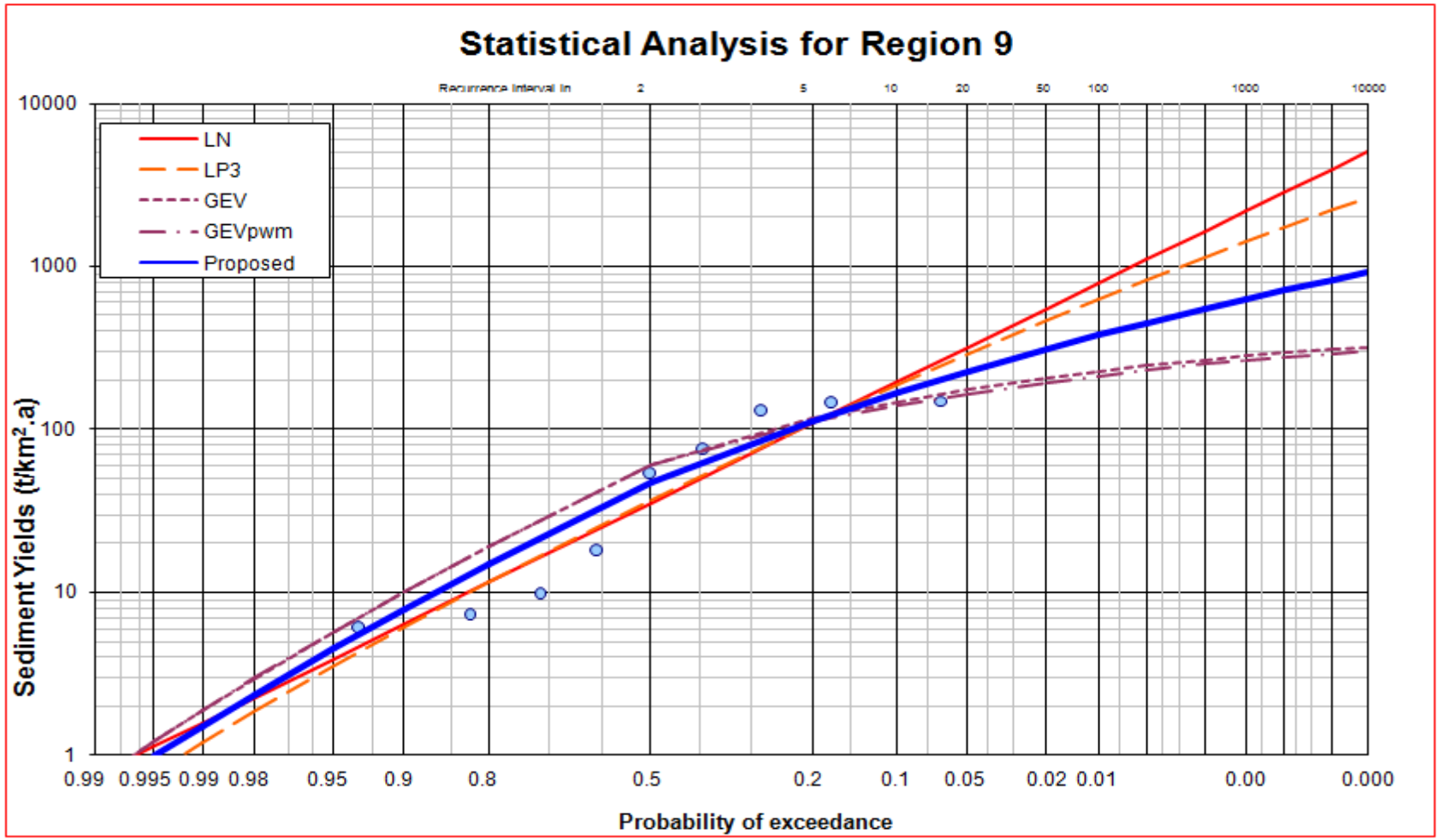

Statistical Analysis for Region 9

APPENDIX E REGIONAL SEDIMENT YIELD CONFIDENCE BANDS

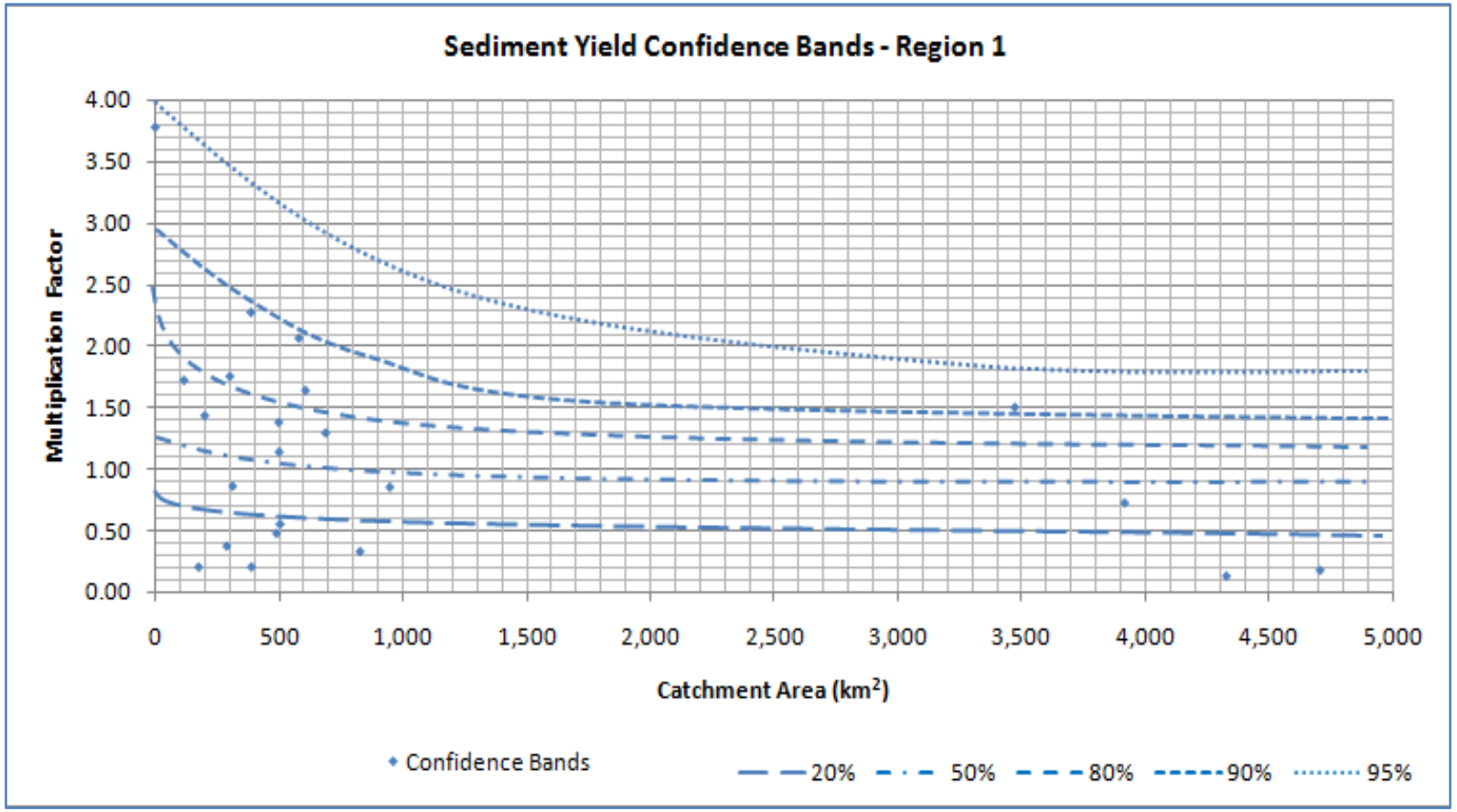
Sediment Yield Confidence Bands - Region 1
Multiplication Factor
4.00
3.50
3.00
2.50
2.00
1.50
1.00
0.50
0.00
0
500
1,000
1,500
2,000
2,500
3,000
3,500
4,000
4,500
5,000
Catchment Area (km²)
Confidence Bands
20%
50%
80%
90%
95%

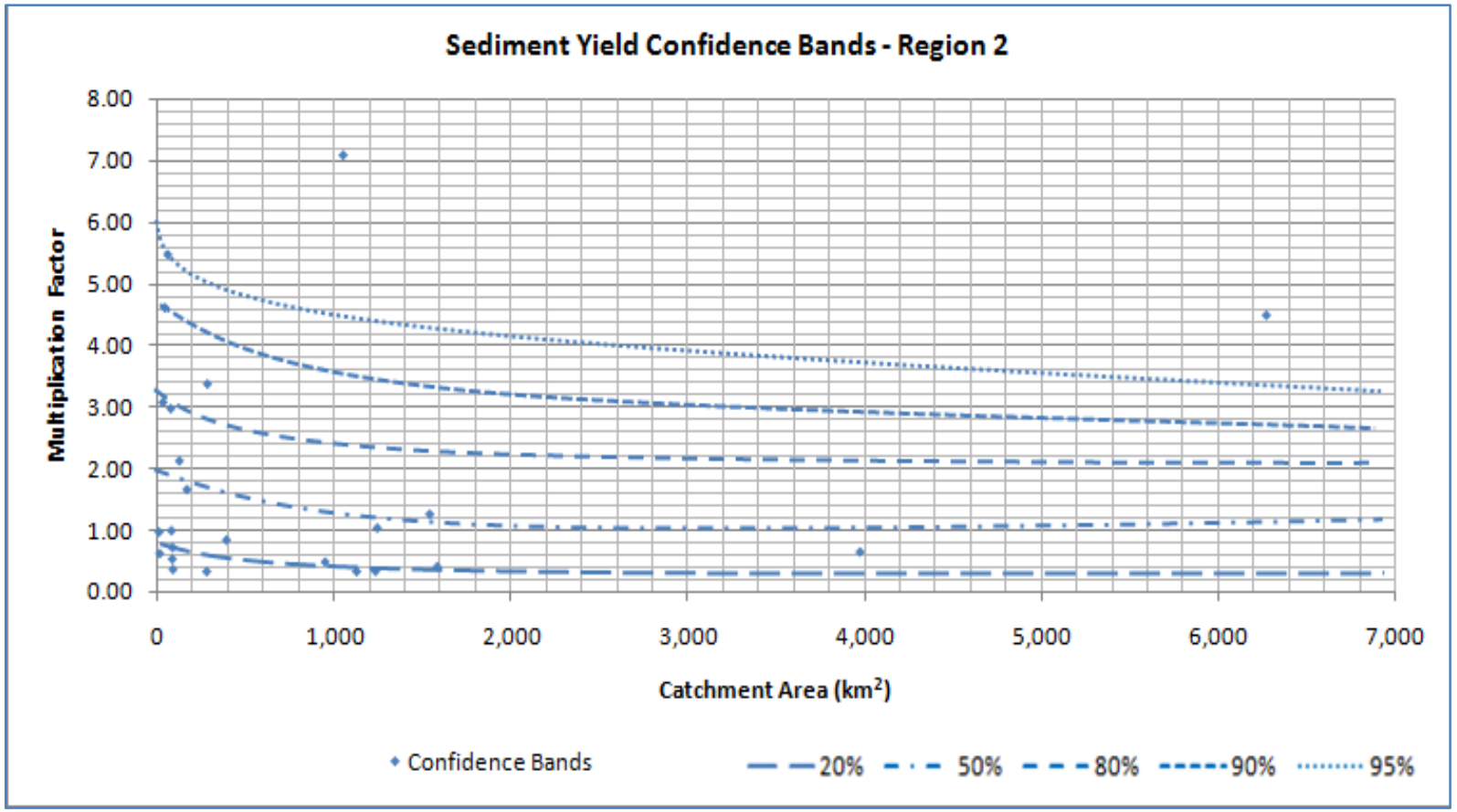
Sediment Yield Confidence Bands - Region 2
Multiplication Factor
8.00
7.00
6.00
5.00
4.00
3.00
2.00
1.00
0.00
0
1,000
2,000
3,000
4,000
5,000
6,000
7,000
Catchment Area (km²)
Confidence Bands
20%
50%
80%
90%
95%

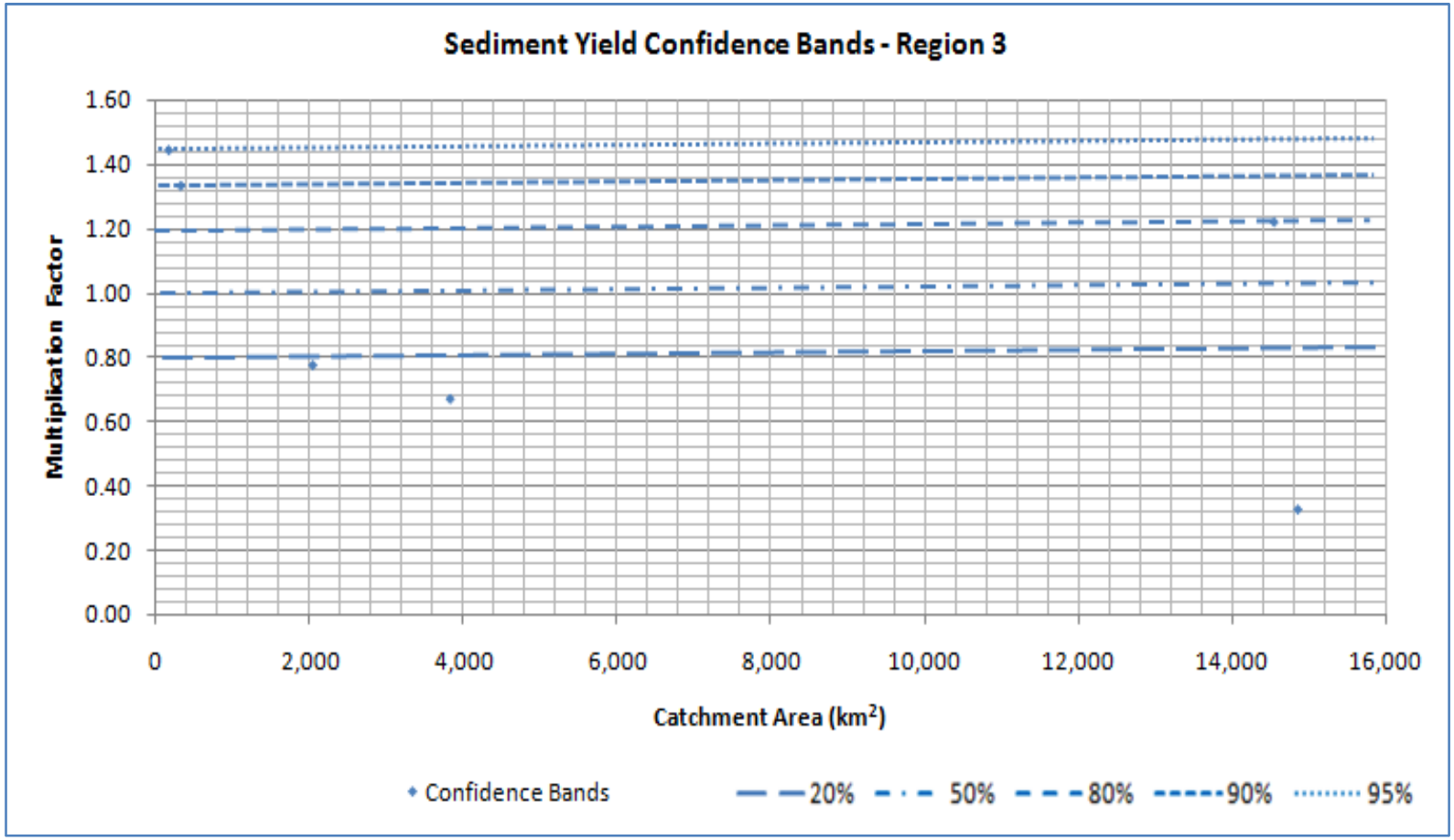
Sediment Yield Confidence Bands - Region 3
Multiplication Factor
1.60
1.40
1.20
1.00
0.80
0.60
0.40
0.20
0.00
0
2,000
4,000
6,000
8,000
10,000
12,000
14,000
16,000
Catchment Area (km²)
Confidence Bands
20%
50%
80%
90%
95%

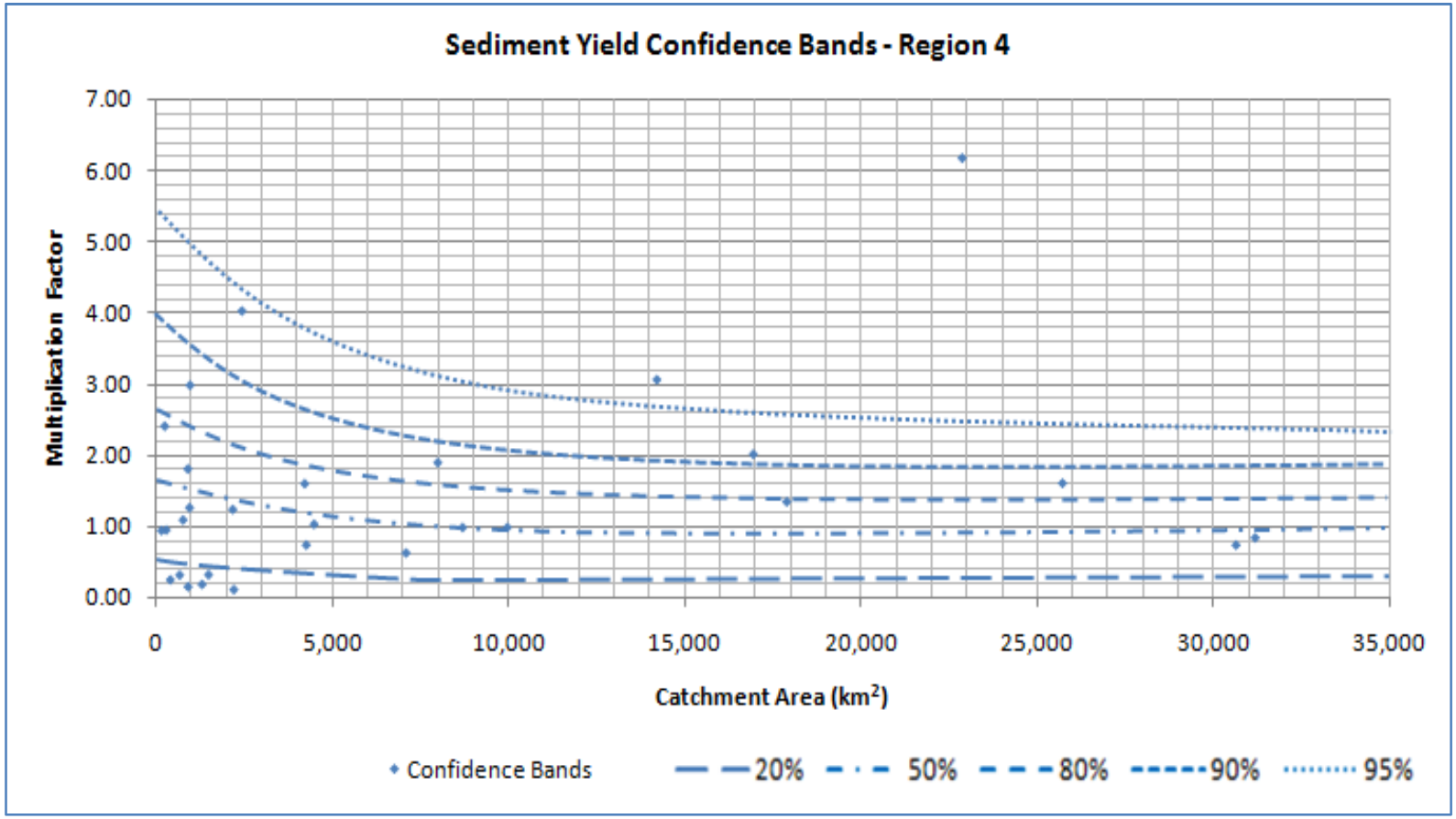
Sediment Yield Confidence Bands - Region 4
Multiplication Factor
7.00
6.00
5.00
4.00
3.00
2.00
1.00
0.00
0
5,000
10,000
15,000
20,000
25,000
30,000
35,000
Catchment Area (km²)
Confidence Bands
20%
50%
80%
90%
95%

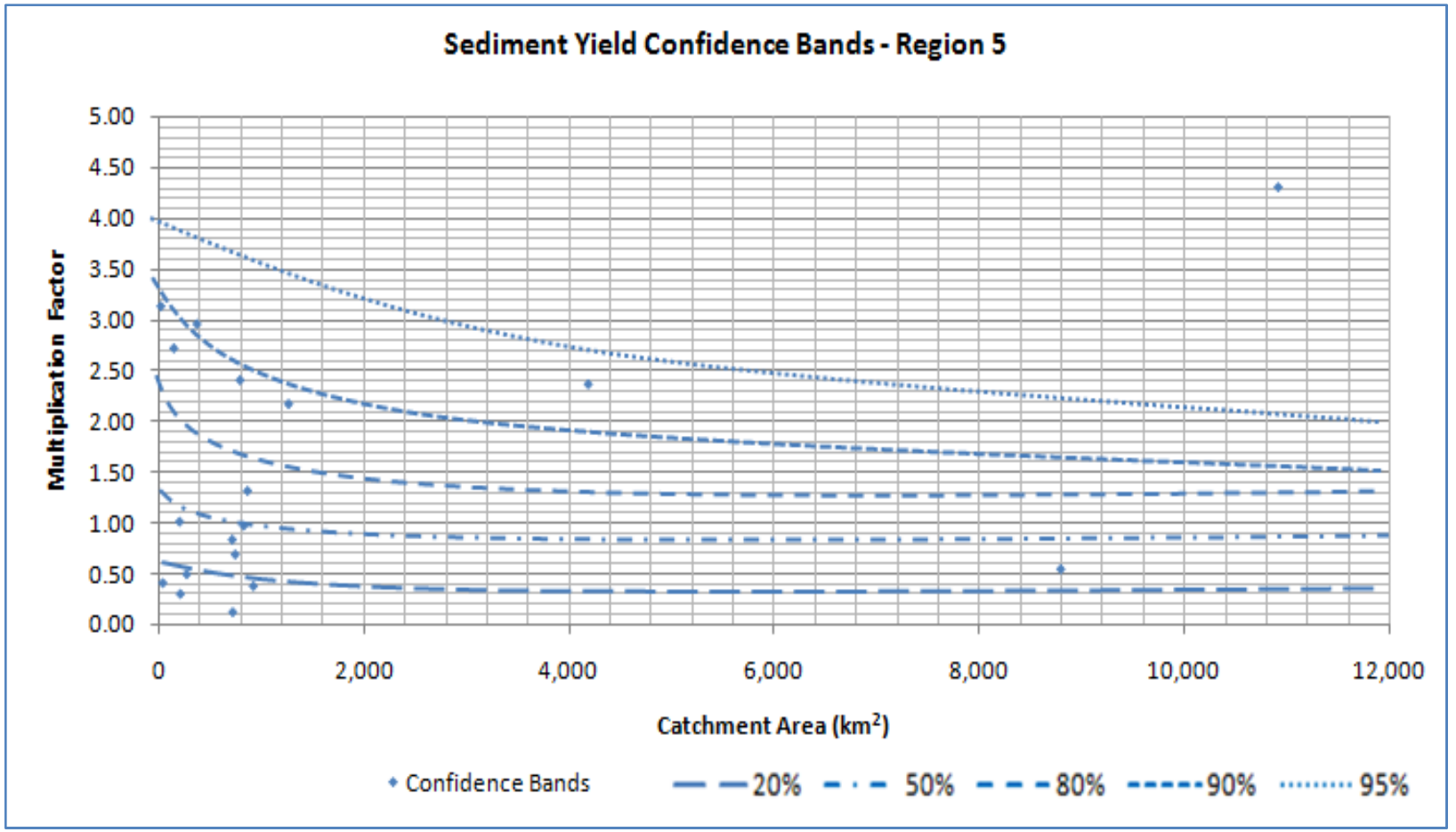
Sediment Yield Confidence Bands - Region 5
Multiplication Factor
5.00
4.50
4.00
3.50
3.00
2.50
2.00
1.50
1.00
0.50
0.00
0
2,000
4,000
6,000
8,000
10,000
12,000
Catchment Area (km²)
Confidence Bands
20%
50%
80%
90%
95%

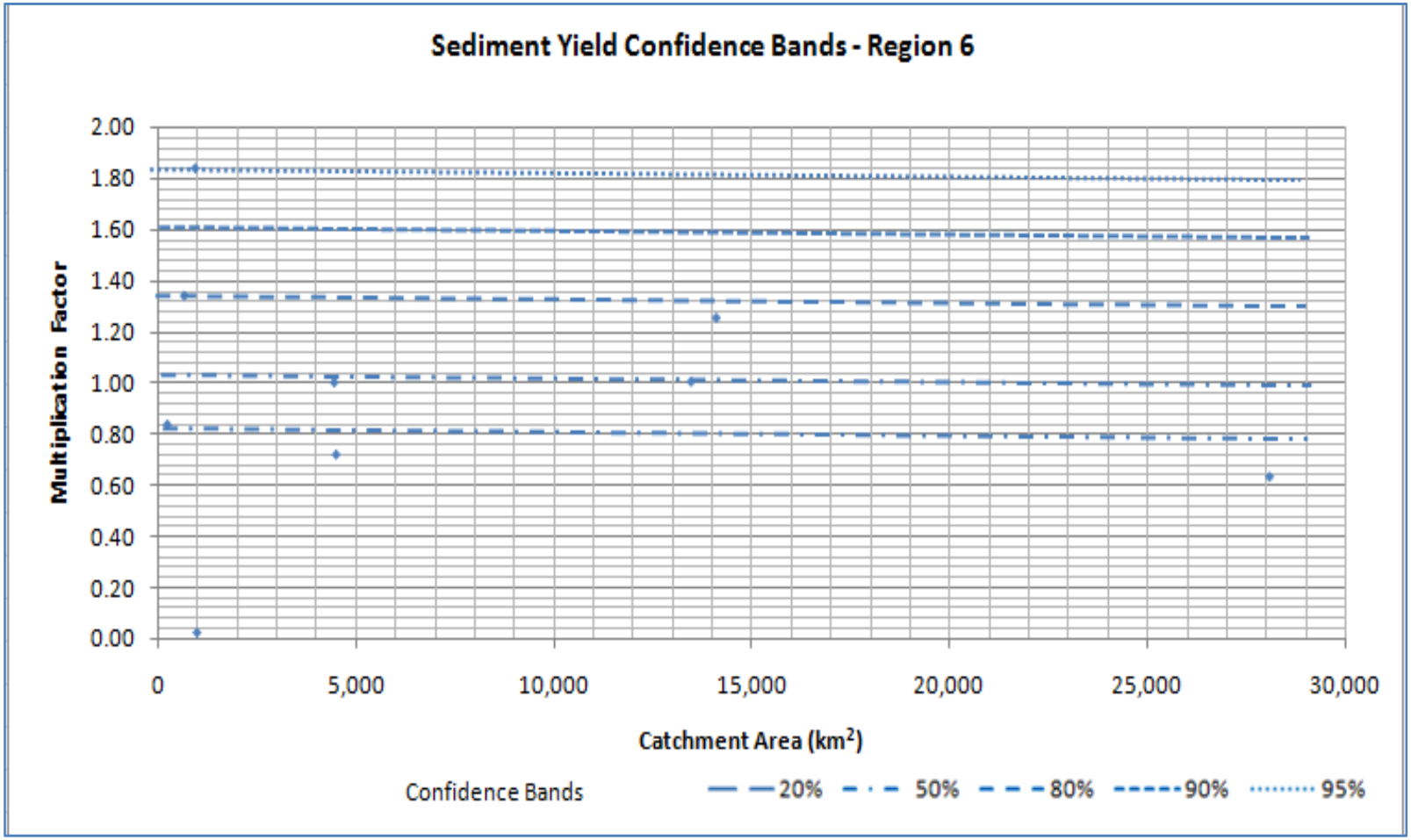
Sediment Yield Confidence Bands - Region 6
Multiplication Factor
2.00
1.80
1.60
1.40
1.20
1.00
0.80
0.60
0.40
0.20
0.00
0
5,000
10,000
15,000
20,000
25,000
30,000
Catchment Area (km²)
Confidence Bands
20%
50%
80%
90%
95%

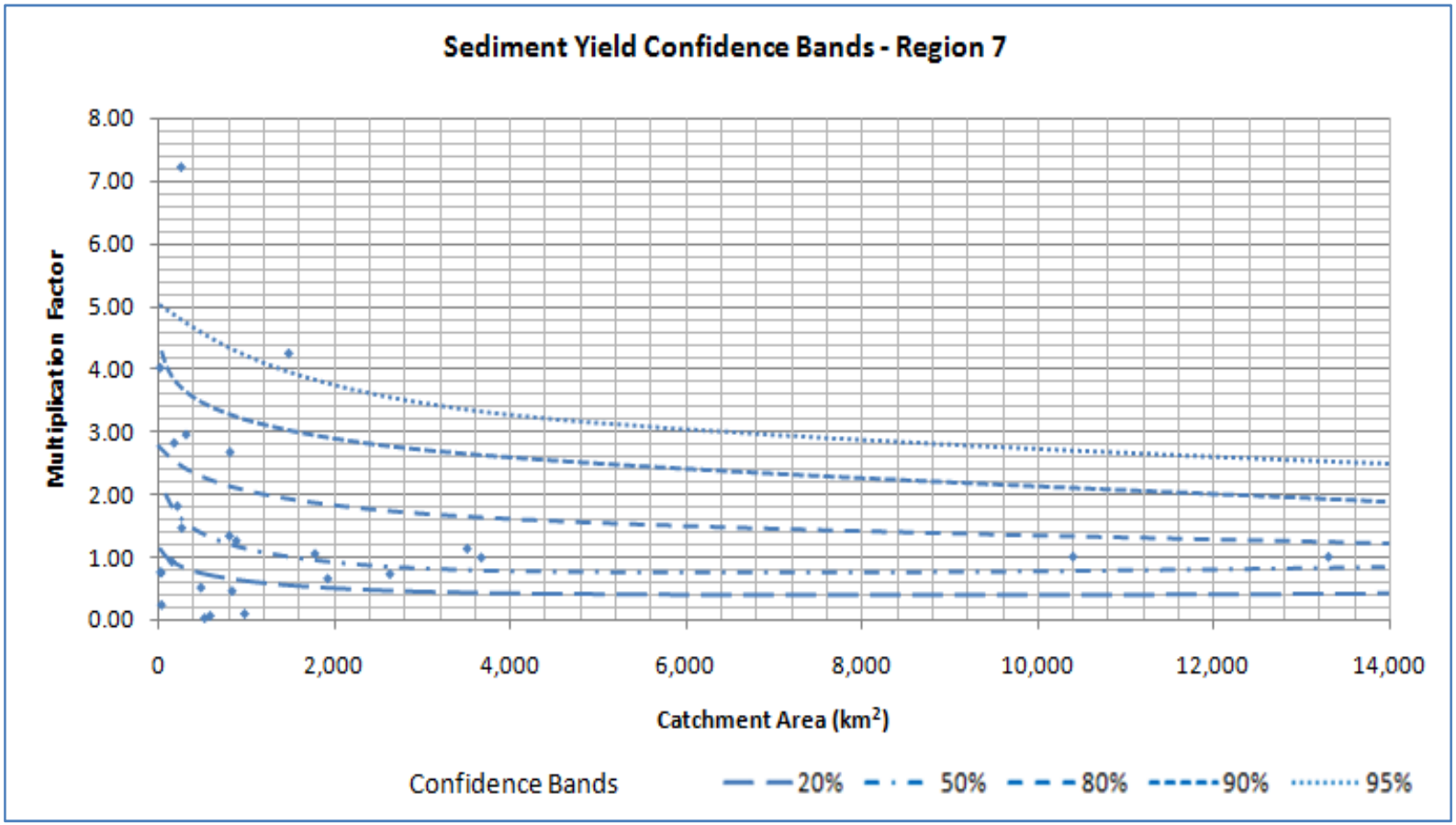
Sediment Yield Confidence Bands - Region 7
Multiplication Factor
8.00
7.00
6.00
5.00
4.00
3.00
2.00
1.00
0.00
0
2,000
4,000
6,000
8,000
10,000
12,000
14,000
Catchment Area (km²)
Confidence Bands
20%
50%
80%
90%
95%

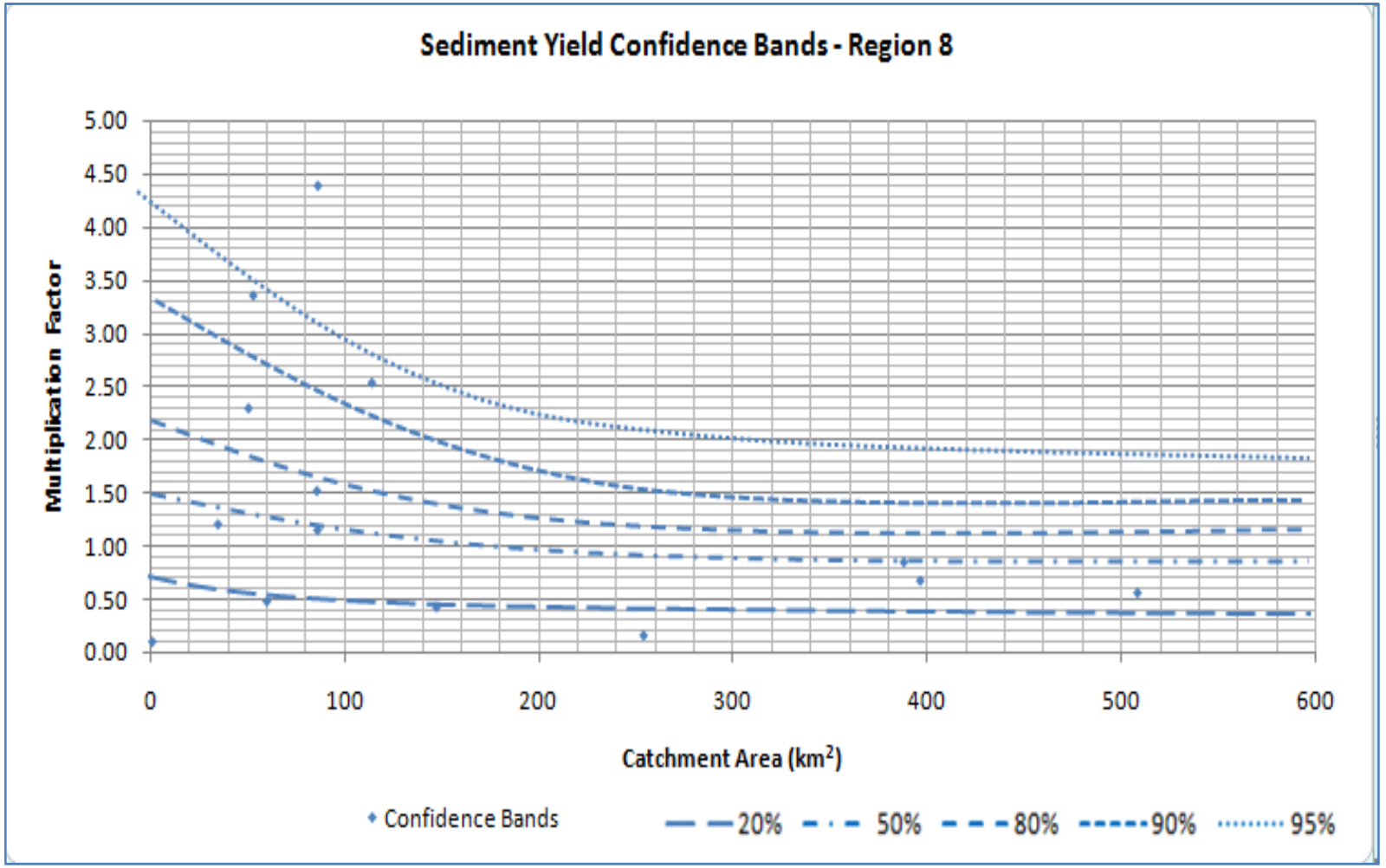
Sediment Yield Confidence Bands - Region 8
Multiplication Factor
5.00
4.50
4.00
3.50
3.00
2.50
2.00
1.50
1.00
0.50
0.00
0
100
200
300
400
500
600
Catchment Area (km²)
Confidence Bands
20%
50%
80%
90%
95%

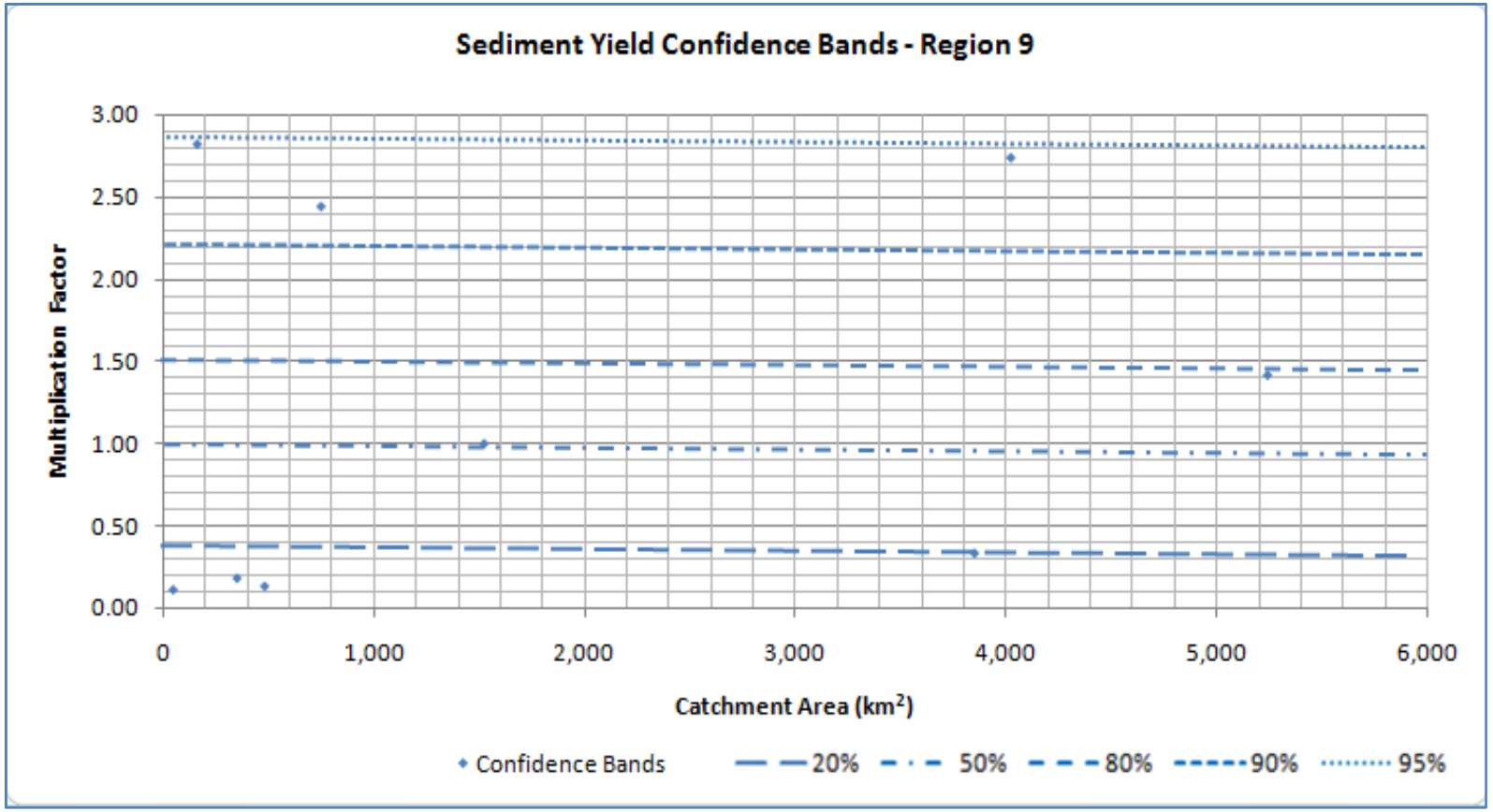
Sediment Yield Confidence Bands - Region 9
Multiplication Factor
3.00
2.50
2.00
1.50
1.00
0.50
0.00
0
1,000
2,000
3,000
4,000
5,000
6,000
Catchment Area (km²)
Confidence Bands
20%
50%
80%
90%
95%

APPENDIX F SIMULATED AND OBSERVED DATA USING THE PROBABILISTIC METHOD

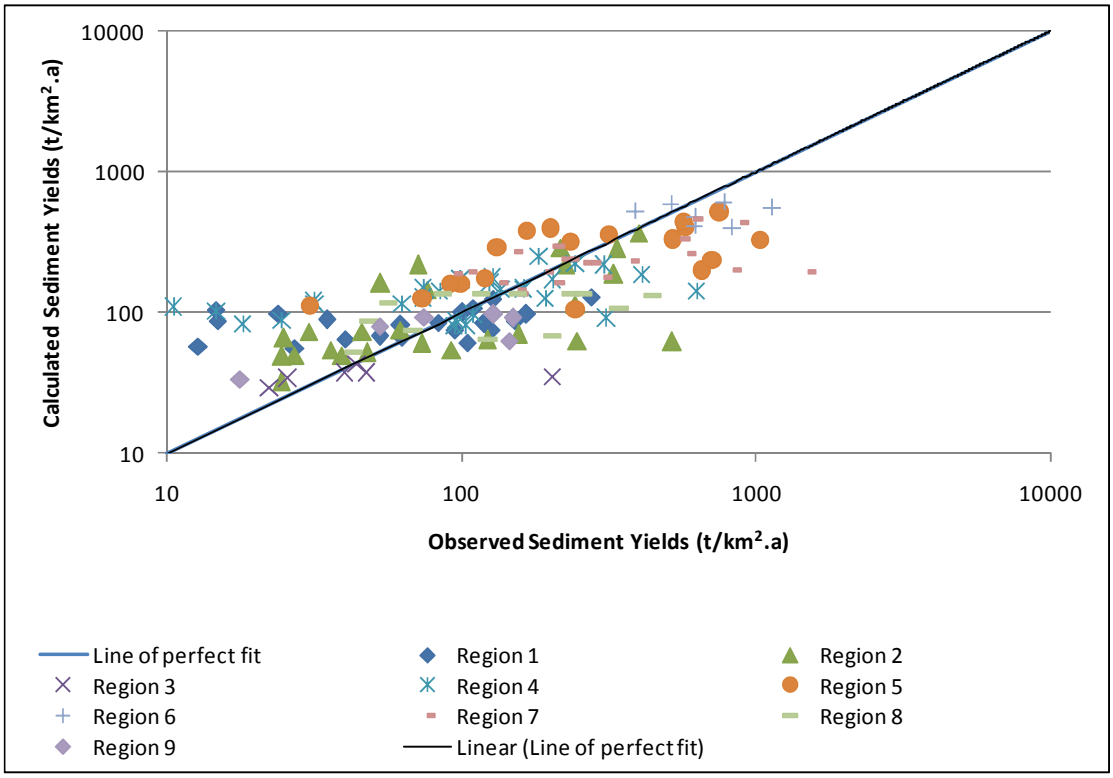

Simulated and observed data for all regions using the probabilistic method

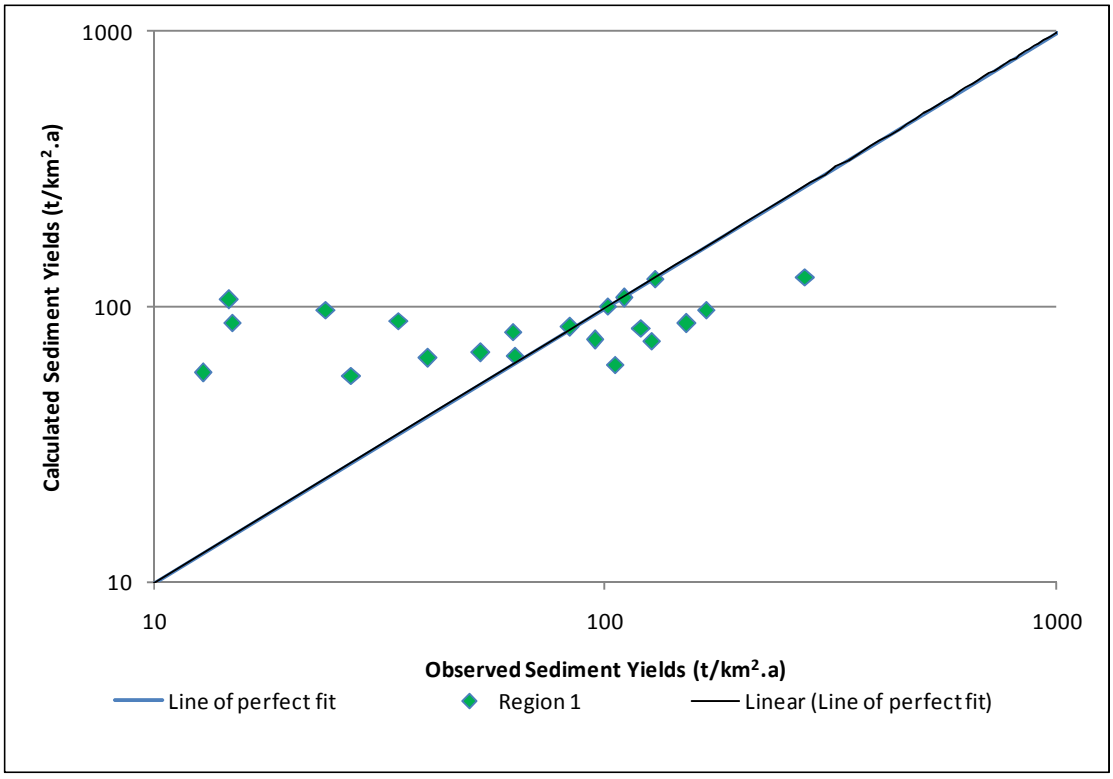

Simulated and observed data for Region 1 using the probabilistic method

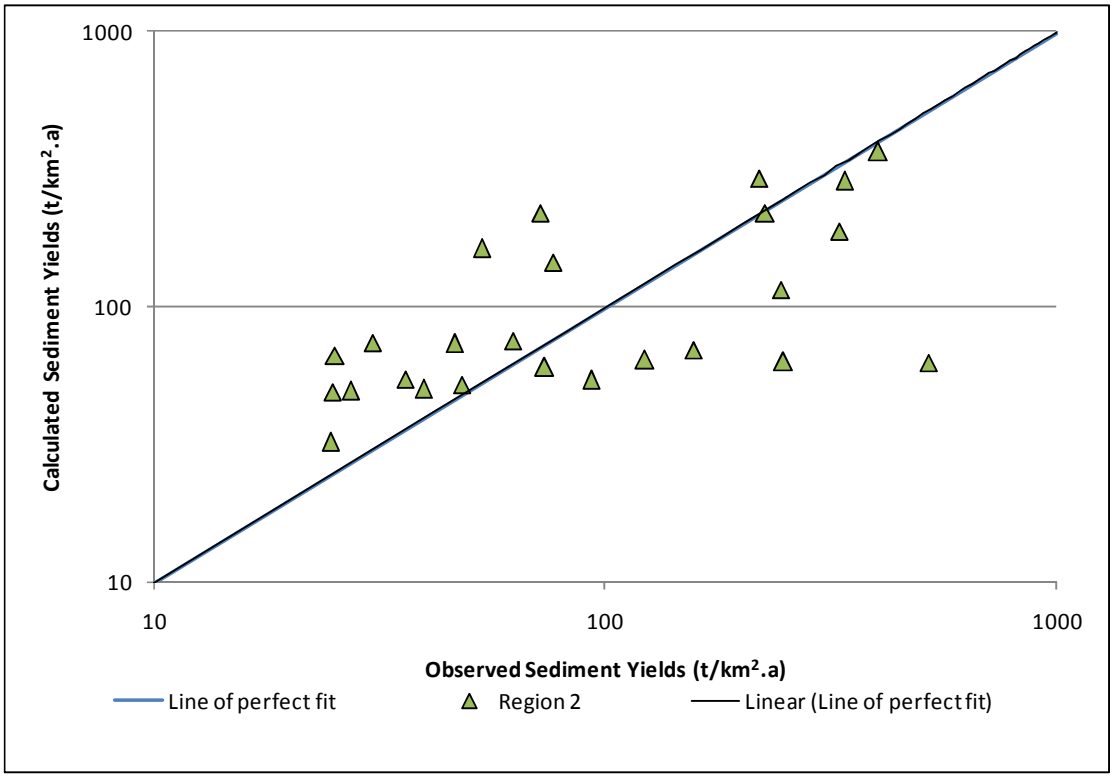

Simulated and observed data for Region 2 using the probabilistic method

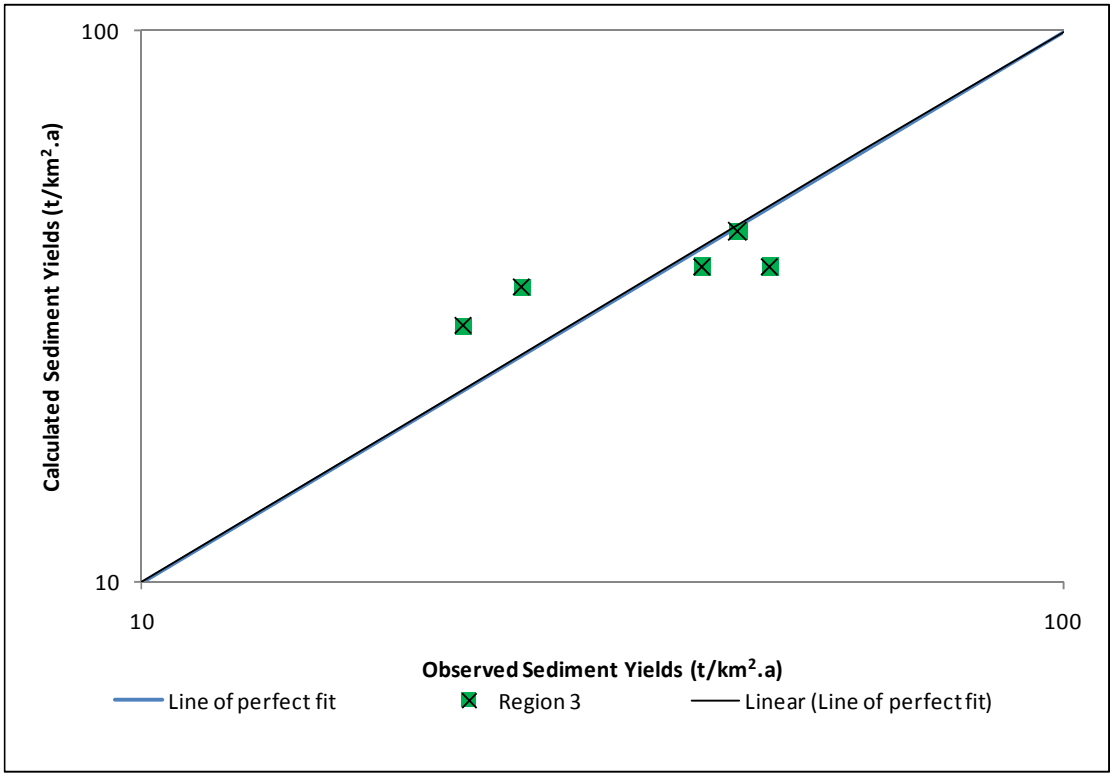

Simulated and observed data for Region 3 using the probabilistic method

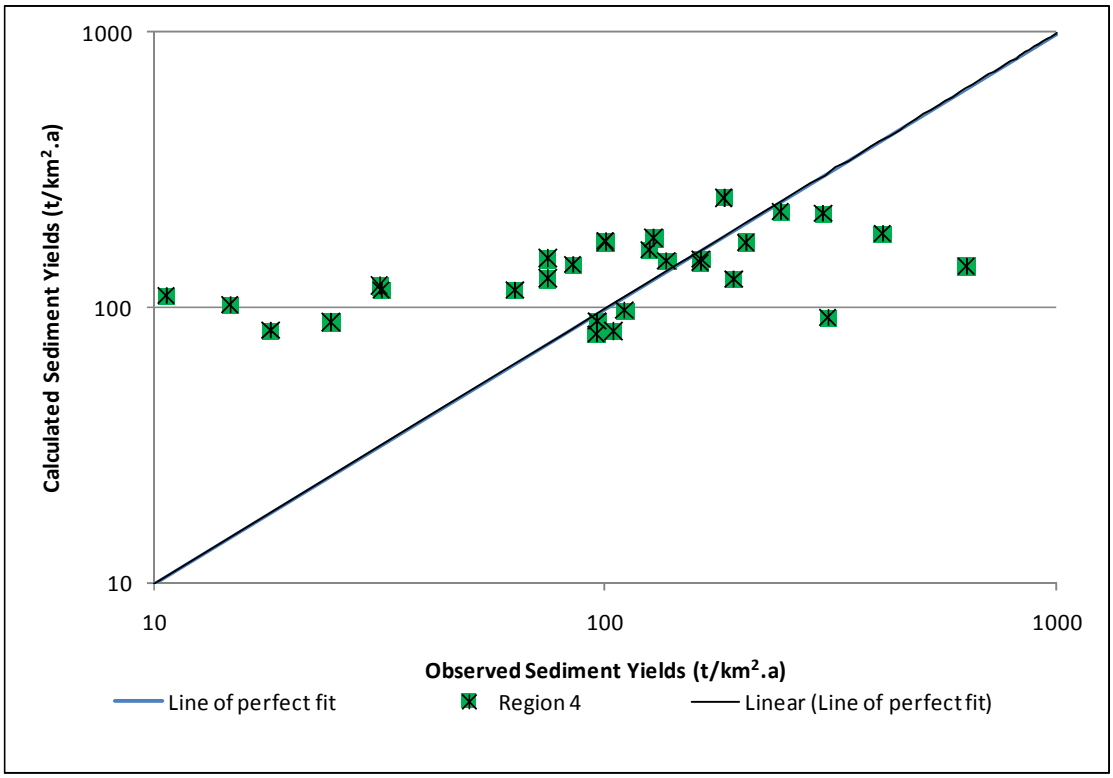

Simulated and observed data for Region 4 using the probabilistic method

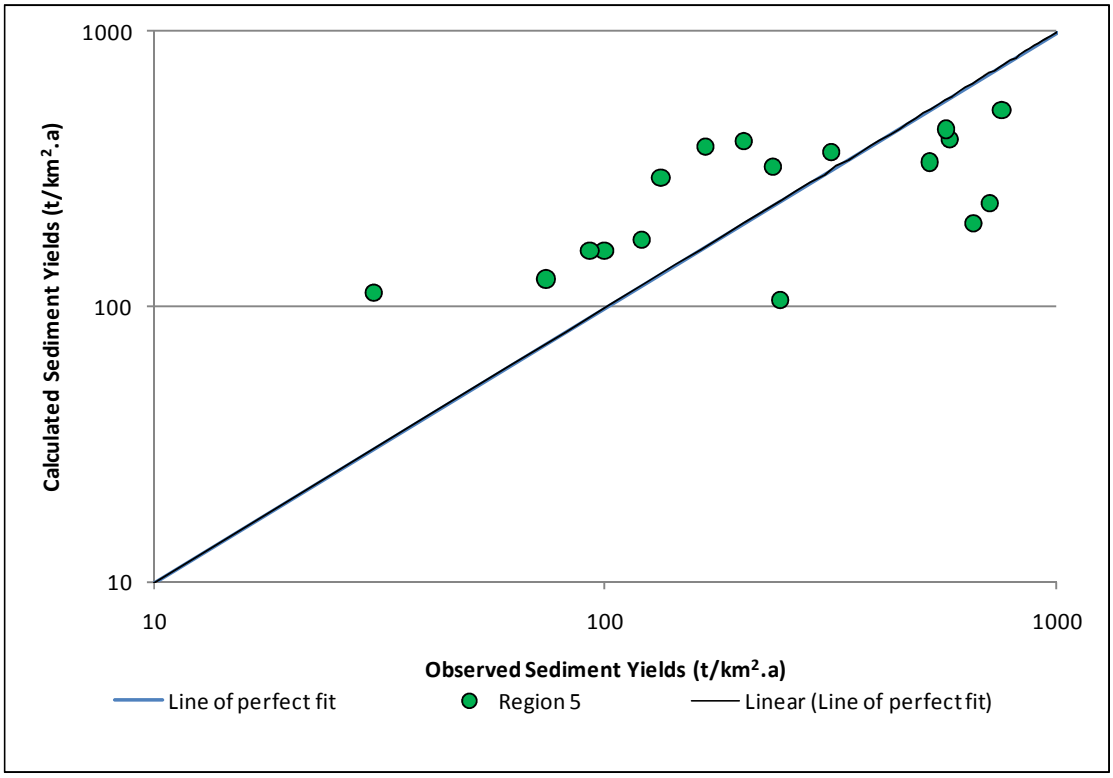

Simulated and observed data for Region 5 using the probabilistic method

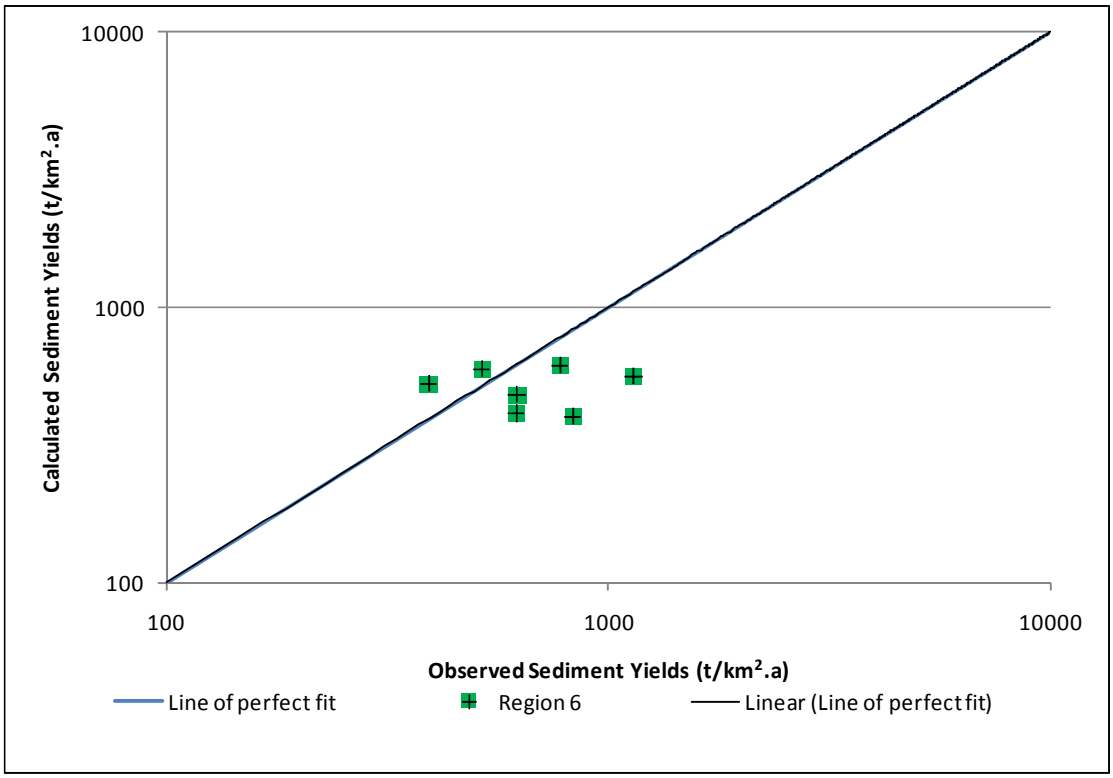

Simulated and observed data for Region 6 using the probabilistic method

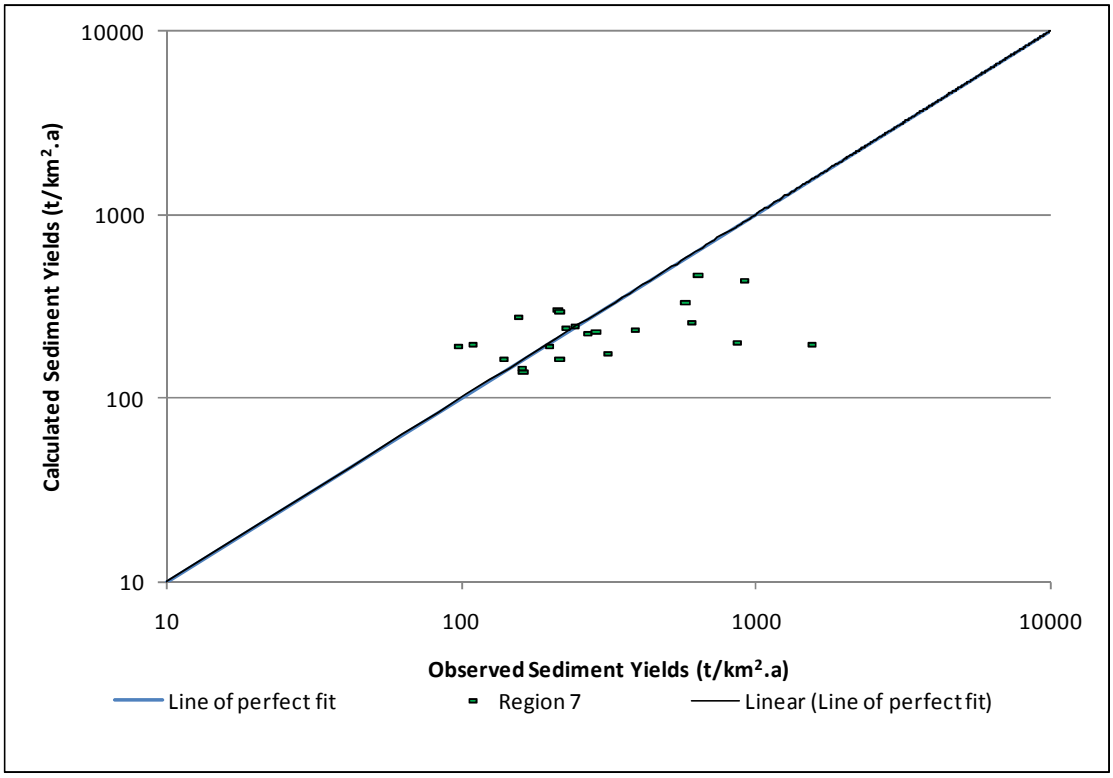

Simulated and observed data for Region 7 using the probabilistic method

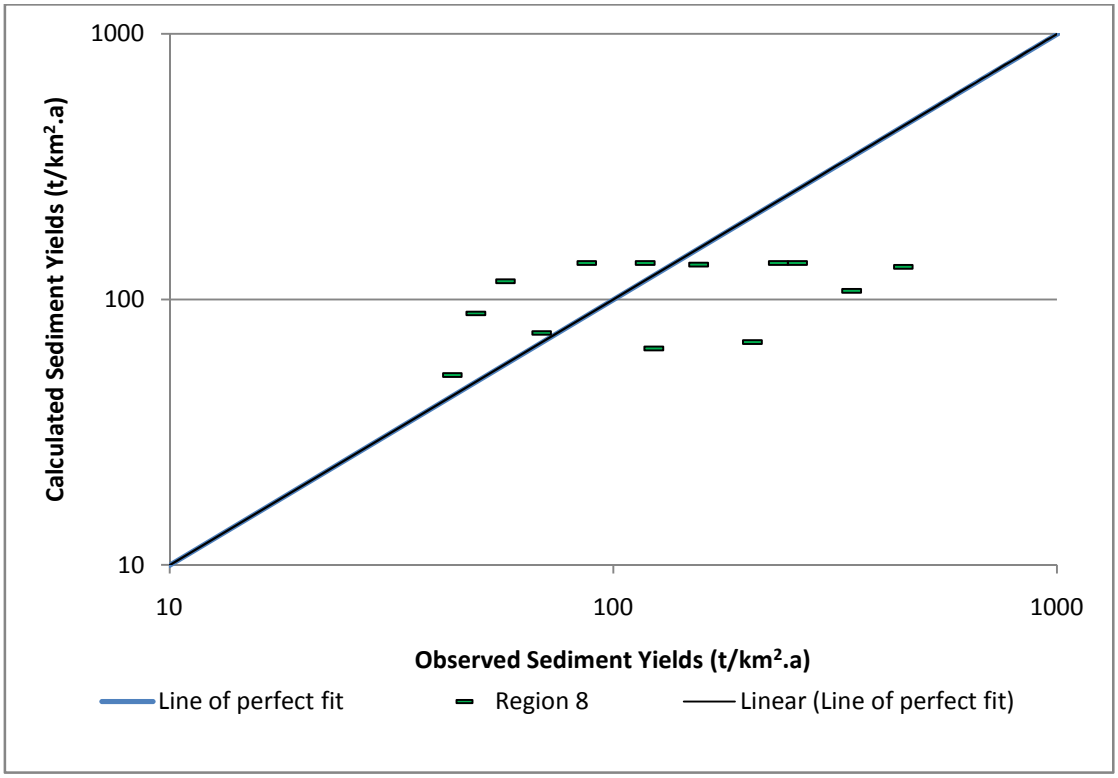

Simulated and observed data for Region 8 using the probabilistic method

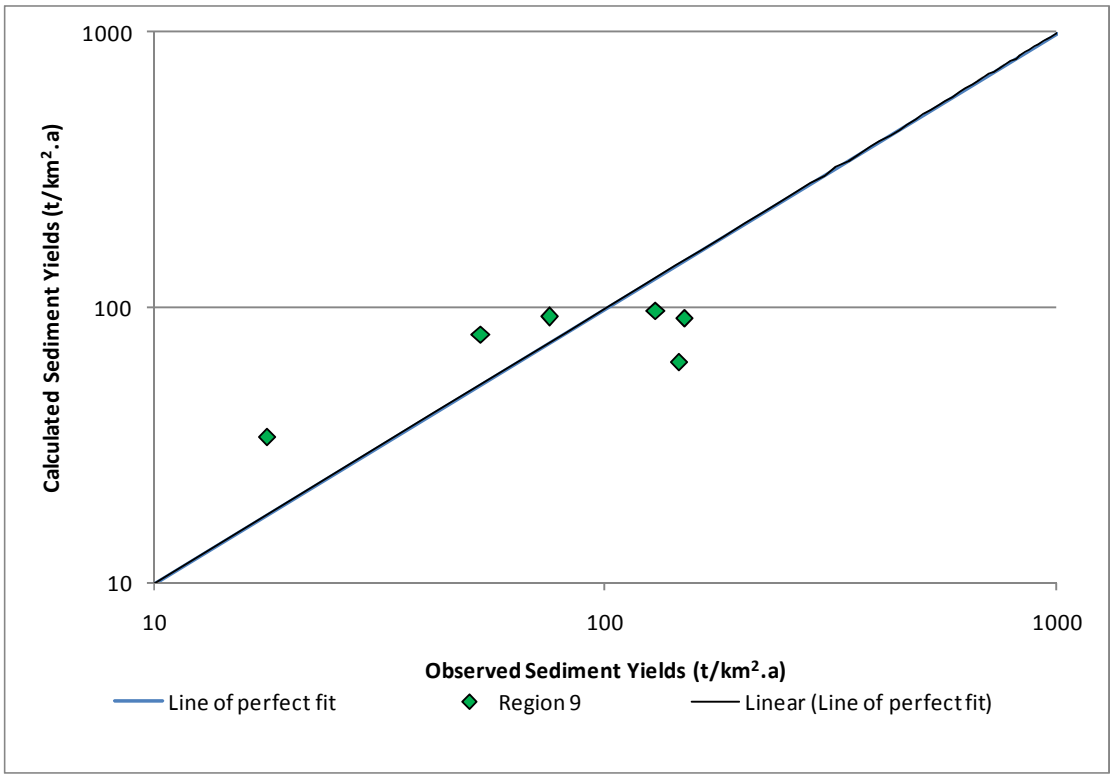

Simulated and observed data for Region 9 using the probabilistic method

APPENDIX G SIMULATED AND OBSERVED DATA USING THE EMPIRICAL METHOD

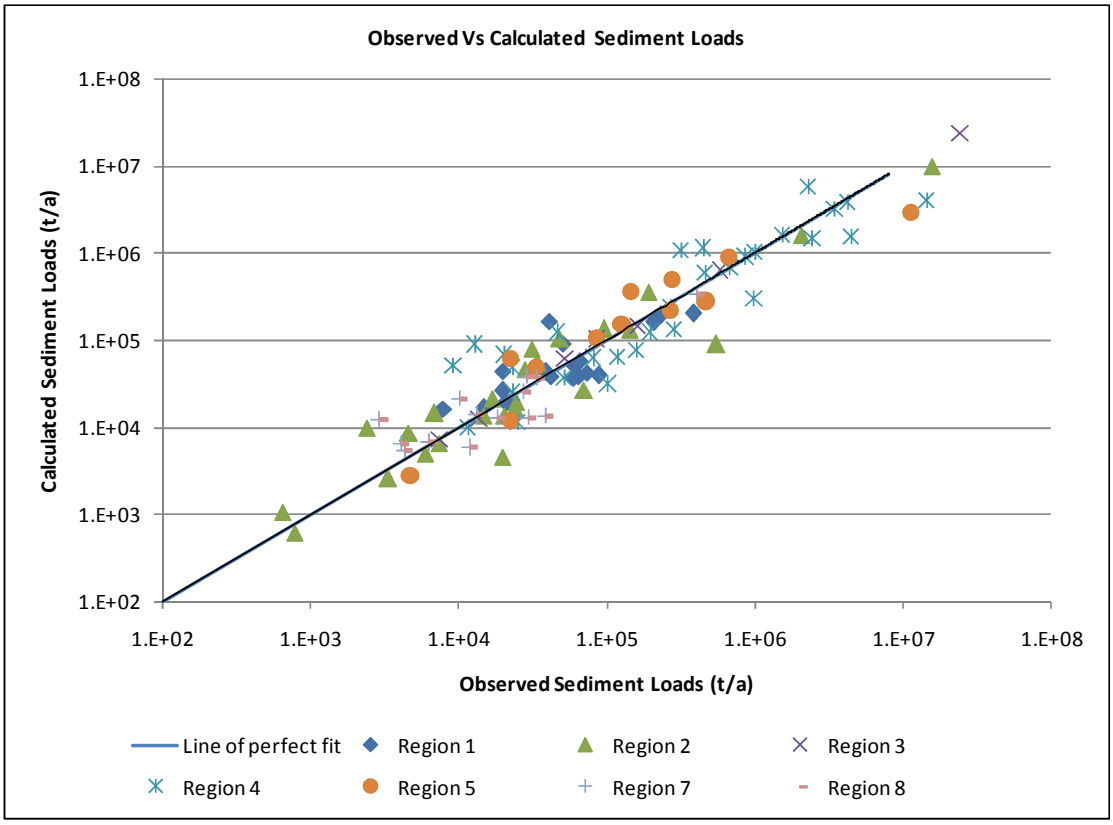

Simulated and observed data for all regions using the empirical method

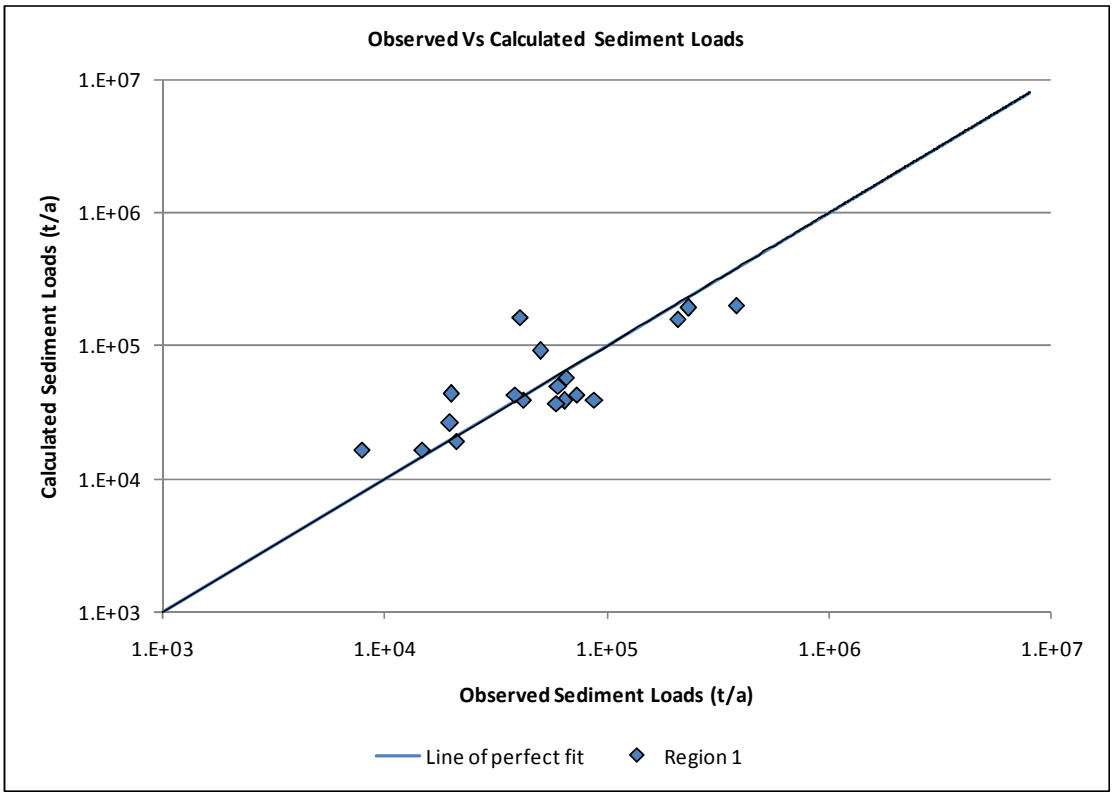

Simulated and observed data for Region1 using the empirical method

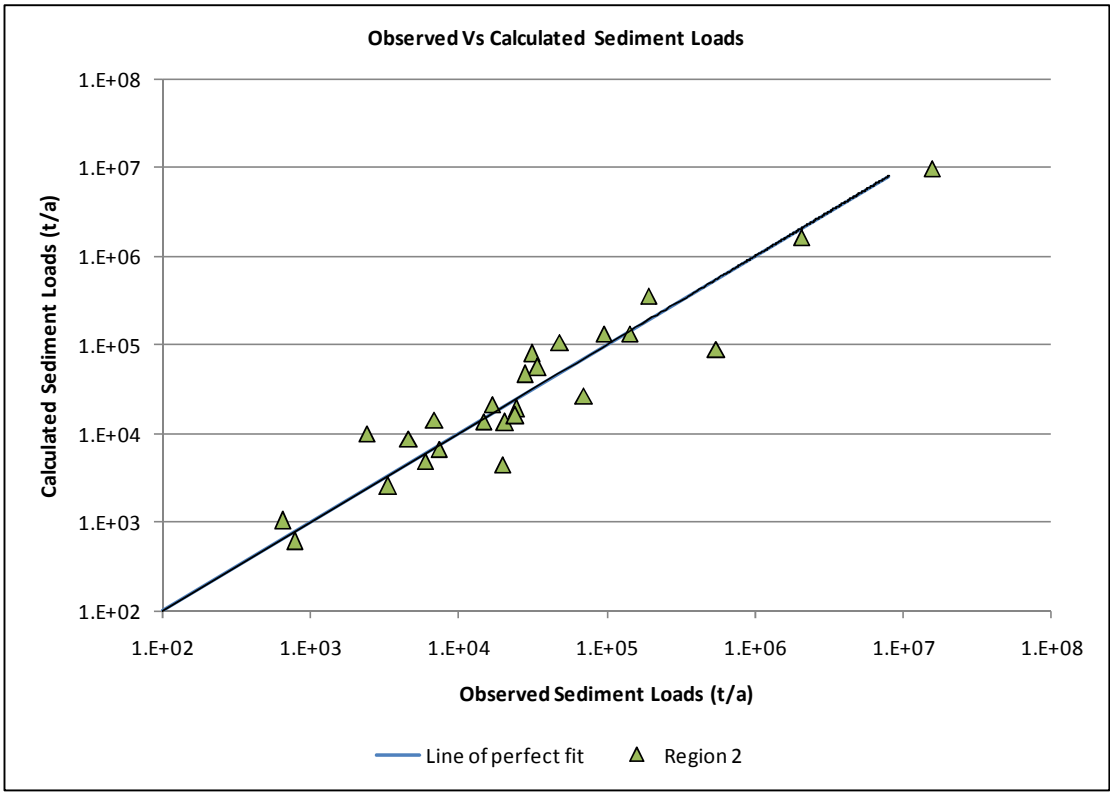

Simulated and observed data for Region 2 using the empirical method

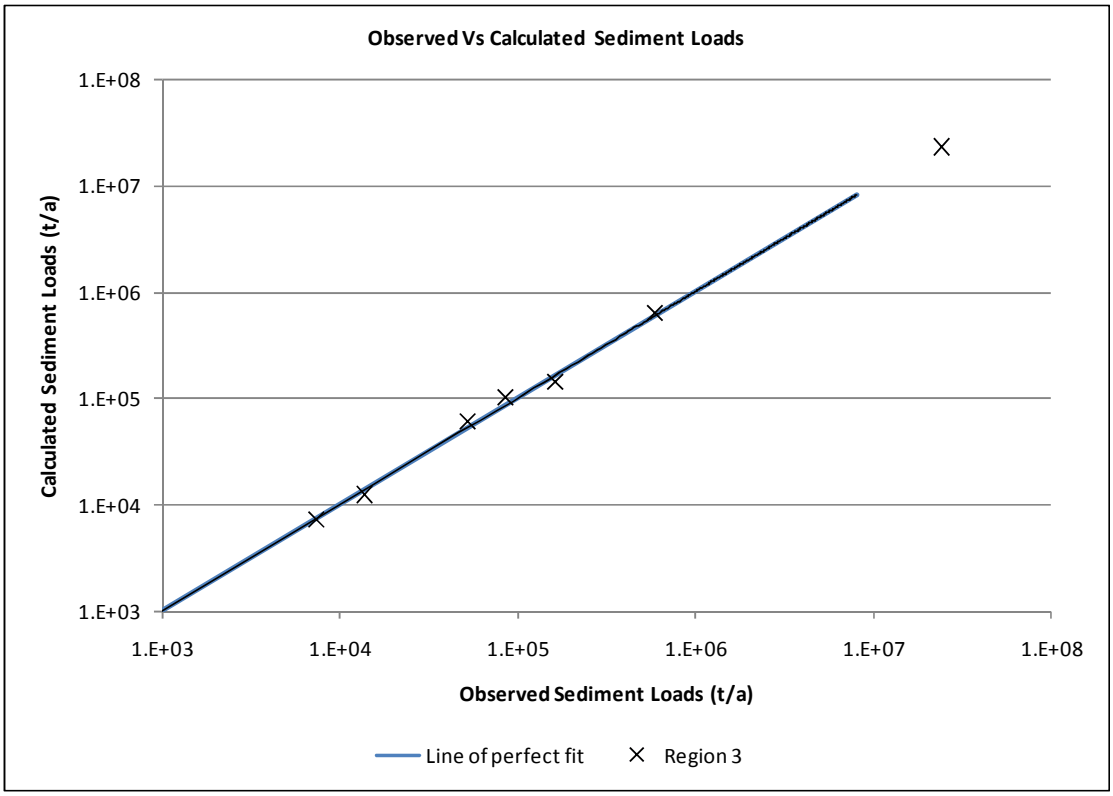

Simulated and observed data for Region 3 using the empirical method

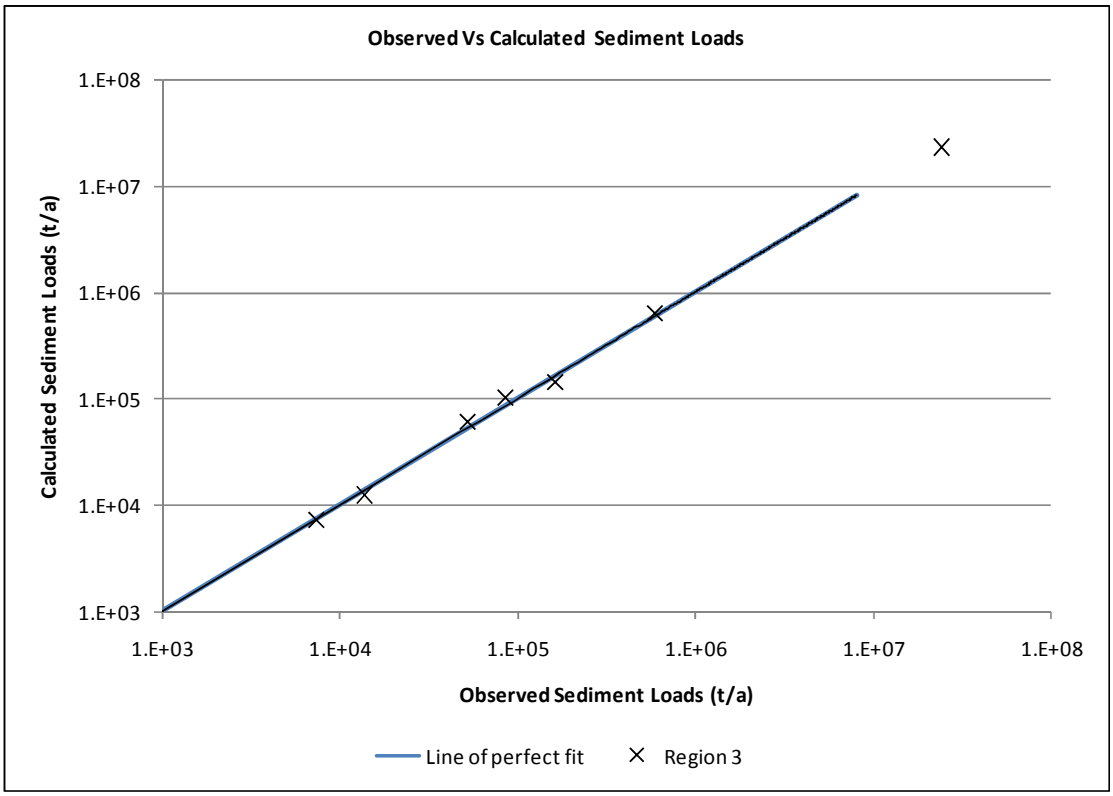

Simulated and observed data for Region 4 using the empirical method

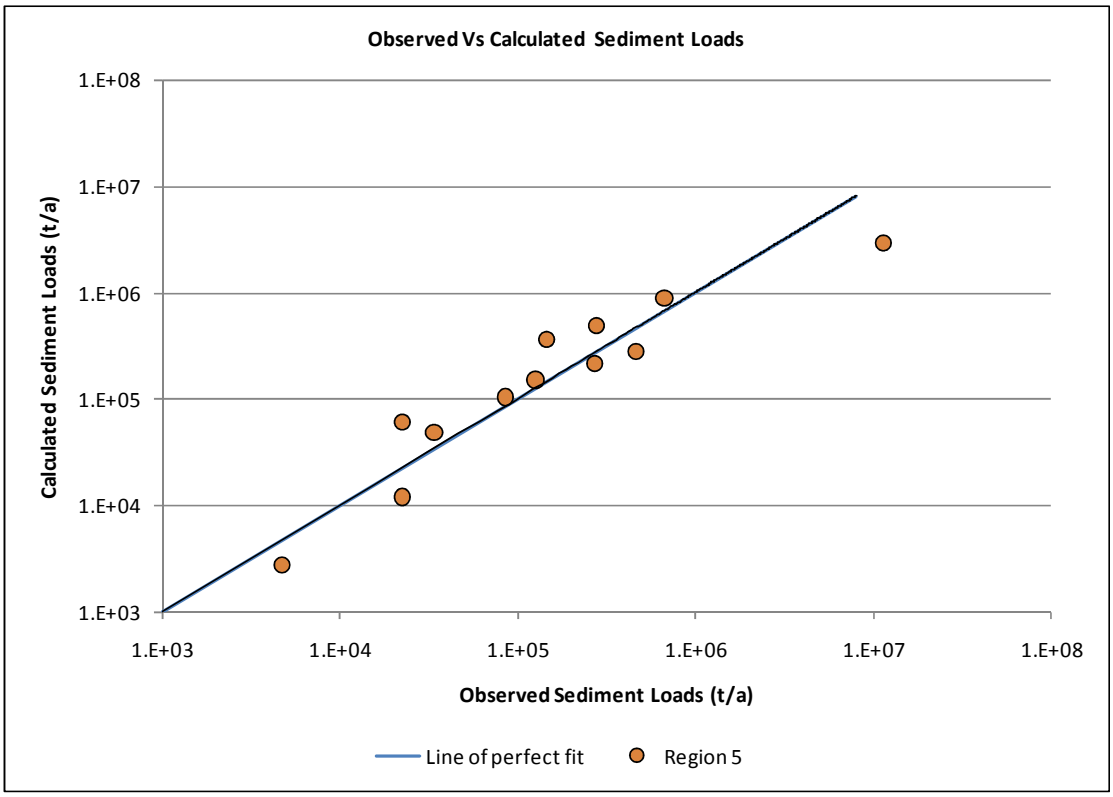

Simulated and observed data for Region 5 using the empirical method

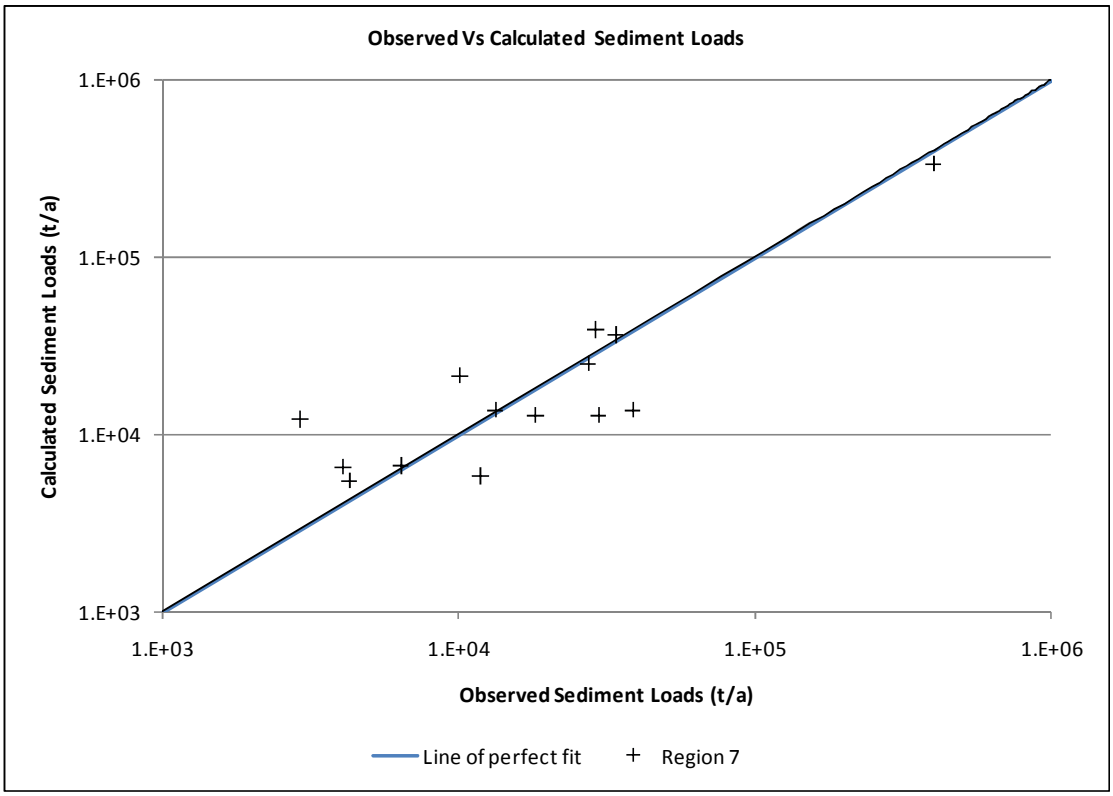

Simulated and observed data for Region 7 using the empirical method

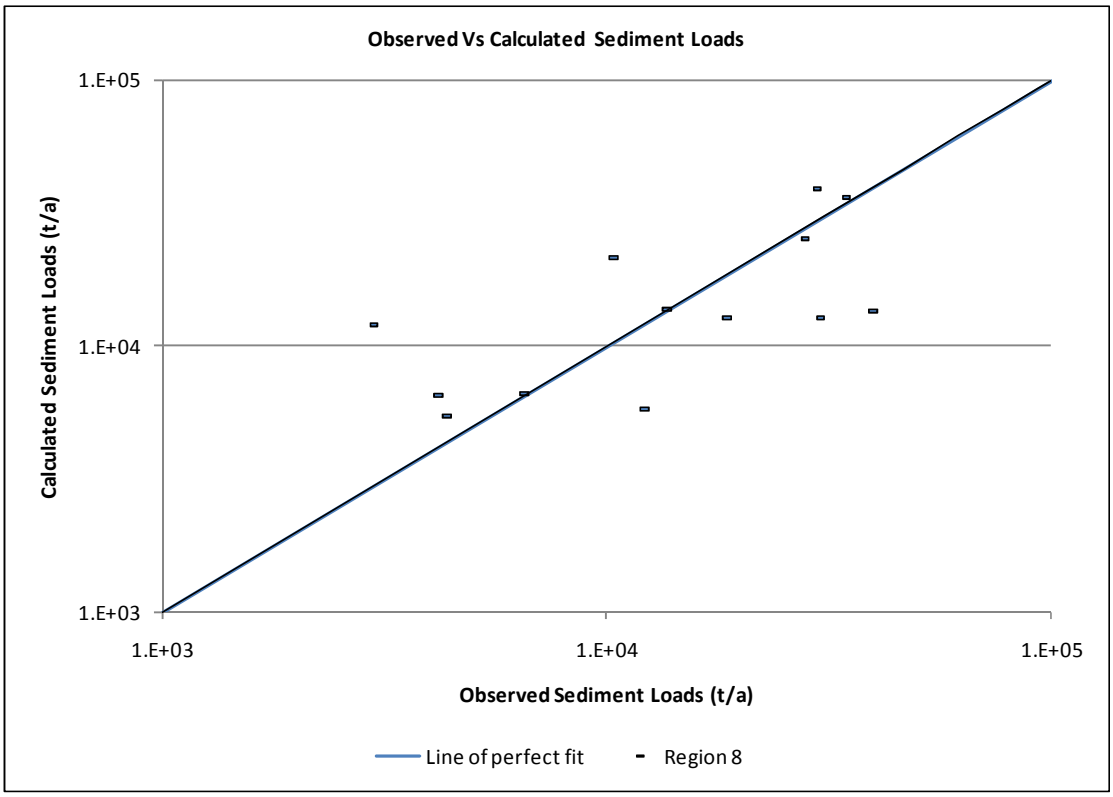

Simulated and observed data for Region 8 using the empirical method

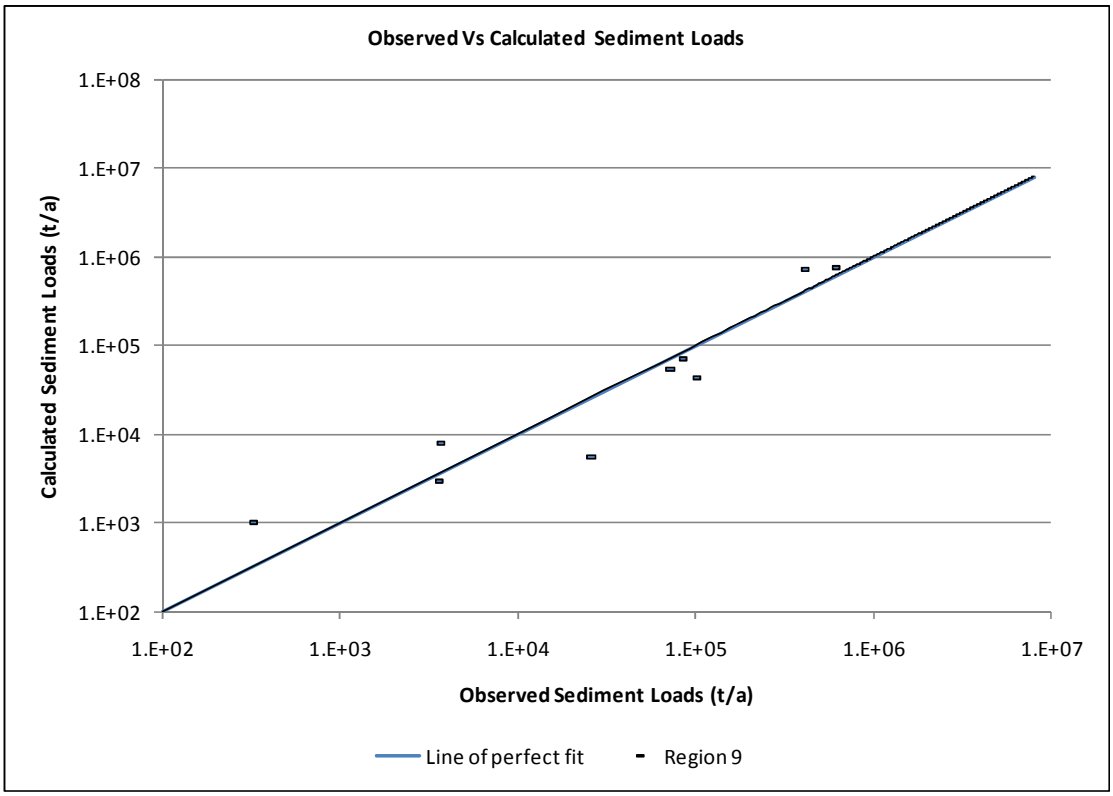

Simulated and observed data for Region 9 using the empirical method

APPENDIX H FLOW CALIBRATION GRAPHS

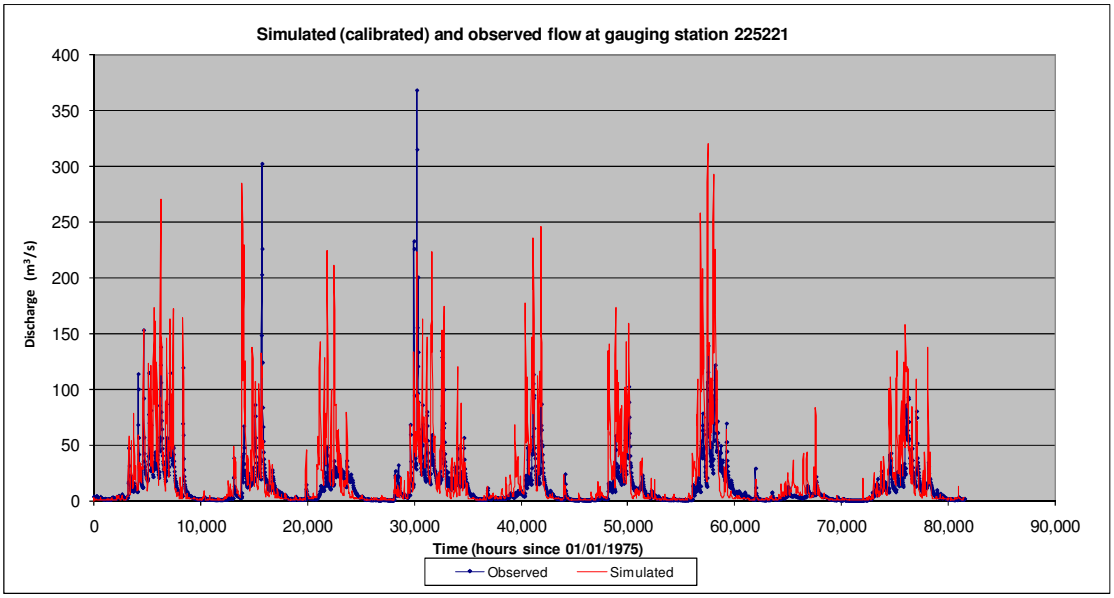

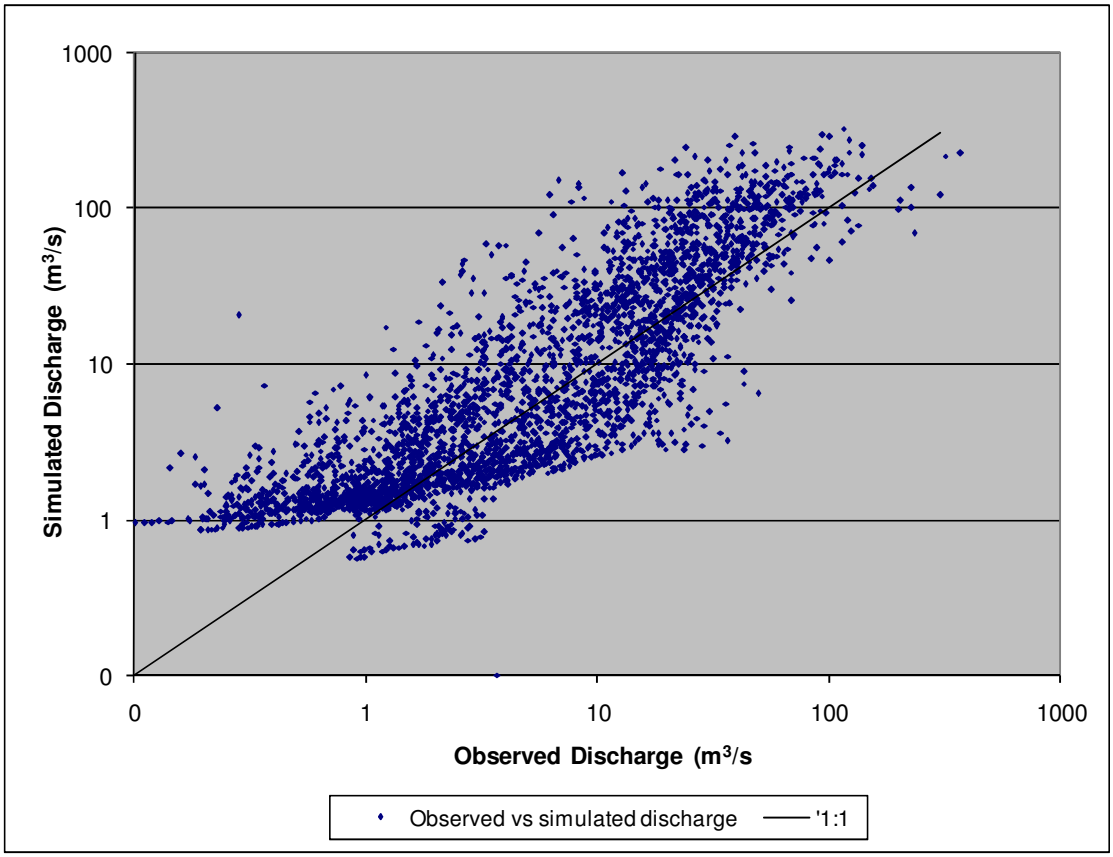

Hydrograph of flow calibration at gauging station 225221 (period from 1975 to 1984) and the relationship between simulated and observed flow along line of perfect fit.

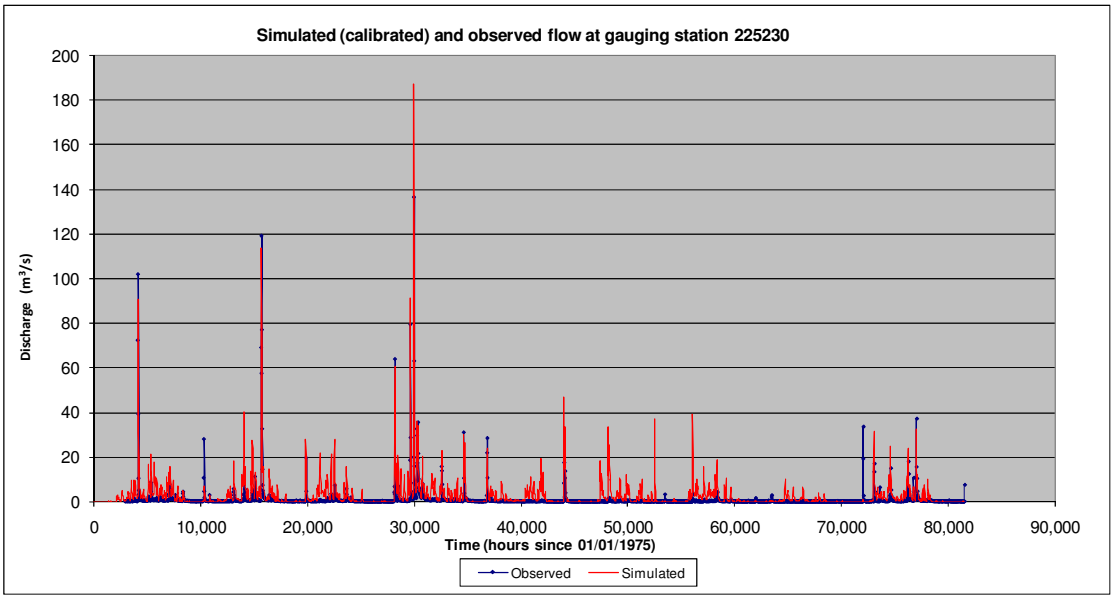

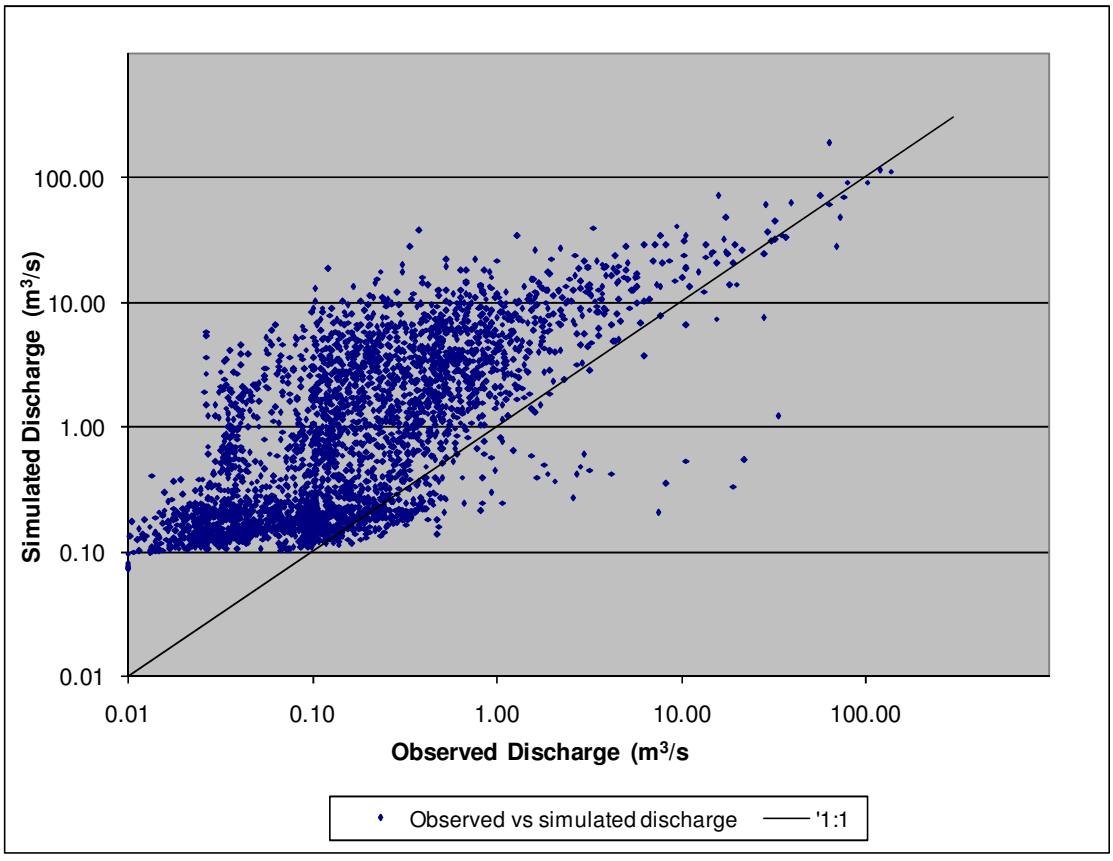

Hydrograph of flow calibration at gauging station 225230 (period from 1975 to 1984) and the relationship between simulated and observed flow along line of perfect fit.

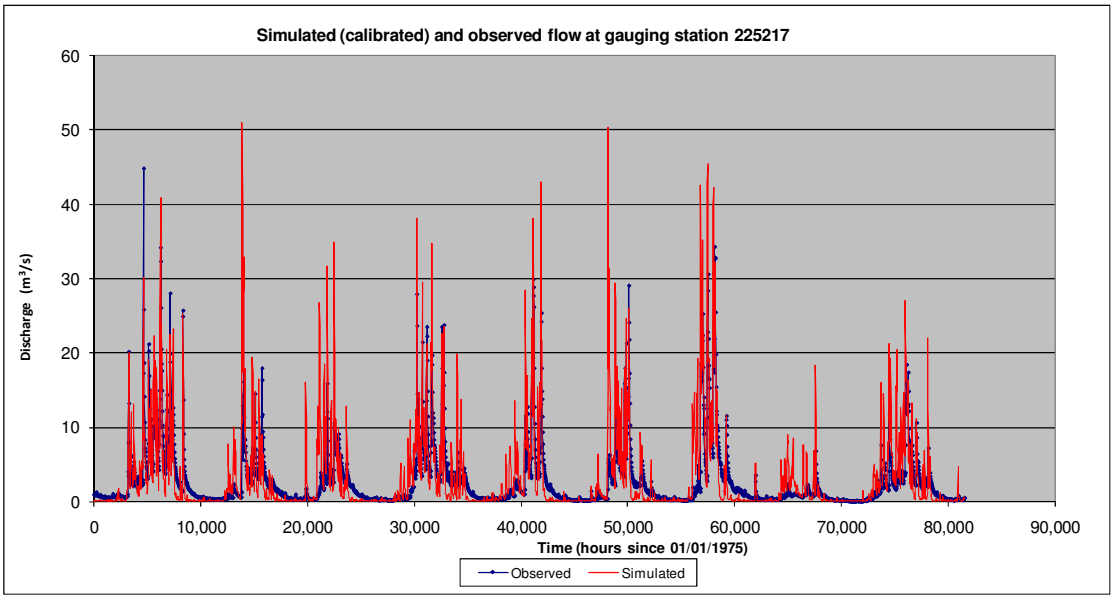

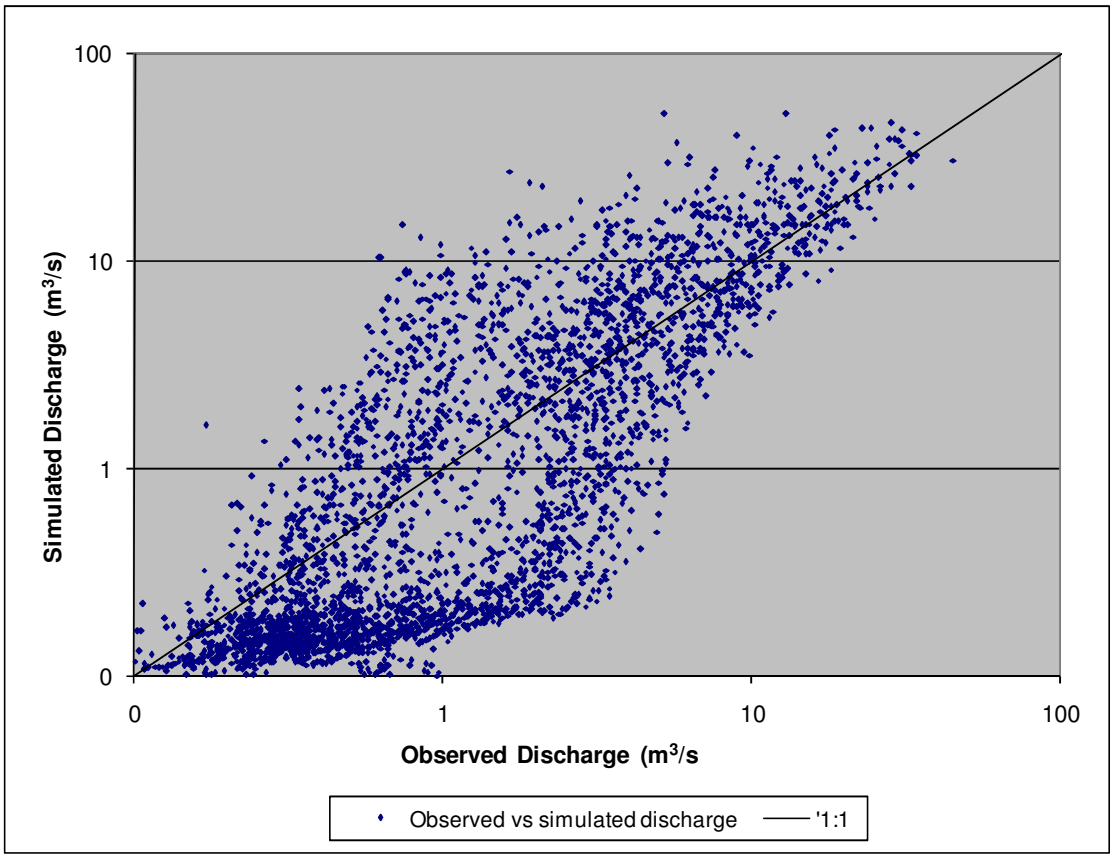

Hydrograph of flow calibration at gauging station 225217 (period from 1975 to 1984) and the relationship between simulated and observed flow along line of perfect fit.

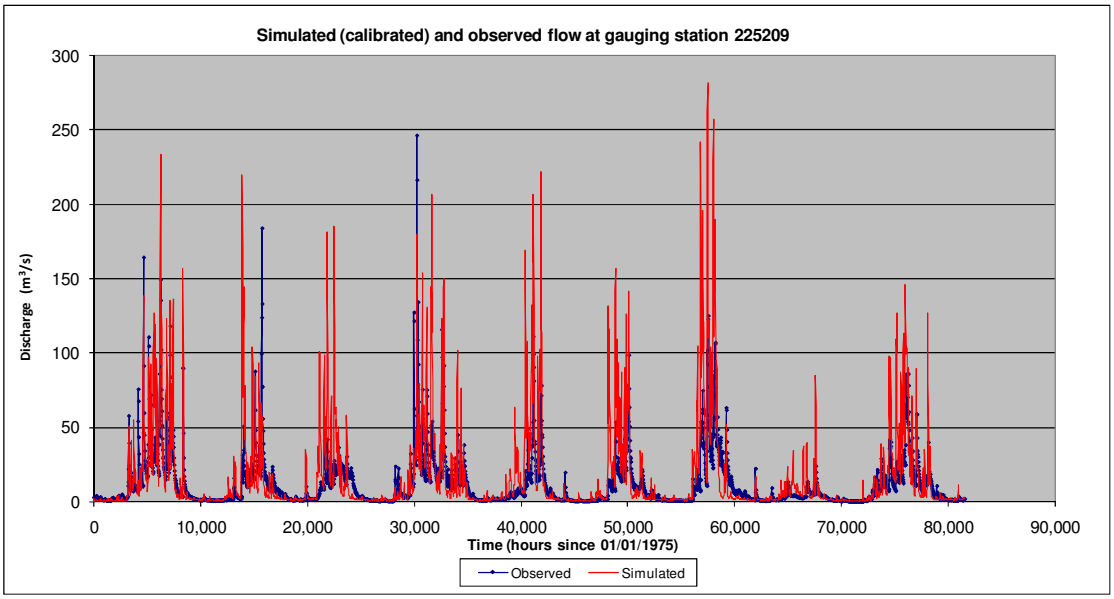

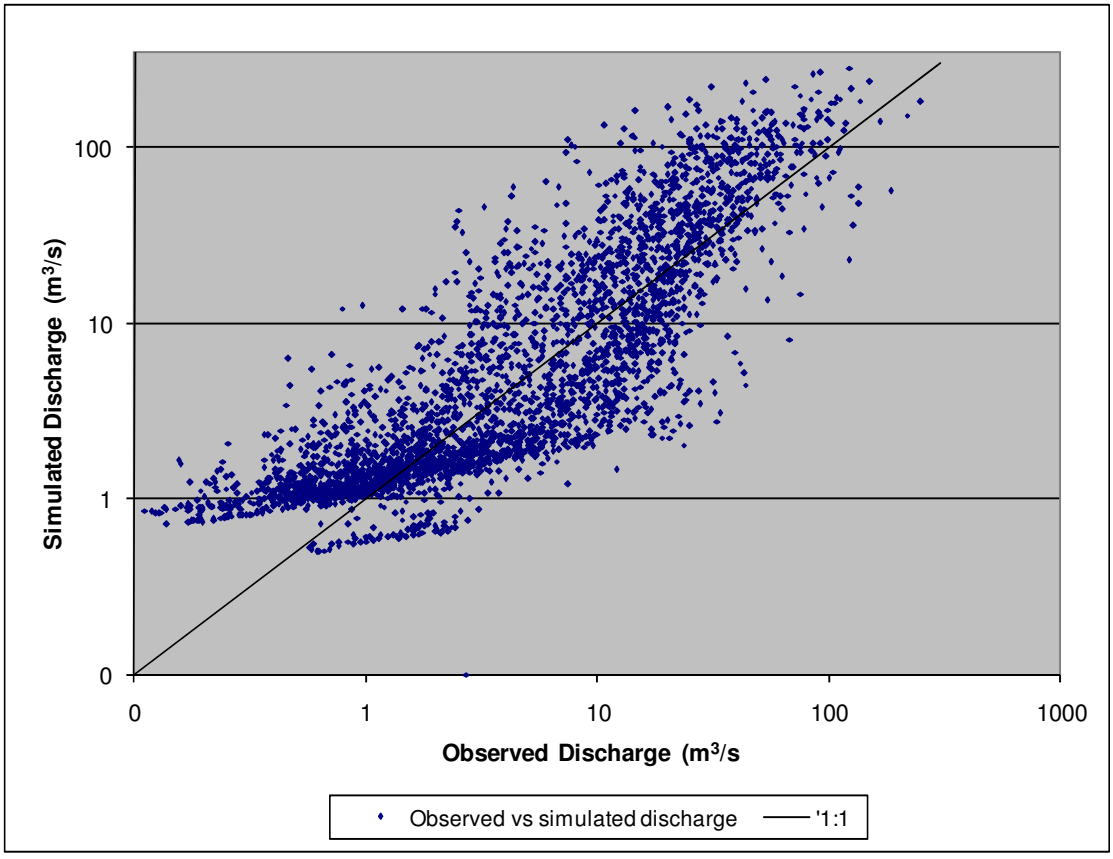

Hydrograph of flow calibration at gauging station 225209 (period from 1975 to 1984) and the relationship between simulated and observed flow along line of perfect fit.

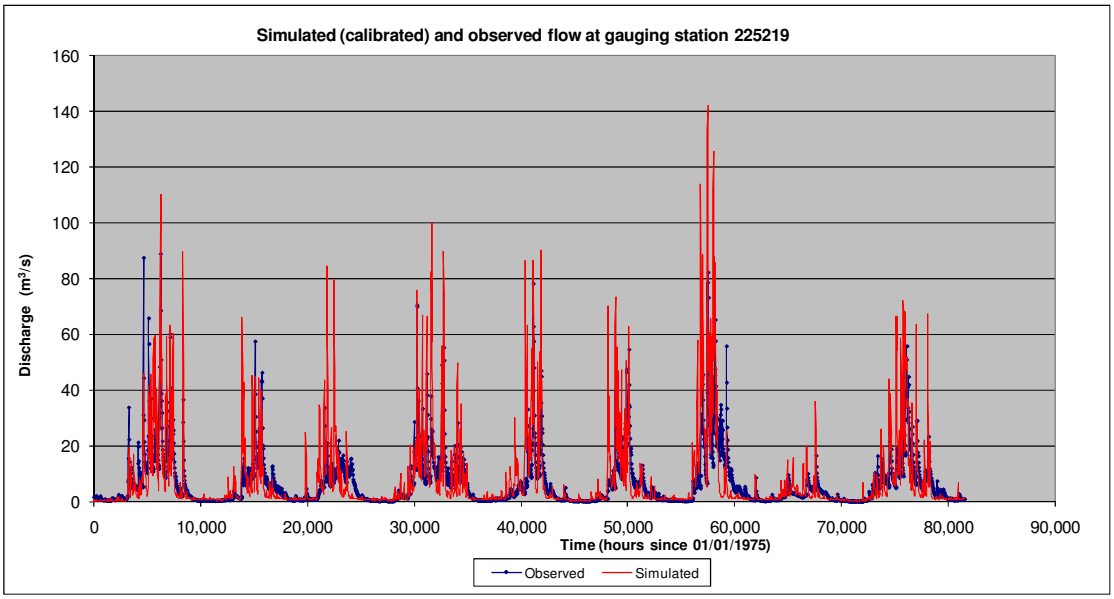

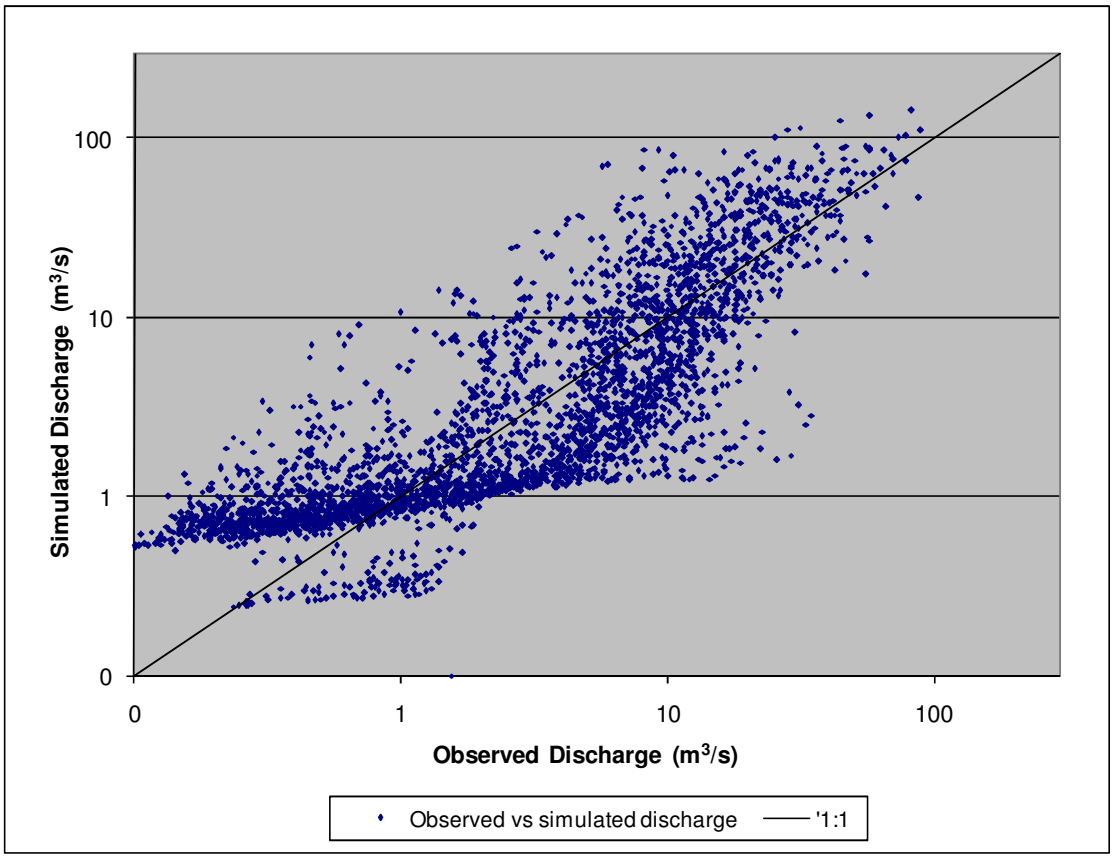

Hydrograph of flow calibration at gauging station 225219 (period from 1975 to 1984) and the relationship between simulated and observed flow along line of perfect fit.

APPENDIX I FLOW VALIDATION GRAPHS

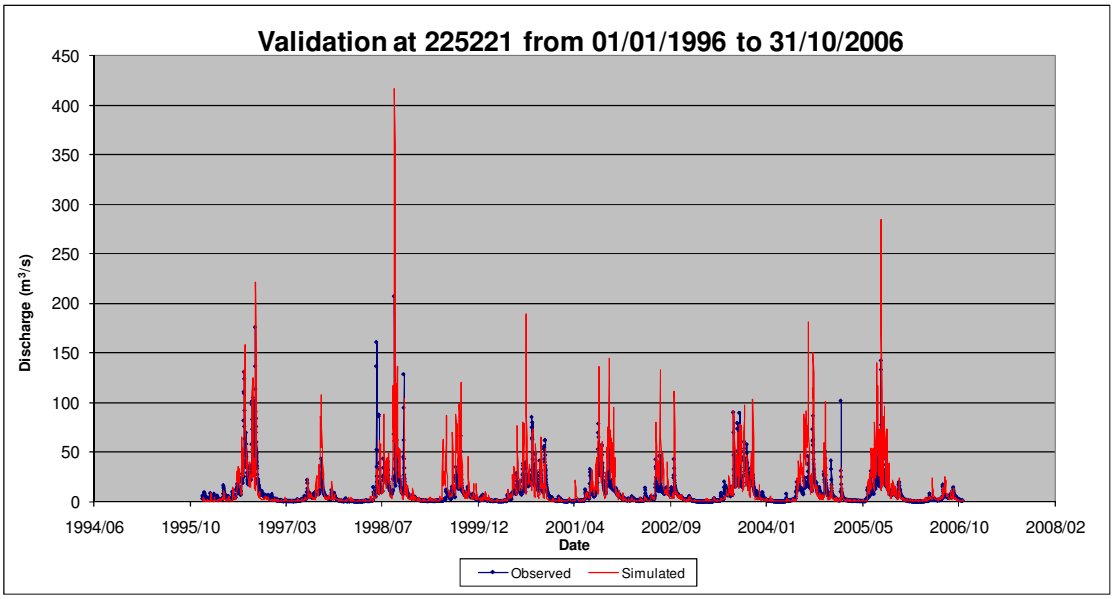

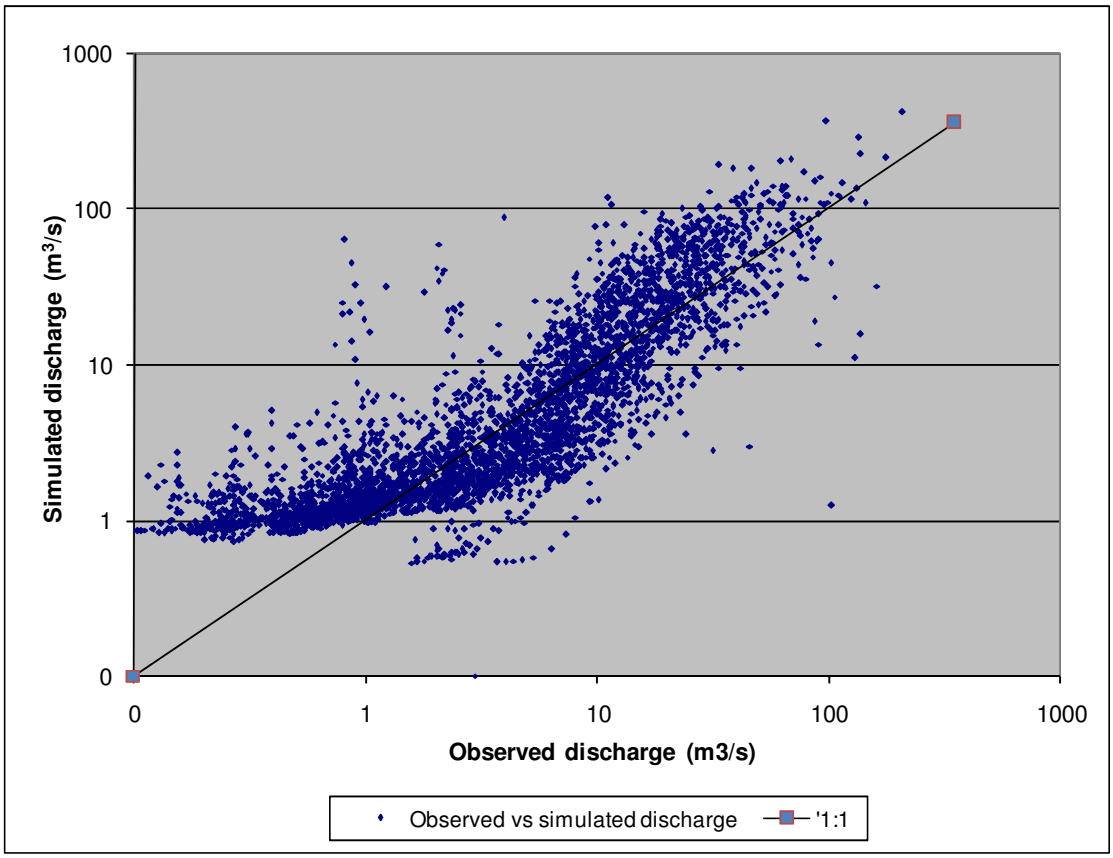

Model validation at gauging station 225221 (during period from 1996 to 2006) and the relationship between simulated and observed flow along line of perfect fit

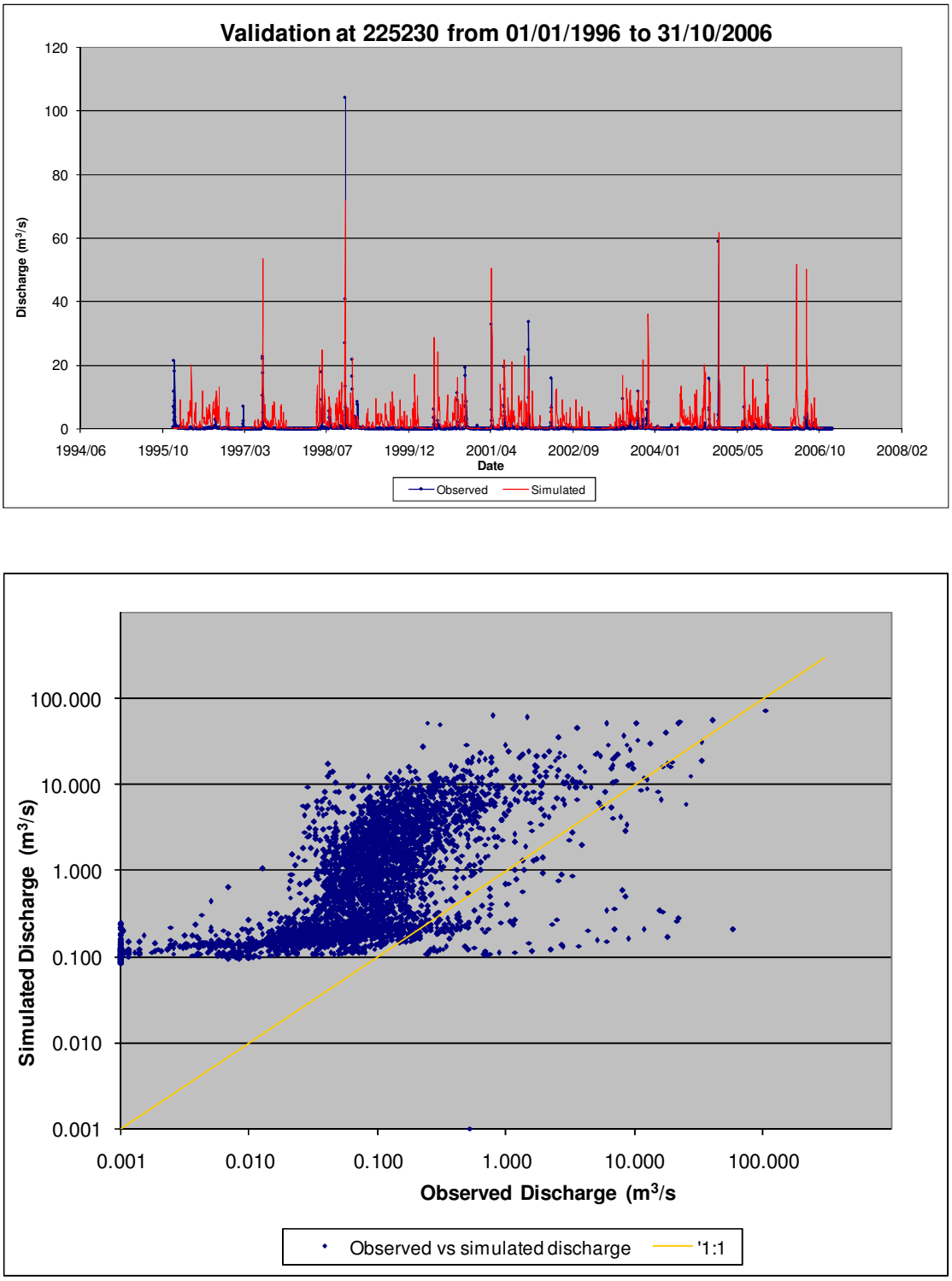

Model validation at gauging station 225230 (during period from 1996 to 2006) and the relationship between simulated and observed flow along line of perfect fit

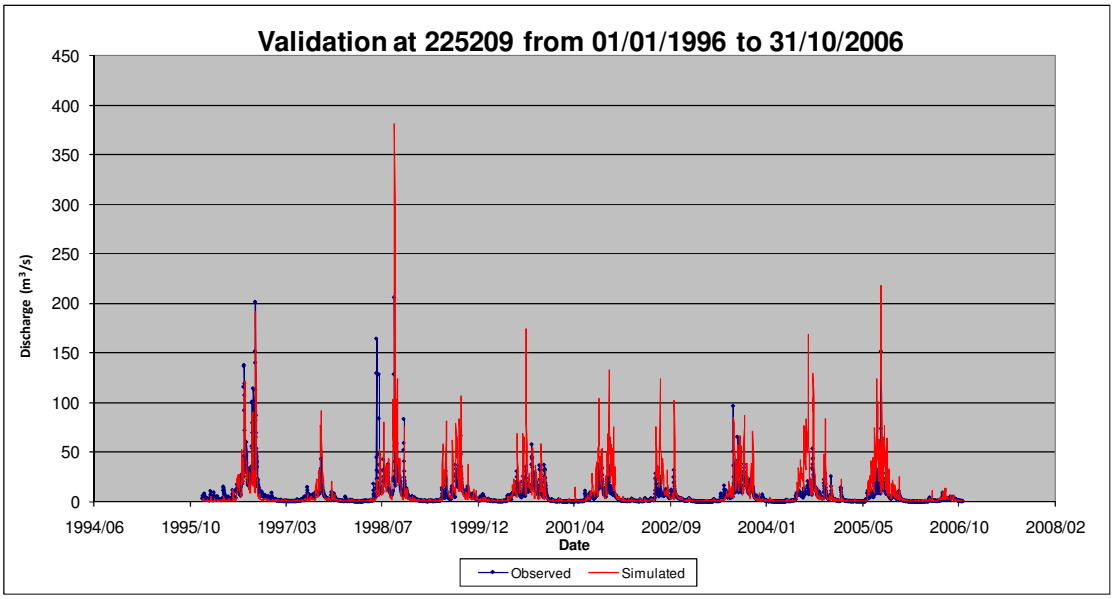

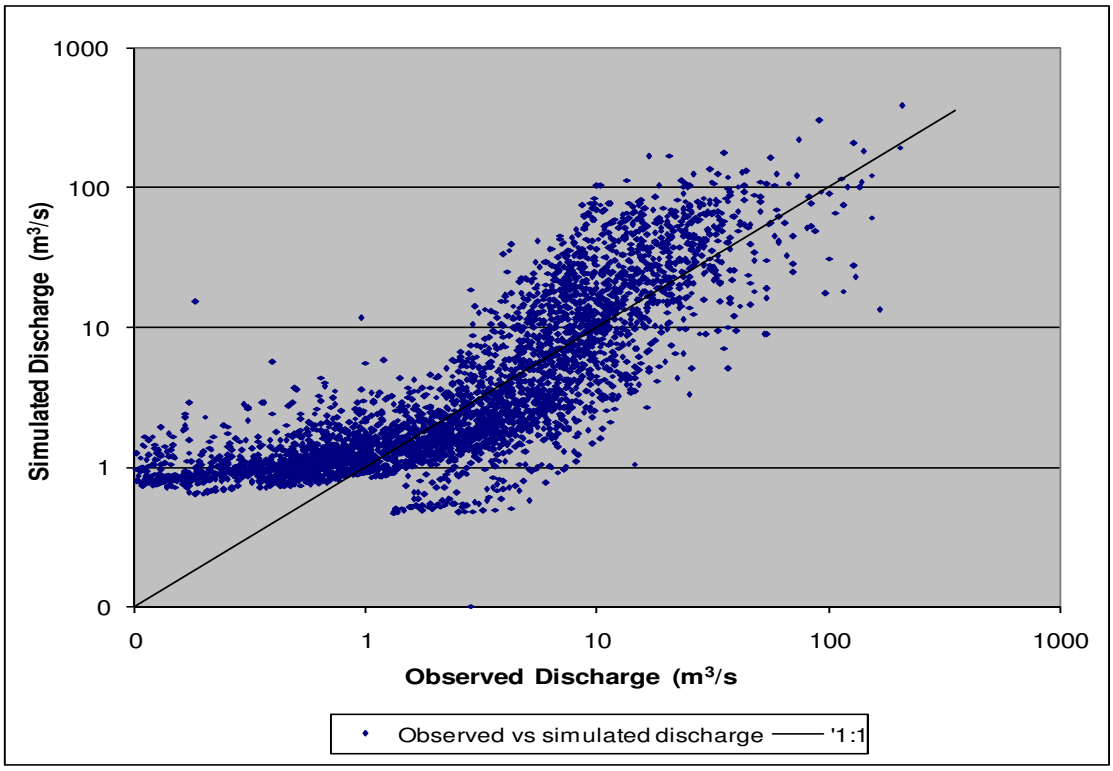

Model validation at gauging station 225209 (during period from 1996 to 2006) and the relationship between simulated and observed flow along line of perfect fit

APPENDIX J SEDIMENT LOAD VALIDATION GRAPHS

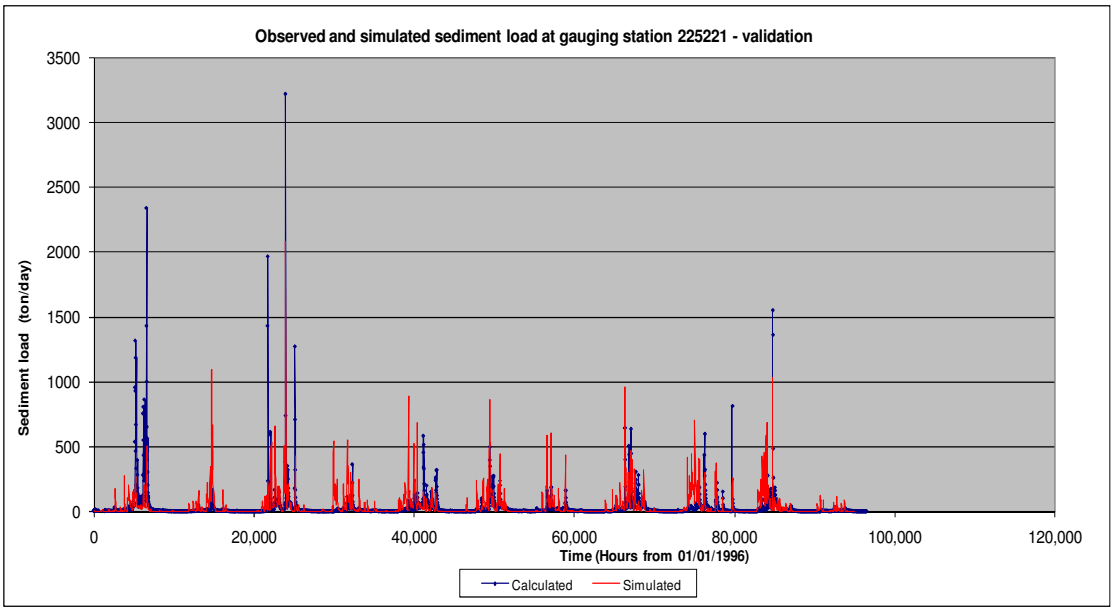

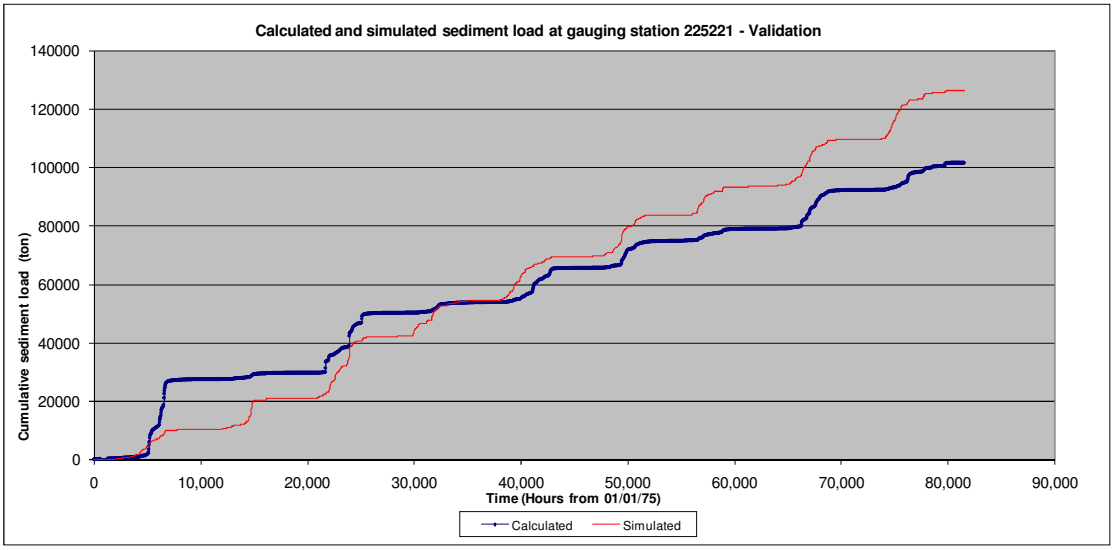

Sediment validation for station 225221 from 1996 to 2006

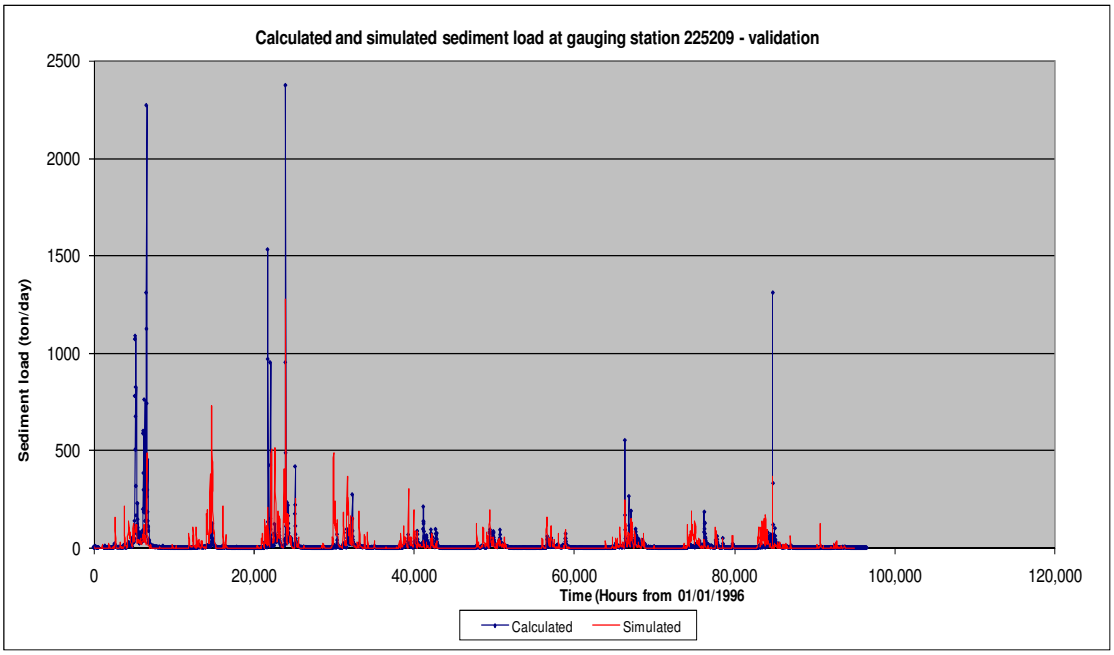

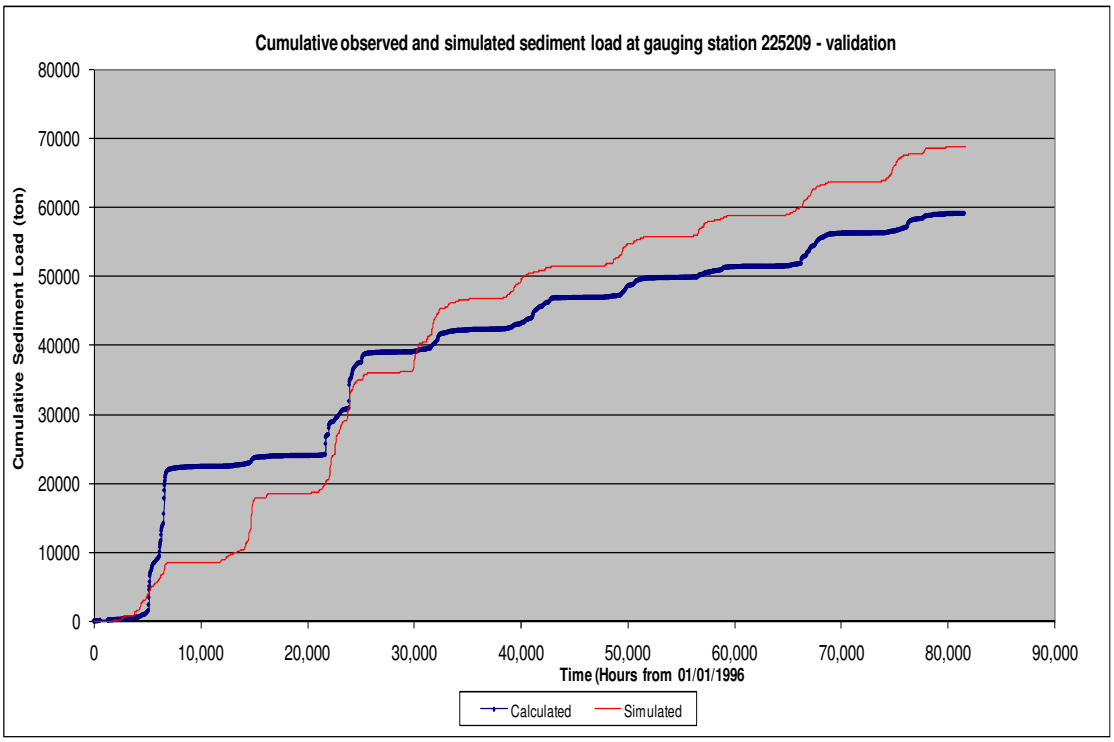

Sediment validation for station 225209 from 1996 to 2006

APPENDIX K CUMULATIVE PLOT OF SEDIMENT LOAD

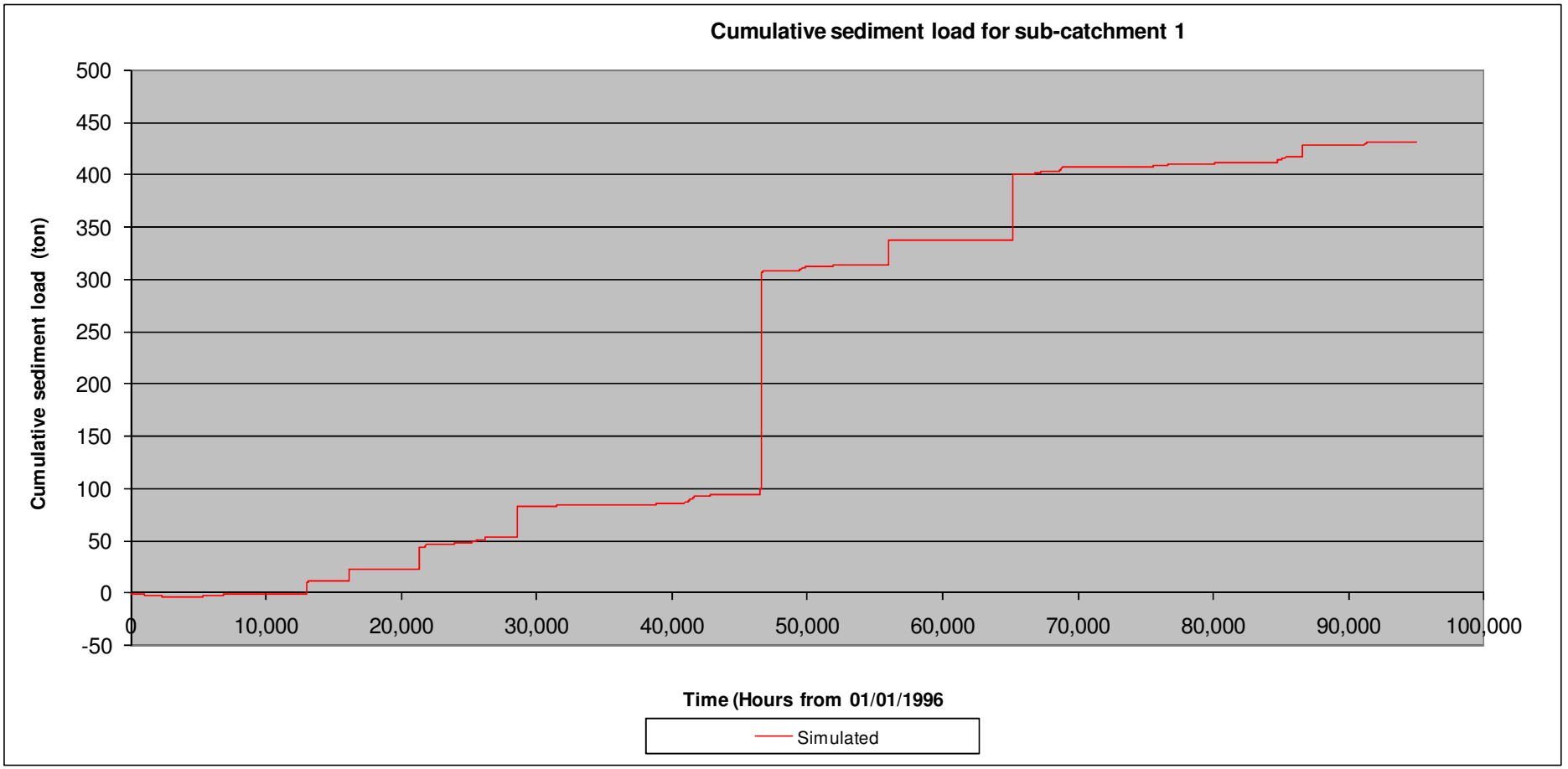
Cumulative sediment load for sub-catchment 1
Cumulative sediment load (ton)
500
450
400
350
300
250
200
150
100
50
0
-50
0
10,000
20,000
30,000
40,000
50,000
60,000
70,000
80,000
90,000
100,000
Time (Hours from 01/01/1996
Simulated

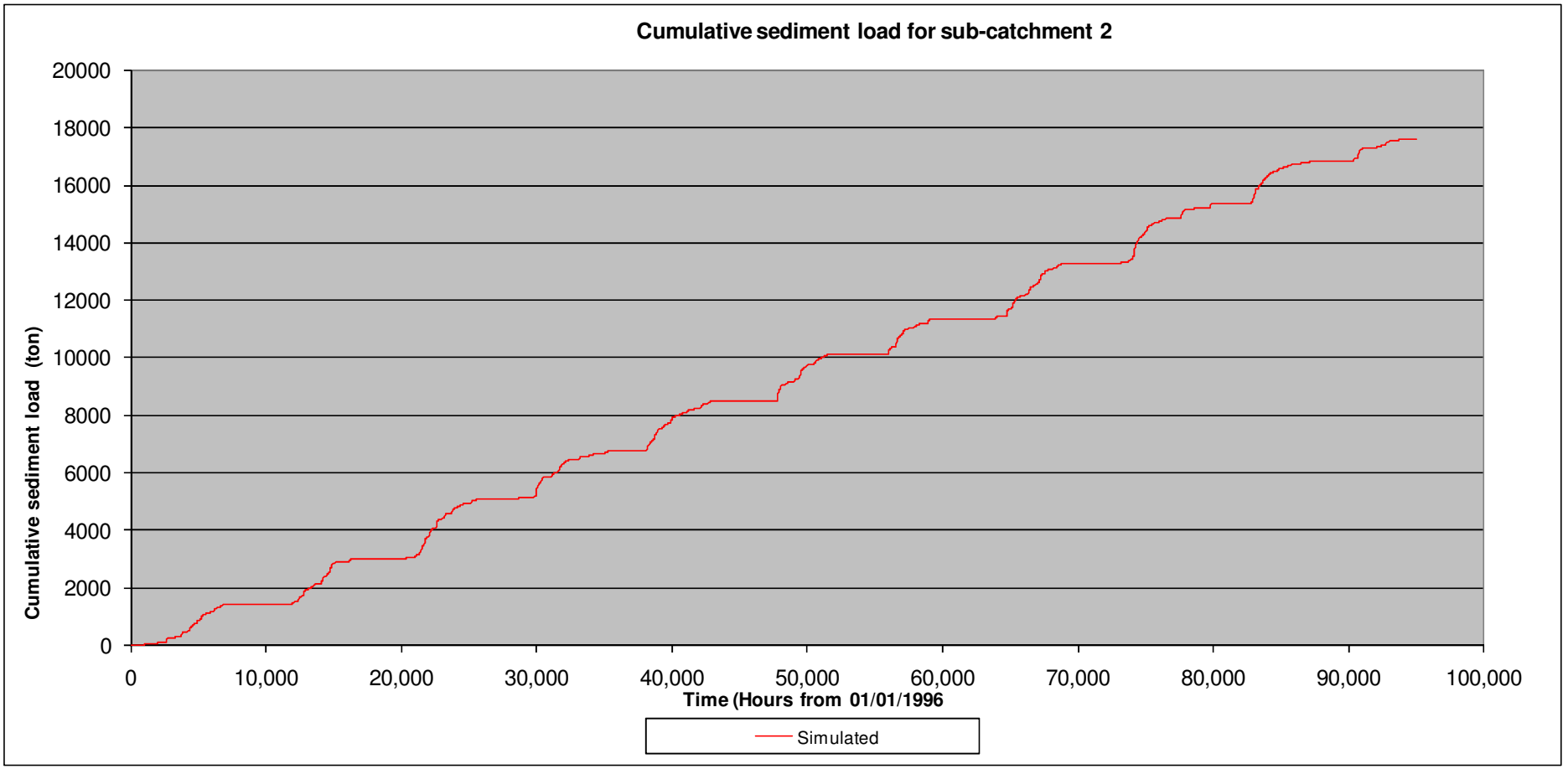
Cumulative sediment load for sub-catchment 2
Cumulative sediment load (ton)
20000
18000
16000
14000
12000
10000
8000
6000
4000
2000
0
0
10,000
20,000
30,000
40,000
50,000
60,000
70,000
80,000
90,000
100,000
Time (Hours from 01/01/1996
Simulated

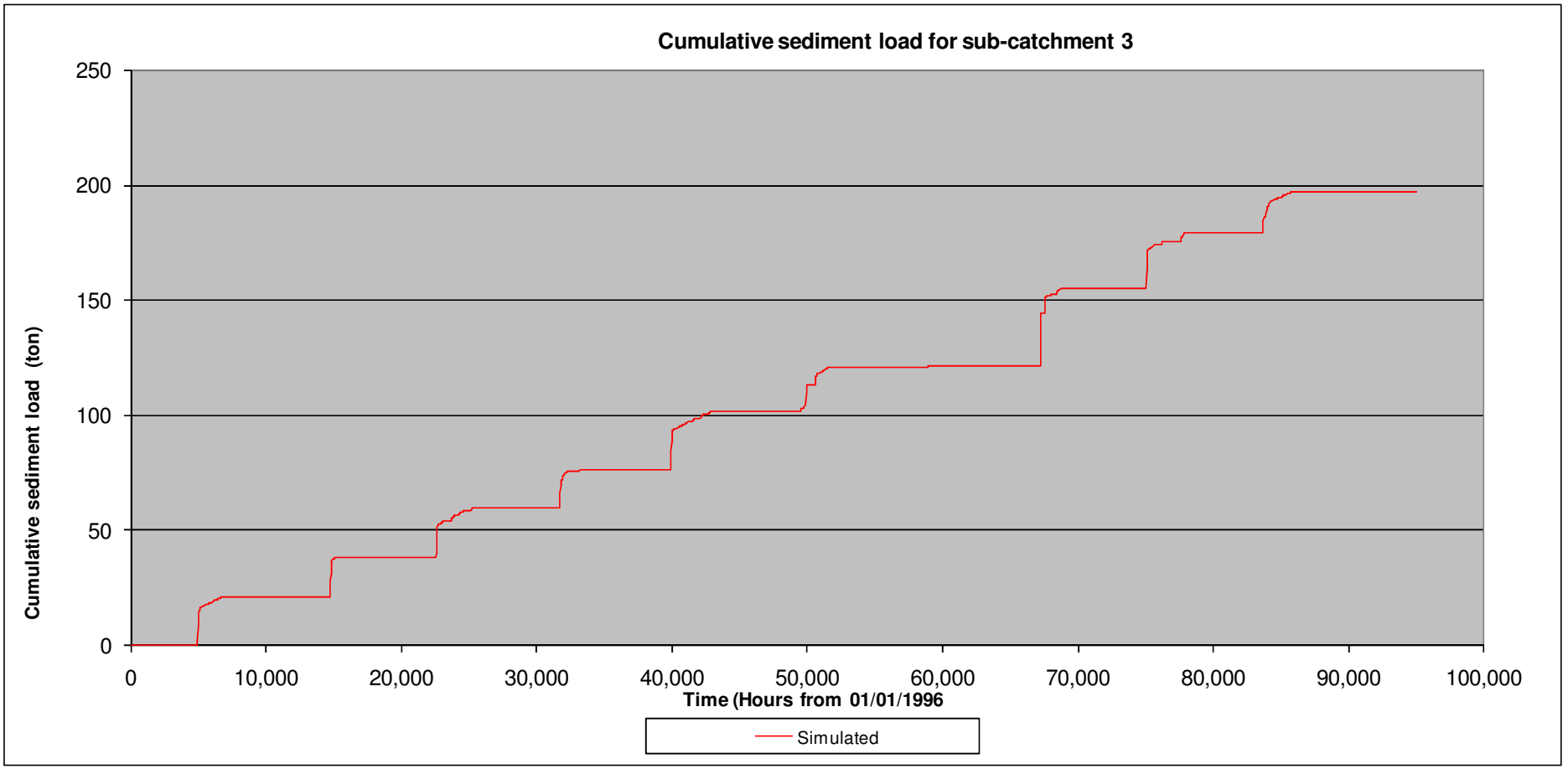
Cumulative sediment load for sub-catchment 3
Cumulative sediment load (ton)
250
200
150
100
50
0
0
10,000
20,000
30,000
40,000
50,000
60,000
70,000
80,000
90,000
100,000
Time (Hours from 01/01/1996
Simulated

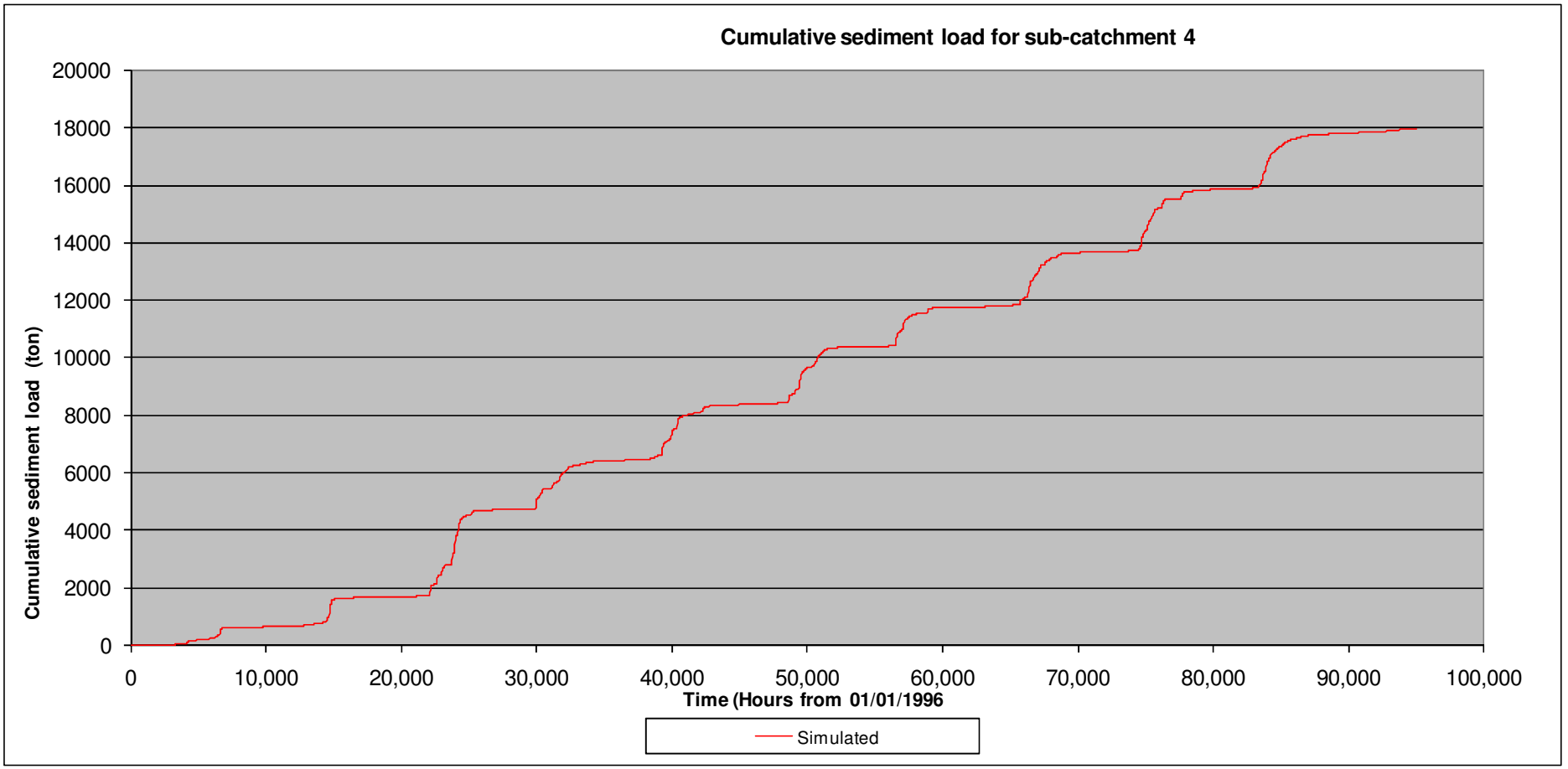
Cumulative sediment load for sub-catchment 4
Cumulative sediment load (ton)
20000
18000
16000
14000
12000
10000
8000
6000
4000
2000
0
0
10,000
20,000
30,000
40,000
50,000
60,000
70,000
80,000
90,000
100,000
Time (Hours from 01/01/1996
Simulated